Award Number: DAMD17-00-1-0277

TITLE: Protease Activated Receptors in the Malignant
            Invasion Process

PRINCIPAL INVESTIGATOR: Rachel Bar-Shavit, Ph.D.
                         Beatrice Vziely, M.D.

CONTRACTING ORGANIZATION: Hadessah Medical Organization
                           Jerusalem, Israel 91120

REPORT DATE: June 2003

TYPE OF REPORT: Final

PREPARED FOR: U.S. Army Medical Research and Materiel Command
               Fort Detrick, Maryland 21702-5012

DISTRIBUTION STATEMENT: Approved for Public Release;
                        Distribution Unlimited

The views, opinions and/or findings contained in this report are
those of the author(s) and should not be construed as an official
Department of the Army position, policy or decision unless so
designated by other documentation.

REPORT DOCUMENTATION PAGE

1. AGENCY USE ONLY (Leave blank)	2. REPORT DATE June 2003	3. REPORT TYPE AND DATES COVERED Final (1 Jun 00 – 31 May 03)

4. TITLE AND SUBTITLE	5. FUNDING NUMBERS
Protease Activated Receptors in the Malignant Invasion Process	DAMD17-00-1-0277

6. AUTHOR(S)
Rachel Bar-Shavit, Ph.D.
Beatrice Vziely, M.D.

7. PERFORMING ORGANIZATION NAME(S) AND ADDRESS(ES)	8. PERFORMING ORGANIZATION REPORT NUMBER
Hadessah Medical Organization Jerusalem, Israel 91120 E-Mail: barshav@md2.huji.ac.il	

9. SPONSORING / MONITORING AGENCY NAME(S) AND ADDRESS(ES)	10. SPONSORING / MONITORING AGENCY REPORT NUMBER
U.S. Army Medical Research and Materiel Command Fort Detrick, Maryland 21702-5012	

11. SUPPLEMENTARY NOTES
Original contains color plates: All DTIC reproductions will be in black and white.

12a. DISTRIBUTION / AVAILABILITY STATEMENT Approved for Public Release; Distribution Unlimited	12b. DISTRIBUTION CODE

13. ABSTRACT (Maximum 200 Words)

Protease-Activated Receptors (PARs) are G-coupled seven transmembrane domain proteins consisting of 4 family members and activated via proteolytic cleavage. In addition to their traditional role in hemostasis, thrombosis and vascular biology, PAR1, thrombin receptor; the first prototype of the family emerges with surprisingly novel functions in tumor biology. We have assigned a central role for PAR1 in breast carcinoma invasion, metastasis and angiogenesis. The notion that *hParl* is one of a series of genes that are part of an invasive program stems from our studies showing that *hParl* is exclusively expressed along the time limited placenta physiological invasion process to the uterus decidua during implantation, completely shuts - off thereafter. The use of breast carcinoma clones over-expressing different forms of *hParl* (e.g., full length, a truncated version and antisense *hParl*) as also tetracycline inducible *hParl* system have enabled the elucidation of a specific "invadopodia" signaling pathway and the relative contribution of *hParl* during breast carcinoma progression and angiogenesis. In parallel, we have established an original line of mice over-expressing MMTV LTR - driven *hPar-1* targeted to the mammary glands. The glands exhibited grossly hyperplastic features as compared with the non transgenic littermates. This phenotype is precociously reminiscent of the effect of several oncogene over-expression in the mouse breast. We propose now a novel pathway of *wnt* activation as a consequence of *hParl* over-expression in the mammary glands. Our approach involving the combined analyses of tissue specific *hParl* transgenes, biopsy specimens and established cell lines are combined to assist evaluating the involvement of *hParl* in breast carcinoma invasion, metastasis and angiogenesis.

14. SUBJECT TERMS	15. NUMBER OF PAGES 163
	16. PRICE CODE

17. SECURITY CLASSIFICATION OF REPORT Unclassified	18. SECURITY CLASSIFICATION OF THIS PAGE Unclassified	19. SECURITY CLASSIFICATION OF ABSTRACT Unclassified	20. LIMITATION OF ABSTRACT Unlimited

Table of Contents

Introduction

In addition to the classical role of *Protease Activated Receptors* (PARs) in hemostasis, thrombosis and vascular biology, it emerges with surprisingly new assignments in tumor biology. The seven transmembrane G-coupled thrombin receptor (PAR1) is the first example of a novel PAR family, consisting of 4 members all of which with a unique mode of activation (see scheme1, in the attached figures). These genes encode their own ligands and serve as substrates for cleavage prior to activation (1-5). While the full repertoire of protease signaling through PARs remains to be defined, this family provides nonetheless, a powerful tool to respond towards a wider range of concentrations, possibly for different rates of signaling. The process by which epithelial cells become invasive involves the acquisition of the ability to migrate through basement membranes and reemerge from blood vessels to establish metastatic colonies at distant sites (see scheme 2). Although the involvement of soluble and matrix-immobilized protease in tumor cell invasion and metastasis is well recognized, the significant impact of protease cell surface receptors, PARs has now beginning to rise.

hPar1 and breast carcinoma invasion. We have identified novel molecular targets belonging to the PAR family, and assigned PAR1 as a potent cellular probe, actively involved in breast carcinoma invasion and metastasis *(Nature Medicine* 4: 909-914, 1998; 6). This was demonstrated by the over-expression of *hPar1* in both tissue biopsy specimens, *in vivo* (Fig. 1, I) and established cell lines, *in vitro* (Figure 2, I&II). Introduction of a *hPar1* antisense sequence (a plasmid containing part of the promoter and the start initiation region of the protein; of 462 bp) markedly diminished the ability of highly metastatic breast cells to invade Matrigel coated filters (see Fig. 2, III&IV; 6). Elucidation of other PAR family members in breast carcinoma metstasis, may help develop an individually based therapy program according to the specific and spatial profile obtained for each patient.

Oncogenic properties of PAR1. PAR1 has recently been reported as an oncogene, promoting transformation in NIH 3T3 cells (7). This function of PAR1 is supported by our prior observations demonstrating that PAR1 is highly over-expressed in series of tissue biopsy specimens of breast (6), colon, esophagus and bladder carcinomas as well as in a collection of differentially metastatic cell lines (6, 8-10).

Models in Breast Epithelia tumor progression: interrelation between *hPar1* and E-cadherin. Early stages of breast cancer (hyperplasia and ductal carcinoma *in situ* (DCIS) are characterized by an increased proliferation of epithelial cells, a loss of acinar organization and filling of the luminal space (11). Later

events involved in the progression toward malignancy are illustrated by the total loss of acinar organization and the acquisition of an invasive behavior. Growth arrested human mammary epithelial acinar structures can be used to study the early stages of carcinogenesis in cells *in vitro* (12, 13). Three dimensiona (3D) basement membrane cultures provide a unique opportunity to model the architecture of the epithelium *in vitro* (14). Unlike monolayer cultures, mammary epithelial cells grown in 3D recapitulate numerous features of breast epithelium in vivo, including the formation growth - arrested polarized acini with a hollow lumen and basal deposition of basement membrane components (12, 14). One of the major components of cell-cell interaction that help maintain the tight constrains of the highly ordered epithelia architecture, is E-cadherin. Loss of E-cadherin expression leads to an invasive phenotype. Therefore, invasive, metastatic tumor cells must be free-roaming capable of detaching from the extra-cellular matrix constrains and neighboring cells. E-cadherin may nonetheless function, as an invasion tumor suppressor gene. We have addressed the interrelation between *hPar 1* and E-cadherin as illustrated in 3D spheroide cultures and in clones over-expressing *hPar1*.

While data accumulated in our Lab show that *hPar1* mediated signaling is significant in the induction of tumor invasion and metastasis (8), the impact of various *hPar1* constructs on E-cadherin expression is further addressed. Does a truncated version of *hPar1* modulate the expression levels of E-cadherin as compared to a full length *hPar1*- is of great interest.

Regulatory sites in *hPar1* promoter: Involvement in spatial expression during tumor invasion. Despite ample data elucidating cellular activation mediated by *hPar1,* little is known about the regulatory process determining the context and pattern of receptor expression. The regulatory region of thrombin receptor *Par1* has been cloned and DNA sequence analysis indicates the presence of several transcription factor-binding elements among of which are two AP-2/Sp1 complexes identified at the proximal 3' region of the promoter (15, 16). Overall these complexes contain four putative AP-2 binding elements and seven Sp1 - binding elements. AP-2 , a 52 kDa protein first purified from HeLa cells, binds to a consensus palindromic sequence, 5' GCCNNNGGC-3' (17, 18). The DNA-binding domain is located within the C-terminal half of the 52-kDa protein and consists of two putative amphipathic α-helices separated by a 92 amino acid intervening span that is both necessary and sufficient for homodimer formation (19). It has been documented that the expression profile of AP-2 in breast carcinoma biopsy specimen is inversely related to ErbB2 protooncogene (20). Recently, Bar-Eli M and *co-workers* (21) have demonstrated that loss of AP-2 expression in metastatic melanoma cells correlates with overexpression of *hPar1*. This may indicate that loss of AP-2 leads to *hPar1* over-expression and melanoma malignancy, strictly down regulated when AP-

is present. Therefore it is plausible that AP-2 may act as a potent suppressor of *hPar1* gene expression. The elucidation of AP-2 expression pattern and spatial localization in our transgenic mice over expressing *hPar1* in the mammary glands may help elucidate, key regulatory elements determining the level of *hPar1* amplification or shut-off.

Body of report

I. Molecular basis of PAR1 induced tumor invasion (see Appendix 1, 8). Part of the molecular mechanism underlying PAR1 induced tumor invasion and metastasis has been described in our stable *hPar1* expressing clones (SB-2 cells). PAR1 is capable of modulating the invasive behavior of the cells by conferring metastatic properties in parental non invasive cells (as evaluated by formation of lung metastatic foci, *in vivo* and migration through Matrigel coated filters, *in vitro*). Activation of PAR1, increased markedly the phosphorylation of paxillin and focal adhesion kinase (pp125 FAK) accompanied by cytoskeletal reorganization of F-actin stress fibers. Distinct focal adhesion complexes (FACs) are observed following PAR1 activation as detected by immunostaining of vinculin, FAK and paxillin. The specific recruitment of $\alpha v\beta 5$ to focal contact sites, but not $\alpha v\beta 3$ or $\alpha 5\beta 1$, is observed. Based on these evidence, we propose that the activation of PAR1 leads to a selective cooperation of $\alpha v\beta 5$ integrin while fostering tumor cell invasion.

II. The pattern of Protease Activated Receptors (PARs) expression during early trophoblast development (see Appendix 2, 9). Human fetal development depends on the ability of the embryo to gain access to maternal circulation. Thus, specialized stem cells of the newly formed placenta, named trophoblast invade the uterus and its arterial network to establish an efficient feto-maternal molecular exchange. To accomplish this task, trophoblast differentiation during the first trimester of pregnancy, involves cell proliferation, invasion and extracellular matrix (ECM) remodeling. Trophoblast invasion shares many features with tumor cell invasion, with the distinction that it is strictly spatially and temporally controlled. We have previously demonstrated that PAR1, the first member of the Protease Activated Receptor (PAR) family, plays a central role in tumor cell invasion. In the present study we have examined the pattern of expression of PAR1 and other PAR family candidates during early human placental development. We show that PAR1 and PAR3 were highly and spatially expressed between the 7th and 10th weeks of gestation but not at the 12th week and thereafter (see . Pathological trophoblast cells may appear occasionally and cause a trophoblastic disease known as Complete Hydatidiform Mole (CHM). Likewise, high expression levels of PAR1 and PAR3 were observed in the cytotrophoblast cells of CHM biopsy specimens as compared to minimal levels in the normal age-matched placenta. Together, our data suggest

3

the involvement of PAR1 and at least PAR3 in the restricted and unrestricted pathological trophoblast invasion process.

III. Tumor angiogenesis and *hPar1* (See appendix 3, 10). While recently it has been shown that PAR1 plays a critical role in endothelial cell embryonic development rescuing *Par 1 -/-* mice from bleeding to death - its function in tumor angiogenesis was unknown. Griffin et al, (22) provided elegant evidence highlighting that loss of PAR1, does not prevent vessel formation but rather impairs stabilization and maturation of the newly forming vessels, thereby causing abnormal fragility and ruptures in the vessel wall (22, 23). Our studies (10) indicate that *Par1* gene expression plays a central role in tumor blood vessel recruitment both in animal models *in vivo,* determined by the "Tet-on" *Par1* inducible prostate system and by the Matrigel micropocket assay. *Par1* induced angiogenesis is mediated via the increased expression of vascular endothelial growth factor splice forms; VEGF121, VEGF145, VEGF165 and VEGF189 or but not VEGF 206.

IV. Establishing *hPar1* over-expressing line of mice targeted to express in the mammary glands: Morphogenesis, hyperplasia and stabilization of β-catenin (*Manuscript in preparation,* see *attached preliminary data).* The opportunity to identify a novel pathway, that recapitulates a fundamental process both in embryogenesis and tumor progression, is best explored in a transgenic mouse model. We have established the original line of mice carrying an MMTV-LTR driven *hPar1* transgenes specifically over-expressed in the mammary glands. Analysis of the whole mount *hPar1* over-expressing glands, showed enhanced complexity of alveolar side branching in the virgin mice , strikingly induced in the pregnant mice (Fig. 6 IV&V). This phenotype is precociously reminiscent of the effect of several oncogenes over-expressed in the mouse breast. *In situ* hybridization analysis on sections of virgin (at 5, 8 and 13 weeks) and pregnant (4d, 8d and 12d) mammary glands, showed high and abundant levels of *hPar*1 at the luminal phase of the mammary epithelium (Fig. 7, I&II).

In search for the elucidation of a molecular mechanism induced by *hPar1* mammary gland morphogenesis and hyperplasia, we reasoned that *Wnt* may play a critical role in the process. Wnt proteins are known to orchestrate many aspects of the cell physiology such as embryogenesis and tumorigenesis (24, 25). The elucidation of early developmental processes by Wnts have been well studied in fly, warm, fish, frog, mouse and human (24). Although there is a broad agreement that Wnts exert these influences on embryonic cells as also in pathological carcinoma progression through cell surface receptors named Frizzled (26), the proximal steps of the signaling cascade beyond Frizzleds are less well understood. The overall downstream targets of Frizzled action are divided into several pathways among of which the major one is:

the canonical Wnt pathway, acting through stabilization of β-catenin and the regulation of gene transcription.

Among the Wnt family members Wnt-4 is a prime candidate to address mammary gland morphogenesis, elegantly demonstrated by Brisken *et al* to play a critical role in ductal side branching (27-29). Our preliminary data indicate that Wnt- 4 expression is markedly induced in the *hPar1* over-expressing glands as compared with age matched wild type mice. This was demonstrated both by RT-PCR (at 5 &13 weeks virgin mice and during pregnancy at 4, 8, and 12 days of gestation) and immunoblotting (Fig. 8). Wnts encode a large family of secreted glycoproteins that carry short-range signals between cells and bind to members of the Frizzled family of seven-trans-membrane receptors. Of the Wnts known to express in the mouse mammary gland in addition to wnt -4; Wnt 7a, 7b; Wnt 5a and 5b and Wnt 6, we find that only Wnt 7b levels are increased as compared with normal controls both in virgin and pregnant *hPar1* over-expressing mice analyzed. The presence of elevated Wnt-4 and Wnt-7 in mammary glands from *hPar1* over-expressing mice suggests that *hPar1* gene either directly or indirectly controls their level of expression.

While ductal side branching is responsible, in part for the mammary glands complexity induced by the over-expression of *hPar1*, the prospect of induced alveoli proliferation was analyzed as well. For this, the status of epithelia proliferation was assessed by performing immunohistostaining analysis of the *proliferating cell nuclear antigen* (PCNA). The proliferation index (PI) is defined as the number of PCNA - positive nuclei of alveolar epithelial cell/total nuclei. Our data (Fig. 9, I&II) indicate that proliferation of alveolar bud epithelium is significantly higher in the *hPar1* over-expressing transgenes as compared with age - matched wild type counterparts. In mammary glands, at 5 weeks of age, the proliferative process is initiated as shown in normal virgin mammary glands, thus, a relatively higher level of PI in the *w.t.* mice is seen, yet the trasgenes exhibit almost a 3 fold increased levels of PCNA. The difference is highlighted especially at the time period of weeks 10 and 13 of virgin mice, where normally alveoli proliferation activity is arrested. In comparison, an induced PCNA staining level is seen in *hPar1* age matched transgenes, exhibiting increased PI index. At pregnancy, while normal on-going PCNA activity takes place also in the *w.t.* mice, again a higher induced activity is seen in the *hPar1* over-expressing mice. We conclude that *hPar1* over-expressing mammary glands are actively engaged in both, ductal side branching as also in alveoli proliferation leading finally to high complexity of the ductal network.

β -catenin, a down stream effector of the *Wnt* pathway, plays a dual role; in cell adhesion as a linker between actin cytoskeleton and E-cadherin cell-cell receptor; on the other hand it may serve as a classical oncogene (30). The canonical Wnt/Wingless signaling pathway directs cell fate in a variety of cell

types and has an integral role in organogenesis. The core of the pathway is the stability of β-catenin. Wnt signaling inhibits the amino terminal phosphorylation and subsequent degradation of β-catenin allowing cytoplasmic pools of β-catenin to enter the nucleus and bind to members of the Lef/Tcf family of DNA binding proteins. Thus, β-catenin acts as a transcription co-factor of the Lef/Tcf family. The later is responsible for inducing a growing list of target genes, among them c-*Myc*, c-*Jun* and cyclin D1 (31). In the absence of Wnt signaling, a multi-protein cyoplasmic complex containing the adenomtous polyposis coli (APC) supports the degradation of phosphorylated β-catenin, via the ubiquitin-proteasome system (32, 33). Cytoplasmic pool of β-catenin is constitutively subjected to sequential phosphorylation of a stretch of four N-terminal residues (e.g., S33, S37 T41 and S45). Following the completion of this phosphorylation cascade, a perfect β-TrCP binding motif is created around phosphoserines 33 and 37 (34, 35). β-catenin degradation is initiated upon the interaction with axin. The later, acting directly or via an adapter protein diversin (36), recruits casein kinase I (CKI) to phosphorylate β-catenin at S45 (60, 61).
S45, in-fact, acts as a single molecular switch of the canonical *Wnt* signaling, and is the most commonly mutated residue of β-catenin in malignancy (37, 38).

The relationship between the Wnt pathway and cancer was first established when Wnt-1, the hot spot of insertional mutagenesis by the mouse mammary tumor virus (MMTV), was cloned (39). Serving as the down-stream effector of this pathway, β-catenin itself is a classic oncogene (38). In addition, β-catenin mutations have been demonstrated in numerous tumors, most notably colon carcinomas and hepatocellular carcinoma (40, 41). The majority of these mutations are clustered in the N-terminus, curtailing the phosphorylation cascade , or hitting residues modeling the β-TrCP binding motif (42). Acting as the single molecular switch of the canonical Wnt signaling, S45 is the most commonly mutated residue of β-catenin in malignancy (37, 42). However, β-catenin stabilization may result also from loss of function of any component contributing to β-catenin degradation. Indeed, APC and axin, which promote β-catenin degradation, function also as tumor suppressors.

We sought to evaluate β-catenin state in *hPar1* over-expressing mammary gland transgenes as compared with *w.t.* age matched counterparts. Our data indicate the striking accumulation and high expression levels of β-catenin, regardless of virgin or pregnant mice over-expressing *hPar1* mammary glands, as compared with very little or almost none in normal counterparts (Fig. 10, I). We are fully engaged at analyzing mediators responsible for β-catenin stabilization in our system. The immediate target is to assess properties of impaired β-catenin phosphhorylation sites. In parallel, because we consistently obtain a 55kDa protein in size, a β-catenin degradation product comparable with the ΔNβ-catenin (lacking the N-terminal portion of 89 a.a., where phosphorylation occurs), we intend to analyze the properties of this

protein band. Immunohistostaining and cellular localization experiments was carried out in parallel, to evaluate the spatial cell distribution of β-catenin within the *hPar1* over-expressing mammary glands. Our launched pilot experiments clearly demonstrate the high and abundant staining of β-catenin in the nuclei of *hPar1* over-expressing glands as compared with very little or no β-catenin in the normal age matched mammary tissues. Hence, in the over-expressing *hPar1* mice mammary glands, stabilized pools of β-catenin is imported to the nuclei where it may further affect gene transcription.

Once stabilized, cytoplasmic pools of β-catenin enter the nucleus and affects target gene expression by interacting with Lef-1/Tcf transcription factors. The lymphoid enhancer factor (Lef1) and T cell factor (Tcf), consist a family of proteins that bind DNA directly and act mostly as repressors. The binding of β-catenin to Lef-1/Tcf is required for the initiation of targeted gene activation. We have investigated *hPar1* gene transcriptional activity as portrayed via the activated Lef-1/Tcf. This was carried out following transfections with TOPFlash-Luc construct, a positive control reporter plasmid containing Lef-1/Tcf binding sites, as compared with FOPFlash-Luc, a negative control plasmid (with a point mutation in Lef-1/Tcf binding sites). We have analyzed various forms of *hPar1* gene in order to establish the critical parameters of Lef-1/Tcf transcriptional activity induced by the *hPar1*. Of the forms we have analyzed, the truncated version of *hPar1* devoid of the entire cytoplasmic tail, compared with the length *hPar1*. Our preliminary data show that following transient transfection of the full length *hPar1* in 293 cells, [utilizing LipofectAMINE PLUS reagent], along with TOPFlash -Luc and FOPFlash-Luc, a marked activity in TOPFlash as compared to minimal activity of FOPFlash – is observed. Activation of *hPar1* showed further enhancement in TOPFLASH activity (see Fig. 10, II). Along this line, over-expression of a truncated version of *hPar1* showed no transcriptional activity – yielding only a basal level of TOPflash activity. This points out the significance of *hPar1* signaling events in the induction of the transcriptional activity. It is imperative to emphasize that the powerful system of mammary mice transgenes allowed the identification of β-catenin stabilization by *hPar1* and hence, the induced transcriptional activation of Lef-1/Tcf. It is most likely that the appropriate context of epithelial mammary gland interactions with the microenvironment stroma enabled β-catenin nuclear localization in the over expressing *hPar1* gene. Needless to emphasize that by merely over-expressing *hPar1* in breast carcinoma cell lines, this novel pathway was not likely to be elucidated. We will further analyze transcriptional activities of discrete thrombin receptors family members, namely *Par3* and *Par4*. The prospect of assigning targeted gene activities by distinct *Par* family members is nonetheless at prime significance.

II. MCf-7 over-expressing *hPar1* clones: Impact different forms of *hPar1* plasmids and Focal Adhesion Complex formation. Cell migration and invasion are both fundamental components of tumor cell metastasis. Cell invasion integrates a complex set of events initiated by either alterations in integrin cell surface expression (43), by the release or activation of protease (that cleaves extracellular matrix components thereby liberating ECM-immobilized proteins to foster tumor progression; 44), and /or by modulations of gene expression during cell transformation (45). Increased focal adhesion kinase (FAK) expression and tyrosine phoshorylation are connected with elevated tumorigenesis. It has been demonstrated for example, that in FAK-/- fibroblasts, cell migration and invasion are impaired and re-expression of FAK, Tyr 397 phosphorylation, and FAK kinase activity are all required for the generation of an invasive cell phenotype (46).

We have demonstrated during the present funding period that activation of *hPar1* is capable of inducing Focal Adhesion Complex (FAC) formation, cytoskeletal re-organization and the selective recruitment of αvβ5 integrin (8). The interrelation between *hPar1* gene constructs, invasion and FAC formation in breast cancer cells were further addressed. For this, we have been engaged at preparing cell transfectants, chimeras of *hPar1* and tetracycline inducible systems for the purpose of adequately address the originally proposed tasks. Our data, gleaned from the combined and converged results using *hPar1*-inducible/regulated systems as well as by various *hPar1* constructs (e.g., full length truncated version devoid of the entire cytoplasmic tail, a GST-C-tail of *hPar1*) - outlined in details bellow:

Establishment of the "Tet-Off" inducible *hPar1* system in the parental MCf-7 breast cells has been carried out. It is demonstrated (Fig. 11), that elevated expression of *hPar1* is seen in the absence of Dox, completely shuts - off in the presence of Dox.

In parallel, we have prepared stable MCf-7 clones over-expressing either full length *hPar1*, and a truncated version of *hPar1* lacking the entire cytoplasmic region. RT-PCR analysis of the clones show the expression of the gene regardless of either a truncated or full length *hPar1* analyzed, as none detected in the mock transfected cells. This was compared to equal amounts applied as determined by a housekeeping gene GAPDH -tested. While by the use of primers directed towards the C-tail of *hPar1* in full length over-expressing clones indicate (as expected) the presence of a C-tail, it is absent in clones expressing the truncated version of *hPar1*. This internal control, provides an additional support and verification that these clones in-fact, provide good vehicles to address the relevant issues raised (Fig. 12). Likewise, the expression of PAR1 protein was shown as demonstrated by either Western blot, immunoflurescence and FACS analyses, indicating that the truncated *hPar1* is well expressed on the cell surface of the, yet lacking

8

the cytoplasmic region. Immunofluorescence analysis provided data regarding the spatial and cellular distribution of the PAR1-protein showing the membrane and cytoplsmic localization in both protein in both the full length *(F.L.) hParl* clones and the *hParl* truncated clones and absent in the mock transfected MCf-7 cells (Fig. 13, I-III).

Next, we wished to determine in these clones, conditions for the activation of the FAC major signaling protein - FAK. Our data show that by utilizing anti pFAK antibodies no discrete localization is seen prior to activation in either *F.L.* or in truncated *hParl* over-expressing clones as also in control mock transfected cells. Following activation however, distinct focal adhesion sites are clearly marked by pFAK and completely absent in cells over-expressing a truncated version of *hParl* regardless of activation (fig. 14).

One of the queries raised during our studies is whether PAR1, a cell surface receptor protein enters FACs following activation. Immunofluorescence analysis in highly invasive MDA-435 cells show that prior to *hParl* activation, no FACs are observed, yet exhibiting high and abundant levels of PAR1, in the cytoplasm of the cells (Fig. 15). Following *hParl* activation however, discrete and abundant sites of FACs are distinctly marked as detected by 4G10 antibodies, directed toward p-Tyr labeled proteins. Concomitantly, altered distribution of the cytoplasmic PAR1 is observed following activation, exhibiting now discrete localization spots as detected by anti PAR1 antibody staining. A merge of both images (anti 4G10 and anti PAR1) gives - rise to discrete yellow staining spots, pointing to co-localization of both *hParl* and 4G10 marking -FACs. We conclude thus, that at least in MDA435 cells PAR1 enters FACs.

In parallel, we have prepared (as outlined above) a construct of a GST-C-tail PAR1, containing Serine (S) 369 /N-terminus and up to residue 425 (T) / COOH. The C-tail was prepared by using the following primers (5' TACTATTACGCTGGATCCTCTGAG-3' and CTGAATTCCTAAGTTAACAGCTT-3') in an RT-PCR reaction. The DNA fragment obtained was further cut using the appropriate restriction enzymes (BamH1 and EcoR1) and ligated into pGEX2T vector (see Fig. 16, I). The desired construct was further separated on a SDS-gel and the appropriate size obtained have further indicated that the fusion protein of the C-tail was adequately prepared (Fig. 16, II). Next, various cell lysates over-expressing either *hParl* or Syk, a tumor suppressor gene in breast carcinoma progression were applied onto the GST-PAR1 - C-tail. The specifically eluted material showed clearly that in lysates of Syk-3T3 cells, Syk was bound to the PAR1 C-tail. No binding was observed when either a control GST- beads were used as a binding column (Fig. 17). Or lysates of 3T3 cells applied under similar conditions. When a GST - C-tail of PAR1 was digested and cleaved from the GST beads (for the purpose of possible competition analysis between GST-C-tail and Syk expressing cells), a marked inhibition of Syk levels was observed (Fig. 17, II). These results

9

further substantiate and strengthen our basic assumption that in-fact, Syk and PAR1 are bound together and physically co- associate (Fig. 18, I&II). We are currently analyzing whether the N-terminal SH2 or the tandem SH2 domains of Syk are involved directly in the binding to PAR1 cytoplasmic portion, leaving the kinase domain free for activation. We are also preparing deletions of PAR1 cytoplasmic tail in order to determine the minimal size necessary for this direct association between PAR1 and Syk. Along this line, activation of PAR1 induced also the association of Src observed as early as 2 min and declined after 20 min activation, as demonstrated by co-IP analysis of PAR1 and Src (see Fig. 19). Furthermore, in cells over-expressing Syk, activation of PAR1 showed increased complex formation between Syk and Src (Fig. 20). We are now in the process of determining whether a complex comprised of three components; Src and Syk attached to the C-tail of PAR1, occurs following PAR1 activation.

In leukocytes, Syk is activated by binding to diphosphorylated immune receptor tyrosine-based activation motifs (pITAMs) (47). Syk also has been recently demonstrated to directly interact with the C-terminal portion of integrin $\beta3$ cytoplasmic tail (48). The possibility that Syk interacts directly with the cytoplasmic region of PAR1 is nonetheless interesting and intriguing. It may implicate that PAR1, a G-coupled receptor is capable of recruiting Syk kinase to couple tyrosine induced pathways, for a protective tumor suppressing outcome.

Notably, both Rac and JNK activation are attenuated in cells incapable of invasion (for example, cells exhibiting FAK-/-). A useful outline of FAK stimulated downstream signaling events, during invasion, may come from lessons in non invasive FAK-/- fibroblasts, re-introduced with the capability to invade (46). FAK expression within FAK-/- cells facilitated the formation of multiprotein signaling complex comprised of v-Src, p130Cas, Crk and Dock180. One should note, that the role of FAK in linking stimulation to Rac and JNK activation is not limited to reconstituted FAK-/- cell, since FAK antisense treatment of human A549 carcinoma cells disrupted the EGF-stimulated formation of a Src-p130Cas signaling complex (49). The loss of FAK expression however, in A549 cells also inhibited EGF-stimulated JNK activation and invasive cell motility. Experiments performed by Hsia *et al*., in a FAK rescue assays in FAK-/-, v-Src cells showed that FAK phosphorylation at Tyr397, FAK kinase activity, and the SH3-binding sites in the FAK-COOH - terminal domain were individually required to facilitate Rac and JNK activation and cell invasion (46).

Our data in cells over-expressing *hPar1* clearly indicate the induced Rac activities in a Rac pull - down assay using a GST-Pak (See Fig. 21). Concomitantly, activation of PAR1 induced the phosphorylation of JNK-1. This phosphrylation was attenuated when Syk, a tandem SH2 tyrosine kinase with potential tumor suppressing activities was introduced into these cells. Overall, elucidation of a pathway

leading to *hPar1* induced *"invadopodia"* involves; phosphorylation of FAK, activation of Rac and JNK-1, downstream combined altogether to foster invasion in these cells. In this context, it is interesting to add, that in Syk over-expressing cells, activation of *hPar1* leads in contrary to attenuated activation of JNK-1 and increased phosphorylation of c-Cbl. No such activation is seen in the absence of Syk (Fig. 22).

c-Cbl, a 120kDa protein contains a proline rich region allowing its interaction with the SH3 domain-containing proteins and several putative docking sites for a wide variety of SH2 -containing proteins. Consistent with the structure of c-Cbl, it has been shown that c-Cbl could bind to various transducing molecules among of which them are: Syk, the p85 subunit of PI-3'-kinase, Shc (50), Grb2, and Crk –II (51). Given the numerous putative tyrosine phosphorylation sites present on c-Cbl and the possible activation of signal transducing molecules downstream, it is suggested that activation by Syk may confer a negative regulation of the cell cycle, via c-Cbl (Fig. 22). Similarly, it was shown that induced expression of another tumor suppressor gene p53, was linked to Ras-mediated negative regulation of cell-cycle components such as; the CDK inhibitor p21waf1 and Gadd45, shown to inhibit entry of cells to S phase; 52), and also to stimulation of DNA excision repair (53). Our preliminary data indicate a similar pattern, showing that upon expression of Syk in invasive breast cells the levels of Gadd45 is dramatically increased (as determined by Northern blot analysis, see Fig. 24). A growth arrest and DNA damage gene 45, (Gadd45), belongs to GADD protein family shown to inhibit the proliferation and stimulate DNA repair and/or apoptosis. GADD genes were originally identified by subtraction hybridization from a cDNA library constructed from UV-irradiated Chinese hamster ovary cells (54). Recently it has been shown that Gadd45 elevated expression is associated with DNA fragmentation as assessed via TUNEL staining in bronchiolar epithelial and parenchyma cells (55). Altogether, our data support the notion that in the presence of Syk gene, negative cell-cycle regulation that ultimately lead to apoptosis - takes place in breast cancer. Activation of Syk via PAR1 confers tumor-suppressor like phenotype (see summary scheme in Fig. 25).

III. Conditional switching of *hPar1* in tumor progression. To gain insight into the properties attributed to *hPar1* during tumor development and metastasis we have established a tetracycline inducible system of *hPar1* expression. Tumor progression is known as a complex process guided by a combination of unregulated gene expression in the invading cells and stereospecific microenvironmental cues. While complex morphogenetic processes are executed in a multifactorial events pending on the context and guided messages transmitted by the microenvironment, addressing an individual gene might be hampered by several problems. The use of cell transfectants, for example, exhibiting a continuos over-expression of

sprouting blood vessels – was analyzed. Alternatively, the perturbation of stability in the mature vessel, similar to the previously suggested role in a developmental system (22), in settings of tumor angiogenesis - was investigated, To evaluate the feasibility of a *hPar1* based future gene therapy we have designed and prepared cells expressing the inducible *hPar1*.

In a low *hPar1* expressing rat prostate carcinoma cells AT2.1, that were stably transfected to express the "Tet-on" promoter, *hPar1* cDNA was introduced and selected for stable clone expression. Two clones of AT2.1/Tet-on/*hPar1* clones (Cl1 and Cl4) were picked showing the regulated levels of *hPar1* strongly induced upon the addition of a tetracycline analog Dox as determined by Northern blot analysis. *Par1* expression was nearly undetectable in the absence of Dox. Following addition of Dox, the levels of the 4.1 kb *Par1* mRNA were increased substantially (39 fold for Cl1 and 52 fold for Cl4; Fig. 26II, D & F). The optimal dose of Dox necessary to induce *Par1* expression was 1-2 µg/ml (not shown). *Par1* mRNA could be detected as early as 4-6 h, and reached maximum levels at 20-24 h after Dox treatment (not shown). AT2.1 cells transfected with the pTet-On vector without the *Par1* gene did not express any detectable *Par1* mRNA levels either in the presence (Fig. 2II, lane B) or in the absence (Fig. 26 II, lane A) of Dox.

To assess the effect of PAR1 on tumor growth *in vivo*, AT2.1/Tet-On/*hPar1* clone Cl4 cells or control transfected cells were injected *s.c.* into rats. The onset of *hPar1* induction in these animals and the duration of expression were tightly controlled though the inclusion or omission of Dox from the drinking water. Rats were then maintained for 2 weeks with either regular drinking water (supplemented with 1% sucrose) or drinking water containing Dox (and 1% sucrose) to induce *Par1*. In all injected rats, marked tumor growth occurred during this time period. In the absence of Dox the mean mass of AT2.1 clone Cl4 tumors was 0.35±0.1 gr (Fig. 26 III, B). When PAR1 expression was induced by Dox in the drinking water, mean AT2.1 clone Cl4 tumor mass increased 3.7 fold to 1.30 ± 0.14 gr. This increase was statistically significant. In addition to being larger, tumors in these Dox –treated animals had a very reddish appearance (Fig. 26 III, C) compared to the pale appearance of tumors from untreated animals (Fig. 26 III, B). In comparison, tumors from control-transfected and non-transfected AT2.1 tumors were significantly smaller and did not increase in mass or change in color when Dox was delivered in their drinking water (Fig. 2 6IV). We conclude, therefore, that the regulated induction of the *Par1* gene markedly enhanced two critical determinants of tumor progression: tumor size and angiogenesis. The enlarged and vascularized tumor obtained in the expression of *hPar1* is supported by data obtained in Matrigel invasion assay *in vitro* showing a 7 fold induction in the invasion levels upon the addition of Dox (Fig. 27).

We applied a Matrigel plug assay to evaluate whether *Par1* can recruit blood vessels *in vivo*. We have characterized a stable *Par1* transfected, non-metastatic SB-2 melanoma cell line (Cl13) (8). Densitometric

12

analysis of a representative Western blot (Fig. 1, ref. 8) revealed that Cl13 cells express 4.2 times more PAR1 than the parent SB-2 line which expresses very little PAR1. For comparison, the highly invasive melanoma cell line SM-A375 was determined to express 1.8 times the levels of PAR1 protein found in SB-2 parental cells. C113 cells were mixed at 4^0C with Matrigel (reconstituted basement membrane (BM) preparation extracted from EHS mouse sarcoma) and injected *s.c.* into BALB/c mice. Upon injection, the liquid Matrigel rapidly formed a solid gel plug that served not only as an inert vehicle for PAR1 producing cells, but also mimicked the natural interactions that exist between tumor cells and the surrounding extracellular matrix (ECM). Non-transfected SB-2 cells were similarly mixed with Matrigel and injected as a control. In some cases, C113 cells were treated with thrombin receptor activating peptide (TRAP) to activate *Par1* prior to embedding in Matrigel. 10 days after injection, the Matrigel plugs were exposed, examined and photographed. Plugs containing control SB-2 cells were pale, containing few blood vessels; however, those containing *Par1*-expressing C113 cells were reddish, indicative of recruited blood vessels. Plugs containing TRAP-activated C113 cells had the most pronounced red coloration (Fig. 28 I). Matrigel plugs were subsequently removed, paraffin-embedded, sectioned, and stained for either collagen (Mallory's staining; Fig.28 II A, C, D&E) or Factor VIII (vWF staining Fig. 28 II, B&F) to allow histological evaluation of blood vessels in the plug. A network of recruited capillary blood vessels is seen in plugs containing C113 cells while few vessels appear in plugs containing non transfected cells (Fig. 1 II). The difference in angiogenesis induced by activated PAR1-transfected cells (Fig. 28 IIF) as compared to non transfected, either untreated or TRAP-treated (Fig. 28II, A&B), is particularly striking. Microscopic counts of the microvessels in Matrigel sections indicated that these differences are statistically significant (Fig. 28 III). While low levels of blood vessels were obtained in SB-2 cells and somewhat induced levels following activation, eight fold increase was seen in Cl13 following TRAP activation (Fig. 28 III). To exclude the possibility that clonal variation is responsible for these effects, we analyzed several other PAR1- transfected SB-2 clones (MixL and Cl15) and found similar angiogenic activity (data not shown).

Next, we have designed a *hPar1* withdrawal experiment. Rats were induced for the expression of *hPar1*, for two weeks (by the addition of Dox) to their drinking water), by the time that the tumor was fully developed we have omitted ("off") Dox , for additional two weeks. The tumors then were processed as described above and further analyzed for the state of the tumor and blood vessels. As one can see in Fig. , no dramatic differences are observed in the tumors either following 2 weeks (left panel) onset of *hPar1* or 4 weeks (middle panel). In- comparison, a comparable tumor of 4 weeks of age whereby in the last 2 weeks *hPar1* was shut-off, massive appearance of nonviable cells is seen. This was detected by PI (*propidium*

13

iodide) staining of nuclei in the bulk of the tumor, in-comparison, to presence of a few viable cells adjacent a nearby an intact blood – vessel (Fig. 29).

We are currently engaged at processing further and evaluate these tumors. This will be carried out by the staining with vonWillebrand Factor (vWF; Dako, Denmark) as also Mallory's for detecting blood vessels. The status of these vessels will be determined upon staining with anti smooth muscle actin For the detection of matured vessels (coated with pericytes).

Enhanced levels of blood vessels are also observed in mammary glands over-expressing *hPar1* as compared to age matched *w.t.* mammary glands, following Mallory's staining (Fig. 30). The combined , data overall points to the distinct role of *hPar1* in tumor angiogenesis.

IV. Interrelation between of *hPar1* and E-cadherin in breast carcinoma. Loss of E-cadherin expression or function in tumors leads to a more invasive phenotype. Epithelial cells associate into intact polarized sheets and communicate through an intricate network of cell-cell junctions and cell-ECM interactions. This architectural restraint of cell-cell junctions underlined by a basement membrane serves as extra-strict boundaries to maintain normal cellular behavior. A critical event in malignant tumor development is the acquisition of the ability to invade through basement membranes, enter the circulatory system, and re-emerge from blood vessels to establish metastatic colonies at distant sites. This task is accomplished via a well-orchestrated set of events including the recruitment of enzymes to remodel targeted locations of the basement membrane microenvironment. Lack of the architectural restraint of cell-cell junctions as portrayed by the loss of E-cadherin is a hallmark tumor progression. Thus the early phases toward malignancy, where epithelia-mesenchyme transition (EMT) occurs the disturbance of cell-cell adherens junctions is the core process. E-cadherin therefore, functions also as an invasion /tumor suppressor protein. The loss of E-cadherin is attributed usually to activation of transcriptional regulators such as the repressor Snail (58) or hypermethylation in the promoter (59).

Although the role of E-cadherin in the regulation of tumor invasion is well established , the mechanism by which it promotes invasion suppressing activity is less understood. Along this line, it is interesting to note a recently reported finding (60) that the invasion suppressor activity of E-cadherin is not attributed to the extracellular portion (mediating cell-cell interactions), but in-fact, to the β-catenin binding domain in the cytoplasmic tail. While β-catenin depletion also results in invasion suppression. However, alteration in β-catenin/TCF transcriptional regulation of target genes is not required for invasion suppression activity of E-cadherin. This may suggest the involvement of other β-catenin binding proteins in the process.

14

During our transfections studies enforcing the expression the full length *hPar1*, we have consistently noted the loss of E-cadherin expression. This consistent loss of E-cadherin as a result of *hPar1* over-expression is accompanied by enhanced migration and filling of a defined vacant space created by a well defined wound in the tissue plate (Fig. 31 I&II).

What are the regulatory processes by which *hPar1* gene conveys the loss of E-cadherin is of prime interest in our laboratory. For this we are analyzing the state of E-cadherin promoter methylation in clones over-expressing *hPar1* as compared with control cells. We have analyzed also morphogenesis of *hPar1* over- expression in 3-dimensional cultures. Human mammary epithelial cells form acini-like structures containing a single layer of polarized, growth - arrested cells when grown within a Matrigel environment; (matrix rich in collagen type IV and laminin derived from the Englebreth-Holm Swarm; EHS tumor) (12-14). The epithelial cells within the acini in cultures as also *in vivo* deposit collagen type IV and secrete sialomucin in their basal and apical surfaces, respectively. They also have a typical apico-basal distribution of polarity markers such as ZO-1, E-cadherin and $\alpha6\beta4$ integrins. These indicate that the acinar structures formed in culture closely mimic the acini in the adult breast. Three-dimensional acinar structures were generated by plating MCF-10A cells on an exogenous basement membrane matrix, Matrigel. After 10-12 days in culture, each cell formed an acinus containing 20-40 cells (Fig. 32 I&II). Confocal immunofluorescence analyses of acini labelled with 4', 6-diamidino-2-phenylinidole (DAPI) revealed that the acinar units had basally localized nuclei and a hollow lumen. Immunostaining for basal surface markers such as collgen type IV (data not shown) and cell-cell junction markers as β-catenin and E-cadherin (Fig. 32 II), indicated that the acinar structures consisted of polarized epithelial cells. In contrast, these cells exhibited highly invasive phenotype of disorganized intrusion structures (Fig. 32 I), when an invasive breast cancer cells highly expressing *hPar1* were plated, under similar conditions.

V. hPar1 expression in human ovarian tissue samples: Correlation with malignant progression and pY397FAK.

We investigated the expression pattern of *hPar1* in ovarian carcinoma tissue samples. High and abundant levels were detected in either borderline or invasive carcinoma, regardless of the cell histological subtype. No *hPar1* expression was detected in normal cell surface ovarian epithelia. The differential expression of *hPar1* was shown by *in situ* hybridization, immunhitochemical analysis and semi-quantitative RT-PCR. In parallel, we have analyzed $\alpha v\beta5$ integrin levels of expression in these tissues. While abundant expression of $\alpha v\beta5$ integrin was seen regardless of the progression stages, activated focal adhesion kinase (FAK), a major focal complex protein was seen in a direct correlation with ovarian tumor progression.

15

Phosphorylated FAK was observed in invasive and bordeline ovarian carcinoma while none in the normal epithelia. The abundant *hPar1* present in borderline and invasive ovarian carcinoma are most likely to transmit signals, induce the phosphorylation of FAK and thereby alter integrins functional state. Altogether our data indicate that *hPar1* and FAK cooperate in concert to promote ovarian cancer progression.

Legends to Figures:

Scheme 1: PAR family comprised of 4 gene members

Scheme 2: Steps in tumor carcinoma progression and metastasis. Normal epithelia consist of polarized sheets of cells with well organized junctions underlined by a basement membrane. In carcinoma *in situ,* epithelial cells proliferate locally, but are still confined by the basement membrane. The transition from epithelial to mesenchyme stage (EMT-epithelial mesenchyme transition) involves further alterations that can induce local dissemination, emergence through the basement membrane, intravasation and extravasation of lymph or blood vessels, and the establishment of metastatic colonies at distant sites. PAR1 is present at high levels in DCIS (ductal carcinoma *in situ*), but not in normal epithelia or dysplastic carcinoma. Active signaling initiated by PAR1 association with $\alpha v \beta 5$ induces reorganization of the cytoskeleton and focal adhesion complex formation, which fosters invasion and metastasis. Part of the scheme is modified from Thiery, JP (*Nature Reviews* June 2002 volume 2 (6)p. 442-454).

Fig. 1: I. *In situ* **hybridization of PAR1 mRNA in normal and cancerous breast tissues specimens.**
Riboprobes probes prepared and labeled by T7 RNA polymrerase (for antisense orientation) or T3 RNA polymerase (for sense orientation - control), using DIG-UTP for labeling mix.Top. IDC staining by PAR1 antisense and sense control (A,B; respectively). Middle. DCIS staining by PAR1 antisense and sense control (C,D; respectively). Bottom. Hyperplasia staining by PAR1 antisense and sense control (E,F; respectively).
II. *In situ* **hybridization of PAR3 in breast carcinoma biopsy specimens.** RNA probes were transcribed and labeled by T7 RNA polymrerase (for antisense orientation) or T3 RNA polymerase (for sense orientation - control), using DIG-UTP for labeling mix. Top panel. IDC (invasive ductal carcinoma) biopsy sample of antisens and sense orientation of PAR1 (*left & right*, respectively). DCIS (ductal carcinoma in situ) antisense and sense (as above, middle panel) and hyperplasia and normal breast tissue (*left & right*, respectively- bottom panel).

Fig. 2: PAR1 expression in human breast carcinoma cell lines. Total RNA isolated from human breast carcinoma cell-lines were analyzed by Northern blotting. These are: MDA-435 (lane A), MDA-231 (lane B) and MCF-7, as well as Ha-ras-transfected breast carcinoma cell lines, MCF10AT3B (lane D), MCF10AT (lane E) and MCF10A (lane F). The blots were probed with ^{32}P-labeled 250 base pair DNA, corresponding to PAR1 (upper part), or with ^{32}P-labeled β-actin DNA (lower part).
II. Western blot analysis of ThR. Western blot analysis of cell lysates (50 μg/lane) of MCF-7 (lane A), MDA-231(lane B) and MDA-435 cells. Specific protein band was detected following incubation with anti ThR antibodies and visualized by the ECL immunoblotting detection system according to the manufacturer's instructions.
III. Inhibiton of MDA-435 Matrigel invasion by PAR1 antisense. MDA-435 cells were transiently transfected with pCDNAIII expression plasmid containing the antisense PAR1 including part of the promoter region (i.e. 462 nucleotides). The level of invasion was compared to untreated MDA-435 (lane A) and MCF-7 (lane B) cells. Control transfections of MDA-435 cells were performed in the presence of vector alone - or DOTAP liposomes alone (Gibco -BRL) (lane D). Nearly confluent (60%) cells were treated with various concentrations of the plasmid: transfection with antisense PAR1 - 5 μg/plate (lane E), transfection with antisense PAR1 - 20 μg/plate (lane F). The invasion assay was performed as described under Materials and Methods, 72 h following transfection.

IV. Western blot analysis of PAR1 antisense transfectants. MDA-435 cell lysates (50 μg/lane) of PAR1 antisense transfectants (A) were applied on SDS-PAGE and the level of receptor protein was compared to cells transfected with vector alone (B) or untreated cells.

Fig. 3: Tissue expression and distribution of PAR1 in the first trimester placenta. I. *In situ* **hybridization of** *Par1*. Normal placental specimens were analyzed for *Par1* mRNA by *in-situ* hybridization, using a DIG-labeled RNA probe for *Par1*. *Par1* antisense riboprobe was applied on tissues from weeks: (A) 6; (B) 7; (C) 8; (D) 10; (E) 10; sense control riboprobe 10; (F) 14. An enlarged view of the placental villi border is shown in section C (note the abundant staining of *Par1* in the cytotrophoblast layer but not in the syncytiotrophoblast). **II. Levels of** *Par1&2* **mRNA. a.** For PCR detection, 0.25 μg of RNA was reverse-transcribed and amplified, using the appropriate set of primers and compared with the control housekeeping gene GAPDH. b. *Par1* mRNA levels were evaluated by Northern blot analysis and compared to the levels of 28S RNA.
III. PAR1 Immunostaining. Immunohistochemical staining of PAR 1 shows high immunoreactivity in placental samples obtained at 7 (A), 8 (B) and 10 (C) weeks of gestation. Minimal levels of staining was observed at week 12 (E) of gestation and in a control sample using bovine IgG at week 10 (D). Data shown are representative of at least 5 independent experiment series of early placenta samples.

Fig. 4: Tissue expression and distribution of PAR3 in the first trimester placenta I. *In situ* **hybridization.** Normal placental specimens were analyzed for *Par3* mRNA by *in situ* hybridization using a DIG-labeled RNA probe. An antisense *Par3*-riboprobe was applied on tissues from placenta villi following weeks: (A) 6; (B) 7; (C) 8; (D) 10; (E) 10; sense control riboprobe, at week: (F) 12. **II. RT-PCR analysis of** *Par3*. For PCR detection as in Fig. 1, using specific primers of *Par3*. **III. Western blot analysis of PAR3.** PAR3 protein levels were detected at weeks 7, 8 and 10 of gestation and was absent at week 12 (D). Equal levels of protein were applied as detected by β- actin house keeping levels. Data shown are representative of at least 3 independent set of experiments of early placenta samples.

Fig. 5: Modulation of EVT villi invasion by over-expressing *hPar1* **either sense or antisense constructs. I.** Introduction of *hPar1* full length enforce villi extension outgrowth in extravillous trophoblast (EVT) grown in Matrigel tissue culture. The *hPar1* over-expressing EVT induced MMP2 and MMP9 as determined by zymography assay. **II.** Inversely, the overexpression of *hPar1* antisense when the villi extension is maximal, resulted in a marked attenuation of villi outgrowth as determined also by a marked reduction in cellular fibronectin synthesis.

Fig. 6: I. Generation of MMTV-*hPar1* transgenic mice. Schematic representation of MMTV-SV40-BSSK- *hPar1* construct for mammary-specific expression (MMTV-*hPar1*-TG). The long form of the MMTV long terminal repeat is used to drive selective expression, and the SV40 splicing and polyadenylation fragment enhance export and translation. Full length of human *Par1* was insert between the sites of HindIII and EcoRI.
II. MMTV-*hPar1* transgenic lines. A) Genotyping of the founder mice using Southern blotting. The tail DNA was digested with BamHI, and a transgene fragment was detected via Southern blotteing. L1-L3, lines 1-3; *w.t.*, wild type, 10, 20 copy numbers.
III. RT-PCR analysis shows the expression of human *Par1* transgene in different organs of a transgenic mouse. The experiment is a representative of at least 5 mice tested.
1. Mammary   2. Ovary   3. Brain   4. Colon   5. Heart   6. Kidney   7. Lung   8. Spleen   9. Salivary   10. Liver   11. Positive control.
IV. Whole mounts analysis of *hPar1* transgenic mice. Whole-mount hematoxylin staining of *w.t.* and *hPar1*-TG mammary glands at different developmental stages. The epithelial tissue derived from the *hPar1* transgenic mammary glands display increased lateral branching, pervasive intraductal hyperplasia in virgin (B: 13wk) and pregnant mammary glands (D&F, day 8,12 of pregnancy respectively) as compared to age matched *w.t.* mice (A, C&E).
V. Histological analyses of hematoxylin and eosin (H&E). Staining showing the fine histology of the same stages depicted in the whole-mount staining, the *w.t.* and *hPar1*-TG glands. V-13wk, 13 week old virgin; P8d, day 8 of pregnancy; P12d, day 12 of pregnancy.

MMTV-LTR driven *hPar1* overexpressed in the mammary gland were analyzed by whole mounts. Mammary glands of 13 weeks old virgin normal mice (A) and *hPar1*+/- mice (B). Normal pregnant mice of 4 and 12 days (at 13 weeks of age)(C &E) as compared to age matched *hPar1* mice (D &F).

Fig.7: I. *In situ* **hybridization analysis of *hPar1* transgenic mammary glands.** I. *hPar1* expression in 10 weeks old virgin (A, B; antisense and sense respectively), pregnant 13 weeks/4day(C, D; antisense and sense respectively), 8days pregnancy (E, F; antisense and sense respectively), 12 days pregnancy (G, H; antisense and sense respectively). Magnification of X20. **II.** Low power magnification (X5) of hPAR1 in *hPar1*+/- transgenic mice of 8d pregnancy (A, B; antisense and sense respectively). Normal age matched mice (C, D; antisense and sense respectively).
II. RT-PCR analysis of *hPar1* in *w.t.* and age matched hPar1 over-expressing mammary gland mice. *hPar1transgenes* virgin (G-I) and pregnant (J-L). Virgin mice at age of 5, 8 and 10 weeks old. Pregnant mice at 4, 8 and 12 days of pregnancy. Wnts levels were compared to *hPar1* expression in control (A-F) and *hPar1*+/- transgenic mice (G-L). *hPar1* and Wnts expression were compared to a house keeping control gene levels L19.

Fig. 8: I. Increasing Wnts expression in the *hPar1* transgeic mammary glands.
I. RT-PCR analysis of Wnts expression in mammary glands of *w.t.* and *hPar1* transgenic mice. Wnt-4 expression is higher in transgenic virgin (5wk-10wk) mammary glands than the *w.t.* (5wk-10wk), especially in pregnant stage (P4d-P12d). Wnt-7b expressions in *hPar1*-TG mammary glands are also higher than the wild type in virgin and pregnant stage. Wnts levels were compared to *hPar1* expression in *w.t.* and transgenic mice. *hPar1* and Wnts expression were compared to a house keeping control gene levels L19.II.
II. Immunoprecipitation analysis of Wnt-4 expression in the *hPar1*-TG and *w.t.* mice. The transgenic mice show higher expression in the pregnant 8 and 12 days (L&N) than the *w.t.* mice (K&M).

Fig. 9: Mammary glands overexpressing *hPar1* epithelium display increasing epithelial proliferation
Immunohistochemical analysis of PCNA (Proliferating Cell Nuclear Antigen) in the glands of *w.t.* and *hPar1*-TG mice revealed hyperplasia in *hPar1*-TG epithelium. High expression of PCNA is noticed in 5-weeks-old trangenic mammary glands as compared to the *w.t.* mice (A and B, respectively). While mammary glands proliferation in the *w.t.* mice were reduced in 8 and 10 weeks (C and E, respectively), trangenic mice show high expression of PCNA at a similar stage (D and F, respectively). During pregnancy, PCNA expressed highly both in *w.t.* and *hPar1*-TG mice, but the transgenic mice show higher levels (G and H for pregnant 4 days, respectively). The histogram shows that the proliferation indexes after count the nuclear staining of the PCNA. The values represent the averaged fraction of PCNA-positive epithelial cells per total number of epithelial cells of three different mice.
II. Western blot analysis of PCNA expression in the *hPar1*-TG and *w.t.* mice. The transgenic mice (B.8wk, D.10wk, F.13wk, H.P4d, J.P8d) show higher level of PCNA expression compared with the *w.t.* mice both in virgin (A, C, E) and pregnant stage (G, I) respectively.
III. Increased Cyclin D1 induction in *hPar1* transgenic mice mammary glands. Western blot analysis of cyclin D1 expression in *w. t.* and *hPar1*-TG mammary glands. β-actin was used as an control. Fold relative increase are indicated bellow with *w.t.* given an arbitrary value of 1.00.

Fig. 10: I. Immunhistostaining of β-catenin in *w.t.* and *hPar1* overexpressing mammary glands.
Pregnant (10 d) w.t. and age matched *hPar1* mammary glands show the distinct nuclear localization in over-expressing *hPar1* mice as compared to no staining in *w.t,* mice.
II. *hPar1* up-regulated β-Catenin/Lef1 promoter activity. HEK 293 cells were cotransfected with ΔNβ-cat1+, human Lef1, TOPFLASH or FOPFLASH promoter luciferase, β-galactosidase, and indicated human *Par1* constructs. Cells were then treated with or without Thrombin 1u/ml for 10 minutes. The results are presented as normalized luciferase activity. Each experiment was repeated three times at least.

Fig. 11: I. "Tet-Off" inducible hPar1 established in MCf-7 cells. A-D, two clones selected expressing *hPar1* in the absence of Dox (A,C) and shut off in the presence of Dox (B,D). hpar1 is not expressed in mock transfected MCf-7 regardless of the presence of Dox (E).

Fig 12: I.   Characterization of breast MCf-7 clones over-expressing *full length* and truncated *hPar1*.
RT-PCR analysis shows *hPar1* expression in cells overexpressing either truncated (B,C) or *F.L. hPar1* as compared to none in mock transfection (A) and a housekeeping gene GAPDH.

Fig 13: PAR1 Protein detection. I. Western blot analysis.   PAR1 is detected in truncated (B,C) and *F.L. hPar1* (E,F) but not in mock transfected MCf-7 cells (A).
II. Immunofluorescence analysis. Cellular distribution in *F.L.* and truncated *hPar1* but not in mock transfected cells.
III. FACS analysis. The *F.L.* and truncated *hPar1* are well expressed on the cell surface.

Fig. 14: Activation of PAR1 induces pFAK phosphorylation in MCf-7 overexpressing *hPar1* but not in a truncated overexpressing clone. FACs are indicated by the immunifluorescence of pFAK.

Fig. 15: Co-localization of PAR1 and FACs in invasive breast MDA-435 cells:
Cells were cultured on coverslips, fixed with cold methanol (-20°C) and stained for either PAR1 (ATAP mAb) or anti-phosphotyrosine (4G10 mAb) followed by a secondary Ab conjugated with cy-5 and cy-2 respectively and for double staining. Upon activation (left panel) co-localization of PAR1 and FACs is observed

Fig. 16: I. PAR1-c-tail cloned into pGEX2T vector. PAR1 –C-tail GST fusion protein separated on SDS-gel indicating the correct size of the C-tail of PAR1.
II.   Verification of *hPar1* C-tail bound to GST beads. Bound GST hPar1 C-tail is separated on SDS-PAGI indicating the adequate size of the tail as compared with GST alone.
III. Specific proteins bound to *hPar1* GST-C-tail. Distinct proteins of the apparent size of 50 and 180 kD are observed. These proteins are currently being analyzed and sequenced.
Fig. 17: I. GST-C-tail of *hPar1* binds specifically Syk. Syk-3TB over-expressing cells show specific binding of Syk as compared with GST only or cells lacking Syk (3TB).
II. PAR1 C-tail competes for PAR1-Syk complex formation. Competition is seen in the presence of released (60nM) *hPar1*-C-tail (B,C) as compared with none specific peptide used for competition (D) and as compared to bound Syk to the GST-C-tail-*hPar1* (A).

Fig. 18: I. PAR1 is physically associated with Syk. Co-immunoprecipitation of PAR1 and Syk. MCF-7 transfected cells (A; mock, B, C; full length h*Par1* Cl-23 and Cl-26 respectively, D; h*Par1* truncated form Cl-1) were lysed and immunoprecipitated with anti PAR1 mAb. Samples were separated on 10% SDS-PAGE, followed by Westren blotting and detection by Syk mAb, (upper panel). The membrane was stripped and re-incubated with anti PAR1 mAb, (lower panel).
II. Co-IP of PAR1 and Syk ,in different epithelial cells. The different cells (A- Syk-3TB, B- 3TB, C-293, D-MDA-435 and E- MCF-7) over expressing h*Par1* were lysed and immunoprecipitated with anti PAR1 mAb. Samples were separated on 10% SDS-PAGE, followed by Westren blotting and detection by Syk mAb (upper panel). The membrane was stripped and re-incubated with anti PAR1 mAb, (lower panel).

Fig. 19: PAR1 activation induced CO-IP of Src with PAR1. MDA-435 cell lysates either activated with thrombin for different periods of time: 2 min (C), 10 min (B), 20 min (A) or not (D). Lysates were immunoprecipitated with anti-PAR1, separated on 10% SDS gel, followed by Western blotting with anti-Src antibody.

Fig. 20: Activation of PAR1 increases complex formation between c-Src and Syk. Immunoprecipitation analysis of Src increases the levels of Syk –c-Src complex following activation of PAR1, distinctly observed in cells overexpressing Syk (C,D; respectively). No complex is seen in cells lacking Syk (A,B and E,F). This is compared to equal amounts precipitated of c-Src.

Fig. 21: Increased Rac activity induced by PAR1 activation: Rac pull-down assay. By the use of Pak-GST it is demonstrated that elevated levels of active Rac is obtained. Maximal increase at 10 and 15 min following PAR1 activation in *hPar1* overexpressing cells as compared with vector alone and total Rac levels (lower panel).

Fig. 22: cCbl phosphorylation is obtained in Syk-3TB cells following PAR1 activation but not in 3TB activated cells. c-Cbl, an immediate substrate of Syk is activated in Syk-3TB cells following PAR1 activation. This however, is not the case in 3TB cells lacking Syk, showing very little or no Cbl phosphorylation. Levels of phosphorylation are compared with Cbl protein levels.

Fig. 23: I&II. Activation of PAR1 in Syk-3TB cells inhibits the otherwise induced JNK phosphorylation following PAR1 activation. PAR1 activation induces JNK phosphorylation within 15 –30 min activation which declines immediately thereafter. Activation of PAR1 however, in Syk-3TB cells, conveyed an inhibitory effect JNK phosphorylation showing a marked reduction in the phosphorylation levels. The phosphorylated levels are compared with a house keeping gene β-actin

Fig. 24: GADD - 45 is over-expressed inn cells expressing Syk. Northern blot analysis shows the increased expression of GADD45 in Syk infected 3TB cells as compared to none in the invasive 3TB cells and actin levels (lower panel).

Fig. 25: Summary Scheme illustrating "invadopodia" initiated by PAR1 activation. PAR1 activates Src, FAK leading to Rac activation and JNK downstream to initiate invasion. Syk over-expression in cells conveys negative cell cycle regulation via p-cCbl inhibition of JNK-1 and expression of GADD45.

Fig. 26: Inducible *Par1* expression in rat carcinoma cells increases tumor mass and angiogenesis. I. Differential expression of *Par1* in the Dunning rat prostate carcinoma cell variants was observed by RT-PCR using primers specific for PAR1. Primers for L19 were used as a loading control. **II.** Inducible *Par1* expression in a rat prostatic carcinoma cell line - AT2.1. AT2.1 cells were transfected with a plasmid containing the human *Par1* coding sequence under the control of a tet-inducible promoter. Two stably transfected clones, AT2.1/Tet-On/*hPar1* clones 4 and 1, were tested for the inducibility of human *Par1* expression by the tetracycline analog, Dox as evaluated by Northern blot analysis. **III.** AT2.1/Tet-On/*hPar1* clone 4 cells and control transfected (vector only) cells were injected into rats *s.c.* Animals were maintained for 2 weeks with regular drinking water or drinking water supplemented with Dox. After 2 weeks, the tumors were excised and examined. Tumors shown were from animals injected with: A. control transfected cells; B. AT2.1/Tet-On/*hPar1*, clone 4; C. AT2.1/Tet-On/*hPar1* clone 4, fed with Dox for 2 weeks. **VI.** Tumor weight. Data shown are the mean at least 3 independent sets of experiments.

Fig. 27: Induced invasion via Matrigel in clones following the regulated expression of *hPar1* in the presence of Dox. Clones over-expressing hPar1 upon the addition of Dox exhibit over 7 fold invasion via Matrigel

Fig. 28: *Par1* induces angiogenesis *in vivo*. Matrigel plugs containing Cl13 (SB-2 cells stably transfected with *Par1)* or non-transfected SB-2 cells were injected *s.c.* into the peritoneal cavity of BALB/c mice in a bilateral fashion. Mice were divided into four groups dependent on the nature of the injected cells: Group A (n=9) untreated SB-2 cells; Group B (n=8) SB-2 cells treated with TRAP (100μM, 8 hours); Group C (n=11) untreated Cl13 cells; and Group D (n=12) Cl13 cells treated with TRAP (100μM, 8 hours).
I. Matrigel plugs under phase microscopy. 10 days after *in vivo* implantation, Matrigel plugs were removed and examined. Matrigel containing SB-2 cells remained pale (A). The appearance of the Matrigel plugs containing SB-2 cells pretreated with TRAP was not significantly different (B). Matrigel plugs containing Cl13 cells exhibited a reddish color (C), which was more pronounced in Cl13 cells pretreated with TRAP (D). Magnification 5X.

II. Histolgical evaluation of Matrigel plugs. Serial sections were prepared from Matrigel plugs, and processed with Mallory's stain. A. Untreated SB-2 cells B. SB-2 cells pretreated with TRAP C. Untreated Cl13 cells D. Cl13 cells pretreated with TRAP. Magnification X 20.

III. Quantification of capillary vessels in Matrigel plugs. Six separate fields of each Matrigel plug stained with H&E and Mallory's' Stain were examined under phase microscopy and capillary vessels were counted. Data shown are representative of at least 3 independent Matrigel plug sets of experiments.

Fig. 29: Withdrawal of *hPar1* expression upon omission of Dox in rat tumor progression. While no difference is seen in the tumor mass by 2 weeks *hPar1* expression and 4 weeks *hPar1* expression. However, by the shut - off *hPar1* expression for 2 weeks, impaired blood vessels in the tumors lead to massive cell death. A few viable cells are seen around a remaining blood vessel.

Fig. 30: Induced blood vessels in mammary glands over-expressing *hPar1*. vWF staining for the detection of blood vessels show increased levels of blood vessels as compared to *w.t.* mammary glands.

Fig. 31: Over-expression of *hPar1* results with loss of E-cadherin. I. *hPar1* over-expressed CaCO2 cells results with induced migration as compared to parental cells.
II. CaCO2 cells express E-cadherin levels. Over-expression of *hPar1* leads to loss of E-Cadherin.

Fig. 32: I. Nearly normal acini formation in 3D cultures, versus highly invasive cell intrusion. Highly organized cell structure acini of MCF10A cells in 3D Matrigel culture. MCF10A cells over-expressing high PAR1 levels and high metastatic properties show an invasive phenotype in 3D cultures. These cells (3TB cells).

II. Morphogenesis of MCF10A acini formed in 3D matrigel cultures. MCF10A cells form growth arrested polarized acinar structures in Matrigel. Morphology of acinar structures formed by MCF10A cells plated in Matrigel for 12 days. Phase – image of acini structure at high magnification is shown. Note the cell-cell contacts and the "hollow-like" inner circle of the acini. Acini were labeled with DAPI, showing the labeled nuclei within the acini. Cell-cell contact within the spheroid is shown by immunofluorescence staining of E-cadherin and β-catenin.

Team Involved in PARs and Breast Carcinoma Invasion and Metastasis

====================================

The team includes Ph.D. students, an experienced laboratory research assistant as well as professional personnel (among of which are:Oncologist, Gynecologist and Pathologist) who can share responsibilities with the PIs.

* **Bar-Shavit, Rachel Ph.D. PI / Team Leader**

- **Uziely, Beatrice, M.D. /Oncologist**

- **Grisaru-Granovsky, Sorina, M.D. /Gynecologist,**
  Project: Physiological invasion processes of placenta, and malignancy of Ovary varcinoma: Aspects of *hParl* involvement

- **Galina Pizov, M.D. /Pathologist**

  ================

  - *Sharona Cohen Even-Ram* Ph.D. student (currently a PostDoc, K. Yammada, NIH)

  - *Maoz Miriam, M.Sc.* / Research Assistant. Involved in various aspects of the project

  - **Virginie Leib, M.Sc.** / Research Assistant. Project: *hParl* released peptide in body fluids.

  - *YongJun Yin Ph.D. student* - Project: PAR1 transgenic mice, Angiogenesis

  - *Vered Katz, M.Sc* – Project: Three dimensional (3D) spheroids in *hParl* over-expression

  - *Salah, Zaidoun Ph.D. student* - project: PAR1 "TET – On" inducible system, solid tumors and hormone regulation of PAR1

  - *Cohen Irit, Ph.D. student* – Characterization of PAR1 in breast clones : truncated PAR1, full length PAR1 and antisense PAR1

Key research accomplishment

Protease-Activated Receptors (PARs) are G-coupled seven transmembrane domain proteins consisting of 4 family members and activated via proteolytic cleavage. All genes belonging to these receptor - family encode their own ligands. In addition to their traditional role in hemostasis, thrombosis and vascular biology, at least PAR1, thrombin receptor; emerges with surprisingly novel functions in tumor biology. We have previously demonstrated an active participation of PAR1 in breast carcinoma progression and metastasis as also during the physiological process of trophoblast implantation to the uterus decidua. *hPar1* thus, behaves as one of a series of genes that are part of an invasive program, exclusively expressed along the time limited physiological invasion process of the placenta, and completely shuts - off thereafter. In-contrast, the involvement of *hPar1* in tumor progression is portrayed by the striking and continuous over-expression of the gene in malignant epithelia as compared to very little or none in normal counterparts.

Originally we have proposed the following specific aims:
Task 1 a&b: To determine the involvement of PAR family members (PAR1 - PAR4) in breast carcinoma
- Determine the expression profile of PAR family members (1-4) in breast carcinoma metastasis (5 months)

- *In situ* hybridization analysis in paraffin sections (6-15 months)

- PAR (1-4) expression during normal physiological invasion of the placenta (7-15 month)

- To establish extravillous trophoblast (EVT) cultures for the modulation of the invasive phenotype by PAR family (14-18 month)
- Computer analysis and evaluation of the level of *In situ* hybridization analysis (16-18 month)

Task 2a: To modulate the malignant cell metastatic behavior by PAR1
- Transfections /selections of the full length PAR1 in non invasive MCF-7 and ZR-75 breast carcinoma cells.

- Tetracyclin (TeT) "on-off" regulation in tissue cultures (19-24 month)

- Animal models for metastasis using the Tet "on-off" PAR1 system. Analysis of the fate of metastatic foci in the presence of PAR1 gene /following activation (25 - 30 month)

- The fate of metastatic foci (i.e for possible regression) upon turning off PAR1 expression (27-36 month)

Task 2b: To study the molecular mechanism underlying PAR1 invassiveness
- Characterization of PAR1 transfected clones: The level of PAR1 mRNA and proteins (6-12 month)

- Modulation of the invasive phenotype by PAR1 (in PAR1 transfected clones)(13-18 month)

- Integrin profile and function in the overexpressing PAR1 clones (19-25 month)

. . . To elucidate focal adhesion plaque formation and integrin signaling in PAR1 overexpressing clones (26-36 month)

⌐ - Chimeras of PAR1 transfection of either the extracellular deficient portion or the cytoplasmic portion, and the assembly of focal adhesion plaque formation (24-36 month)

Elucidation in part of the molecular mechanism induced by *hPar1:* Cooperation with αvβ5 integrin (*Appendix 1, J Biol Chem* 276: 10952-10962, 2001)

We have elucidated in part, the molecular mechanism of PAR1 induced tumor invasion and metastasis. Activation of PAR1 leads to integrin-mediated adhesion to various extracellular matrix substrata. This takes place, via "inside-out" signaling events and the formation of focal adhesion contact sites. PAR1 promotes invasion properties by the induction of cytoskeletal reorganization of F-actin, increased phosphorylation of FAK and paxillin and the induced formation of focal contact complexes. Following activation of PAR1 the selective recruitment of αvβ5 integrin to focal contact sites - takes place. This recruitment does not occur in the presence of a truncated form of PAR1, devoid of the entire cytoplasmic region. Therefore, signaling transmitted by the cytoplasmic tail of *hPar1* is essential to selectively activate αvβ5 to foster cell adhesion and invasion .

The role of *hPar1* in tumor angiogenesis (*Appendix 3, FASEB J*, 17: 163-174, 2003)

The recruitment of new blood vessels is a prerequisite for tumor growth and metastasis. While it has been shown that *Par1* plays a critical function in vascular embryonic development, rescuing *Par1*-/- mice from bleeding to death after re-expression directly in endothelial cells, its role however, in tumor angiogenesis is poorly explored. We have demonstrated that *Par1* gene expression plays a central function in the induction of blood vessel recruitment in animal models *in vivo,* as determined by the "Tet-on" *Par1* inducible prostate system and by the Matrigel micropocket assay. *Par1* induced angiogenesis is mediated via the increased expression of vascular endothelial growth factor splice forms; VEGF$_{121}$, VEGF$_{145}$, VEGF$_{165}$ and VEGF$_{189}$ or but not VEGF $_{206}$.

Generation of monoclonal antibodies for the detection of the released PAR1 N-terminal peptides in body fluids.

One consequence of the mechanism by which PAR1 is activated, is the release of an N-terminal peptide from the receptor - cell surface. Therefore, the mirror image reflection in body fluids, of over-expressed and activated PAR1 (as it happens to be the case during breast carcinoma progression), is the released PAR1 N-terminal peptide. We have developed now means to detect PAR1 released fragment/s.

The prospect of high *hPar1* released peptide present in body fluids of advanced cancer patients (planned to be analyzed on patients of the Hadassah-University Hospital, the Department of Oncology), as compared to low levels in healthy individuals - is intriguing. This is intended to be carried out by immunodetection of body fluids of breast cancer patients by the utilization of a series of monoclonal antibodies raised against the cleaved peptide. The monoclonal antibodies are developed against several discrete and overlapping epitope regions along the released 41 amino acid fragment.

Over-expression of *hPar1* in mice mammary gland : Morphogenesis, hyperplasia and stabilized β-catenin . In order to gain insight to the role of *hPar1* gene in breast carcinoma progression and mammary gland morphogenesis, we have established a line of mice over-expressing MMTV LTR - driven *hPar-1* targeted to the mammary glands. These glands exhibited grossly hyperplastic features as compared with the non transgenic littermates. The growing branch ends showed enhanced complexity of alveolar side branching as compared with normal virgin glands, especially highlighted in the pregnant *hPar 1* over-expressing mice. This phenotype is precociously reminiscent of the effect of several oncogene over-expression in the mouse breast. The utilization of transgenic mice over-expressing oncoproteins in the mammary gland provided classical milestones in highlighting genetic pathways engaged in breast cancer. We are guided by the notion that understanding genetic pathways, is a prerequisite for the development of molecular and pharmacological therapeutics to treat and prevent cancer. The opportunity to identify a novel path, that recapitulates a fundamental process both in embryogenesis and tumor progression, induced by *hPar1* gene is best explored in a transgenic mouse model. Indeed, many properties seen in the embryo are mimicked, by the mammary gland during ductal and alveolar development, such as pattern formation of the ductal tree and inductive interactions that take place between the epithelium and mesenchyme. While studies in tissue culture cells, permit the dissection of events in a single cell, analysis in mice integrates the entire complexity of an organ recapitulating the dynamics and physiological status of the animal and enabling to explore a particular gene in the context of intact organs. In our *hPar1* over-expressing mammary gland mice, we have found a striking stabilization and accumulation of β-catenin. This high /stabilized pools of β-catenin enters the nuclei where it is now abundantly localized. The novel oncogenic-like pathway of *hPar1* inducing *Wnt* signaling and β-catenin stabilization; an arising theme in tumor development – is now being proposed. Our approach involving the combined analyses of tissue specific

hParl transgenes, biopsy specimens and established cell lines may help elucidate the involvement of *hParl* in tumor formation, metastasis and angiogenesis. This will lead nonetheless, to the device of therapeutic medicaments, a task which is beyond the scope of the present report.

Outlined list of key research accomplishments:

- Elucidation in part of the molecular mechanism induced by *hParl*: Cooperation with $\alpha v \beta 5$ integrin (*Appendix 1, J Biol Chem* 276: 10952-10962, 2001)

- The pattern of expression of *Protease Activated Receptors* (PARs) during throphoblast development (*Appendix 2, J Pathol,* 200: 47-52, 2003)

- The role of *hParl* in tumor angiogenesis (*Appendix 3, FASEB J,* 17: 163-174, 2003)

- Human *Protease-Activated Receptor 1* expression in malignant epithelia: a role in invasiveness (*Appendix 4, Arterioscler Thromb Vasc Biol. Perspective* Jun 1;23(6):940-9444, 2003)

- Elucidation of "invadopodia" -signaling pathway in *hParl* over-expressing breast clones. (Manuscript *in preparation*)

- Interrelation between Syk and *hParl* in breast carcinoma: Illustration of a negative cell-cycle regulation (Manuscript *in preparation*).

- Interrelation between *hParl* and E-cadherin: A role for *hParl* signaling ?

- Over-expression of *hParl* in mice mammary gland : Morphogenesis, hyperplasia and stabilized β-catenin (Manuscript submitted)

Reportable outcome:
Appendix 1: Molecular mechanism of *hParl* induced tumor invasion and metastasis : cooperation with the $\alpha v \beta 5$ integrin *J Biol Chem* 276: 10952-10962, 2001

Appendix 2: The pattern of expression of protease-activated receptors (PARs) during early trophoblast development. *J Pathol* 2003 May;200(1):47-52.

Appendix 3: Oncogenic transformation induces tumor angiogenesis: a role for PAR1 activation. *FASEB J.* 2003 Feb;17(2):163-174.

Appendix 4: Human protease-activated receptor 1 expression in malignant epithelia: a role in invasiveness. *Arterioscler Thromb Vasc Biol. Review.* 2003 Jun 1;23(6):940-944.

Concluding Remarks

Our original tasks were centered around the elucidation of the involvement of PAR family members (PAR1-4) in breast carcinoma progression. The approach taken was initially based on correlation studies

(performed by *in situ* hybridization, RT-PCR and Northern blots) carried out both in malignant carcinoma biopsy specimens and normal tissue samples of first trimester placenta. This is based on the notion that genes that are part of an invasive program will be exclusively expressed along the time limited physiological invasion process (during implantation) and completely shuts - off thereafter. Next we aimed at elucidating in part, the molecular mechanisms of *hPar1* induced breast carcinoma invasion and metastasis. For this we were engaged at preparing molecular probes of *hPar1* (e.g., full length, truncated version of *hPar1* and *hPar1* antisense) as also creating tetracycline inducible clones of the gene. We have analyzed these forms of *hPar1* in traditional cell lines stably expressing these constructs as also in three dimensional cultures recapitulating at large the glandular structure of breast acini *in vitro*. This enabled us to illustrate an "invadopodia" pathway induced by *hPar1*. Essentially this pathway is initiated by the recruitment of integrin signaling machinery; activation of FAK and paxillin, followed by Rac activation (as determined by a Rac pull - down assay) and JNK1 downstream. Focal Adhesion Complex (FAC) formation is observed following the activation of PAR1, entirely absent when a truncated version of the gene is utilized. We were able to modulate the invasive behavior of the cells by either over-expressing *hPar1* in non metastatic cells (JBC, Appentix 1) or confer antisense expression in a highly metastatic cells. In parallel we have demonstrated the role of *hPar1* in tumor angiogenesis. By *in vivo* injection of either Matrigel plugs containing *Par1*-expressing cells or in a tetracycline-inducible *Par1* expression cells, we have shown that *Par1* significantly enhanced both angiogenesis and tumor growth. Activation of PAR1 markedly augments the expression of VEGF mRNAs and of functional VEGFs as determined by *in vitro* assays for endothelial tube alignment and bovine aortic endothelial cell proliferation. In-fact, several VEGF splice forms VEGF 121, 145, 165, 189 but VEGF 206 are induced in cells expressing *Par1*. Withdrawal studies of *hPar1* gene (shut-off by omitting Dox) in animal models, preliminary points to effect primarily blood vessels recruited to the tumor mass.

With regard to animal models we have been engaged at establishing an original line of mice over-expressing MMTV LTR - driven *hPar-1* targeted to the mammary glands. These glands exhibited grossly hyperplastic features as compared with the non transgenic littermates. The phenotype obtained is precociously reminiscent of the effect of several oncogene over-expression in the mouse breast. Our studies strengthen and support the notion that *hPar1* may act as a potent oncogene to foster tumor progression and metastasis.

While originally we have proposed to study the expression pattern of the four PAR family members (showing the involvement of PAR1 and –3 in breast carcinoma malignancy and physiological trophoblast invasion), we have turned our attention to focus mostly on the role of *hPar1*. However, were committed during the funding period to prepare *hPar1* molecular probes, inducible system for the regulated expression of *hPar1* and transgenic mouse models. the role of *hPar1* in breast carcinoma progression and angiogenesis.

We have demonstrated the relevance of *hPar1* initiated signaling in breast tumor progression and addressed the role of tumor suppressor gene - Syk during this process. Our transgenic mice over-expressed in the mammary gland revealed nonetheless a novel mechanism of *Wnt* activation induced by *hPar1*. This defines now new avenues in the role of the gene during breast cancer progression (beyond the scope of the present funding period).

***Innovation* "So what":** The main outcome of the present final report stems from our prior observation that thrombin receptor, PAR1, plays a central role in breast carcinoma invasion and metastasis (6). We have established now the original MMTV LTR - driven *hPar-1* mice, targeted to the mammary glands. Transgenic mouse model is best explored for the possible identification of a novel pathway, that integrates fundamental processes both in embryogenesis and tumor progression. The *hPar1* over-expressing mammary glands exhibited grossly hyperplastic features as compared with the non transgenic littermates, precociously reminiscent of the effect of several oncogene expression in the mouse breast. While studies in tissue culture cells, permit the dissection of events in a single cell, analysis in mice integrates the entire complexity of an organ, recapitulating the dynamics of hormonal and physiological status of the animal and enabling to investigate a particular gene in the context of intact organs. Hence we propose now a novel pathway of *hPar1* induced breast hyperplasia and tumorigenicity via the striking stabilization and elevated accumulation of β-catenin. This high /stabilized pools of β-catenin in the *hPar1* mammary glands, enters the nuclei where it is now abundantly localized capable of potently induce transcription of down stream genes. Needless to emphasize, that we are guided by the notion that understanding genetic pathways, is a prerequisite for the development of molecular and pharmacological therapeutics to treat and prevent cancer. This will lead nonetheless, to the device of potentially powerful carcinoma therapeutic medicaments based on *hPar1* gene. We have also elucidated the role of *hPar1* in tumor angiogenesis and addressed the relevance of *hPar1* initiated signaling in tumor invasion. Our approach involving the combined analyses of tissue specific PAR1 transgenes, biopsy specimens and established cell lines is expected to elucidate the involvement of PARs in tumor metastasis and angiogenesis.

References

1. Vu, T-K., Hung, H.D.T., Wheaton V.I., & Coughlin, S.R. 1991. Molecular cloning of a functional thrombin receptor reveals a novel proteolytic mechanism of receptor activation. *Cell* 64:1057-1068.

2. Rasmussen UB, Vouret-Craviari V, Jallat S, Schlesinger Y, Pages G, Pavirani A, Lecocq JP, Pouyssegur J, Van Obberghen-Schilling E. 1991. cDNA cloning and expression of a hamster α-thrombin receptor coupled to Ca^{+2} mobilization. *FEBS Lett* 288: 123-128.

3. Gerszten RE, Chen J, Ishii M, Ishii K, Wang L, Nanevicz T, Turck CW, Vu TK, Coughlin SR. 1994. Specificity of the thrombin receptor for agonist peptide is defined by its extracellular surface. *Nature (London)* 368: 648-649.

4.   Kahn ML, Zheng YW, Huang W, Bigornia V, Zeng D, Moff S, Farese RV Jr, Tam C, Coughlin SR.1998. A dual thrombin receptor system for platelet activation *Nature*. 394: 690-694.

5.   Nakanishi-Matsui M, Zheng YW, Sulciner DJ, Weiss EJ, Ludeman MJ, Coughlin SR 2000. PAR3 is a cofactor for PAR4 activation by thrombin. *Nature*. 404: 609-613.

6.   Even-Ram, S., Uziely, B., Cohen, P.,Ginzburg, Y., Reich, R. Vlodavsky, I. and Bar-Shavit, R. 1998. Thrombin receptor overexpression in physiological and malignant invasion process. *Nature Medicine* 4: 909-914.

7.   Martin, CB., Mahon, GM., Klinger, MB., Kay, RJ, Symons, M., Der, CJ., and Whitehead IP., 2001. *Oncogene*, 20: 1953-1963.

8.   Cohen Even-Ram, S., Maoz, M., Pokroy, E., Reich , R. Katz, B-Z., Gutwein, P., Altevogt, P., and Bar-Shavit, R. 2001. Tumor cell invasion is promoted by activation of protease activated Receptor-1 in cooperation with $\alpha v \beta 5$ integrin. *J. Biol. Chem* 276: 10952-10962.

9.   Even-Ram SC, Grisaru-Granovsky S, Pruss D, Maoz M, Salah Z, Yong-Jun Y, Bar-Shavit R. 2003. The pattern of expression of protease-activated receptors (PARs) during early trophoblast development. *J Pathol* May;200(1):47-52.

10.   Yin, Y-J., Salah, Z., Maoz, M., Cohen Even Ram, S., Ochayon,, S., Neufeld, G., Katzav, S., and Bar- Shavit, R. 2003. Oncogenic transformation induces tumor angiogenesis: A role for PAR1 activation. *FASEB J* Feb;17(2):163-74.

11.   Bissell, M.J., and Radisky, D. 2001. Putting tumors in context. *Nat. Rev. Cancer* 1, 46-54.

12.   Muthuswamy, S.K., Li, D., Lelievre, S., Bissel, M.J., and Brugge, J.S. 2001. ErbB2, but not ErbB1, reinitiates proliferation and induces luminal repopulation in epithelial acini. *Nat. Cell Biol.* 3:531-537.

13.   Debnath J, Mills KR, Collins NL, Reginato MJ, Muthuswamy SK, Brugge JS.2002. The role of apoptosis in creating and maintaining luminal space within normal and oncogene-expressing mammary acini. *Cell*. Oct 4;111(1):29-40.

14.   O'Brien, L.E., Zegers,M.M., and Mostov, K.E. 2002. Opinion: building epithelial architecture: Insight from three-dimensional culture models. *Nat. Rev. Mol. Cell Biol.* 3: 531-537.

15.   Li F, Baykal D, Horaist C, Yan CN, Carr BN, Rao GN, Runge MS. 1996. Cloning and identification of regulatory sequences of the human thrombin. *J Biol Chem.* 1 Oct 18;271(42):26320-8.

16.   Schmidt VA, Vitale E, Bahou WF. 1996 . Genomic cloning and characterization of the human thrombin receptor gene. Structural similarity to the proteinase activated receptor-2 gene. *J Biol Chem.* Apr 19;271(16):9307-12.

17.   Bauer R, Imhof A, Pscherer A, Kopp H, Moser M, Seegers S, Kerscher M, Tainsky MA, Hofstaedter F, Buettner R. 1994. The genomic structure of the human AP-2 transcription factor. *Nucleic Acids Res.* Apr 25;22(8):1413-20.

18.   Williams T, Admon A, Luscher B, Tjian R. 1988. Cloning and expression of AP-2, a cell-type-specific transcription factor that activates inducible enhancer elements. *Genes Dev.* Dec;2(12A):1557-69.

19.   Williams T, Tjian R. 1991. Analysis of the DNA-binding and activation properties of the human transcription factor AP-2. *Genes Dev.* Apr;5(4):670-82.

29

20. Gee JM, Robertson JF, Ellis IO, Nicholson RI, Hurst HC. 1999. Immunohistochemical analysis reveals a tumour suppressor-like role for the transcription factor AP-2 in invasive breast cancer. *J Pathol.* Dec;189(4):514-520.

21. Tellez C, Bar-Eli M. 2003. Role and regulation of the thrombin receptor (PAR-1) in human melanoma. *Oncogene.* May 19;22(20):3130-7.

22. Griffin, C.T., Snirivasan, Y., Zheng, Y-W., Haung, W., and Coughlin, S.R. 2001. A role for thrombin receptor signaling in endothelial cells during embryonic development. *Science* 293, 1666-1670.

23. Carmeliet, P. 2001. Clotting factors build blood vessels. *Science* 293: 1602-1604.

24. Wodarz A, Nusse R. 1998. Mechanisms of Wnt signaling in development. *Annu Rev Cell Dev Biol.* 14:59-88.

25. Peifer M, Polakis P. 2000. Wnt signaling in oncogenesis and embryogenesis--a look outside the nucleus. *Science.* Mar 3;287(5458):1606-1609.

26. Bhanot P, Brink M, Samos CH, Hsieh JC, Wang Y, Macke JP, Andrew D, Nathans J, Nusse R. 1996. *Nature* Jul 18;382(6588):225-230.

27. Brisken C, Heineman A, Chavarria T, Elenbaas B, Tan J, Dey SK, McMahon JA, McMahon AP, Weinberg RA. 2000. Essential function of Wnt-4 in mammary gland development downstream of progesterone signaling. *Genes & Dev.* 14: 650-654.

28. Siegel PM, Hardy WR, Muller WJ. 2000. Mammary gland neoplasia: insights from transgenic mouse models. *BioEssay* 22: 554-563,

29. Brisken C, Park S, Vass T, Lydon J, O'Malley B, Weinberg, RA. 1998. A paracrine role for the epithelial progesterone receptor in mammary gland development. *Proc. .Natl. Acad. Sci. USA* 95: 5076-5081.

30. Roelink, H Wagenaar,E Silva, SLD and Nusse, R. 1990.Wnt-3, A Gene Activated by Proviral Insertion in Mouse Mammary Tumors, is Homologous to int-1/Wnt-1 and is Normally Expressed in Mouse Embryos and Adult Brain. *Proc. .Natl. Acad. Sci. USA.* 87: 4519-4523.

31. Nusse R. WNT targets. 1999. Repression and activation. *Trends Genet.* Jan;15(1):1-3.

32. Hinoi T, Yamamoto H, Kishida M, Takada S, Kishida S, Kikuchi A. 2000. Complex formation of adenomatous polyposis coli gene product and axin facilitate glycogen synthase kinase-3 beta-dependent phosphorylation of beta-catenin and down-regulates beta-catenin. *J Biol Chem.* Nov 3;275(44):34399-406.

33. Hart MJ, de los Santos R, Albert IN, Rubinfeld B, Polakis P. 1998. Downregulation of beta-catenin by human Axin and its association with the APC tumor suppressor, beta-catenin and GSK3 beta. *Curr Biol.* May 7;8(10):573-81.

34. Amit S, Hatzubai A, Birman Y, Andersen JS, Ben-Shushan E, Mann M, Ben-Neriah Y, Alkalay I. 2002. Axin-mediated CKI phosphorylation of beta-catenin at Ser 45: a molecular switch for the Wnt pathway. *Genes Dev.* May 1;16(9):1066-1076.

35.   Liu C, Li Y, Semenov M, Han C, Baeg GH, Tan Y, Zhang Z, Lin X, He X. 2002. Control of beta-catenin phosphorylation/degradation by a dual-kinase mechanism. *Cell.* Mar 22;108(6):837-847.

36.   Schwarz-Romond T, Asbrand C, Bakkers J, Kuhl M, Schaeffer HJ, Huelsken J, Behrens J, Hammerschmidt, M, Birchmeier W. 2002. The ankyrin repeat protein Diversin recruits Casein kinase Iepsilon to the beta-catenin degradation complex and acts in both canonical Wnt and Wnt/JNK signaling. *Genes Dev.* Aug 15;16(16):2073-2084.

37.   Wong CM, Fan ST, Ng IO. 2001. beta-Catenin mutation and overexpression in hepatocellular carcinoma: clinicopathologic and prognostic significance. *Cancer.* Jul 1;92(1):136-45.

38.   Polakis P. 2000. Wnt signaling and cancer. *Genes Dev.* Aug 1;14(15):1837-1851.

39.   Roelink H, Wagenaar E, Lopes da Silva S, Nusse R. 1990. Wnt-3, a gene activated by proviral insertion in mouse mammary tumors, is homologous to int-1/Wnt-1 and is normally expressed in mouse embryos and adult brain. *Proc Natl Acad Sci U S A.* Jun;87(12):4519-23.

40.   Taniguchi K, Roberts LR, Aderca IN, Dong X, Qian C, Murphy LM, Nagorney DM, Burgart LJ, Roche PC, Smith DI, Ross JA, Liu W. 2002. Mutational spectrum of beta-catenin, AXIN1, and AXIN2 in hepatocellular carcinomas and hepatoblastomas. *Oncogene.* Jul 18;21(31):4863-71.

41.   Morin PJ, Sparks AB, Korinek V, Barker N, Clevers H, Vogelstein B, Kinzler KW. 1997. Activation of beta-catenin-Tcf signaling in colon cancer by mutations in beta-catenin or APC. *Science.* Mar 21;275(5307):1787-1890.

42.   Polakis P.1999. The oncogenic activation of beta-catenin. *Curr Opin Genet Dev.* Feb;9(1):15-21.

43.   Hood JD, Cheresh DA. 2002. Role of integrins in cell invasion and migration. *Nat Rev Cancer.* Feb;2(2):91-100.

44.   McCawley LJ, Matrisian LM. 2000. Matrix metalloproteinases: multifunctional contributors to tumor progression. *Mol Med Today.* Apr;6(4):149-156.

45.   Ozanne BW, McGarry L, Spence HJ, Johnston I, Winnie J, Meagher L, Stapleton G. 2000. Transcriptional regulation of cell invasion: AP-1 regulation of a multigenic invasion programme. *Eur J Cancer.* Aug;36(13 Spec No):1640-1648.

46.   Hsia DA, Mitra SK, Hauck CR, Streblow DN, Nelson JA, Ilic D, Huang S, Li E, Nemerow GR, Leng J, Spencer KS, Cheresh DA, Schlaepfer DD. Differential regulation of cell motility and invasion by FAK. *J Cell Biol.* Mar 3;160(5):753-767.

47.   Chu DH, Morita CT, Weiss A. 1998. The Syk family of protein tyrosine kinases in T-cell activation and development. *Immunol Rev* 165:167-80.

48.   Woodside DG, Obergfell A, Leng L, Wilsbacher JL, Miranti CK, Brugge JS, Shattil SJ, Ginsberg MH. 2001. Activation of Syk protein tyrosine kinase through interaction with integrin beta cytoplasmic domains. *Curr Biol* 13;11(22):1799-804.

49.   Hauck CR, Sieg DJ, Hsia DA, Loftus JC, Gaarde WA, Monia BP, Schlaepfer DD. 2001. Inhibition of focal adhesion kinase expression or activity disrupts epidermal growth factor-stimulated signaling promoting the migration of invasive human carcinoma cells. *Cancer Res.* Oct 1;61(19):7079-7090.

50.   Panchamoorthy G, Fukazawa T, Miyake S, Soltoff S, Reedquist K, Druker B, Shoelson S, Cantley L, Band. H. 1996. p120cbl is a major substrate of tyrosine phosphorylation upon B cell antigen

receptor stimulation and interacts in vivo with Fyn and Syk tyrosine kinases, Grb2 and Shc adaptors, and the p85 subunit of phosphatidylinositol 3-kinase. *J Biol Chem.* Feb 9;271(6):3187-194.

51. Husson H, Mograbi B, Schmid-Antomarchi H, Fischer S, Rossi B. 1997. CSF-1 stimulation induces the formation of a multiprotein complex including CSF-1 receptor, c-Cbl, PI 3-kinase, Crk-II and Grb2. *Oncogene.* May 15;14(19):2331-238.

52. Carrier F, Smith ML, Bae I, Kilpatrick KE, Lansing TJ, Chen CY, Engelstein M, Friend SH, Henner WD, Gilmer TM, et al. 1994. Characterization of human Gadd45, a p53-regulated protein. *J Biol Chem.* Dec 23;269(51):32672-7.

53. Smith ML, Chen IT, Zhan Q, Bae I, Chen CY, Gilmer TM, Kastan MB, O'Connor PM, Fornace AJ Jr.1994. Interaction of the p53-regulated protein Gadd45 with proliferating cell nuclear antigen. *Science.* Nov 25;266(5189):1376-1380.

54. Fornace AJ Jr, Nebert DW, Hollander MC, Luethy JD, Papathanasiou M, Fargnoli J, Holbrook NJ. 1989. Mammalian genes coordinately regulated by growth arrest signals and DNA-damaging agents. *Mol Cell Biol.* Oct;9(10):4196-4220.

55. O'Reilly MA, Staversky RJ, Watkins RH, Maniscalco WM, Keng PC. 2000. p53-independent induction of GADD45 and GADD153 in mouse lungs exposed to hyperoxia. *Am J Physiol Lung Cell Mol Physiol.* Mar;278(3):L552-L559.

56. Huang YQ, Li JJ, Hu L, Lee M, Karpatkin S. 2001. Thrombin induces increased expression and secretion of VEGF from human FS4 fibroblasts, DU145 prostate cells and CHRF megakaryocytes. Thromb Haemost. Oct;86(4):1094-8.

57. Jin E, Fujiwara M, Pan X, Ghazizadeh M, Arai S, Ohaki Y, Kajiwara K, Takemura T, Kawanami O. 2003. Protease-activated receptor (PAR)-1 and PAR-2 participate in the cell growth of alveolar capillary endothelium in primary lung adenocarcinomas. Cancer. Feb 1;97(3):703-713.

58. Poser I, Dominguez D, de Herreros AG, Varnai A, Buettner R, Bosserhoff AK. 2001. Loss of E-cadherin expression in melanoma cells involves up-regulation of the transcriptional repressor Snail. *J Biol Chem.* Jul 6;276(27):24661-6. Epub 2001 Apr 25.

59. Chan AO, Lam SK, Wong BC, Wong WM, Yuen MF, Yeung YH, Hui WM, Rashid A, Kwong YL. 2003. Promoter methylation of E-cadherin gene in gastric mucosa associated with Helicobact pylori infection and in gastric cancer.pylori infection and in gastric cancer. *Gut.* Apr;52(4):502-506.

60. Wong AS, Gumbiner BM. Adhesion-independent mechanism for suppression of tumor cell invasion by E-cadherin. *J Cell Biol.* 161: 1191-1203.

PI: *Bar-Shavit, R.* PhD

Scheme 1:

PAR-Protease Activated Receptor family

PAR-1: Thrombin receptor I
hPAR-1 Internal Ligand:
AA 37-61 TLDPR SFLLRNP NDK YEPF

PAR-2: An orphan receptor
hPAR-2 Internal Ligand:
AA 32-56 SSKGR SLIGKV DGTSHVTGKG

PAR-3: Thrombin receptor
hPAR-3 Internal Ligand:
AA 34-57 TLPIK TFRGAPP N SFEEFPFSALE

PAR-4: Thrombin receptor
hPAR-4 Internal Ligand:
AA 28-52 LPAPR GYPGQV CANDSDT

Internal ligand

outside

1 2 3 4 5 6 7

inside

Scheme 2:

Normal epithelium
Basement membrane

Dysplastic Carcinoma

Carcinoma in situ

Loss of E-cadherin
Invasive carcinoma

ECM RGD

Matrix degradation

PAR1 cross-talk with α₅β₅ integrin during invasion

Fig2:

Fig1:
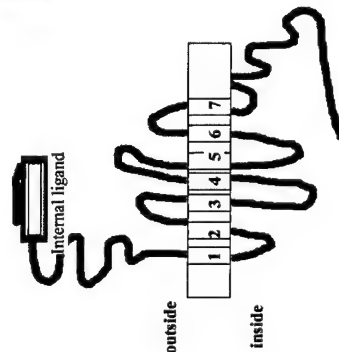
I. *In situ* hybridization analysis of PAR1 in breast tissue biopsy specimens

IDC   DCIS

Normal

Normal ———— Dysplasia ———— Hyperplasia
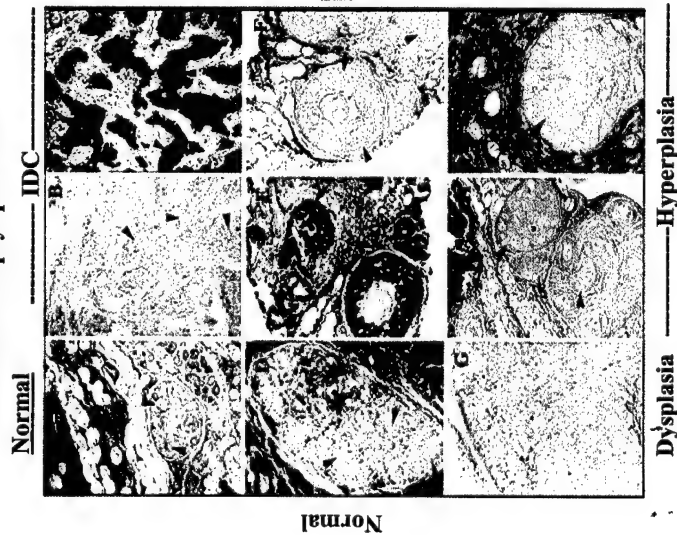
II. PAR3 Expression in Normal and Cancerous Breast

IDC   DCIS   Hyperplasia   Normal
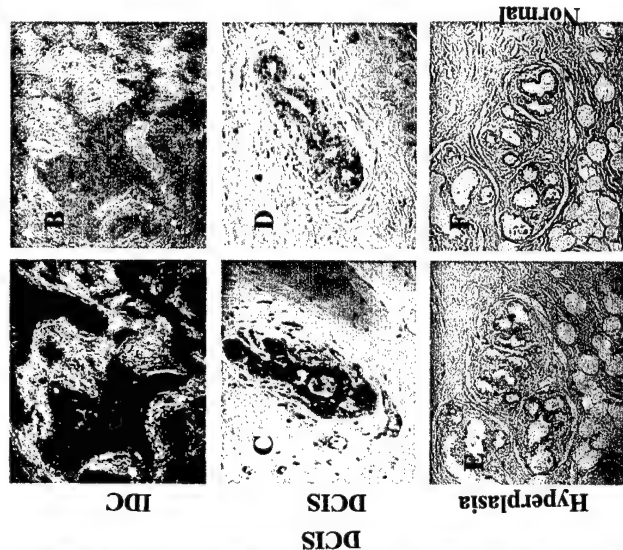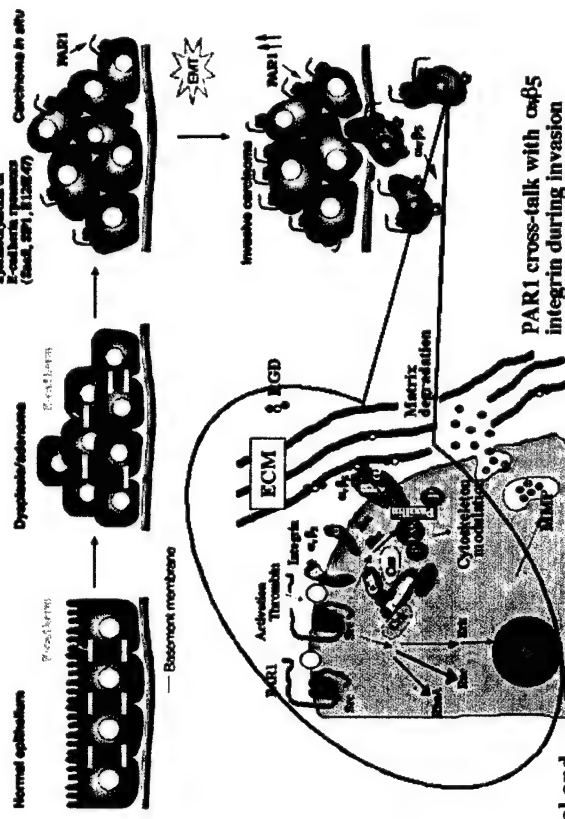
I. *Differential expression of PAR1 in Various Metastatic Cell Lines*

A B C D E F

Par1

β-actin

II.

A B C

PAR1

III. *PAR1 Antisense inhibits highly metastatic cell invasion* **IV.**
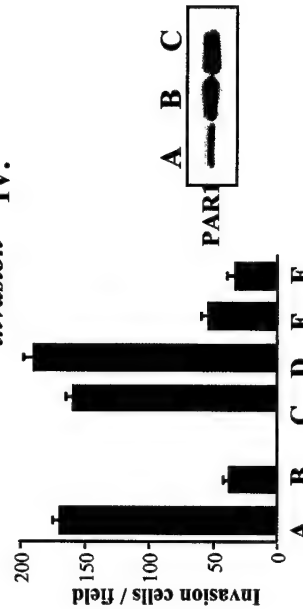
Invasion cells / field

200 150 100 50 0

A B C D E F

A B C

PAR1

Fig3: Tissue expression and distribution of *Par1* in the first-trimester placenta

I. In situ

II a. RT-PCR

II b. Northern

Fig4: Tissue expression and distribution of *Par1* in the first-trimester placenta

PI: *Bar-Shavit, R.* PhD

I. In situ

II. RT-PCR

III. Western blot
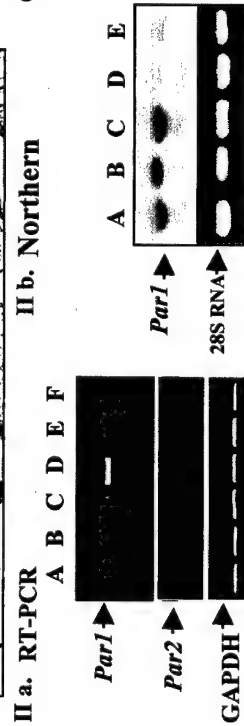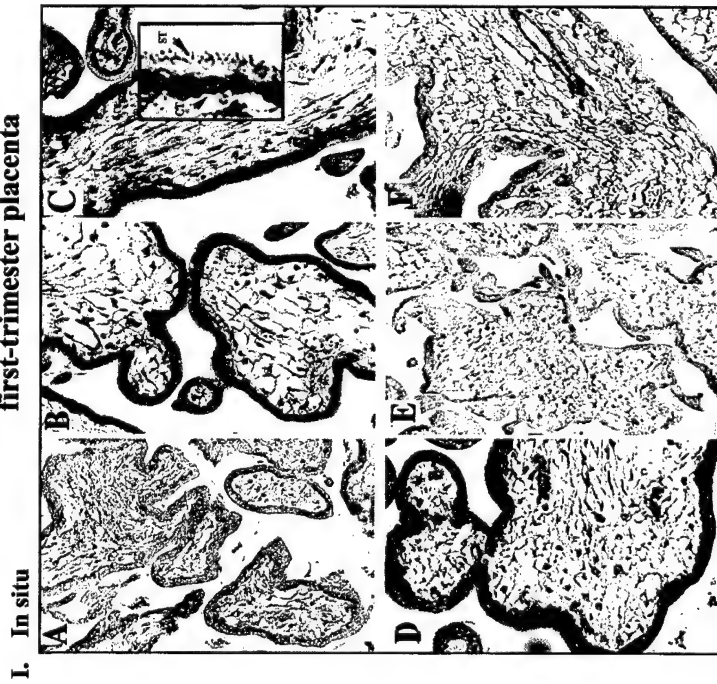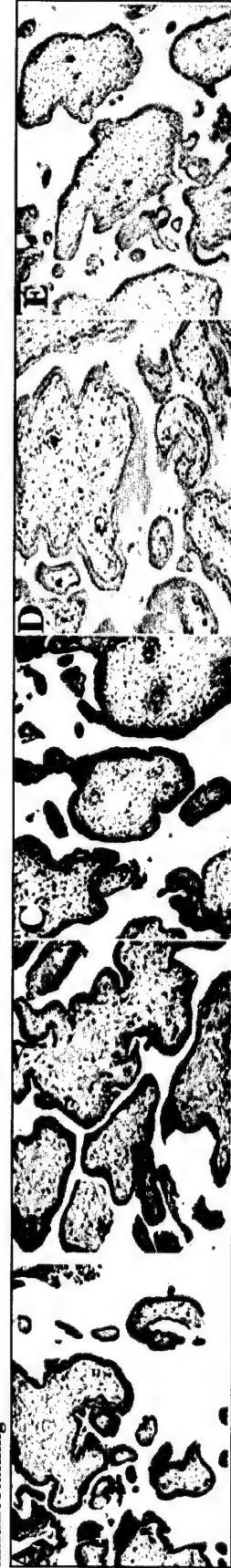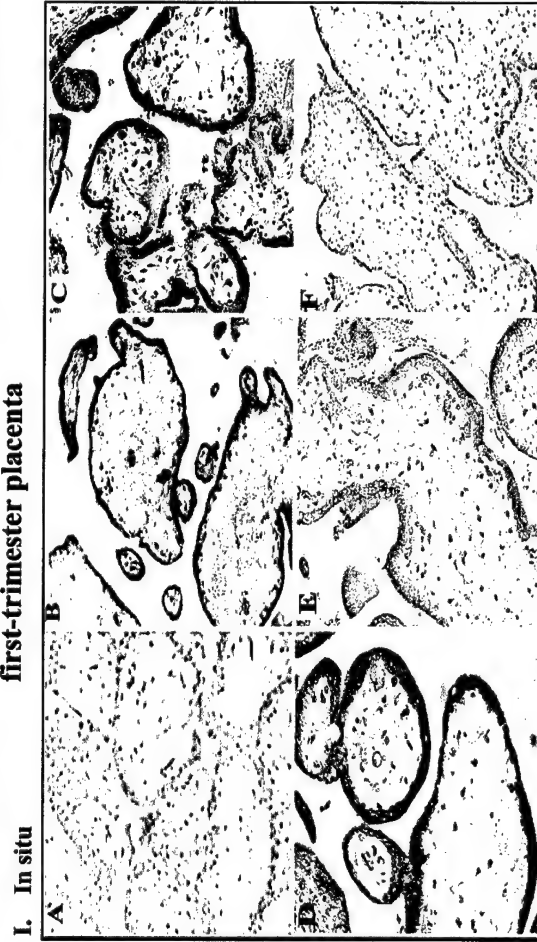
Fig5: Modulation of EVT villi Growth

I. Introduction of *hPar1* EVT villi growth

II. *hPar1* antisense inhibits EVT villi growth

II. Immunostaining
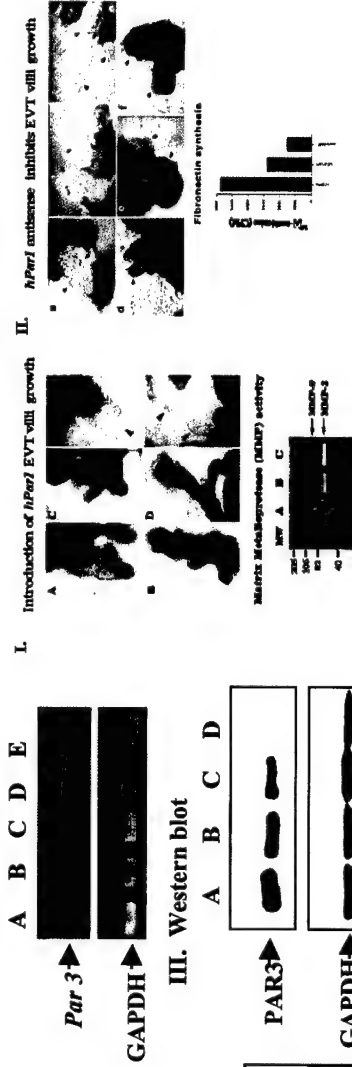
Figure 6: Overexpression of an MMTV LTR Driven *hPar1* Transgenes

I.
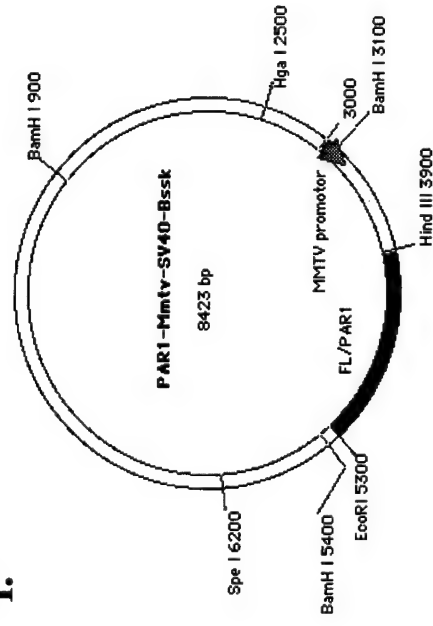
MMTV-*hPar1* transgenic construct. Full length human *Par1* (1.4kb) DNA was inserted into the multiple cloning site between *HindIII* and *EcoRI*. The plasmid was digested with the restriction endonucleases SpeI to generate the DNA fragment for injection.

II.

Genomic DNA/Mice tail Southern Blot

Genomic DNA/Mice tail PCR

III.

IV. Whole Mount
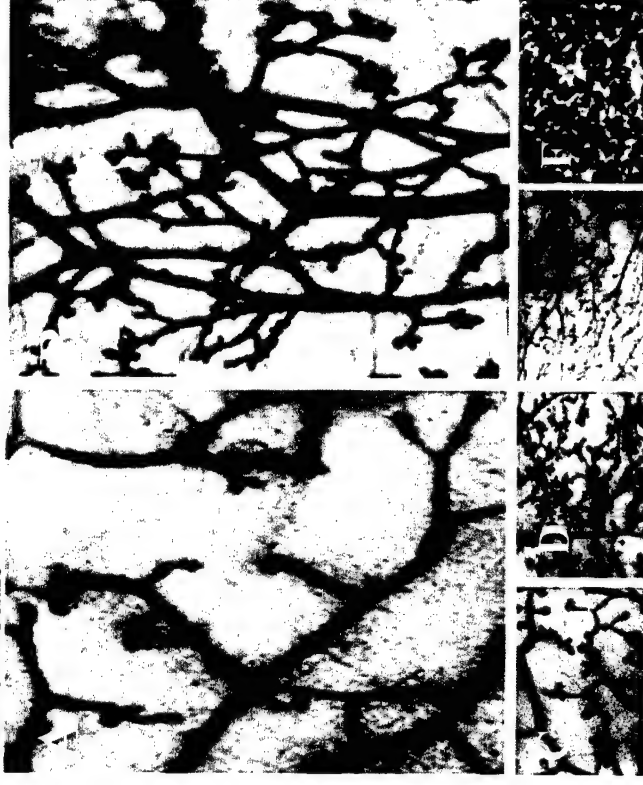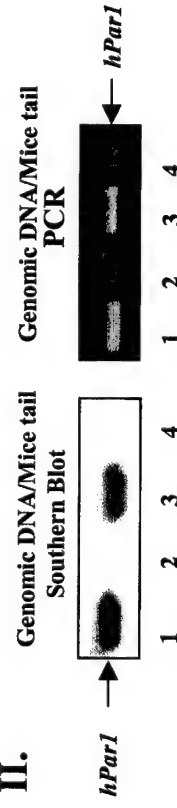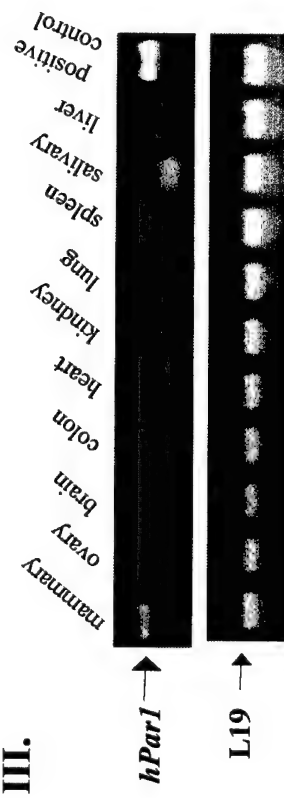
V. H&E Staining g
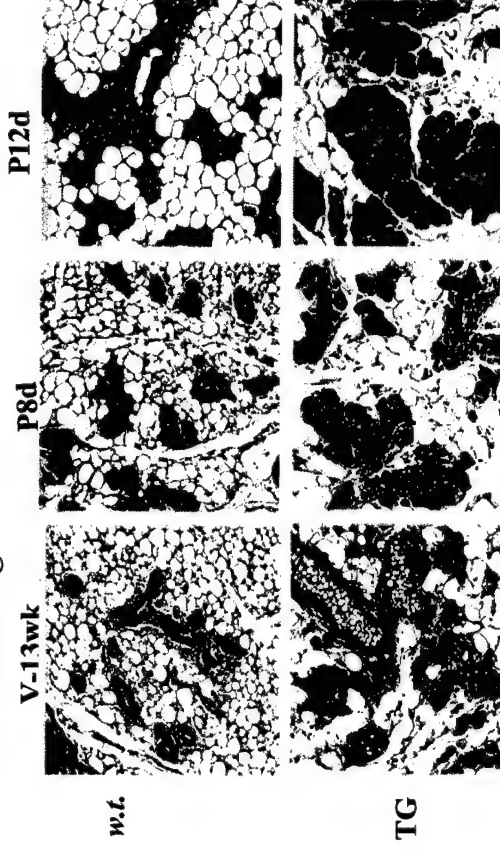
Figure 7:

I. *in situ* hybridization of *hPar1* in the transgenic mammary gland
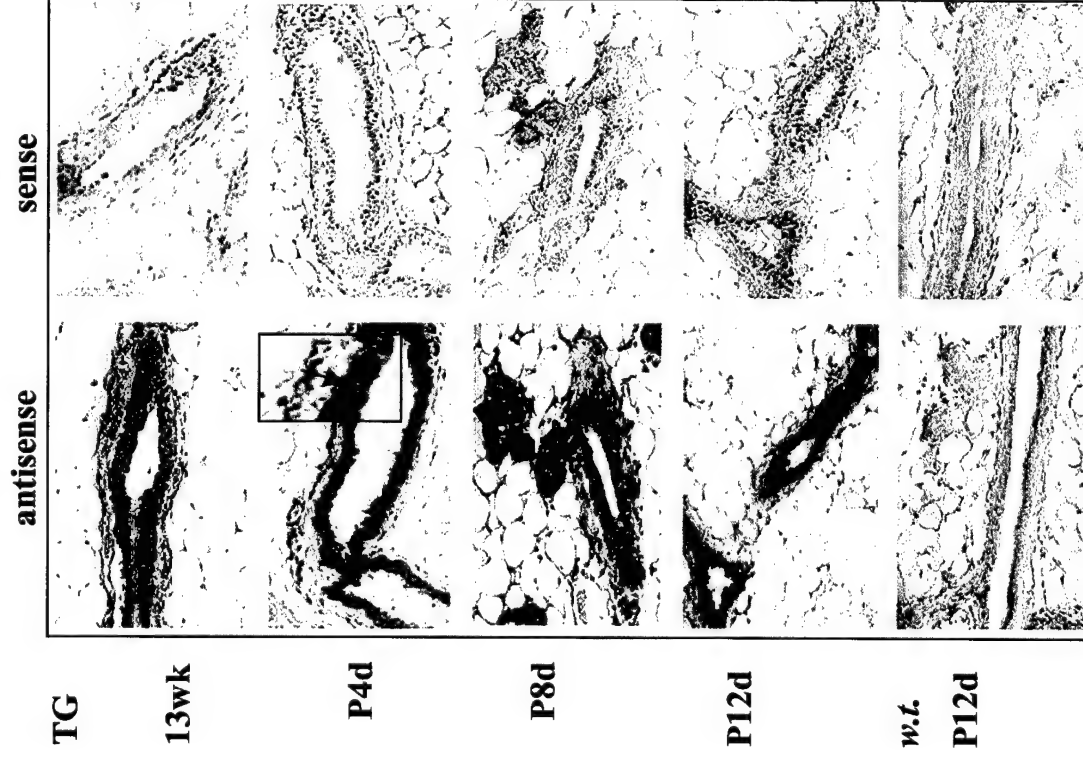
II. RT-PCR analysis of levels (virgin and Pregnant P4d-P12d)
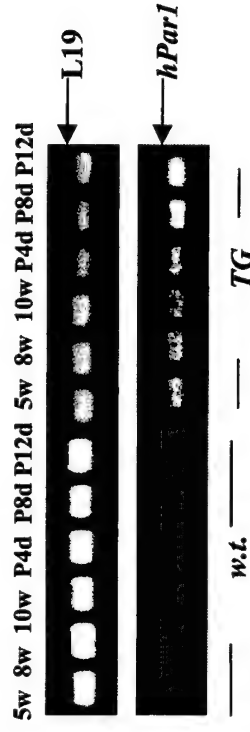
Figure 8:

I. Wnt pattern in *hPar1* overexpressing TG mice
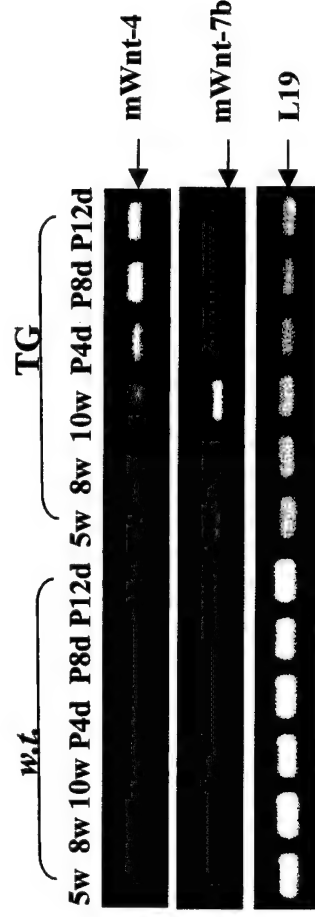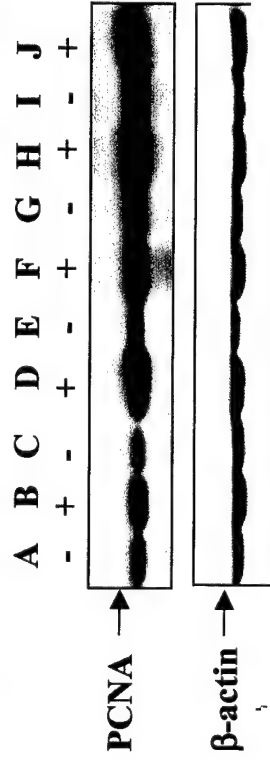

II. Immunoblot of Wnt-4 in *w.t.* and age matched *hPar1* TG mice
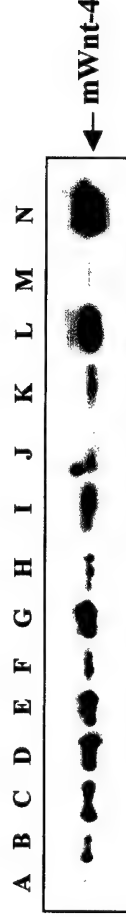
Figure 9:

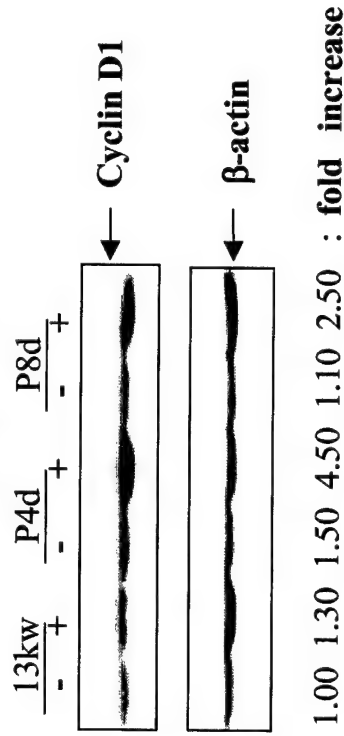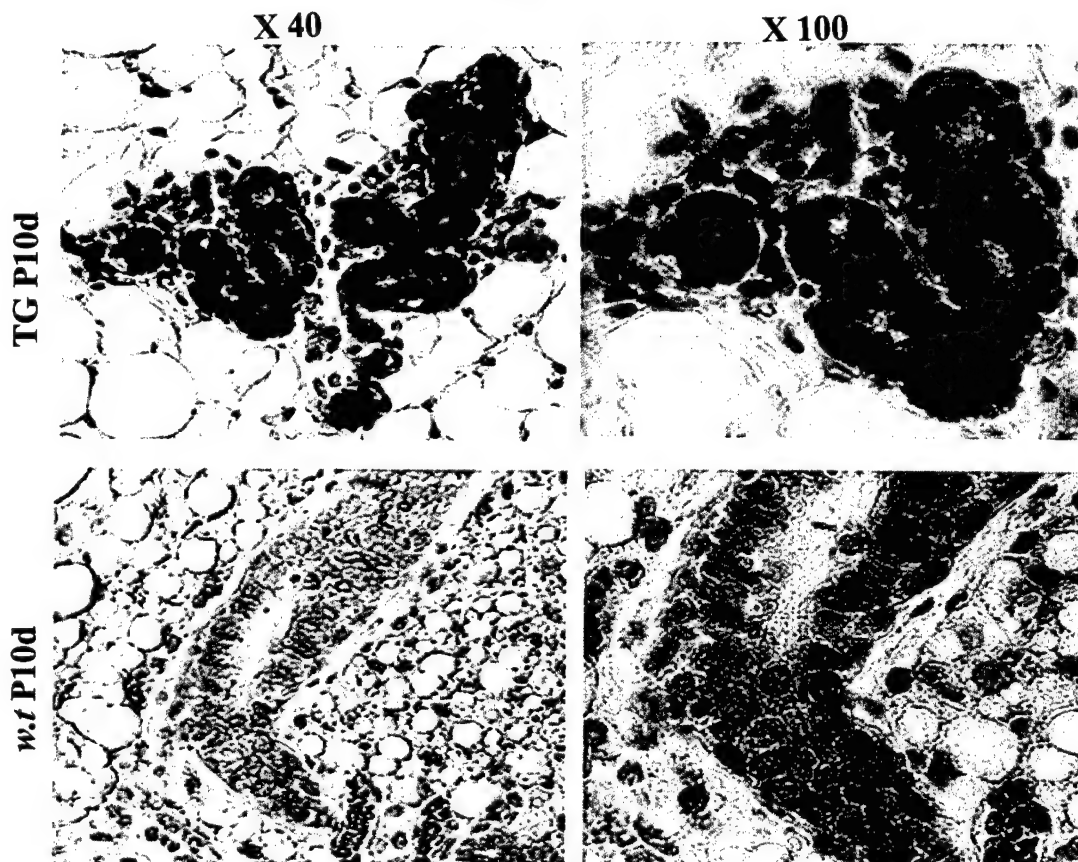## I.   PCNA immunostaining in *w.t.* and age-matched TG mice
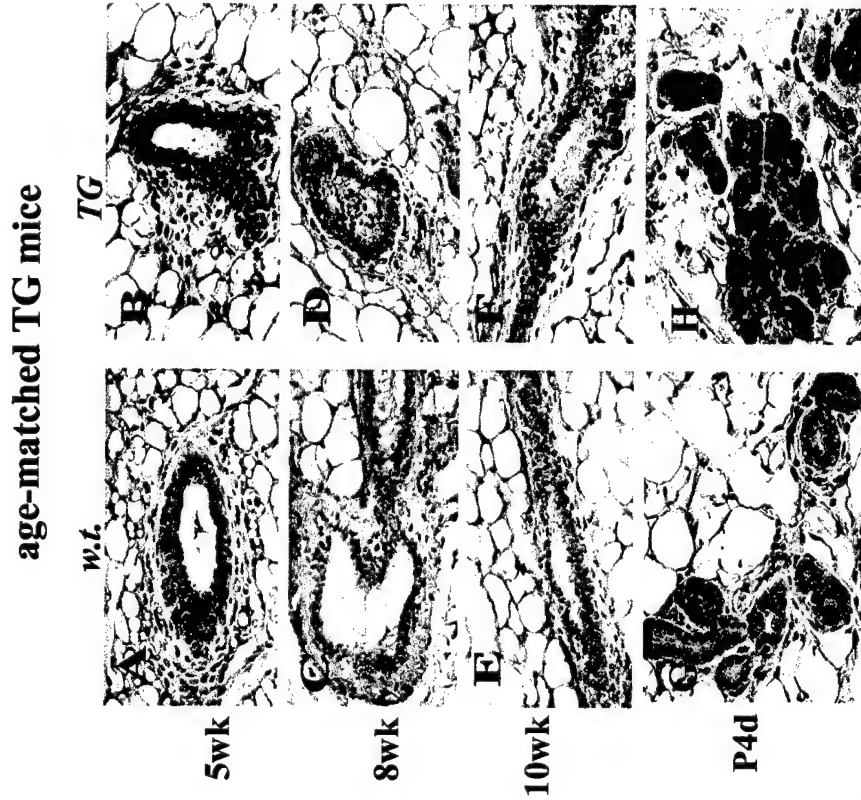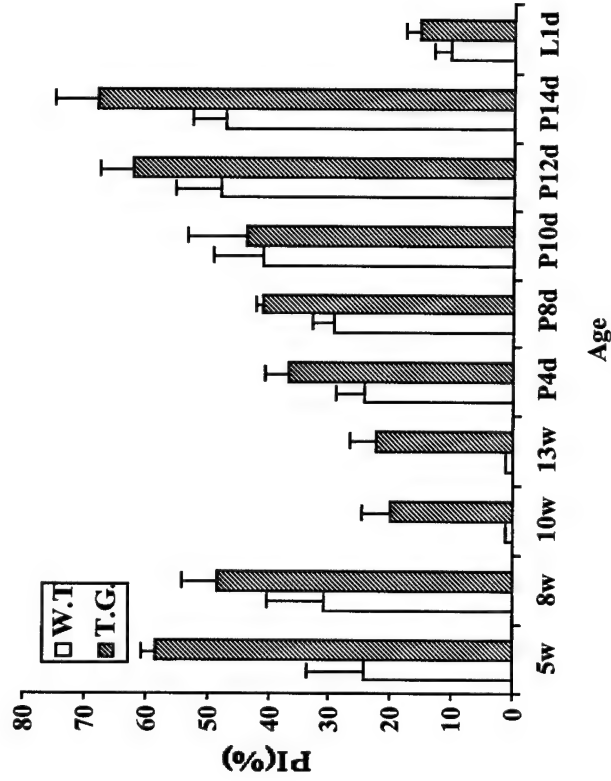
The proliferation index (PI) was defined as the number of PCNA-positive nuclei of mammary gland epithelial cells/total nuclei(500).

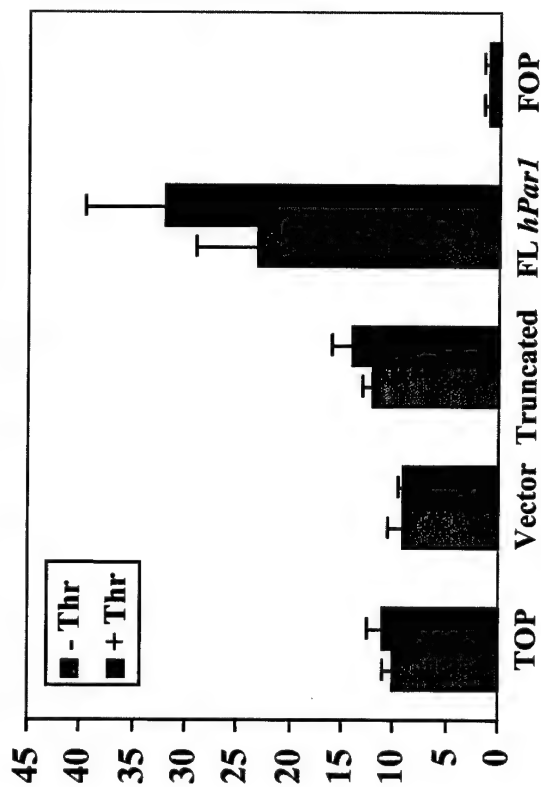## III.   Western blot analysis of Cyclin D1 in *w.t.* and TG mice

1.00 1.30 1.50 4.50 1.10 2.50 : fold increase

II.   Western blot

PI: *Bar-Shavit, R.* PhD

Figure 10:

I. Immunolocalization of β-catenin in *w.t.* and age-matched TG mammary gland

II. 293 transfected with TOP/FOPlash: Effects of FL *hPar1* and truncated *hPar1*

Figure 30:

Angiogenesis by *hPar1* in overexpressing mammary gland

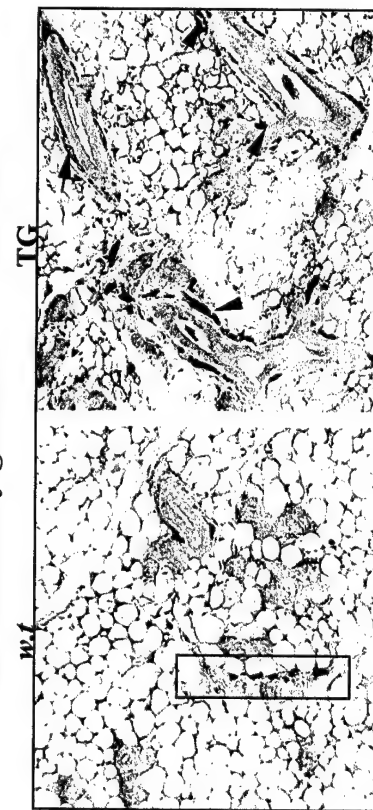Von Willebrand Factor (vWF) staining in the mammary glands of TG and *w.t.*
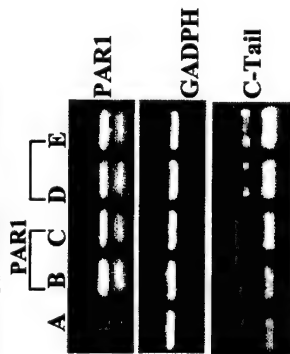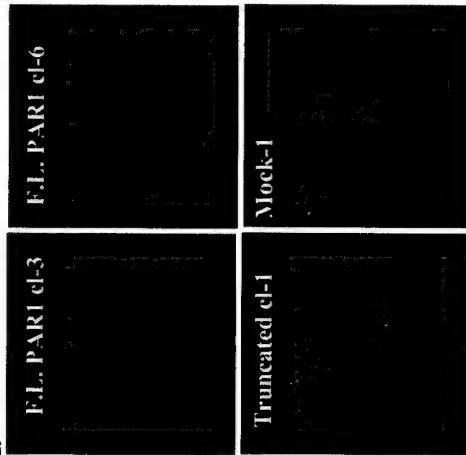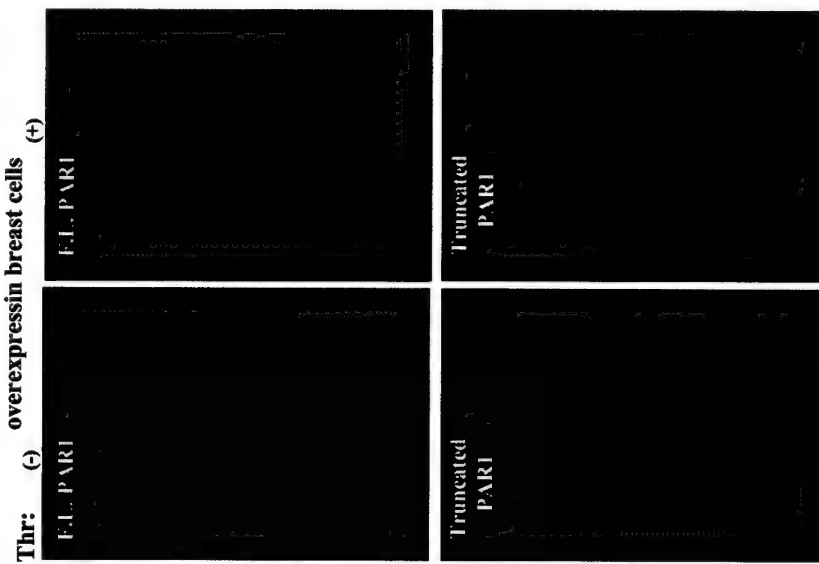
Fig. 11: "Tet-off" inducible cell lines

Fig. 14: FAC formation followin PAR1 activation in overexpressin breast cells
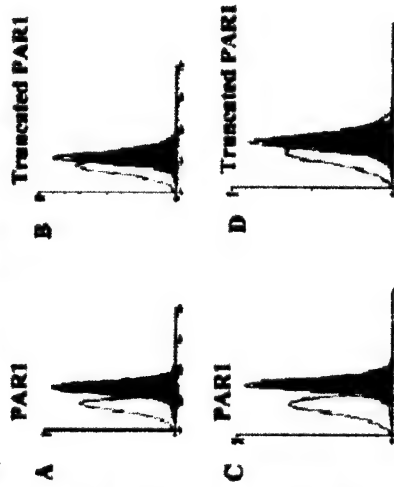
Fig. 15: PAR1 enters FAC in MD-435   PI: *Bar-Shavit, R.* PhD

Dox: - + - + - +
A B C D E F
Par1
β-actin

Fig. 12

Mock Truncated F.L. PAR1
PAR1
A B C D E
PAR1
GADPH
C-Tail

Fig. 13:

I. Mock truncated F.L. PAR1
A B C D E F
PAR1
β-actin

II.

F.L. PAR1 cl-3   F.L. PAR1 cl-6

Truncated cl-1   Mock-1

Thr: (-)   (+)
F.L. PAR1   F.L. PAR1
Truncated PAR1   Truncated PAR1

III.
A PAR1   B Truncated PAR1
C PAR1   D Truncated PAR1

Thr: (-)   (+)
4G10
PAR1
Merge

Fig. 16:

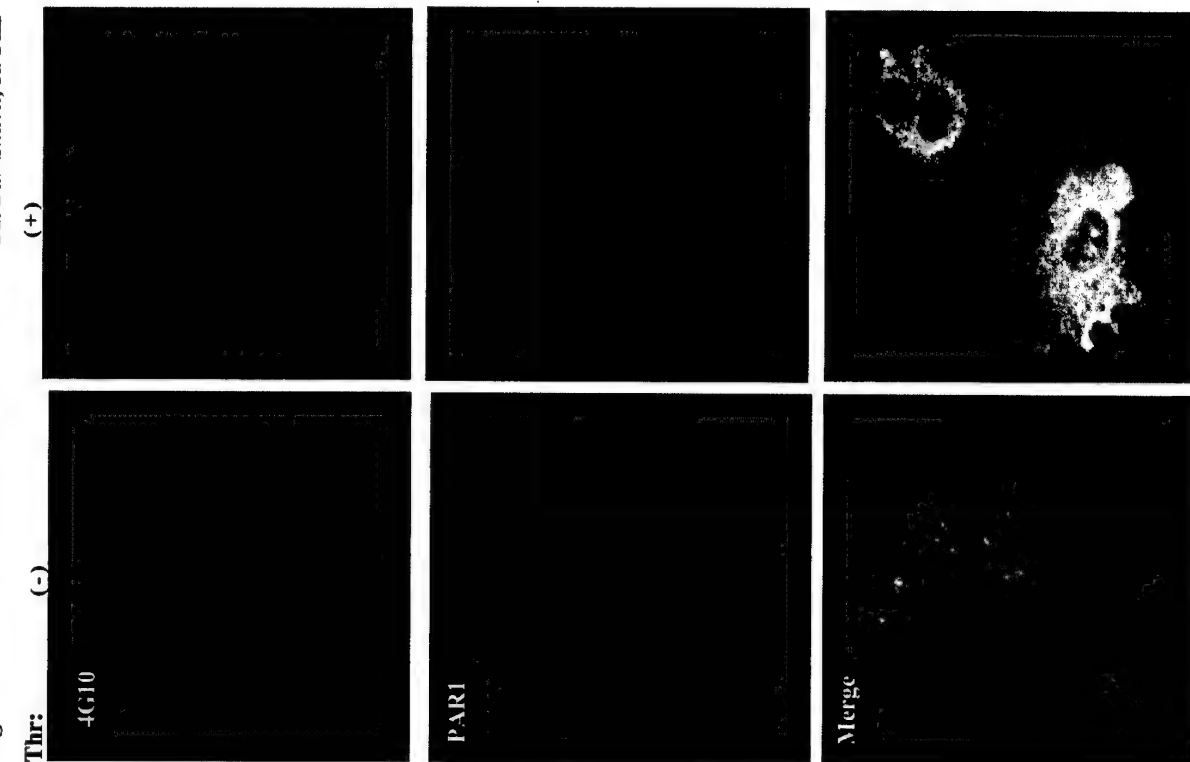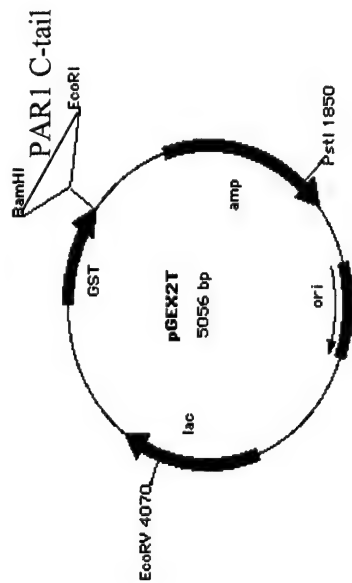**I. PAR1 c-tail cloned in pGEXT2 in order to get GST-C-tail fusion protein**

Scheme 3: PAR1 different forms:

WT   Truncated   Y397Z
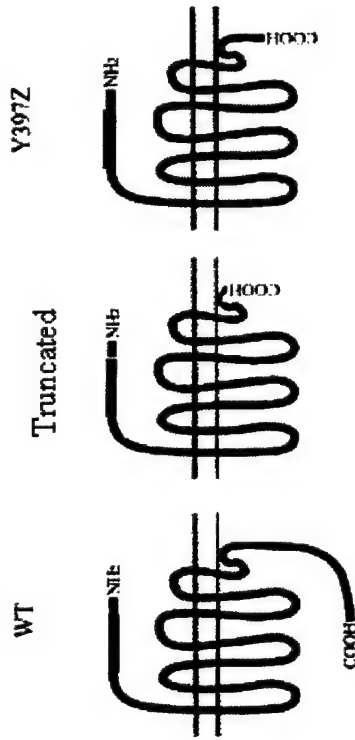
Fig. 25: Pattern of invadopodia induced by hPAR1: Inhibition by Syk

PAR1

Integrin

Src Syk Cbl p85 PI3K p110

αv

FA Rac Jnk

GADD

Akt

Erk

Negative regul

Lamellipodi

Invadopodia

II.

GST   GST C-tail

A   B

32kD →
27kD →

III. Specific interaction of proteins with PAR1 GST-C-tail

MCF-7   MDA-435

C-tail - + - +
        A B C D

~180 kD →
~50 kD →

pGEX2T
5056 bp

GST
lac
EcoRV 4070
ori
amp
PstI 1850
BamHI
EcoRI
PAR1 C-tail

Fig. 21:

PI: *Bar-Shavit, R. PhD*

Rac pull-down assay

Thr Activ.

| | Vect | | Caco2/hPar1 | |

Active Rac

Total Rac

Thr Activ.   - 2' 5 10' 15' 30' - 2' 5' 10' 15' 30'

Fig. 24:

GADD45 expression in Syk transfected breast carcinoma cells

Thr Activ.   - 3TB 10min Thr | 3TB 30min Thr | SYK3TB | SYK3TB 30min Thr

GADD45

Actin

II. Induction of p-JNK1 upon PAR1 activation is inhibit in Syk-3TB cell

α-Thr	-	+	+	+	+	+
min	0	5	10	15	20	30	60

←64 kDa
←50 kDε

P-JNK1→
P-JNK1→

β-actin→

Fig. 17:

Syk is bound to PAR1 GST-C-tail

I.

Syk 3TB   3TB

Syk

GST
GST-C tail

	+			
		+		
			+	
				+
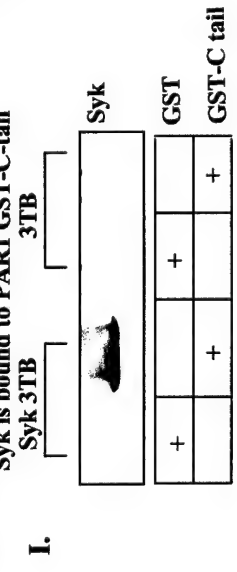
II. PAR1 C-tail competes for PAR1-Syk complex in MCF-7 overexpressing PAR1

A   B   C   D   - PAR1 C-tail peptide
-   +   +   +

Syk

PAR1

Fig. 19:

Thrombin activation in MDA-435 cells induces Src association with PAR1

	A	B	C	D
Thrombin	+	+	+	-
min	20	10	2	0

Src
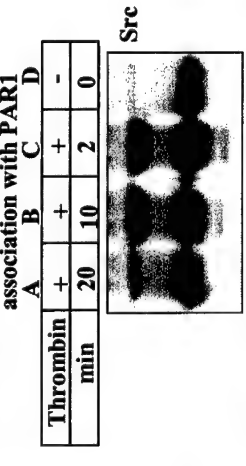
Fig. 20:

Activation of PAR1 C-tail increase the level of c-src Syk complex

MCF-7   Sky 3TB   3TB

	A	B	C	D	E	F
Thrombin:	-	+	+	-	-	+

Syk

Src
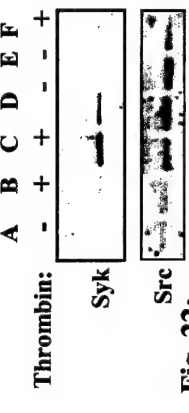
Fig. 22:

p-Cbl is induced in Syk 3TB cells

Syk-3TB

Thr	-	+	+	+	+
Min	0	5	20	30	60

3TB

+	+	+	+
0	5	20	30	60

pCbl

Cbl
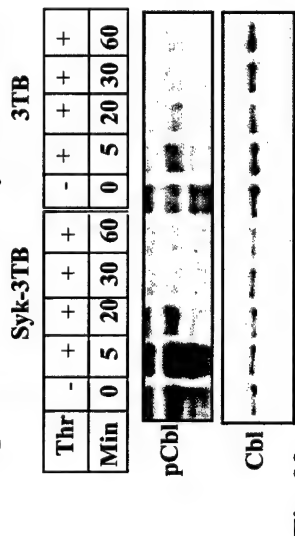
Fig. 23:

I. PAR1 activation induces p-JNK1 in 3TB cell

α-Thr	-	+	+	+	+	+
min	0	5	10	15	20	30	60

64 kDa
50 kDa

P-JNK1→
P-JNK1→

β-actin→

Fig. 18:

I. Syk is physically associated with PAR1

Mock   F.L. cl-23   Truncated F.L. cl-26

Syk

PAR1

II. Co-IP of PAR1 and Syk in different epithelial cells

Syk-3TB   3TB   293   MDA-435   MCF-7 F.L.

Syk

PAR1

Fig. 26:

PI: *Bar-Shavit, R.* PhD

Fig. 27:

Fig. 28:

hPar1 'Tet-on' system

I.

A   B   C

→ m-PAR1

→ L19

A- AT2.1   B- AT3.1   C- Baf 210

II.

- + - + - + Dox

A B C D E F

→ *h*-PAR1

→ β- actin

A- AT2.1/cont/ non induced
B- AT2.1/cont/ induced by Dox
C- Clone 1/PAR1/ non induced
D- Clone 1 /PAR1/ induced by Dox
E- Clone 4 /PAR1/ non induced
F- Clone 4 /PAR1/ induced by Dox

III.

A   B   C

IV.

	Vector +Dox	Cl4	Cl4 +Dox
Mass weight	0.56	0.35	1.3

Tet on prostate *hPar1* induced invasion
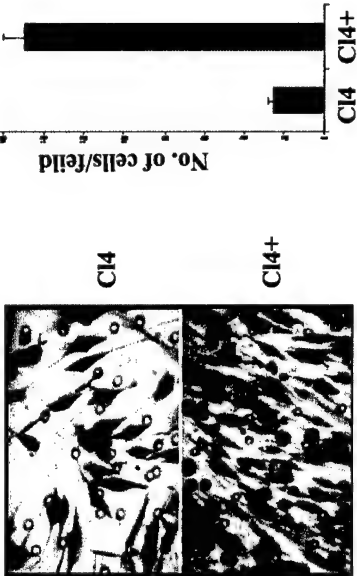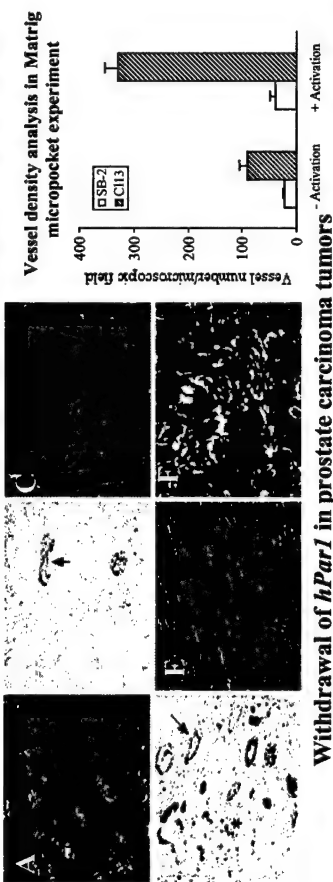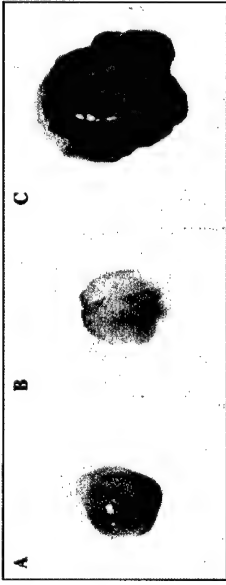
Cl4

Cl4+

No. of cells/feild

Cl4   Cl4+

II.

A   C

F   E

Vessel density analysis in Matrig micropocket experiment

□ SB-2   ▨ Cl13

Vessel number/microscopy field

- Activation   + Activation

hPar1 induced angiogenesis *in vivo*

Fig. 29:

Withdrawal of *hPar1* in prostate carcinoma tumors

50X

100X

Dox: 2wk(+)   4wk(+)   2wk(+),2wk(-)

Fig. 31: **The over-expression of** *hPar1* **in non-invasive Caco2 cells:Enhanced migration and loss of E-Cadherin**

I. Migration

Caco2   Caco2/vect   Caco2/*Par1*

Control

16hr

Fig. 31

II. E-cadherin expression levels

A B C D

← PAR1

← E-cadherin

← β-actin

A- MD435   B- Caco2   C- Caco2/vect.   D- Caco2/*Par1*

Fig. 32:

I.

MCF-10A

hPar1 overexpressing

II.

Phase image

E-cadherin

DAPI

β-catenin

Tumor Cell Invasion Is Promoted by Activation of Protease Activated Receptor-1 in Cooperation with the $\alpha_v\beta_5$ Integrin*

Sharona Cohen Even-Ram‡, Miriam Maoz‡, Elisheva Pokroy‡, Reuven Reich§, Ben-Zion Katz¶, Paul Gutwein‖, Peter Altevogt‖, and Rachel Bar-Shavit‡**

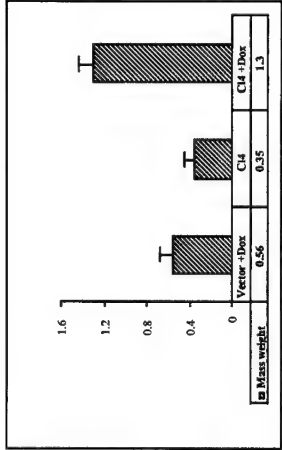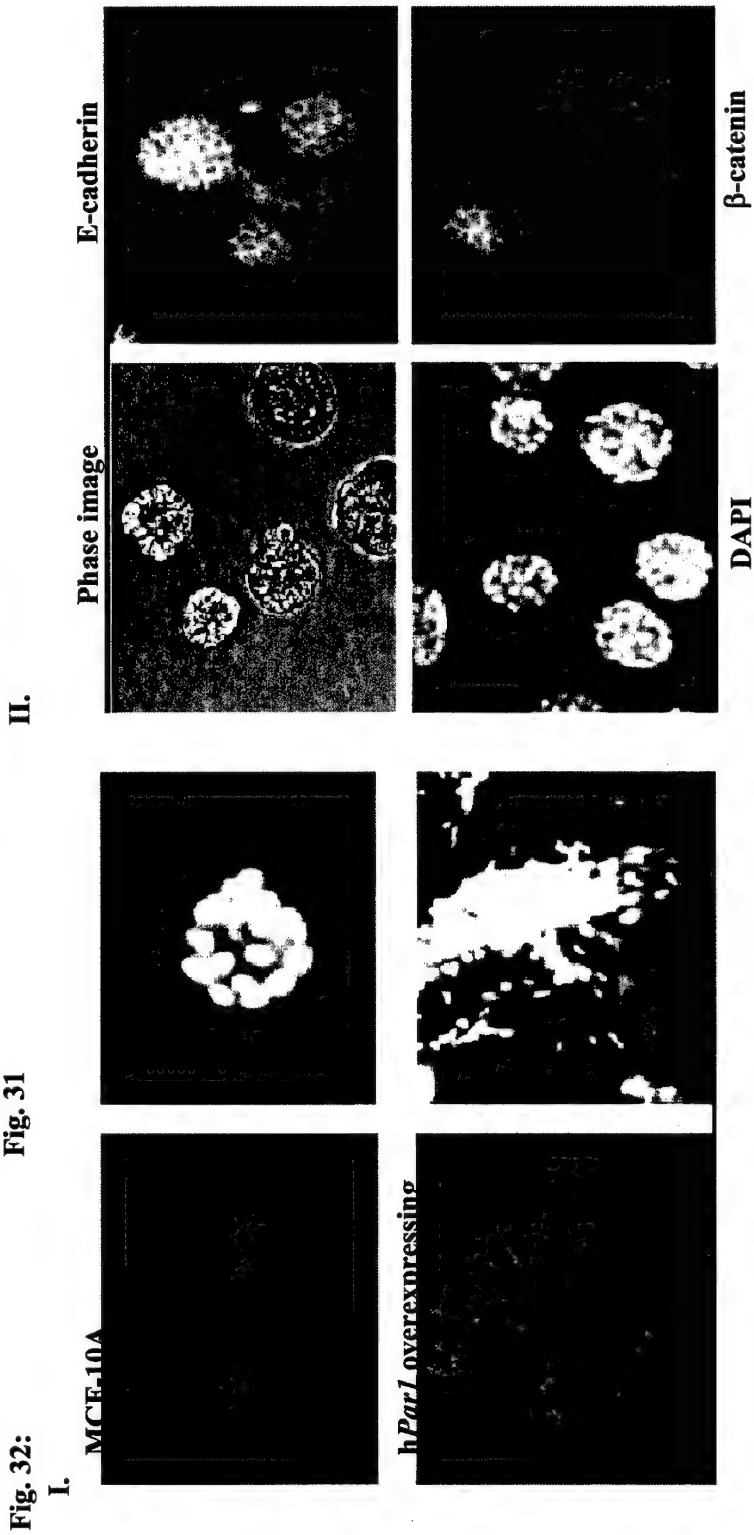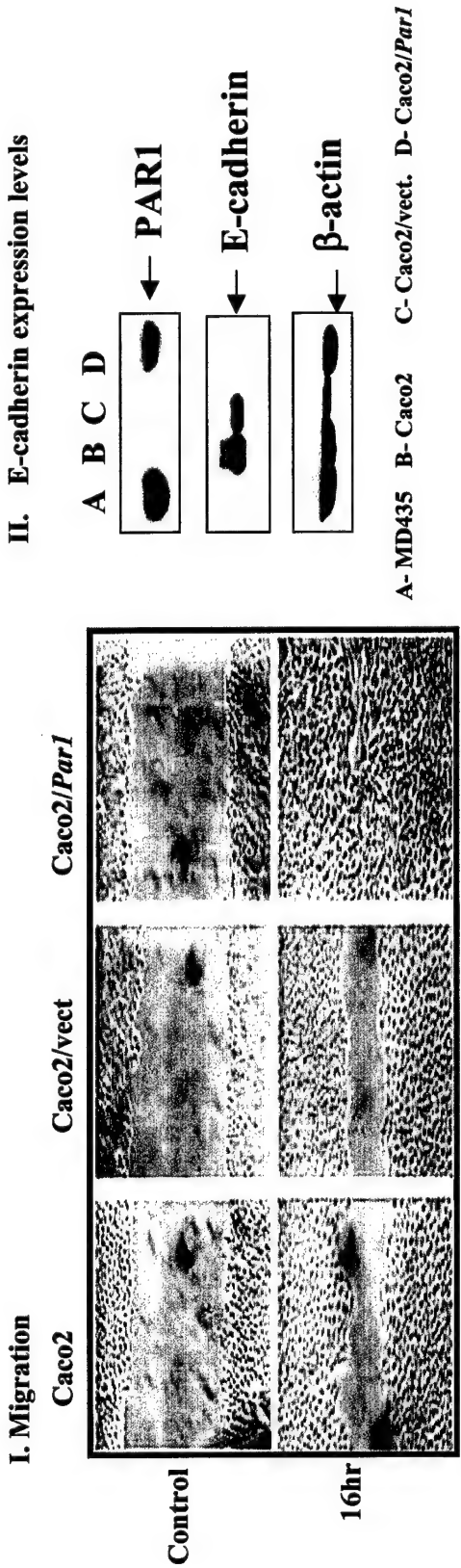From the Departments of ‡Oncology and §Pharmacology at the Hadassah-Hebrew University Hospital, Jerusalem 91120, Israel, the Department of ¶Hematology, Medical Center, Tel Aviv 64239, Israel, and the ‖Tumor Immunology Program, German Cancer Research Center, D-69120 Heidelberg, Germany

The first prototype of the protease activated receptor (PAR) family, the thrombin receptor PAR1, plays a central role both in the malignant invasion process of breast carcinoma metastasis and in the physiological process of placental implantation. The molecular mechanism underlying PAR1 involvement in tumor invasion and metastasis, however, is poorly defined. Here we show that PAR1 increases the invasive properties of tumor cells primarily by increased adhesion to extracellular matrix components. This preferential adhesion is accompanied by the cytoskeletal reorganization of F-actin toward migration-favoring morphology as detected by phalloidin staining. Activation of PAR1 increased the phosphorylation of focal adhesion kinase and paxillin, and the induced formation of focal contact complexes. PAR1 activation affected integrin cell-surface distribution without altering their level of expression. The specific recruitment of $\alpha_v\beta_5$ to focal contact sites, but not of $\alpha_v\beta_3$ or $\alpha_5\beta_1$, was observed by immunofluorescent microscopy. PAR1 overexpressing cells showed selective reciprocal co-precipitation with $\alpha_v\beta_5$ and paxillin but not with $\alpha_v\beta_3$ that remained evenly distributed under these conditions. This co-immunoprecipitation failed to occur in cells containing the truncated form of PAR1 that lacked the entire cytoplasmic portion of the receptor. Thus, the PAR1 cytoplasmic tail is essential for conveying the cross-talk and recruiting the $\alpha_v\beta_5$ integrin. While PAR1 overexpressing cells were invasive in vitro, as reflected by their migration through a Matrigel barrier, invasion was further enhanced by ligand activation of PAR1. Moreover, the application of anti-$\alpha_v\beta_5$ antibodies specifically attenuated this PAR1 induced invasion. We propose that the activation of PAR1 may lead to a novel cooperation with the $\alpha_v\beta_5$ integrin that supports tumor cell invasion.

The ability of tumor cells to invade beyond controlled hemostatic boundaries and re-emerge from blood vessels to establish new metastatic colonies continuous to present a major obstacle in cancer cure. It is well known that in tumor invasion and metastasis, the pericellular proteolytic systems, consisting of proteases and their specific cell surface receptors, are tightly regulated to modulate cellular functions and degrade selective matrix barriers (1, 2). We have previously demonstrated that the proteolytically activated receptor 1 (PAR1,[1] thrombin receptor) plays a central role in the malignant and physiological invasion processes of both breast carcinoma metastasis and placental implantation (3). At the molecular level, tumor invasion is mediated via the combined interactions of the host cell signaling machinery and the regulation of the stromal extracellular matrix (ECM). Extensive proteolysis in the tumor microenvironment is also responsible for the activation of several enzymatic precursors, like plasminogen, pro-matrix metalloproteinase, and prothrombin (4–6). In addition, the extravascular deposition of fibrin within the tumor microenvironment is well established (7), pointing to the significant role of the coagulation proteins in tumor progression. Indeed, the tissue factor (TF), a protease receptor that plays a central role in hemostasis, has also been implicated in angiogenesis and tumor cell metastasis by means of intracellular events mediated by its cytoplasmic tail and by the perivascular extracellular proteolysis (8–10). These features are shared by other cellular receptors involved in the proteolytic modification of the tumor environment. Among these is the receptor for the serine protease urokinase, which, when bound to its cell surface receptor (uPAR), converts plasminogen to plasmin; plasmin, in turn, is known to effectively degrade various matrix glycoproteins (1, 11). It has been shown also that uPAR serves as an adhesion receptor for vitronectin (12) and that the vitronectin receptor $\alpha_v\beta_3$ not only supports the migration of tumor cells on various matrix-proteins but also binds matrix metalloproteinase-2, thus presenting an immobilized enzyme with improved matrix-collagen degradation properties at the invasive front (13). Additional cell surface protease receptors include the PAR family, which are proteolytically cleaved G-coupled receptors of seven transmembrane-spanning domains. Unlike most cellular growth factor receptors, the PAR family members do not require the traditional ligand-receptor complex formation for ac-

---

** To whom all correspondence should be addressed. Permanent address: Dept. of Oncology, Sharett Inst., Hadassah University Hospital, P.O. Box 12000, Jerusalem 91120, Israel. Tel.: 972-2-677-7563; Fax: 972-2-642-2794; E-mail: barshav@md2.huji.ac.il. Current address (during the academic year 2000–2001): Dept. of Cell Biology, Harvard Medical School, 240 Longwood Ave., Boston, MA 02115. Tel.: 617-432-3971/3972; Fax: 617-432-3969; E-mail: rachel_barshavit@hms.harvard.edu.

[1] The abbreviations used are: PAR, protease activated receptor; FAC, focal adhesion complex; FAK, focal adhesion kinase; ECM, extracellular matrix; TRAP, thrombin receptor-activating peptide; AS, antisense; FACS, fluorescence-activated cell sorting; DMEM, Dulbecco's modified Eagle's medium; FCS, fetal calf serum; FITC, fluorescein isothiocyanate; mAb, monoclonal antibodies; BSA, bovine serum albumin; PBS, phosphate-buffered saline; TF, tissue factor; uPA, urokinase; uPAR, urokinase receptor.

tivation. Instead, they are activated by a specific cleavage within their extracellular N-terminal portion to unmask a new amino acid terminus, which serves then as an internal ligand for activation (14–18). Until now, four members of the PAR family have been identified and of these, three (PAR1, PAR3, and PAR4) have been established collectively as "thrombin receptors," possibly serving as a redundant receptor system for the coagulation protease cellular response (14).

Since solid tumors are in close contact with ECM components, malignant cell invasion into the surrounding tissues is facilitated by mutual interactions that convey essential signaling cues to the cells (19, 20). These cell-ECM interactions are mediated by integrins, a family of adhesion receptors that mediate the attachment of the cell to both structural and matrix-immobilized proteins to promote cell survival, proliferation, and migration (21, 22). It is widely recognized that integrins perform a significant function in cellular invasion and metastasis (23–26). Non-ligated integrins are generally distributed diffusely over the cell surface with no apparent linkage to the actin cytoskeleton. However, ECM-bound integrins frequently cluster into specialized structures termed focal adhesion complexes (FACs), thus providing a convergence site for multiple signaling components (26, 27) and also physically linking the receptors to the actin filaments (28–30). The known signaling events that follow receptor clustering include tyrosine phosphorylation of proteins like focal adhesion kinase (FAK) and paxillin (31), as well as the recruitment of other FAC components like vinculin, talin, tensin, and p130 Cas (32–36). A growing number of studies indicate that signals driven by integrins act in concert with signals initiated by the G-protein-coupled receptors and with receptors for tyrosine kinase to promote the pathological tumor cell invasion process, on the one hand, and physiological activities like angiogenesis and wound healing (37, 38) on the other. The combined signals involved with the activation of focal adhesion proteins indicate that the cooperation between the signaling pathway takes place most likely within these FAC structures.

In the present work, we have studied the molecular mechanism of PAR1 involvement in tumor cell invasion. We show here that PAR1 modulates the invasive phenotype of melanoma cell lines, inducing the otherwise non-invasive cells to migrate effectively through Matrigel barriers. This process is accompanied by the increased adherence of the cells to various matrix components, actin stress fiber formation, and adhesion-triggered signaling, with no alteration of the cell surface integrin levels. We demonstrate now, for the first time, that PAR1 mediates these functions via selective cross-talk with the $\alpha_v\beta_5$ integrin to confer FAC formation, distinct signaling events, and cytoskeletal reorganization. Combined, these processes promote tumor cell invasion.

EXPERIMENTAL PROCEDURES

Cells—SB-2 non-invasive human melanoma and A375-SM "super-metastatic" human melanoma cells (kindly provided by J. Fidler and M. Bar-Eli, Department of Cell Biology, University of Texas, M. D. Anderson Cancer Center, Houston, TX) were grown in 10% FCS-DMEM supplemented with 50 units/ml penicillin and streptomycin (Life Technologies, Inc.) and maintained in a humidified incubator with 8% CO_2 at 37 °C. The PAR1 stable transfectants, clone 13 and clone Mix L, were grown under the same conditions; for long term maintenance, these were supplemented also with 200 μg/ml G418 antibiotics. MCF-7 cells were maintained as previously described (3).

Cell Transfection—Cells were grown to 30–40% confluence and then transfected with 0.5–2 μg/ml plasmid DNA in Fugene 6 transfection reagent (Roche Molecular Biochemicals) according to the manufacturer's instructions. After 10 days of selection, stable, transfected clones were established in medium containing 400 μg/ml G418. Antibiotic-resistant cell colonies were transferred to separate culture dishes and were grown in 200 μg/ml G418 medium. Forty-eight hours after trans-

fection, transiently transfected cells were collected and tested by immunoprecipitation analyses (see below).

Preparation of Truncated PAR1—Using polymerase chain reaction, we constructed a PAR-1 mutant protein truncated in its cytoplasmic tail after the amino acid Leu-369. As a template, we used PAR-1 cDNA in the pCDNA 3 vector. For amplification, we used a T7 sense primer and the reverse primer GGTCTAGAAAACTATAGGGGGTCGATG-CACGAGCT containing a STOP codon and an *Xba*I site. The amplified DNA fragment was subcloned using the polymerase chain reaction-blunt technique (Invitrogen) and confirmed by DNA sequencing. The insert was released from the vector by *Xba*I digestion and cloned into plasmid pCDNA3. To confirm the functional integrity of the DNA constructs, wild type and mutant cDNAs were transiently expressed in 293 cells that were subsequently stained with a PAR-1-specific antibody (WEDE15, Immunotech, Cedex, France).

Western Blot Analysis—Cells were solubilized in lysis buffer containing 10 mM Tris-HCl, pH 7.4, 150 mM NaCl, 1 mM EDTA, 1% Triton X-100, and protease inhibitors (5 μg/ml aprotinin, 1 μM phenylmethyl-sulfonyl fluoride, and 10 μg/ml leupeptin) at 4 °C for 30 min. The cell lysates were subjected to centrifugation at 10,000 $\times$ g at 4 °C for 20 min. The supernatants were saved and their protein contents were measured; 50 μg of the lysates were loaded onto 10% SDS-polyacrylamide gels. After the proteins were separated, they were transferred to an Immobilon-P membrane (Millipore). Membranes were blocked and probed with 1 μg/ml amounts of the appropriate antibodies as follows: anti-PAR1 thrombin receptor mAb, clone II aR-A (Biodesign Int.); anti-paxillin monoclonal antibody (mAb), clone 349 (Transduction Laboratories, Lexington KY); anti-human focal adhesion kinase, rabbit polyclonal IgG (Upstate Biotechnology Inc., Lake Placid, NY); anti-phosphotyrosine mAb, clone 4G10 (Upstate Biotechnology Inc.); anti-vinculin mAb (Transduction Laboratories). The antibodies were suspended in 1% BSA in 10 mM Tris-HCl, pH 7.5, 100 mM NaCl, and 0.5% Tween 20. After washes with 10 mM Tris-HCl, pH 7.5, 100 mM NaCl, and 0.5% Tween 20, the blots were incubated with secondary antibodies conjugated to horseradish-peroxidase. Immunoreactive bands were detected by the enhanced chemiluminescence (ECL) reagent using Luminol and p-cumaric acid (Sigma).

Immunoprecipitation—Cells were treated for 30–60 min with thrombin at a concentration of 1 NIH unit/ml of serum-free DMEM medium (0.5% BSA), and then lysed as described above. We used 400 μg of total protein for immunoprecipitation of $\alpha_v\beta_3$, $\alpha_v\beta_5$, paxillin, FAK, or both paxillin and FAK. All the antibodies were used at a concentration of 10 μg/ml. After overnight incubation, Protein A-Sepharose beads (Amersham Pharmacia Biotech) were added to the suspension (50 μl) that was subsequently rotated at 4 °C for 1 h. Elution of the reactive proteins was made by re-suspending the beads in protein 2$\times$ sample buffer (63 mM Tris-HCl, pH 6.8, 20% glycerol, 20% SDS, 0.01% bromphenol blue, 5% β-mercaptoethanol, 0.02 M dithiothreitol) and boiling for 5 min. The supernatant was loaded on a 10% SDS-polyacrylamide gel followed by the same procedure as in Western blotting.

Matrigel Invasion Assay—We used blind-well chemotaxis chambers with 13-mm diameter filters. Polyvinylpyrrolidone-free polycarbonate filters with 8-μm pores (Costar Scientific Co., Cambridge, MA) were coated with basement membrane Matrigel (25 μg/filter) as described previously (39). Briefly, the Matrigel was diluted to the desired final concentration with cold distilled water, applied to the filters, dried under a hood, and reconstituted with serum-free medium. In the upper compartment of the Boyden chamber, we placed 2–3 $\times$ 10^5 cells suspended in DMEM containing 0.1% bovine serum albumin. As a chemoattractant, into the lower compartment of the Boyden chamber, we put 3T3 fibroblast conditioned medium. Assays were carried out in 5% CO_2 at 37 °C. After 2 h of incubation, we observed that more than 90% of the cells were attached to the filter. At this time, the cells on the upper surface of the filter were removed by wiping with a cotton swab. The filters were fixed in DifQuick system (American Scientific Products) and stained with hematoxylin and eosin. Cells from various areas of the lower surface were counted. Each assay was performed in triplicate. For chemotaxis studies (a control of Matrigel invasion), the filters were coated with collagen type IV alone (5 mg/filter) to promote cell adhesion. Cells were added to the upper chamber and conditioned medium to the lower compartment.

Adhesion Assay—The medium of cells grown in 10% FCS was replaced by DMEM with 0.5% BSA, and the cells were detached from the plate by treating with 0.05% trypsin in a solution of 0.02% EDTA in 0.01 M sodium phosphate, pH 7.4 (Biological Industries, Beit Ha'emek, Israel). After washing, 0.5 $\times$ 10^6 cells/ml cells were re-suspended in a serum-free DMEM medium (as above) and laid on 13-mm culture dishes pre-coated with either 100 μg/ml fibronectin or Th-1, a thrombin-de-

rived RGD (arginine-glycine-aspartic acid) peptide. After a 45-min incubation period to allow cell adhesion, the excess cells were washed away. The adhered cells were fixed to the plates with 4% formaldehyde in PBS, pH 7.4, for at least 2 h. After fixation, the plates were washed in 1% boric acid solution and the cells were stained with 1% methylene blue reagent (Sigma) in 1% boric acid for 30 min. After extensive washing with tap water, the methylene stain was eluted by the addition of 500 μl of 1 M HCl. The intensity of the color staining was measured by color spectrometry at a wavelength of 620 nm.

Immunofluorescence—Cells were plated on glass coverslips in 16-mm culture dishes; after the cells had grown to subconfluence, they were washed with PBS, permeabilized in 0.5% Triton X-100-containing 3.5% paraformaldehyde/PBS solution on ice for 2 min, and finally fixed with 3.5% paraformaldehyde/PBS for 20 min. Reactions with the appropriate antibodies were performed in room temperature for 60 min, after which the cells were washed extensively in PBS. The antibodies included the following: anti-$\alpha_v\beta_3$ mAb clone LM609, anti-$\alpha_v\beta_5$ clone P1F6, and anti-$\alpha_5\beta_1$ clone JBS5, (all from Chemicon Int.). After the 60-min incubation with the primary antibodies, followed by extensive washes in PBS, an additional 60-min incubation was carried out in the dark with secondary antibodies, goat-anti-rabbit or goat-anti-mouse IgG each conjugated with Cy-3 (Jackson Immunoresearch Laboratories) diluted 1:700. Labeling of filamentous actin by 1 μ g/ml FITC-conjugated phalloidin (Sigma) was performed similarly. The labeled cells were visualized and photographed by fluorescent confocal microscopy (MRC-1024 confocal imaging system, Bio-Rad).

Flow Cytometry Analysis—The medium of cells grown in 10% FCS-DMEM was replaced by serum-free DMEM containing 0.5% BSA. Thrombin at a concentration of 1 IU/ml was added to the plates that were activated by incubation for 60 min. The plates were washed with PBS, and the cells were detached from the plates by treatment with 0.05% trypsin in a solution of 0.02% EDTA in 0.1 M sodium phosphate at pH 7.4 (Biological Industries). After being washed twice in PBS, the cells were re-suspended in 200 μl of PBS and the appropriate antibodies were added to a concentration of 10 μg/ml. These reactions, performed at room temperature for 60 min, were followed by extensive washing in PBS. A 1-h incubation with a secondary antibody goat-anti-mouse IgG (Jackson Immunoresearch Laboratories) conjugated with FITC and diluted 1:500 was carried out in the dark. The treated cells were washed extensively, re-suspended in 100 μl of PBS, and analyzed by FACS.

RESULTS

Altering the Expression of PAR1 Affected Tumor Cell Invasiveness—In previous work (3), we showed that there is a direct correlation between PAR1 expression and the metastatic potential of primary tumor biopsies and tumor cell lines, as reflected by their *in vitro* potential to invade through a Matrigel barrier.[2] In a physiological invading model system of placenta trophoblast implantation, we have also shown that PAR1 is part of the invasive program of trophoblast, as evaluated by their villi extension and matrix metalloproteinase synthesis.[3] Here, to clarify how high levels of PAR1 may confer invasiveness, we transfected a non-invasive melanoma cell line (SB-2 cells) with PAR1 cDNA and compared the properties of the transfected cells to those of the highly invasive melanoma cell line A375SM. We used PAR1 cDNA under the control of the cytomegalovirus viral promoter in the pCDNA3 expression vector. We selected several stable clones that expressed high levels of PAR1, as evaluated by Western blot analysis (Fig. 1a) and Northern blot analysis (data not shown). The selected clones were then tested for their ability to invade through Matrigel-coated filters. Indeed, clones expressing high levels of PAR1 had an increased ability to invade the Matrigel layer, as compared with control clones transfected with empty vectors or SB-2 cells that had not been transfected at all (Fig. 1b). In addition, we observed that, whereas highly invasive A375SM cells invaded Matrigel coated membranes more efficiently than

did non-metastatic cells (Fig. 1b, *SB-2*), activating the A375SM cells with PAR1 increased their ability to invade Matrigel to an even higher level (Fig. 1b, *activ. A375SM*). In addition, the invasiveness of PAR1-transfected cells was further increased when they were either activated by thrombin, as shown in two separate PAR1-transfected clones (Fig. 1b, *clones 13* and *Mix L*), or when they were treated with the thrombin-receptor-activating peptide (TRAP) that corresponds to PAR1 internal ligand SFFLRN (data not shown).

Circulating tumor cells can invade into a new metastatic site only if they can adhere to the basement membrane. We analyzed the adhesion properties of cells suspended in a serum-free medium and then incubated for 60 min on plates coated with either fibronectin, a major component of the ECM, or with Th-1, an 11-amino acid peptide, corresponding to the thrombin RGD motif (40). Highly invasive A375 SM melanoma cells adhered strongly to both Th-1 and fibronectin; however, under the same conditions, the non-invasive SB-2 cells failed to adhere. We observed a marked increase in the adherence to both of these matrices of PAR1-transfected SB-2 cells (Fig. 2, *a* and *b*). The level of adherence of these PAR1 transfectants was directly correlated both with their level of PAR1 expression and with their ability to invade the Matrigel barrier. To assure that this increase in their adherence was actually caused by the presence of PAR1, we asked if reducing the expression of PAR1 in malignant cells would reduce the adhesion properties of these cells. To do this, we evaluated the effect of transfection by PAR1 antisense DNA on the adhesion properties of the invasive A375SM cells. We used a 462-base pair oligonucleotide fragment corresponding to the 5' region of PAR1 that included part of the near promoter sequence and the coding region for the internal ligand. We cloned this DNA segment into pCDNA3 mammalian expression vector in an antisense orientation, selecting for stable clones expressing the plasmid bearing the PAR1 antisense DNA as compared with cells transfected by empty vectors or non-transfected control cells. Northern blot analysis (Fig. 2d) indicated that, whereas empty vector transfection (Fig. 2d, B) had no significant effect on PAR1 expression (Fig. 2d, A), clones AS -3 (Fig. 2d, C) and AS-4 (Fig. 2d, D), which were transfected by the PAR1 antisense DNA, did exhibit reduced PAR1 expression. When we analyzed clones AS-3 and AS-4 for their adhesion properties, we found that the cell adherence properties to fibronectin (Fig. 2c) and to Th-1 (data not shown) of both of these clones were significantly lower than those of the A375 SM parental cells.

The organization of the cytoskeleton is critically influenced by adhesion interactions. To explore the effect of PAR1 activation on cytoskeletal reorganization, we plated PAR1-transfected cells (clone 13) and control non-transfected cells (SB-2 cells) on glass coverslips and then treated them with TRAP for various periods of time (Fig. 2e). After activation by TRAP, the cells were permeabilized, fixed, and stained with FITC-labeled phalloidin to detect filamentous actin (F-actin). Cytoskeletal reorganization was observed as early as 15 min after activation by TRAP (Fig. 2e). Thirty to 60 min after PAR1 activation, we observed a transition in the PAR1 transfectants from elongated spindle-like shapes to spreading, jellyfish-like structures. Ninety minutes to 2 h after activation, the cells became rounder and we observed the appearance of a ringlike bundle of actin filaments at the base of the cells (typical of migrating cells). These changes occurred more rapidly and were more dramatic in PAR1-overexpressing cells than they did in the non-transfected control cells. Altogether, these data show that the adhesive properties of tumor cells were affected by changes in PAR1 expression.

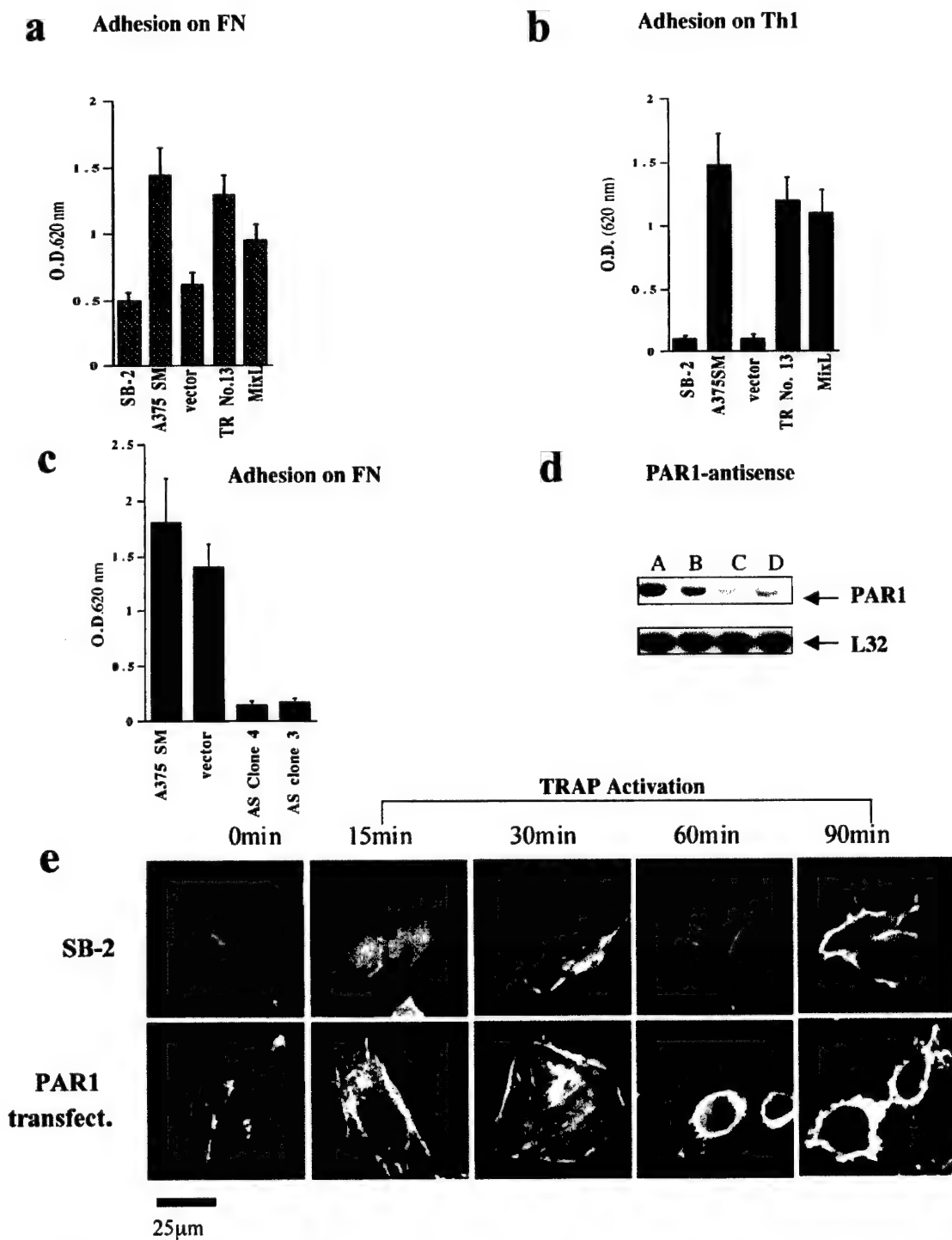*PAR1 Activation Induced Signaling and Led to Establish-*

---

a
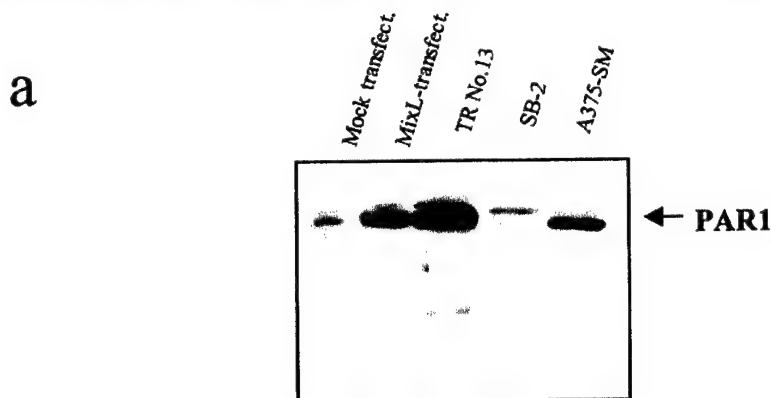
← PAR1

FIG. 1. **Transfection by PAR1 DNA confers invasive properties on non-metatastic melanoma cells.** The expression of PAR1 and cellular invasive properties were measured in SB-2 non-metatastic human melanoma cells, in A375 SM highly metatastic human melanoma cells, in stable PAR1 transfectants clone 13 and clone Mix L, and in mock-transfectant SB-2 cells transfected by empty vectors. Stable PAR1 clones were screened for PAR1 expression (*a*) using anti-PAR1 thrombin receptor mAbs on a Western blot of 50 μg of lysates total protein. *b*, the invasive capabilities of the selected clones were determined by the Matrigel invasion assay. Cell lines marked "*activ.*" were activated by 1 unit/ml thrombin for 1 h before being used in the invasion assay. The data presented here are the averages of data from at least three replicate experiments.

b

Matrigel invasion
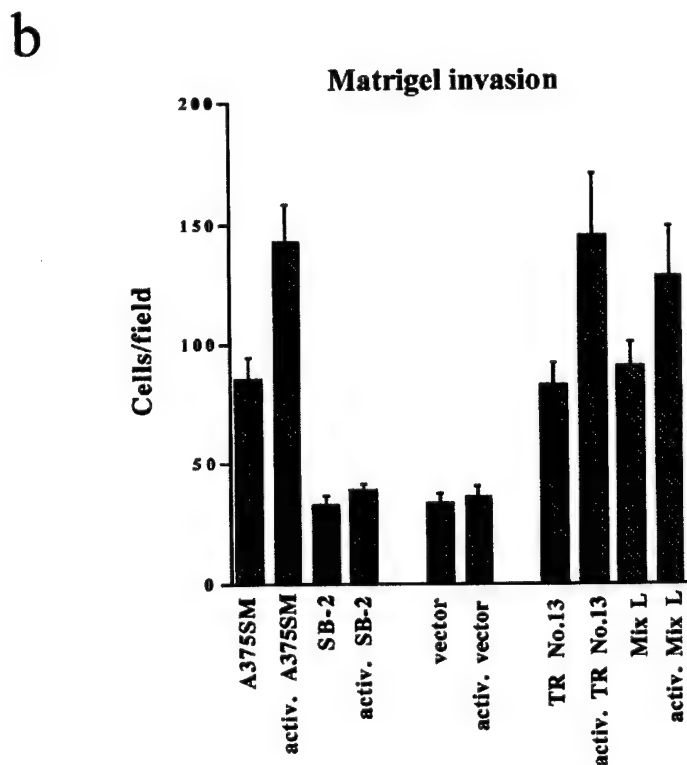
ment of Focal Contacts—Integrin activation typically leads to the assembly of focal adhesion contacts; this takes place by phosphorylation on tyrosine leading to the recruitment of various signaling and structural molecules. FAK and paxillin are the most common signaling components of FAC that are phosphorylated upon integrin activation. To analyze the phosphorylation levels of FAK and paxillin in PAR1-transfected cells, we immunoprecipitated these proteins from cell lysates of either thrombin-activated or non-activated control cells. The immunoprecipitated proteins were blotted onto a nylon membrane and probed with anti-phosphotyrosine mAb to detect their phosphorylation levels. FAK and paxillin proteins from parental, non-invasive SB-2 cells exhibited low levels of phosphorylation (Fig. 3a). On the other hand, FAK and paxillin from PAR1 transfectant cells exhibited increased phosphorylation to high levels similar to those observed in the metastatic line A375 SM (Fig. 3a). By immunofluorescent analysis using anti-phosphotyrosine mAb followed by a Cy-3 fluorescence-labeled secondary antibody, we detected FAC formation as soon as 15 min following PAR1 activation, reaching a maximum

a   Adhesion on FN   **b**   Adhesion on Th1

c   Adhesion on FN   **d**   PAR1-antisense

TRAP Activation

0min   15min   30min   60min   90min

e

SB-2

PAR1
transfect.

25μm

Fig. 2. **Altering PAR1 expression affected cell adhesion and actin fiber re-organization.** Stable PAR1-transfected clones and PAR1 antisense selected clones were analyzed for their adhesive properties to substrates coated with fibronectin (*a* and *c*) or Th-1 RGD peptide (*b*). Cell adhesion was measured by Methylene blue staining of formaldehyde-fixated cells. The eluted stain was detected by spectrophotometry using a $\lambda = $ 620 nm filter. The cells tested (*a* and *b*) were the same as those described in Fig. 1. In addition, we show that in highly metastatic human melanoma A375SM cells stably transfected by PAR1 antisense cDNA (AS clone 4 and AS clone 3), reduced adhesion was observed (*c*) as compared with A375SM cells that were not transfected or that were transfected by an empty vector. These clones exhibited low PAR1 levels as shown by Northern blot analysis (*d*) of RNA samples from A375SM (*A*), A375SM cells transfected with vector only (*B*), AS clone 3 (*C*), and AS clone 4 (*D*). The data presented here are the averages of data from at least three replicate experiments. L32 is a ribosomal RNA that we have used as a housekeeping control gene for these experiments. *e*, SB-2 cells and PAR1 transfectant clone13 were subjected to actin staining by FITC-phalloidin after PAR1 activation by TRAP. Note that the PAR1 transfectants exhibited a more rapid change in actin fiber re-organization and cellular morphology than did the naive SB-2 cells.

FIG. 3. **Activation of PAR1-induced phosphorylation of FAK and paxillin and their recruitment to FACs.** *a*, the tyrosine-phosphorylated levels of immunoprecipitated FAK (*upper section*) and paxillin (*lower section*) were measured by anti-phosphotyrosine mAb (4G10, UBI) in SB-2 naïve cells, in A375SM metastatic cells, and in the stable PAR1 transfectant clone 13. Note that FAK was observed to co-precipitate with paxillin (*lower section*). *b*, immunofluorescent staining of phosphotyrosine in PAR1-transfected clone 13 was performed by specific incubations with mAbs (4G10) at 0, 15, and 60 min. Detection was made by Cy3-labeled goat anti-mouse IgG, using confocal microscopy. Following activation by 100 μM TRAP, the FACs were observed to be enriched with phosphorylated proteins with a peak at 60 min. *c*, immunofluorescent staining with anti-vinculin, anti-FAK, and anti-paxillin in the stable PAR1 transfectant clone 13 activated with 100 μM TRAP for 1 h or not (*NA*). When the cells were stained with anti-FAK and anti-paxillin, distinct FAC staining was observed only in the activated cells. When the cells were stained with anti-vinculin, FACs were detectable at a low level in the non-activated (*NA*); this level was increased following receptor activation by TRAP.
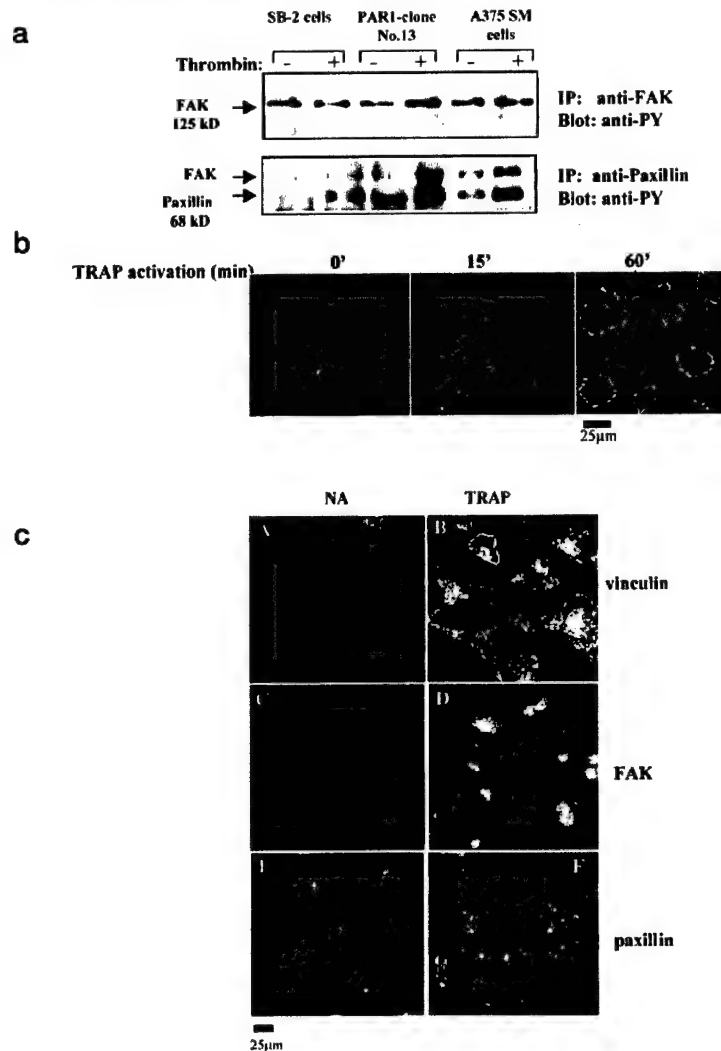
after 60 min (Fig. 3*b*). Together, these data demonstrate that, following activation, overexpressed PAR1 is capable of initiating high levels of integrin signaling.

We characterized FAC assembly by immunofluorescent staining, using mAb anti-vinculin, anti-paxillin, and FAK polyclonal antibodies. Following activation, we observed some FAC formation in all of the cell types that we examined; however, the complexes in the activated PAR1 transfectants were far more distinct and larger than those that we observed in non-activated cells (Fig. 3*c*), in cells that had been transfected by empty vectors, or in cells that had not been transfected (data not shown). In the activated PAR1 clones, vinculin staining of FACs was intense; however, we also observed clear, although less intense, vinculin staining of FACs in activated non-transfected and mock-transfected cells. This may be explained by the fact that, rather than having a signaling function, vinculin functions mainly as a structural protein, and it has been reported to play a role in the maintenance of the FAC and adherence junctions (41). It has also been reported that both vinculin and talin are phosphorylated even under basal conditions (42).

The $\alpha_v\beta_5$ *Integrin Is Specifically Recruited to FACs in Response to PAR1 Activation without Alteration of the Cell-surface Integrin Level*—Having established that signaling was induced

by PAR1 ligand activation, that also led to establishment of focal contacts, we asked whether altering the adhesive phenotype would be accompanied by *de novo* integrin expression. Here we used flow cytometry analysis carried out with a battery of anti-integrin antibodies directed against the $\alpha_v\beta_3$, $\alpha_5\beta_1$, and $\alpha_v\beta_5$ integrins. Following activation, we observed no significant differences between the cell-surface integrin profiles of the PAR1 transfectants and of the parental cells (Fig. 4*a*). Nevertheless, the fact that PAR1 activation did not alter integrin expression does not exclude the possibility of affinity modulation of the integrins in an inside-out manner.

We then asked which of these integrins would respond to PAR1 by participating in the induction of the cytoskeleton signaling events. We examined the cell surface integrins by immunofluorescent visualization before and after PAR1 activation. Although $\alpha_5\beta_1$ and $\alpha_v\beta_3$ (Fig. 4*b*, *B* and *C*) are distributed diffusely over the cell surface both before and after PAR1 activation, after PAR1 activation we found that $\alpha_v\beta_5$ was localized to distinct sites of FACs (Fig. 4*b*, *D*). However, we only detected $\alpha_v\beta_5$ within the focal contacts in the activated PAR1-overexpressing cells (Fig. 4*b*, *E*) but not in the PAR1-transfected cells prior to PAR1 activation cells (Fig. 4*b*, A), nor in the mock transfectants or in the parental non-transfected cells (data not shown). Based on our results, we hypothesized that

PAR1 Activation Promotes Integrin Signaling and Invasion

a

b

25μm
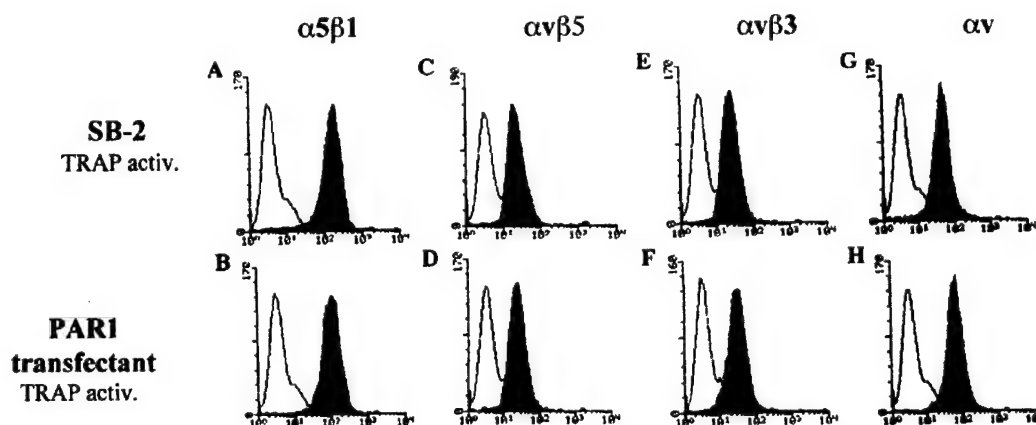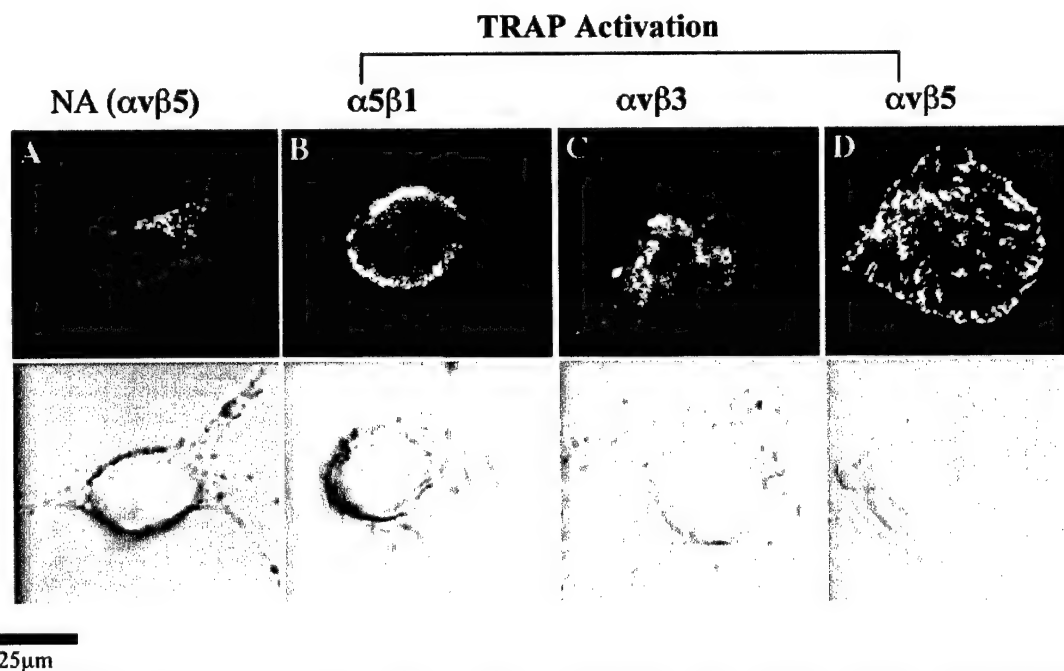
FIG. 4. **PAR1 activation did not alter the levels of integrin expression but did induce $\alpha_v\beta_5$ recruitment to FACs.** *a*, integrin expression levels were measured by flow cytometry in SB-2 naive cells and in PAR1 clone13, each activated with thrombin at a concentration of 1 unit/ml. The levels of $\alpha_5\beta_1$ (*A* and *B*), $\alpha_v\beta_5$ (*C* and *D*), $\alpha_v\beta_3$ (*E* and *F*), and the integrin α_v chain (*G* and *H*) were detected by incubating the cells with the appropriate specific mAb, followed by incubation with FITC-labeled anti-mouse IgG. The *white peaks* correspond to the expression levels of control secondary isotype-specific mouse IgG antibodies. Note that no significant changes were observed in the levels of any of the integrins examined. *b*, the distribution of integrins was detected by immunofluorescent staining (*upper panel*). Cy-3 red fluorescence was visualized by confocal microscopy. The *lower panel* shows the same cells as in the *upper panel*, but visualized by phase-contrast microscopy. Non-activated (*NA*) PAR1 clone 13, stained by anti-$\alpha_v\beta_5$ mAbs revealed a diffused pattern (*A*). After activation by TRAP, the integrin $\alpha_5\beta_1$ was detected in a random perinuclear position (*B*); the integrin $\alpha_v\beta_3$ was randomly scattered over the cell membrane (*C*); the integrin $\alpha_v\beta_5$ was localized to distinct "spikes" of focal adhesion contacts (*D*).

the $\alpha_v\beta_5$ integrin would respond to signals conveyed by the activated PAR1. It seemed that $\alpha_v\beta_5$ was specifically recruited to the focal adhesion contacts, where it played a major role in the reorganization of the cytoskeleton. Our hypothesis was confirmed by the results of the following reciprocal co-precipitation experiments. We analyzed the co-precipitation of paxillin with either $\alpha_v\beta_5$ or with $\alpha_v\beta_3$ in cell lysates of naive SB-2 cells and of the stable PAR1 transfectant clone 13 that was either thrombin-activated or not. The blotted membranes were incubated with the mAb of the anti-β_5 subunit. As we expected, in the parental cells, we found only basal levels of paxillin precipitation with either of the two integrins (Fig. 5, *a* and *b*). In the PAR1 clone 13, we found that paxillin co-precipitated with $\alpha_v\beta_3$ at a low level, and that level was not increased significantly by thrombin activation of PAR1 (Fig. 5*b*). However, in PAR1 clone 13, we did find a high level of co-precipitation of $\alpha_v\beta_5$ with paxillin, and that level was significantly increased by thrombin activation of PAR1. We also analyzed co-immunoprecipitation of paxillin and FAK from cell lysates of SB-2 cells and from the stable PAR1 transfectant clone 13, both of which were thrombin-activated or not. Again, the blotted membranes were incubated with the mAb of anti-β_5 subunit. As we expected, there was no co-immunoprecipitation in the parental cells, whether or not they were activated; however, there was a significant level of co-precipitation of β_5 subunit in the PAR1 clone 13, that was greatly increased upon activation by thrombin (Fig. 5*c*). When, instead of anti-$\alpha_v\beta_5$, we used anti-$\alpha_v\beta_3$ to probe the same blot, we found no evidence of the β_3 subunit (data not shown). These results indicate that $\alpha_v\beta_5$ and the typical signaling molecules, paxillin and FAK, were tightly associated and thus co-precipitated. We found that this kind of association was likely to occur within focal adhesions rather than in other cellular compartments, as demonstrated by the induced assembly and signaling of FACs. Furthermore, this association appeared to be labile and seemed to occur in response to PAR1 activation, indicating that the $\alpha_v\beta_5$ integrin was present within newly assembled FACs. Our data do not exclude the possibility that $\alpha_v\beta_3$ is present on the cell surface. Our data do suggest, however, that the $\alpha_v\beta_3$ integrin probably does not cooperate with PAR1-specific signaling to induce the cellular responses described here.

To substantiate the cooperative cross-talk and the recruitment of $\alpha_v\beta_5$ following PAR1 activation, we used a truncated form of PAR1, consisting of the extracellular and seven transmembrane domains but lacking the entire cytoplasmic portion of the receptor, and compared its function to the intact receptor. We carried out these experiments in MCF7 cells, which are non-invasive cells that naturally express very low levels of PAR1. These parental cells were transiently transfected with cDNA coding for either the intact PAR1 or truncated PAR1; 48 h after transfection, the transient transfectants were either activated or not and then subjected to immunoprecipitation analysis as described above. In lysates of the MCF7 PAR1 transient transfectants, we detected high levels of co-precipitation of FAK, paxillin, and $\alpha_v\beta_5$ after PAR1 activation by thrombin but not without activation. In lysates of truncated PAR1 transfectants, we observed no co-precipitation of FAK with paxillin, and $\alpha_v\beta_5$ regardless of whether the cells were thrombin activated or not (Fig. 5*d*, *upper panel*). In the PAR1 transfectants, tyrosine phosphorylated paxillin co-precipitated with $\alpha_v\beta_5$ and the level of this precipitation increased following thrombin activation of PAR1; in truncated PAR1-transfected cells, we detected only minor levels of phosphorylated paxillin with or without thrombin activation (Fig. 5*d*, *lower panel*). As seen by the results of the flow cytometry (FACS) analysis (Fig. 5*e*), the failure to immunoprecipitate FAK by anti-$\alpha_v\beta_5$ in

PAR1-truncated transfectants did not result from the inability to express properly on the cell surface. Transfectants of either PAR1 (Fig. 5*e*, *A*) or truncated PAR1 (Fig. 5*e*, *B*) showed cell surface expression of the truncated receptor protein as determined by flow cytometry (FACS) analysis (Fig. 5*e*). Using anti-PAR1 WEDE15 mAbs, we found similar levels of expression in both the PAR1 (Fig. 5*e*, *A*, *second peak*) and the truncated PAR1 (Fig. 5*e*, *B*, *second peak*) transfectants, relative to the expression levels in naive cells (Fig. 5*e*, *A* and *B*, *first peaks*). We obtained similar results when we compared the levels of expression of the transfectants (Fig. 5*e*, *C* and *D*, *second peaks*) to those of empty vector-transfected cells (Fig. 5*e*, *C* and *D*, *first peaks*). The results of these experiments strongly support the notion that following activation the PAR1 cytoplasmic tail recruits and activates the $\alpha_v\beta_5$ integrin. That the PAR1 molecule participates in other signaling activities is supported by our finding that, although Shc was phosphorylated in the presence of the full-length activated PAR1, this was not the case in the presence of the activated truncated PAR1 (data not shown). We conclude that, although, like the full-length PAR1, the truncated PAR1 is expressed and assembled on the cell surface, unlike the full-length PAR1, the truncated PAR1 is incapable of carrying out PAR1 signaling. To ascertain that in fact the $\alpha_v\beta_5$ integrin may cooperate with PAR1 during tumor invasion, we asked whether neutralizing the activity of the $\alpha_v\beta_5$ integrin would affect the invasive properties of the highly invasive A375 SM cells. A375 SM cells were activated or not with 1 unit/ml thrombin; the activated cells were then either not treated at all or treated with anti-$\alpha_v\beta_5$-blocking mAbs antibodies (clone P1F6) or with nonspecific IgG. The cells were then subjected to a Matrigel invasion assay. As one can see, PAR1 activation further induced the invasive properties of the cells by 60% while the addition of anti-$\alpha_v\beta_5$ antibodies attenuated this induction; the addition of a non-related IgG led to no significant effect (Fig. 5*f*).

DISCUSSION

In this study, we have shown that changes in the expression of PAR1 in a cell affect its invasive capabilities. These changes come about through the specific recruitment of the $\alpha_v\beta_5$ integrin, through cytoskeletal reorganization, and through distinct signaling at FACs. The fact that PAR1 alters the invasive properties of tumor cells reinforces our initial observations that PAR1 expression correlates with the invasive potential of both the malignant invasion processes of breast carcinoma (3) and the physiological invasion processes of placenta trophoblast implantation (3)[8] emphasizing the central role of PAR1 during invasion. The on-going process of invasion by cells is characterized by extensive proteolytic remodeling, in part by serine proteases, of the tumor microenvironment (1, 2). Serine proteases also serve as ligands for several cell-surface receptors, among which is uPAR, which, through binding uPA, efficiently converts plasminogen to plasmin (11). TF is another protease cell surface receptor that binds factor VII, thereby initiating the coagulation pathway during perivascular hemostasis (43). It is interesting that, in addition to their involvement in hemostasis, these receptors are also implicated as central players in tumor progression and metastasis (8–10). The extracellular proteolytic activation of factor VII by TF is also responsible for the generation of thrombin from circulating plasma prothrombin (44, 45). In fact, thrombin production is probably the direct result of disseminated overactivation of the coagulation system, a widely described pathology among cancer patients (46). The abundant localization of either soluble or immobilized thrombin in the vicinity of the tumor milieu enables the excessive activation of PAR1 and the subsequent cellular response during invasion. In fact, although the repertoire of signaling

PAR1 Activation Promotes Integrin Signaling and Invasion

PAR1 activation promotes integrin signaling and invasion
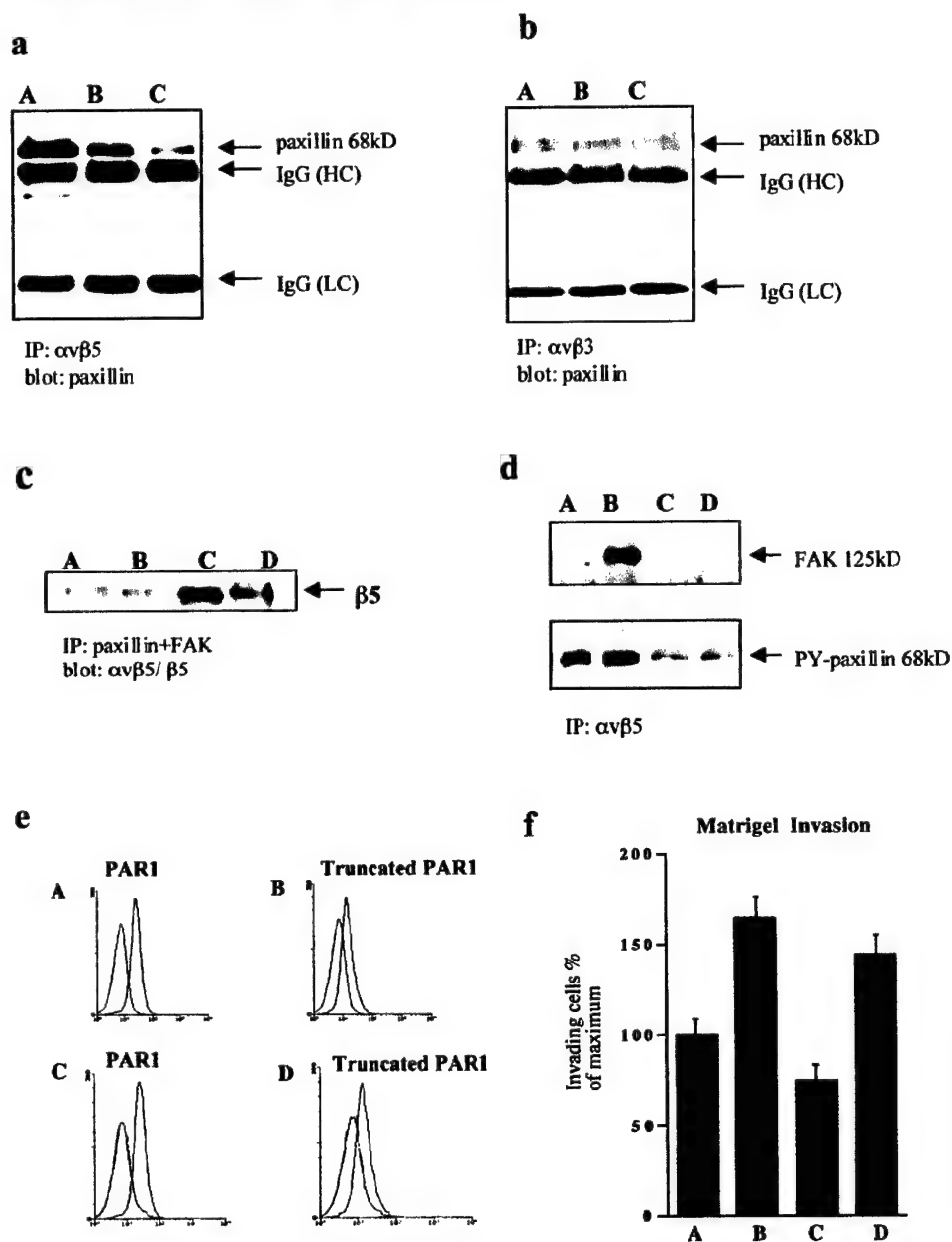
FIG. 5. **Activation of full-length PAR1 but not of truncated PAR1 led to the co-precipitation of $\alpha_v\beta_5$ with paxillin and FAK and reduced invasiveness in the presence of anti-$\alpha_v\beta_5$ antibodies.** Co-precipitation of paxillin with $\alpha_v\beta_5$ (*a*) or with $\alpha_v\beta_3$ (*b*) was measured in cells lysates of naive SB-2 cells (*C*) and of a stable PAR1 transfectant clone 13 that was either thrombin-activated (*A*) or not (*B*). *c*, paxillin and FAK were immunoprecipitated from cell lysates of SB-2 cells that had been thrombin-activated (*A*) or not (*B*) and from the stable PAR1 transfectant clone 13 that was either thrombin-activated (*C*) or not (*D*). The blotted membrane was incubated with anti-β_5 subunit mAb. *d*, non-invasive MCF7 cells, naturally expressing very low levels of PAR1, were transfected with cDNA expression vectors coding either for PAR1 or for truncated PAR1. In lysates of the PAR1 transfectants, co-precipitation of FAK and paxillin was detected after PAR1 activation by thrombin (*B*) but not without activation (*A*). In lysates of truncated PAR1 transfectants, no co-precipitation of FAK with paxillin with $\alpha_v\beta_5$ was observed regardless of whether the cells were thrombin-activated (*D*) or not (*C*). Tyrosine-phosphorylated paxillin co-precipitated with $\alpha_v\beta_5$ (*lower panel*) in PAR1-transfected cells (*A*); the level of this precipitation increased following thrombin activation of PAR1 (*B*); in truncated PAR1-transfected cells, only minor levels of phosphorylated paxillin were detected with (*D*) or without (*C*) thrombin activation. *e*, PAR1 expression levels were measured by FACS analysis using anti PAR1 mAb (WEDE15, Immunotech, Cedex, France), followed by incubation with FITC-labeled anti-mouse IgG. The analysis was carried out on MCF7 cells following transfection by DNA coding for the full-length PAR1 (*A* and *C*) or for the truncated PAR1 (*B* and *D*). Their levels were compared with non-transfected cells (*first peak, B* and *A*). This is true also when PAR1 or truncated PAR1 expression was measured relative to empty vector-transfected cells (*first peak, C* and *D*, respectively). *f*, A375SM cells were activated with 1 unit/ml thrombin (*B–D*) or not (*A*). The activated cells were then treated with 20 μ g/ml either anti-$\alpha_v\beta_5$-blocking mAbs (*C*) or nonspecific IgG (*D*). The treated cells were then subjected to a Matrigel invasion assay. The data presented here are the averages of data from at least three replicate experiments. One hundred percent invasion by the metastatic cells corresponded to 48 ± 3 invading cells as compared with 17 ± 1.5 invading cells by SB-2 non-metastatic cells (data not shown).

pathways is limited, it can be harnessed to integrate the information obtained from multiple receptors for a wide range of cellular responses. Here we have presented evidence showing that the overexpression of PAR1 increases the invasiveness of melanoma cells (Figs. 1b and 5f) and is also associated with an increase in the adhesion properties of the cell (Fig. 2, a–c). The activation of PAR1 resulted in the phosphorylation of the focal adhesion proteins FAK and paxillin that are typical of integrin signaling (Fig. 3a). Although the levels of the cell surface integrins were not affected (Fig. 4a), there was notable change in their mode of distribution. In particular, in response to PAR1 activation, the integrins $\alpha_v\beta_3$ and $\alpha_5\beta_1$ remained diffusely distributed but, in contrast, we found that the integrin $\alpha_v\beta_5$ was uniquely recruited to the sites of focal adhesion contacts (Fig. 4b).

It is well established that there is cooperation between integrins and other cell surface receptors, and further, that this cooperation may operate at several levels (47–50). Physical interactions between the extracellular domains of integrins and non-integrin receptors may result in mutual or sequential activation. For example, the results of several parallel studies demonstrate a physical link of uPAR with the integrin $\alpha_3\beta_1$ in keratinocytes (51), with the β_2 integrin Mac-1 in leukocytes (52), and with $\alpha_v\beta_5$ in breast cancer (53). The interaction of uPAR with integrin β_1 has also been shown to involve the functional cooperation of integrins with cell surface receptors via caveolin in a manner dependent on the conformational state of the receptors (54, 55). Alternatively, the activation state of integrins can be modified in an "inside-out" manner. Internal signals conveyed by intersecting cascades react with the cytoplasmic domain of the integrin β subunit and thereby increase the affinity to their ligands of the extracellular portion of the integrins. Activation of G-protein-coupled receptor initiates a signal transmission through the C-terminal cytoplasmic domain of the receptor that leads to the assembly of adaptor proteins, non-receptor tyrosine kinases, and small G-proteins. Signals that are transduced in forking pathways, like Ras-Raf-mitogen-activated protein kinase and phosphatidylinositol 3-kinase-Akt/PKB, are also largely shared by integrin and thymidine kinase receptors. In endothelial cells (56), astrocyte cell rounding (57), and nuerite retraction (58), cytoskeletal responses to thrombin are known to involve the activation of the Ras-dependent ERK1/2 mitogen-activated protein kinase pathway during gap formation. These responses have been found to be Rho-dependent and require Rho-specific guanine nucleotide exchange factors (57, 59). More specifically, the Rho-dependent pathway controls barrier maintenance and stress fiber formation while Rac induction and myosin light chain kinase activation are both implicated in barrier dysfunction (56). Together, these facts imply that integrin-related signaling can be intersected by PAR1 signaling at the intracellular level.

Thrombin contains a cryptic RGD epitope that can potentially be recognized by integrins (40). The transient binding of thrombin to its receptor, prior to receptor cleavage, may serve as an RGD-exposing event that enables integrin binding during PAR1 activation. Thus, it seems that, at least theoretically, cooperation between PAR1 and the vitronectin receptor $\alpha_v\beta_5$ may occur at the extracellular level. Using a truncated PAR1 construct that lacks the entire cytoplasmic tail domain, we demonstrated here that it was the cytoplasmic portion of the PAR1 molecule that was responsible for cooperation with the $\alpha_v\beta_5$ integrin. We found that the truncated PAR1 was unable to transmit intracellular signals, and therefore, was unable to recruit $\alpha_v\beta_5$ and to initiate the typical integrin-associated signals. The other vitronectin receptor, $\alpha_v\beta_3$, has been widely

implicated in both angiogenesis and melanoma cell invasion and metastasis (60, 61). Nevertheless, many tumor cells that lack $\alpha_v\beta_3$ can still readily metastasize (62). In cells that express both $\alpha_v\beta_5$ and $\alpha_v\beta_3$, $\alpha_v\beta_3$ is constitutively capable of inducing cell spreading and migration, while $\alpha_v\beta_5$ cannot promote cell spreading and migration without an additional exogenous soluble factor (60, 63). Based on our results, we propose that during the invasion process $\alpha_v\beta_5$ is the dominant integrin involved in PAR1-ECM signaling interactions. This is consistent with previous suggestions (64) that $\alpha_v\beta_5$ has a role in mediating human keratinocyte locomotion. Filardo *et al.* (36) also showed that $\alpha_v\beta_5$, as the sole integrin expressed in melanoma cells, could promote cell spreading and migration in cooperation with insulin-like growth factor signaling. It has also been postulated that $\alpha_v\beta_5$-mediated cell migration is protein kinase C θ-dependent (66). Whether, as has been shown for endothelial cell migration (67), PAR1-mediated association of $\alpha_v\beta_5$ during tumor invasion is under the regulation of protein kinase C θ associated to TAP20 (theta-associated protein) remains to be determined.

The adhesion of tumor cells to the basement membrane is an essential step in the process of invasion. In contrast to the passive, non-active nature of non-malignant cells, the dynamic nature of tumor cell adherence to the underlying ECM precedes matrix degradation and migration. The interactions of the cell matrix involve the activation of integrins as well as the initiation, through focal adhesion structures, of signaling cascades that lead to cytoskeletal reorganization. This has been shown to be the case during tumor progression where TF supports cell adhesion, migration, and spreading through the action of the cytoplasmic portion of the TF molecule (10). The interaction of uPA with its cell surface receptor uPAR is necessary for vitronectin-dependent human pancreatic carcinoma (FG) cell adhesion and migration mediated via the $\alpha_v\beta_5$ integrin (65). The convergence point of the PAR1 and the $\alpha_v\beta_5$ signaling pathways is not yet known and is currently under study in our laboratory. Nevertheless, the data that we have presented here suggest that this unique mode of cooperation specifically promotes the invasive properties of tumor cells. We believe that the PAR1 and the $\alpha_v\beta_5$ signaling pathways that we have studied here may prove to be crucial for other PAR1 functions in vascular biology and embryonic development.

REFERENCES

1. Mignatti, P., and Rifkin, D. B. (1993) *Physiol. Rev.* **73**, 161–195
2. Johnsen, M., Lund, L. R., Romer, J., Almholt, K., and Dano, K. (1998) *Curr. Opin. Cell Biol.* **10**, 667–671
3. Even-Ram, S., Uziely, B., Cohen, P., Grisaru-Granovsky, S., Maoz, M., Ginzburg, Y., Reich, R., Vlodavsky, I., and Bar-Shavit, R. (1998) *Nat. Med.* **4**, 909–914
4. Carroll, V. A., and Binder, B. R. (1999) *Semin. Thromb. Hemost.* **25**, 183–197
5. Kurschat, P., Zigrino, P., Nischt, R., Breitkopf, K., Steurer, P., Klein, C. E., Krieg, T., and Mauch. C. (1999) *J. Biol. Chem.* **274**, 21056–21062
6. Al-Mondhiry, H. (1975) *Thromb. Diath. Haemorrh.* **34**, 181–193
7. Shoji, M., Hancock, W. W., Abe, K., Micko, C., Casper, K., Baine, R. M., Wilcox, J. N., Danave, I., Dillehay, D. L., Matthews, E., Contrino, J., Morrissey, J. H., Gordon, S., Edington, T. S., Kudryk, B., Kreutzer, D. L., and Rickles, F. R. (1998) *Am. J. Pathol.* **152**, 399–411
8. Bromberg, M. E., Konigsberg, W. H., Madison, J. F., Pawashe, J. F., and Garen, A. (1995) *Proc. Natl. Acad. Sci. U. S. A.* **92**, 8205–8209
9. Mueller, B. M., and Ruff, W. (1998) *J. Clin. Invest.* **101**, 1372–1378
10. Ott, I., Fischer, E. G., Miyagi, Y., Mueller, B. M., and Ruff, W. (1998) *J. Cell Biol.* **40**, 1241–1253
11. Vassali, J. D., Sappino, A. P., and Belin, D. (1991) *J. Clin. Invest.* **88**, 1067–1072
12. Wei, Y., Lukashev, M., Simon, D. I., Bodary, S. C., Rosenberg, S., Doyle, M. V., and Chapman, H. A. (1996) *Science* **273**, 1551–1555
13. Brooks, P. C., Montgomery, A. M., Rosenfeld, M., Reisfeld, R. A., Hu, T., Klier, G., and Cheresh, D. A. (1994) *Cell* **79**, 1157–1164
14. Kahn, M. L., Hammes, S. R., Botka, C., and Coughlin, S. R. (1998) *J. Biol. Chem.* **273**, 23290–23296

15. Cupit, L. D., Schmidt, V. A., and Bahou, W. F. (1999) *Trends Cardiovasc. Med.* **9,** 42–48
16. Vu, T. K., Hung, D. T., Wheaton, V. I., and Coughlin, S. R. (1991) *Cell* **64,** 1057–1068
17. Nystedt, S., Emilsson, K., Larsson, A. K., Strombeck, B., and Sundelin, J. (1995) *Eur. J. Biochem.* **232,** 84–89
18. Ishihara, H., Connolly, A. J., Zeng, D., Kahn, M. L., Zheng, Y. W., Timmons, C., Tram, T., and Coughlin, S. R. (1997) *Nature* **386,** 502–506
19. Liotta, L. A., Rao, C. N., and Barsky, S. H. (1983) *Lab. Invest.* **49,** 636–649
20. Crowe, D. L., and Shuler, C. F. (1999) *Histol. Histopathol.* **14,** 665–671
21. Giancotti, F. G., and Ruoslahti, E. (1999) *Science* **285,** 1028–1032
22. Bissell, M. J., Weaver, V. M., Lelievre, S. A., Wang, F., Petersen, O. W., and Schmeichel, K. L. (1999) *Cancer Res.* **59,** 1757s–1763s; Discussion 1763s–1764s
23. Hynes, R. O. (1992) *Cell* **69,** 11–25
24. Clark, E. A., and Brugge, J. S. (1995) *Science* **268,** 233–239
25. Schwartz, M. A., Schaller, M. D., and Ginsberg, M. H. (1995) *Annu. Rev. Cell Dev. Biol.* **11,** 549–599
26. Howe, A., Aplin, A. E., Alahari, S. K., and Juliano, R. L. (1998) *Curr. Opin. Cell Biol.* **10,** 220–231
27. Gilmore, A. P., and Burridge, K. (1996) *Structure* **4,** 647–651
28. Wang, N., Butler, J. P., and Ingber, D. E. (1993) *Science* **260,** 1124–1127
29. Felsenfeld, D. P., Choquet, D., and Sheetz, M. P. (1996) *Nature* **383,** 438–440
30. Sheetz, M. P., Felsenfeld, D. P., and Galbraith, C. G. (1998) *Trends Cell Biol.* **8,** 51–54
31. Burridge, K., Turner, C. E., and Romer, L. H. (1992) *J. Cell Biol.* **119,** 893–903
32. Hildebrand, J. D., Schaller, M. D., and Parsons, J. T. (1995) *Mol. Biol. Cell* **6,** 637–647
33. Chen, H. C., Appeddu, P. A., Parsons, J. T., Hildebrand, J. D., Schaller, M. D., and Guan, J. L. (1995) *J. Biol. Chem.* **270,** 16995–16999
34. Schlaepfer, D. D., Hauck, C. R., and Sieg, D. J. (1999) *Prog. Biophys. Mol. Biol.* **71,** 435–478
35. Bockholt, S. M., and Burridge, K. (1993) *J. Biol. Chem.* **268,** 14565–14567
36. Filardo, E. J., Deming, S. L., and Cheresh, D. A. (1996) *J. Cell Sci.* **109,** 1615–1622
37. Ishida, T., Ishida, M., Suero, J., Takahashi, M., and Berk, B. C. (1999) *J. Clin. Invest.* **103,** 789–797
38. Ojaniemi, M., and Vuori, K. (1997) *J. Biol. Chem.* **272,** 25993–25998
39. Albini, A. (1998) *Pathol. Oncol. Res.* **4,** 230–241
40. Bar-Shavit, R., Sabbah, V., Lampugnani, M. G., Marchisio, P. C., Fenton, I. I. J. W., Vlodavsky, I., and Dejana, E. (1991) *J. Cell Biol.* **112,** 335–344
41. Rudiger, M. (1998) *Bioessays* **20,** 733–740
42. Schaphorst, K. L., Pavalko, F. M., Patterson, C. E., and Garcia, J. G. (1997) *Am. J. Respir. Cell Mol. Biol.* **17,** 443–455
43. Ruf, W., and Edgington, T. S. (1994) *FASEB J.* **8,** 385–390
44. Cavanaugh, P. G., Sloane, B. F., and Honn, K. V. (1988) *Haemostasis* **18,** 37–46
45. Zucker, S., Mirza, H., Conner, C. E., Lorenz, A. F., Drews, M. H., Bahou, W. F., and Jesty, J. (1998) *Int. J. Cancer* **75,** 780–786
46. Rickles, F. R., Edwards, R. L., Barb, C., and Cronlund, M. (1983) *Cancer* **51,** 301–307
47. Plopper, G. E., McNamee, H. P., Dike, L. E., Bojanowski, K., and Ingber, D. E. (1995) *Mol. Biol. Cell* **6,** 1349–1365
48. Miyamoto, S., Teramoto, H., Gutkind, J. S., and Yamada, K. M. (1996) *J. Cell Biol.* **135,** 1633–1642
49. Baron, V., Calleja, V., Ferrari, P., Alengrin, F., and Van Obberghen, E. (1998) *J. Biol. Chem.* **273,** 7162–7168
50. Schneller, M., Vuori, K., and Ruoslahti, E. (1997) *EMBO J.* **16,** 5600–5607
51. Ghosh, S., Brown, R., Jones, J. C., Ellerbroek, S. M., and Stack, M. S. (2000) *J. Biol. Chem.* **275,** 23869–23876
52. Simon, D. I., Wei, Y., Zhang, L., Rao, N. K., Xu, H., Chen, Z., Liu, Q., Rosenberg, S., and Chapman, H. A. (2000) *J. Biol. Chem.* **275,** 10228–10234
53. Carriero, M. V., Del Vecchio, S., Capozzoli, M., Franco, P., Fontana, L., Zannetti, A., Botti, G., D'Aiuto, G., Salvatore, M., and Stoppelli, M. P. (1999) *Cancer Res.* **59,** 5307–5314
54. Wei, Y., Yang, X., Liu, Q., Wilkins, J. A., and Chapman, H. A. (1999) *J. Cell Biol.* **144,** 1285–1294
55. Chapman, H. A. (1997) *Curr. Opin. Cell Biol.* **9,** 714–724
56. Vouret-Craviari, V., Boquet, P., Pouyssegur, J., and Van Obberghen-Schilling, E. (1998) *Mol. Biol. Cell* **9,** 2639–2653
57. Majumdar, M., Seasholtz, T. M., Goldstein, D., de Lanerolle, P., and Brown, J. H. (1998) *J. Biol. Chem.* **273,** 10099–10106
58. Jalink, K., van Corven, E. J., Hengeveld, T., Morii, N., Narumiya, S., and Moolenaar, W. H. (1994) *J. Cell Biol.* **126,** 801–810
59. Majumdar, M., Seasholtz, T. M., Buckmaster, C., Toksoz, D., and Brown, J. H. (1999) *J. Biol. Chem.* **274,** 26815–26821
60. Brooks, P. C., Klemke, R. L., Schon, S., Lewis, J. M., Schwartz, M. A., and Cheresh, D. A. (1997) *J. Clin. Invest.* **99,** 1390–1398
61. Seftor, R. E. (1998) *Am. J. Pathol.* **153,** 1347–1351
62. Nip, J., and Brodt, P. (1995) *Cancer Metastasis Rev.* **14,** 241–252
63. Klemke, R. L., Yebra, M., Bayna, E. M., and Cheresh, D. A. (1994) *J. Cell Biol.* **127,** 859–866
64. Kim, J. P., Zhang, K., Chen, J. D., Kramer, R. H., and Woodley, D. T. (1994) *J. Biol. Chem.* **269,** 26926–26932
65. Yebra, M., Goretzki, L., Pfeifer, M., and Mueller, B. M. (1999) *Exp. Cell. Res.* **250,** 231–240
66. Tang, S., Morgan, K. G., Parker, C., and Ware, J. A. (1997) *J. Biol. Chem.* **272,** 28704–28711
67. Tang, S., Gao, Y., and Ware, J. A. (1999) *J. Cell Biol.* **147,** 1073–1084

The pattern of Protease Activated Receptors (PARs) expression during early trophoblast development

Sharona Cohen Even-Ram,[#] Sorina Grisaru-Granovsky,[#]

Diana Pruss,[1] Miriam Maoz, Zaidoun Salah, Yin Yong-Jun, and Rachel Bar -Shavit

Depts. of Oncology, Pathology,[1] Hadassah University Hospital,

P.O.B. 12000, Jerusalem 91120, Israel

Short title: PARs expression in normal and in pathological (Complete Hydatidiform Mole) placenta

[#]These authors should be considered as equal first authors.

*Word count of the text - 2, 317

Declaration

1. No information or prior duplication of the present work was submitted or published elsewhere.

2. No conflict of interest will result from publication of this work.

3. The manuscript has been read and approved by all the authors. The requirements for authorship have been met and each authors agrees that the manuscript represent an honest work.

4. Correspondence should be addressed to:

R. Bar-Shavit, Ph.D.

Department of Oncology,
Hadassah - University Hospital,
POB 12000 Jerusalem 91120, Israel
Tel: 972-2-677-7563
Fax: 972-2-642-2794

E-mail: barshav@md2.huji.ac.il

Abstract

Human fetal development depends on the ability of the embryo to gain access to maternal circulation. Thus, specialized stem cells of the newly formed placenta, named trophoblast invade the uterus and its arterial network to establish an efficient feto-maternal molecular exchange. To accomplish this task, trophoblast differentiation during the first trimester of pregnancy, involves cell proliferation, invasion and extracellular matrix (ECM) remodeling. Trophoblast invasion shares many features with tumor cell invasion, with the distinction that it is strictly spatially and temporally controlled. We have previously demonstrated that PAR1, the first member of the Protease Activated Receptor (PAR) family, plays a central role in tumor cell invasion. In the present study we have examined the pattern of expression of PAR1 and other PAR family candidates during early human placental development. We show that PAR1 and PAR3 were highly and spatially expressed between the 7th and 10th weeks of gestation but not at the 12th week and thereafter. Pathological trophoblast cells may appear occasionally and cause a trophoblastic disease known as Complete Hydatidiform Mole (CHM). Likewise, high expression levels of PAR1 and PAR3 were observed in the cytotrophoblast cells of CHM biopsy specimens as compared to minimal levels in the normal age-matched placenta. Together, our data suggest the involvement of PAR1 and at least PAR3 in the restricted and unrestricted pathological trophoblast invasion process.

Key words: PARs, thrombin-receptor, human trophoblast cells, gestational trophoblastic disease, proteases, extracellular matrix

Introduction

During early human placentation, specialized placenta epithelial cells, termed

cytotrophoblast (CTB) differentiate, proliferate, and invade the uterine wall and the spiral arteries

(1). Although poorly understood, the molecular basis of CTB invasion shares many features with

the process of tumor cell invasion (1-3). A subpopulation of CTB cells must detach from the

fetal basement membrane where it currently resides and invade the uterine wall where it can

survive. Cytotrophoblast cells in anchoring villi either fuse to form the syncytiotrophoblast layer

or break through the syncytium to form columns of extravillous trophoblast (EVT) cells that

connect the embryo to the uterine wall. Since the tumor-like properties of this subset population

are critical for the appropriate fetal maternal interactions the molecular mechanisms involved are

carefully programmed and tightly regulated (4). Furthermore, the etiological basis of diseases

during pregnancy involves unregulated trophoblastic invasion. Shallow invasiveness of the uterus

leads to preeclampsia and restriction of fetal growth (5) while excessive proliferation and invasion

may result in gestational trophoblastic disease and choriocarcinoma (6).

The interaction of differentiating CTB cells with the surrounding ECM is a critical feature

of the invasion program identified by the specific integrin switching profile (5, 7, 8). CTB cells

within the uterine spiral arteries, however express a typical vascular integrin profile such as VE-

cadherin, VCAM-1 and PECAM-1 of the IgG family as the integrins $\alpha v\beta 3$ and $\alpha 1\beta 1$ (5, 7, 9). A

potent marker for cytotrophoblast invasion has been recently assigned to the activated form of

focal adhesion kinase (FAK), the major signaling molecule of integrin clustering. While the

expression of FAK is found at all stages of placenta differentiation, the auto-phosphorylated

FAK (pY397FAK) was specifically expressed under conditions facilitating CTB invasion and

inhibited under conditions that abrogated CTB invasion (10, 11).

In the process of trophoblast invasion, both serine- and matrix metallo-proteases (MMPs)

play a central role in the remodeling of the placenta microenvironment as well as in trophoblast

outgrowth (12, 13). One outcome of the enhanced proteolytic function is the activation of a family

of cell surface receptors, collectively named as Protease-Activated Receptors (PARs) (14).

Presently, there are four members of the PAR family termed PAR 1- 4. While PAR 1, 3, and 4 are

activated by thrombin (15), PAR2 is activated by trypsin, tryptase as well as the coagulation

factors VIIa and Xa but not by thrombin (16). This family shares a similar mode of activation, the

exposure of an internal ligand following a unique cleavage site within the N-terminal exo-domain

of the seven transmembrane receptor. Thus PARs are G-coupled receptors that carry their own

ligand and are activated either by cleavage of thrombin or by tethered binding of a peptide that

mimicks the internal ligand sequence.

We have previously shown that PAR1 is overexpressed in biopsy specimens of breast

carcinomas as well as in a collection of differentially metastatic cell lines (17). Activation of

PAR1 led to focal adhesion complex formation, cytoskeletal re-organization and the recruitment of $\alpha_V\beta_5$ integrin into focal adhesion sites (18). This study, was undertaken to assess the expression pattern of three members of the PAR family (PAR1-3), during of the first trimester of pregnancy. The expression levels of PARs in proliferating and potentially invasive trophoblast cells of Complete Hydatidiform Mole (CHM) (6) will assist in evaluating the significance of PARs involvement in early normal placenta development.

Methods

Placental specimens.

Placental specimens were obtained from elective terminations of pregnancies as described

(19). Paraffin-embedded Complete Hydatidiform Mole (CHM) biopsies were obtained from the

Hadassah - Hospital, Department of Pathology archives.

PCR detection of PAR levels

RNA was isolated using TRI-REAGENT (SIGMA) from pure villi preparation that had been

dissected from the placental structures under a dissecting microscope (Zeiss, Schott KL1500,

Germany). cDNA was reverse-transcribed by MMLV reverse-transcriptase (Promega, Wisconsin,

USA) and amplified by PCR using the following sets of primers:

PAR1: 1) 5' ATG GGA TTC TGC CAC CTT AGA TCC 3' (sense)
      2) 5' ATG GGA TCC GGA GGC TGA CTA CAA 3' (antisense)
PAR2: 1) 5' TGC TCC GAT ATC TTT GTA CAG GAC 3' (sense)
      2) 5' TAG GTG GTA GGA AAG CTT CAG GGG 3' (antisense)
PAR3: 1) 5' GCT GAC ACA TGG AAC TGA GGT 3' (sense)
      2) 5' GAG GTA GAT GGC AGG TAT CAG 3' (antisense)

These primers were selected to include the coding region for the specific internal ligand of each

of the genes which is a unique, conserved region.

Northern blot analysis. Par1 mRNA expression was carried out as previously described (17).

In-situ hybridization

Specimens of placenta (8 samples for each week of gestation) were fixed in 4%

paraformaldehyde and embedded in paraffin. Fifteen CHM biopsies were selected from the

Pathology Department archives. Hybridization was carried out as previously described (17).

Immunohistochemistry

Placental tissue samples of 6-15weeks were fixed in 4% paraformaldehyde, and processed as

described (17). The tissue was further denatured for 4 min in a microwave oven in a citrate

buffer (0.01mol/L, pH6.0), then blocked in 0.2% glycine, 3% H_2O_2 in methanol and 5% goat

serum. The sections were incubated overnight at 4°C with either an antibody to PAR1 [(C-18):

sc-8202, Santa Cruz Biotechnology, Inc, CA USA)] at 1 μg/ml, or a control IgG at the same

concentration as anti-PAR1. Detection was performed using a horseradish peroxidase-

conjugated goat-anti-mouse IgG + IgM antibody (Jackson, Bar-Harbor, ME), followed by

Zymed aminoethyl carbozole (AEC) substrate kit (Zymed, South San Francisco, CA) and

counter stained with Mayer's hematoxylin.

Western Blot Analysis

Placental villi were solubilized in lysis buffer as described (19). Membranes (Immobilon - P ;

Millipore) were blocked and probed with 1 μg/ml of anti PAR3 receptor (anti-human rabbit

polyclonal IgG) and detected as described (17).

Results

PAR family expression in human placental villi

To study the pattern of expression and specific localization of *Par1* we have performed *in situ* hybridization analysis. *Par1* mRNA was detected predominantly in the cytotrophoblast layer and not in the syncytiotrophoblast layer (Fig. 1 IC, insert). This expression was found in the 7th, 8th, and 10th week specimens, compatible with the Northern blot and RT-PCR data (Fig1 II a&b). Minimal expression was observed at weeks 12 and 14 of gestation and thereafter. Quantification of the PAR family (*Par1-3*) mRNA was carried out via RT-PCR and Northern blot analysis (Fig. 1 II and Fig. 2). *Par1* expression was first observed in the 7th week of gestation and peaked in the 8th and 10th weeks (Fig. 1 II). By the 12th week, *Par1* expression was no longer detectable (Fig. 1 IIa), and remained undetectable until at least the end of the first trimester (data not shown). The same pattern of *Par1* mRNA levels was detected using Northern blot analysis (Fig. 1 IIb). The levels of *Par2* mRNA on the other hand, as detected by PCR, were relatively low and remained constant throughout the first trimester of pregnancy (Fig. 1 IIa).

Immunohistochemical staining of PAR1 within the cytotrophoblast layer at 7th, 8th and 10th weeks gestation showed high expression, recapitulating essentially the RNA pattern of expression. No staining was detected within the villous stroma at 12th week placenta sample (Fig. 1 IIID&E) or when a control IgG was applied.

While no expression of *Par3* was observed in the 6th week of gestation (Fig. 2IA), high and abundant expression levels were found in the cytotrophoblast layer of weeks 7-10 of gestation (Fig. 2 I B-D). These levels declined thereafter (Fig. 2 IF). This pattern of cell distribution, corresponded to the expression data observed by RT-PCR analysis (Fig. 2II). The expression profile of the RNA levels was confirmed by Western blot analysis for the PAR3 protein quantification similar to the mRNA pattern (Fig. 2 III).

CHMs are linked with a failure to down-regulate the trophoblast expression of PAR1 and PAR3

Trophoblast cells of CHM proliferate rapidly, often show cytologic atypia, and bear an approximately 20% risk of becoming a trophoblastic malignancy (6). This pathological condition of uncontrolled trophoblast hyperplasia provides an opportunity to study the expression levels of *Par1* and *Par3* genes in pathological proliferative placental villi. We have compared tissue localization of *Par1* and *Par3* mRNAs in biopsies of CHM (12-14 weeks of gestation) with that of age-matched normal placentas. *In situ* hybridization analysis of *Par1* RNA probes revealed a high level of expression in the CHM trophoblast cells (Fig. 3II A,B), with very little or no expression detected in trophoblast cells from the normal age matched pregnancies (Fig. 3II C,D). Immunohistological staining showed that specific PAR1 protein is localized within the molar cytotrophoblast cells in a tissue distribution similar to that of RNA (Fig. 3I). *Par3* was highly expressed in CHM (Fig. 3II E, F) and absent from normal placenta of the same gestational age (Fig. 3II H). The protein levels of PAR3 have essentially recapitulated the mRNA profile (data not shown). Overall, our results show that in complete molar trophoblast cells high levels of PAR1 and PAR3 are found. In contrast, these levels are very low in normal age matched placenta. Our data indicate that PAR1 and 3 are involved in the invasive phase of trophoblast cells.

This was shown in the expression pattern of normal developing placenta during the

first trimester of pregnancy as well as in the overexpression demonstrated in

pathological trophoblast of CHM.

Discussion

Human placental development involves the differentiation of CTB stem cells (organized in a polarized fashion on top of a basement membrane) toward a non-polarized cytotrophoblast sub-population (that subsequently loose cell-cell contact and invade). During early pregnancy cytotrophoblast cells proliferate, differentiate and become motile. While the net invasiveness of trophoblast during early placenta development is regulated in part by integrin mediated ECM interactions, a specific pattern of integrins was identified to either facilitate or restrain invasion (5, 7,8). Indeed, FAK a major focal adhesion complex (FAC) protein was reported to be highly expressed between 5 to 8 weeks of gestation, localized especially to both villous stem cell cytotrophoblasts and extravillous trophoblast cells (10, 11). We have previously demonstrated a central role for PAR1 in tumor invasion via the activation of integrins, cytoskeletal re-organization and the posphorylation of FAK and paxillin during the assembly of FACs (17, 18). We show here that PAR1 and PAR3 are highly and abundantly expressed during early placenta differentiation, specifically at weeks 7 to 10 of gestation. This time-frame coincides with the period when the developing trophoblast cells in early pregnancy proliferate, differentiate and become motile.

During early pregnancy several critical proteins are upregulated: HIF1α, $\alpha6\beta4$ and $\alpha5\beta1$ integrins, fibronectin and metalloproteinases MMP2 (5, 19-21). Our preliminary observations

indicated that over expression of *Par1* cDNA in EVT cultures facilitated villi outgrowth and induced

MMP2 and MMP9 activities (unpublished results). This strengthens the notion that PAR1

contributes to the invasion-like properties of trophoblast cells. The high expression levels of PAR1

and PAR3 occur when the oxygen levels in trophoblast cells are low (22, 23). It appears that the

low oxygen tension provides a critical regulator of trophoblast differentiation through the HIF1α

transcription factor (24). We currently examine whether the expression of PARs in villous explants,

cultured in low (3%) O2 environment is elevated as compared with normal (20%) O2 environment.

Collectively, our data are the first to demonstrate that PAR1 and PAR3 are over expressed

in pathological trophoblast cells of CHM and during a limited time period of normal early

pregnancy (7 -10 weeks gestation). The relation between PARs and trophoblast invasiveness is

reaffirmed by the over-expression of PAR1 and PAR3 in pathological trophoblast cells from

CHM tissues. In these tissues, the uncontrolled trophoblast proliferation is associated with an

increased invasive/malignant potential as described in 56% of the patients 50 years of age and

older (6). We suggest that the extended expression levels of PAR1 and PAR3 in molar

trophoblast cells is directly correlated with their invasive phenotype although their role remains

yet to be fully elucidated.

The trophoblast differentiation system, during early pregnancy, provides an opportunity to

study the physiological pattern of PARs in the invading cytotrophoblast cells. These data

complement our earlier observation that PAR1 is overexpressed in a collection of tumor biopsy specimens and plays a central role in tumor invasion and metastasis (17, 18). Yet, the fact that PAR1 and PAR3 are temporally and spatially expressed and their expression is turned off at weeks12 and thereafter - is intriguing. The nature of the molecular mechanisms involved in the shut-off expression of PAR1 and PAR3 are currently being explored.

Acknowledgments

References

1. Cross JC, Werb Z, Fisher SJ. Implantation and the placenta: key pieces of the development puzzle. *Science* 1994; **266:**1508-1518, Review.

2. Damsky CH, Fisher SJ. Trophoblast pseudo – vasculognesis: Faking with endothelial adhesion receptors. *Curr Opin Cell Biol* 1998; **10:** 660-666, Review.

3. Pijnenborg R, Bland JM, Robertson WB, Dixon G, Brosens I. The pattern of interstitial trophoblastic invasion of the myometrium in early human pregnancy. *Placenta* 1981; **2:**303-316.

4. Flamigni C, Bulletti C, Polli V, Ciotti PM, Prefetto RA, Galassi A, Di Cosmo E. Factors regulating interaction between trophoblast and human endometrium. *Ann N Y Acad Sci* 1991; **622:**176-190, Review.

5. Zhou Y, Damsky CH, Chiu K, Roberts JM, Fisher SJ. Preeclampsia is associated with abnormal expression of adhesion molecules by invasive cytotrophoblasts. *J Clin Invest* 1993; **91:**950-960.

6. Coukos G, Makrigiannakis A, Chung J, Randall TC, Rubin SC, Benjamin I. Complete hydatidiform mole. A disease with a changing profile. *J Reprod Med* 1999; **44:** 698-704.

7. Damsky CH, Fitzgerald ML, Fisher SJ. Distribution patterns of extracellular matrix components and adhesion receptors are intricately modulated during first trimester cytotrophoblast differentiation along the invasive pathway, *in vivo*. *J Clin Invest* 1992; **89:**210-222.

8. Damsky CH, Librach C, Lim KH, Fitzgerald M. Integrin switching regulates normal trophoblast invasion. Development 1994; **120:** 3657-3666.

9. Vicovac L, Jones CJ, Aplin JD. Trophoblast differentiation during formation of anchoring villi in a model of the early human placenta *in vitro*. *Placenta* 1995; **16:** 41-56.

10. Ilic D, Genbacev O, Jin F, Caceres E, Almeida EA, Bellingard-Dubouchaud V, Schaefer EM, Damsky CH, Fisher SJ. Plasma membrane-associated pY397FAK is a marker of cytotrophoblast invasion *in vivo* and *in vitro*. *Am J Ppathol* 2001; **159:** 93-108.

11. MacPhee DJ, Mostachfi H, Han R, Lye SJ, Post M, and Caniggia I. Focal adhesion kinase is a key mediator of human trophoblast development. *Laboratory investigations* 2001; **81:** 1469-1483.

12. Hurskainen T, Seiki M, Apte SS, Syrjakallio-Ylitalo M, Sorsa T, Oikarinen A, Autio-Harmainen H. Production of membrane-type matrix metalloproteinase-1 (MT-MMP-1) in early human placenta. A possible role in placental implantation? *J Histochem Cytochem* 1998; **46:**221-229.

13. Librach CL, Werb Z, Fitzgerald ML, Chiu K, Corwin NM, Esteves RA, Grobelny D, Galardy R, Damsky CH, Fisher SJ. 92-kD type IV collagenase mediates invasion of human cytotrophoblasts. J Cell Biol 1991; **113:**437-449.

14. Coughlin SR. How the protease thrombin talks to cells. *Review. Proc Natl Acad SciUSA*1999; **96:**11023-11027, Review.

15. O'Brien PJ, Molino M, Kahn M, Brass LF. Protease activated receptors: theme and variations. *Oncogenes* 2001; **20 (13):** 1570-1581, Review.

16. Camerer E, Huang W, Coughlin SR. Tissue factor-and factor X - dependent activation of protease activated receptor 2 by factor VIIa. *Proc Natl Acad Sci USA* 2000; **97(10):** 5255-5260.

17. Even-Ram S, Uziely B, Cohen P, Grisaru-Granovsky S, Maoz M, Ginzburg Y, Reich R, Vlodavsky I, Bar-Shavit R. Thrombin receptor overexpression in malignant and physiological invasion processes. *Nat Med* 1998; **4:** 909-914.

18. Even-Ram Cohen S, Maoz M, Pokroy E, Reich R, Katz B-Z, Gutwein P, Altevogt P, Bar-Shavit R. Tumor cell invasion is promoted by activation of protease Activated Receptor-1 in cooperation with $\alpha v \beta 5$ integrin. *J Biol Chem* 2001; **276:** 10952-10962.

19. Caniggia I, Grisaru-Gravnosky S, Kuliszewsky M, Post M, Lye SJ. Inhibition of TGF-beta 3 restores the invasive capability of extravillous trophoblasts in preeclamptic pregnancies. *J Clin Invest* 1999; **103**(12):1641-50

20. Caniggia I, Taylor CV, Ritchie JW, Lye SJ, Letarte M. Endoglin regulates trophoblast differentiation along the invasive pathway in human placental villous explants. *Endocrinology* 1997; **138:** 4977-4988.

21. Cannigia I, Mostachfi H, Winter J, Gassmann M, Lye SJ, Kuliszewski M, and Post M. Hypoxia-inducible factor-1 mediates the biological effects of oxygen on human trophoblast differentiation through TGFbeta(3). *J Clin Invest* 2000; **105:** 577-587.

22. Genbacev O, Joslin R, Damsky CH, Polliotti BM, Fisher SJ. Hypoxia alters early gestation human cytotrophoblast differentiation /invasion in vitro and models the placental defects that occur in preeclampsia . *J Clin Invest* 1996; **97:** 540-550.

23. Genbacev O, Zhou Y, Ludlow JW, Fisher SJ. Regulation of human placental development by oxygen tension. *Science* 1997; **277:** 1669-1672.

24. Cannigia I, Winter J, Lye SJ, and Post M. Oxygen and placental development during the first trimester: implications for the pathophysiology of pre- eclampsia. *Placenta* 2000; **21** (Suppl A): S25-S30.

FIGURE LEGENDS

FIGURE 1: **Tissue expression and distribution of PAR1 in the first trimester placenta. I.** *In situ* **hybridization of** *Par1*. Normal placental specimens were analyzed for *Par1* mRNA by *in-situ* hybridization, using a DIG-labeled RNA probe for *Par1*. *Par1* antisense riboprobe was applied on tissues from weeks: (A) 6; (B) 7; (C) 8; (D) 10; (E) 10; sense control riboprobe 10; (F) 14. An enlarged view of the placental villi border is shown in section C (note the abundant staining of *Par1* in the cytotrophoblast layer but not in the syncytiotrophoblast). **II. Levels of** *Par1***&2 mRNA.** a. For PCR detection, 0.25 μg of RNA was reverse-transcribed and amplified, using the appropriate set of primers and compared with the control housekeeping gene GAPDH. b. *Par1* mRNA levels were evaluated by Northern blot analysis and compared to the levels of 28S RNA.

III. PAR1 Immunostaining. Immunohistochemical staining of PAR 1 shows high immunoreactivity in placental samples obtained at 7 (A), 8 (B) and 10 (C) weeks of gestation. Minimal levels of staining was observed at week 12 (E) of gestation and in a control sample using bovine IgG at week 10 (D). Data shown are representative of at least 5 independent experiment series of early placenta samples.

FIGURE 2: **Tissue expression and distribution of PAR3 in the first trimester placenta I.** *In situ* **hybridization.** Normal placental specimens were analyzed for *Par3* mRNA by *in situ* hybridization

using a DIG-labeled RNA probe.   An antisense *Par3*-riboprobe was applied on tissues from placenta villi following weeks: (A) 6; (B) 7; (C) 8; (D) 10; (E) 10; sense control riboprobe, at week: (F) 12.

II. RT-PCR analysis of *Par3*. For PCR detection as in Fig. 1, using specific primers of *Par3*. **III. Western blot analysis of PAR3.** PAR3 protein levels were detected at weeks 7, 8 and 10 of gestation and was absent at week 12 (D). Equal levels of protein were applied as detected by β- actin house keeping levels. Data shown are representative of at least 3 independent set of experiments of early placenta samples.
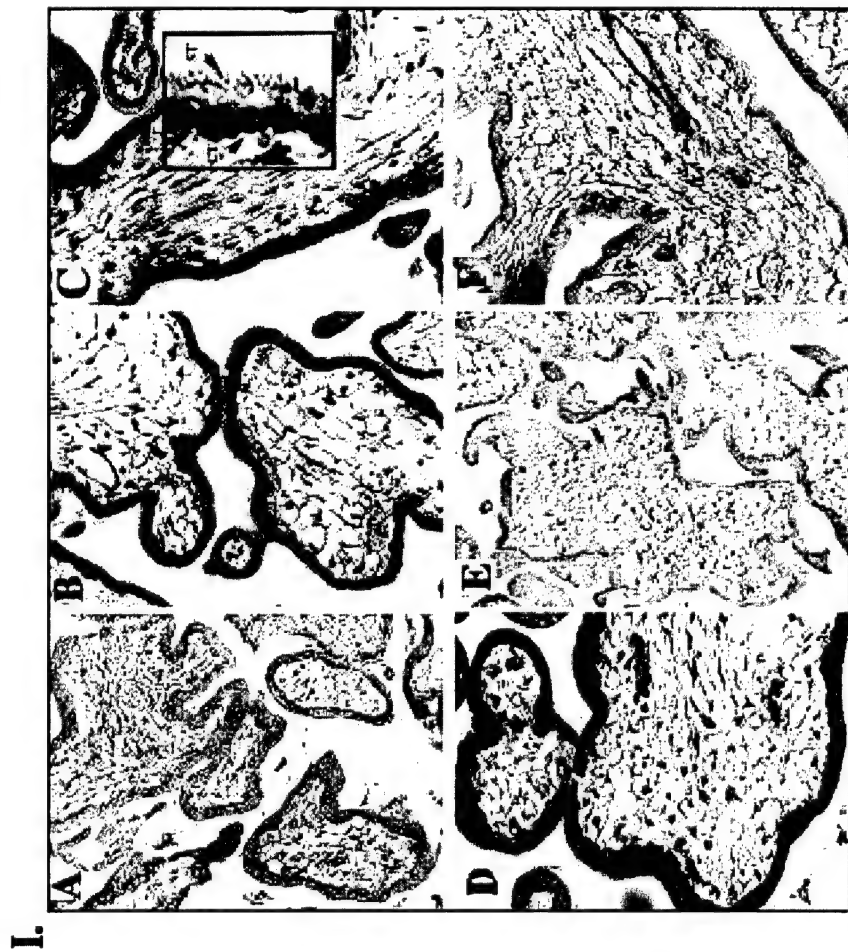
FIGURE 3: ***Par1* and *Par3* expression levels remain high in CHM. I. Immunohistochemistry of PAR1.** A representative experiment of immunohistochemical staining of CHM trophoblast cells, showed strong staining of PAR1 (A) using PAR 1 antibodies. No staining was observed when a control (B) bovine IgG was applied.
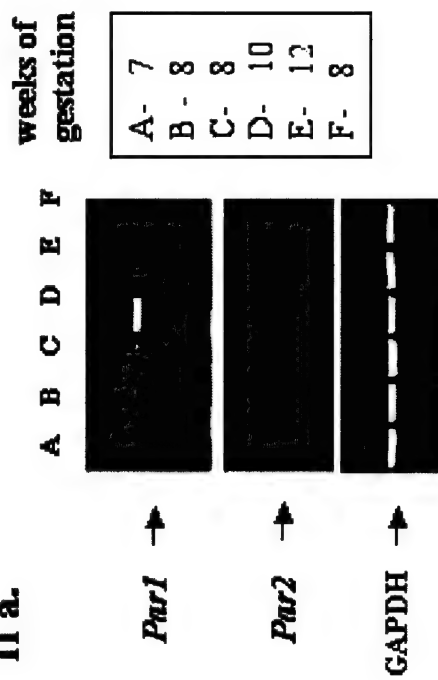
II. *In situ* hybridization of *Par1* and *Par3*. *Par1* and *Par3* mRNA levels were evaluated in biopsy specimens of CHM that were evacuated at the 12th and 14th weeks of gestation. These samples were compared with normal age- matched placental tissues. (A) P*ar1* from CHM placentas at the 12th gestational week; (B) *Par1* from CHM placentas at the 14th gestational week; as compared to normal age matched placenta ; (C) normal villi from placentas at the 12th week, (D) normal villi at the 14th week. (E) and (F) *Par3* from CHM placentas at the 12th and 14th gestational week; respectively (G) *Par3* sense control from CHM placentas at the12th gestational week; (H) *Par3* antisense on normal villi placenta at 14th gestation week.

Figures to
Manuscript

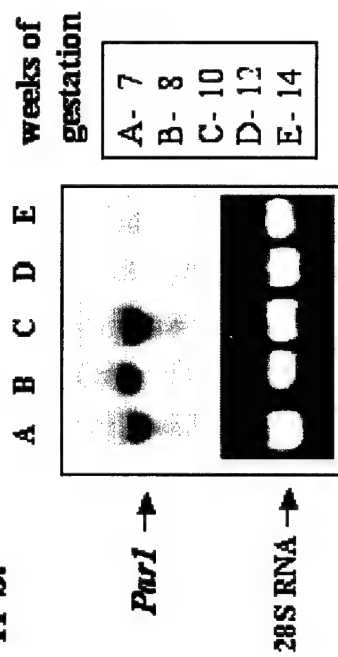Fig Figure 1 Appendix 2

weeks of gestation
A- 7
B - 8
C- 8
D- 10
E- 12
F- 8

II a.

Par1 →

Par2 →

GAPDH →

weeks of gestation
A- 7
B- 8
C- 10
D- 12
E- 14

II b.

Par1 →

28S RNA →

I.

III.

Figure 2   Appendix 2

I.

II.

Par-3 ▲

GAPDH ▲
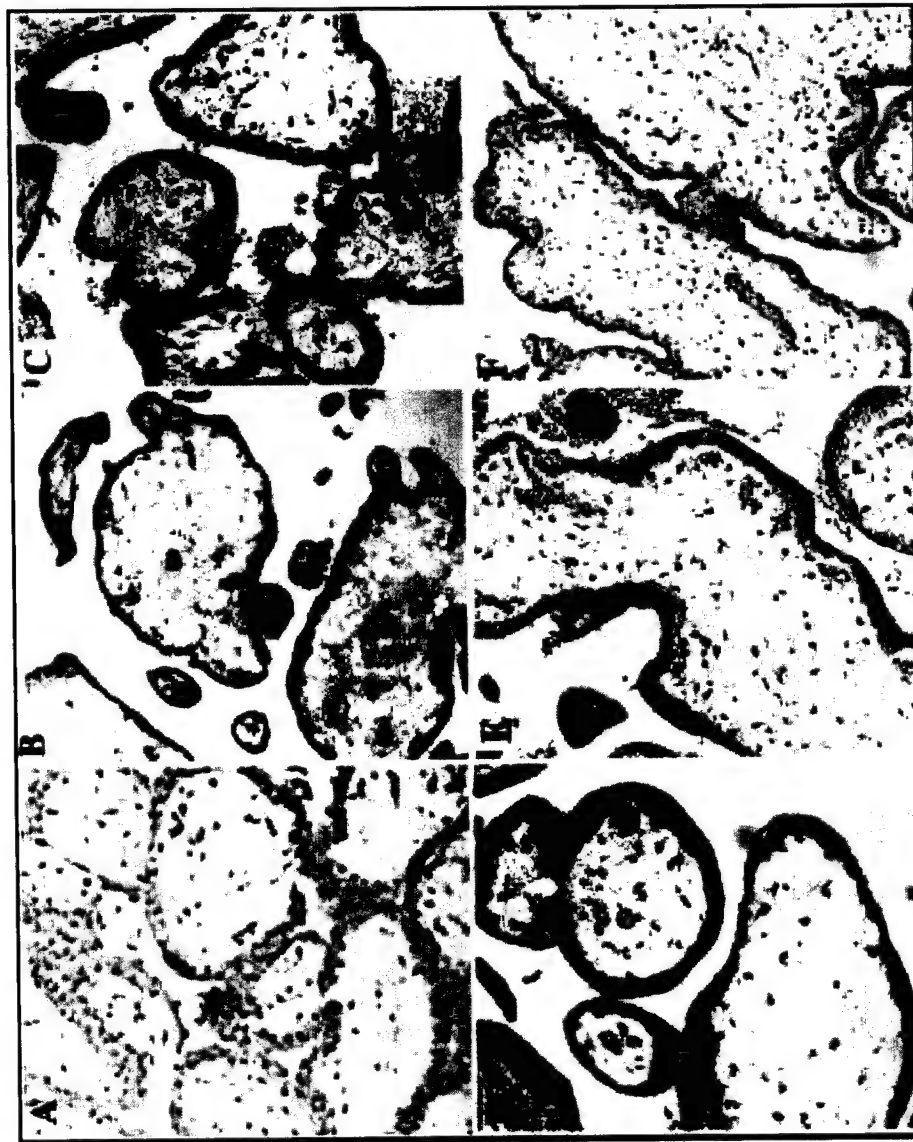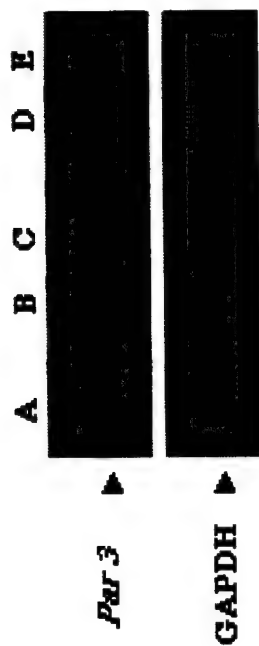
Weeks of
gestation
A - 7
B - 8
C - 10
D - 12
E - 14

III.

PAR 3 → ▲

β- actin → ▲
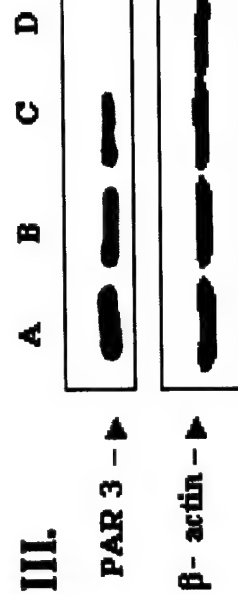
Weeks of
gestation
A - 7
B - 8
C - 10
D - 12

Figure 3   Appendix 2
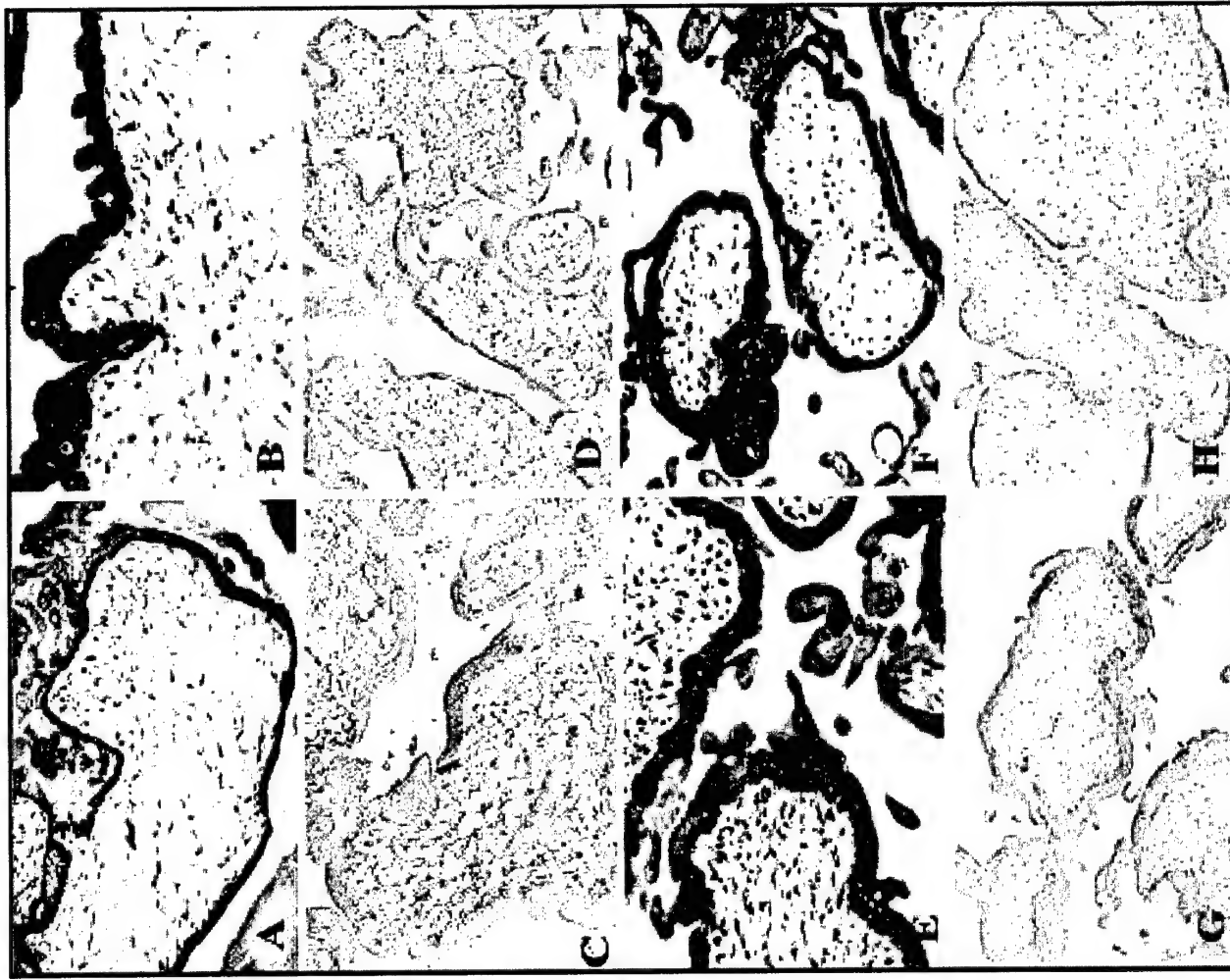
Oncogenic transformation induces tumor angiogenesis: A role for PAR1 activation

Yong-Jun Yin,[1] Zaidoun Salah, [1] Myriam Maoz, [1] Sharona Cohen Even Ram, [1] Shalom Ochayon, [1] Gera Neufeld, [2] Shulamit Katzav[3] and Rachel Bar-Shavit[1] *Departments of Oncology[1],The Hubert H. Humphrey Center for Experimental Medicine & Cancer Research[3], The Hebrew University-Hadassah Medical School, Jerusalem 91120 and The Department of Biology[2], Technion, Israel Institute of Technology, Haifa 32000, Israel*

Running title: *Par1* induced tumor angiogenesis

Correspondence Address:
Rachel Bar-Shavit, Ph.D.
Department of Oncology
Hadassah-University Hospital
POB 12000, Jerusalem 91120
Israel

Phone: 972-2-6777563
Fax: 972-2-6422794
e-mail: barshav@md.huji.ac.il

ABSTRACT

The formation of new blood vessels is a critical determinant of tumor progression. We find that *Par1* gene expression plays a central role in blood vessel recruitment in animal models. By *in vivo* injection of either Matrigel plugs containing *Par1*-expressing cells or of rat prostatic carcinoma cells transfected with tetracycline-inducible *Par1* expression vectors, we show that *Par1* significantly enhances both angiogenesis and tumor growth. Several VEGF splice forms are induced in cells expressing *Par1*. Activation of PAR1 markedly augments the expression of VEGF mRNAs and of functional VEGFs as determined by *in vitro* assays for endothelial tube alignment and bovine aortic endothelial cell proliferation. Since neutralizing anti-VEGF antibodies potently inhibited *Par1*-induced endothelial cell proliferation, we conclude that *Par1*-induced angiogenesis requires VEGF. Specific inhibitors of PKC, Src and PI3K inhibit *Par1*-induced VEGF expression, suggesting the participation of these kinases in the process. We also show that oncogenic transformation by genes known to be part of PAR1 signaling machinery is sufficient to increase VEGF expression in NIH3T3 cells. These data support the novel notion that initiation of cell signaling either by activating PAR1 or by the activated forms of oncogenes is sufficient to induce VEGF and hence angiogenesis.

Key words: Thrombin-receptor, VEGF (vascular endothelial growth factor), invasion, metastasis

INTRODUCTION

The formation of new blood vessels (vasculogenesis and angiogenesis) involves the coordinated functions of endothelial cell proliferation, migration and tube alignment. The emergence of new blood vessels from pre-existing vasculature is a process that is highly affected

by growth factor receptors such as KDR/*flk-1* and *flt-1* and by a spectrum of adhesion molecules, primarily integrins (1,2). Angiogenesis has been designated a hallmark of cancer and determined to be a prerequisite for tumor growth (3, 4) as well as for various ischemic diseases such as retinopathy of prematurity (3). This process takes place as a consequence of an angiogenic genetic switch, which allows the recruitment of blood vessels from neighboring tissues (5). The critical determinants of this angiogenic switch remain to be elucidated.

The relationship between thrombosis and cancer/metastasis was first recognized by the classical observations of Trousseau in 1872 (6). Many studies since have described a systemic activation of the blood coagulation cascade in patients with cancer (7-9). During initiation of the thrombosis/hemostasis cascade, a complex of factors Va and Xa (Va/Xa) acts to convert prothrombin to the serine protease thrombin. Thrombin ligates the Protease Activated Receptor (PAR) family to initiate cellular functions. We have shown previously that PAR1, the first identified member of the PAR family, plays a direct role in both normal (physiological placental implantation) and pathological (malignancy) cell invasion processes (10). Molecular mechanisms underlying PAR1 involvement in tumor invasion and metastasis include increased phosphorylation of focal adhesion complex proteins, cytoskeletal reorganization, and the recruitment of $\alpha v\beta 5$ integrin after PAR1 ligation (11).

PARs are G-coupled cell surface proteins mediating intracellular responses to the serine protease thrombin (12, 13). PAR1 was recently recognized as an oncogene, promoting transformation in NIH 3T3 cells. In addition to its potent focus forming activity, constitutive over-expression of PAR1 in NIH-3T3 cells promoted the loss of anchorage- and serum-dependent growth. PAR1 activity was found to be directly linked to Rho A and inhibited by pertussis toxin and thus mediated via the $G\alpha 13$ subunit (14). The oncogenic function of PAR1 is

especially significant in light of our observation that PAR1 is over-expressed in a series of biopsy specimens of breast tumors (10) as well as in a collection of cell lines exhibiting differential metastatic potentials (11).

Mouse embryos lacking *Par1* or several coagulation factors die with varying frequencies at midgestation, often with signs of bleeding (15-21). Recently (22) it has been shown that *Par1* plays a critical role in endothelial cell embryonic development, rescuing *Par 1* $^{-/-}$ mice from bleeding to death; however, its function in tumor angiogenesis is unknown. It was unclear whether bleeding in embryos lacking *Par1* results from impairment of hemostasis or of blood vessel formation. Griffin *et al* (22) provided elegant evidence demonstrating that loss of *Par1* does not prevent vessel formation but rather impairs the stabilization and maturation of the newly forming vessels, thereby causing abnormal fragility and ruptures in the vessel wall (22, 23). By initiating the PAR1 signaling cascade in endothelial cells, Griffin *et al* were able to rescue *Par1* deficient mouse embryos from bleeding to death. These results demonstrate that activation of PAR1 and its signaling pathway in endothelial cells is essential for vascular integrity. It is interesting to note the phenotypic similarities between *Par1*$^{-/-}$ embryos and various coagulation factor knock out embryos (e.g. factor V$^{-/-}$, tissue factor $^{-/-}$ and prothrombin $^{-/-}$). Most die at midgestation with yolk sac defects and bleeding (16-24).

The major angiogenic factor VEGF acts mainly through two tyrosine kinase receptors present almost exclusively on endothelial cells, VEGF receptor-1 (VEGF-1; also termed *flt*-1) and VEGF receptor-2 (*KDR/flk-1*) (25, 26), and via neuropilins expressed on tumor cells (27). The importance of the VEGF/VEGFR system in angiogenesis is strongly supported by data showing early embryonic lethality in mice either heterozygous or completely deficient in VEGFR (25, 27-31). The crucial biological role of VEGF in angiogenic related functions were

shown in studies using targeted gene disruption in mice. Since VEGFR-2 is required for the differentiation of endothelial cells and the recruitment of endothelial cell precursors (31), embryos lacking the VEGFR-2 gene die before birth because the blood vessels do not form (32). Likewise, inhibition of VEGF activity using neutralizing antibodies or by the introduction of dominant negative VEGF receptors into endothelial cells derived from tumor-associated blood vessels resulted in the inhibition of tumor growth and even in tumor regression. This indicates that VEGF is a major initiator of tumor angiogenesis (32, 33). Furthermore, VEGF expression is potentiated by hypoxia and the induced VEGF production in hypoxic areas of solid tumors contributes significantly to tumor angiogenesis (34-36). VEGF also functions as a survival factor for immature blood vessels. These vessels become VEGF independent once they recruit periendothelial cells and undergo maturation. However, the newly formed vascular network will regress if VEGF is prematurely withdrawn. Thus, VEGF deprivation may lead not only to inhibition of further angiogenesis, but also to regression of already formed, immature, tumor vessels (37).

Several VEGF isoforms are produced from the VEGF gene by alternative splicing. Five human VEGF mRNA splice forms have been identified, encoding VEGFs of various lengths (121, 145, 165, 189 and 206 amino acids; VEGF 121-206) (29-36, 38, 39). They are mainly distinguished by their heparin and heparan sulfate binding ability. While VEGF121 lacks the amino acids encoded by exons 6 and 7 of the VEGF gene (40) and does not bind heparin or extracellular matrix (41), VEGF165 includes exon 7 and does bind heparin (40, 41) and VEGF145 includes exon 6 and binds tightly to the extracellular matrix (ECM) (42). VEGF189 and VEGF 206 contain the amino acids encoded by both exons 6 and 7 and display a higher affinity for heparin and heparan sulfate than VEGF145 or VEGF165. It is not clear which of these splice

forms are involved in VEGF's known effects on angiogenesis and tumor growth. In addition, it is not known whether the effects of VEGF and PAR1 on tumor progression are inter-related in any way. We investigated this question and explored the role of PAR1 in tumor angiogenesis.

MATERIALS AND METHODS

Cells- SB-2 non-invasive human melanoma (kindly provided by J. Fidler and M. Bar-Eli, Dept. of Cell Biology, University of Texas, M. D. Anderson Cancer Center, Houston) were grown in 10% FCS-DMEM supplemented with 50 U/ml penicillin and streptomycin (GIBCO-BRL, Gaithersburg, MD, USA) and maintained in a humidified incubator with 8% CO_2 at 37^OC. The *Par1* stable transfectants, clone 13 and clone MixL were grown under the same conditions; for long-term maintenance these were supplemented with 200 µg/ml G418 antibiotics (11). MCF-7 (adenocarcinoma) and MDA435 cells (ductal carcinoma) were maintained as previously described (10). NIH 3T3 cells transfected with Vav, Src and Ras were grown in DMEM supplemented with 10% calf serum.

Cell transfection - Cells were grown to 30-40% confluency and then transfected with 0.5-2 µg/ml of plasmid DNA in Fugene 6 transfection reagent (Boehringer Mannheim, Germany) according to the manufacturer's instructions (11). After 10 days of selection, stable, transfected clones were established in medium containing 400 µg/ml G418. Antibiotic resistant cell colonies were transferred to separate culture dishes and were grown in 200 µg/ml G418 medium. Forty-eight hours after transfection, transiently transfected cells were collected and tested (RNA was extracted either for RT-PCR and/or Northern blot or for preparation of conditioned medium).

Densitometric evaluations - The relative intensities of PAR1 protein bands (obtained by Western blot analysis) were determined by Fluor-S^{TM} Multi Imager and Multi-Analyst/PC software (Bio-

Rad laboratories, Herecules, CA) normalized to the total amount of protein loaded, and expressed relative to PAR1 levels in parental SB-2 cells.

Preparation of conditioned medium- Cells at 90% confluence were fed with fresh medium and incubated for 24 hours. For TRAP activation, 100 µM TRAP was added to the medium 8 or 24 hours prior to medium collection. Conditioned medium was then collected and centrifuged at 1,000 rpm for 5 minutes. The supernatant was either used immediately or stored at 4^0C prior to use.

Thrombin receptor-Activating Peptide (TRAP)- H-Ser-Phe-Leu-Leu-Arg-Asn-Pro-Asn-Asp-Lys-NH2 (SFLLRNPNDK).

ELISA- Quantification of the levels of VEGF secreted by PAR1 expressing clones was carried out using an ELISA (Quantikine /human VEGF; R&D Systems, MN, USA) performed according to the manufacturer's instructions.

RNA extraction and reverse transcriptase - polymerase chain reaction (RT- PCR) - Total RNA was prepared, using the *TRI REAGENT* (Molecular Research Center, Inc. Ohio) as described by the manufacturer. One microgram of RNA was used for complementary DNA (cDNA) synthesis, employing M-MLV reverse transcriptase and oligo dT (both from Promega, Heidelberg, Germany). VEGF transcripts were amplified, using Taq polymerase (Bioline, London, UK) for 20ul total PCR reaction. 95˚C for 3 minutes for initial melting was followed by 24-30 cycles of 95˚C for 1 minute, 59˚C for 30 seconds, and 72˚C for 1 minute; 7 minutes at 72˚C was used for final extension following cycling. PCR primers were as follows: upstream mouse L19, 5'-CTGAAGGTGAAGGGGAATGTG-3'; downstream mouse L19, 5'-GGATAAAGTCTTGATGATCTC-3'(24cycles); upstream human GADPH, 5'-

CCACCCATGGCAAATTCCATGGCA-3'; downstream human GADPH, 5'-

TCTAGACGGCAGGTCAGGTCCACC(26cycles); upstream VEGF, 5'-

TCGGGCCTCCGAAACCATGA-3'; downstream VEGF, 5'-

CCTCCTGAGAGATCTGGTTC-3' (30cycles). For VEGF, sequences in the 3' and 5'

translated regions were used, allowing the amplification of the known splice variants

(516 base pair [bp], 648bp, 720bp, and 771bp) (46). PCR products were separated on a

2% Nusieve (FMC; Rockland, ME) 3:1 agarose gel, stained with ethidium bromide, and

visualized under UV light.

Northern Blot Analysis - Total RNA (20μg) was electrophoresed on 1% formaldehyde-agarose

gels and transferred to Hybond-N$^+$ membranes (Amersham Pharmacia Biotech UN Limited). The

membranes were hybridized (42°C, 18h) with α ^{32}P-dCTP labelled (Rediprimer II, Amersham

Biosciences UK Limited) probe for human VEGF165 (690 bp obtained by RT-PCR). After

hybridization, membranes were washed and exposed to X-ray films. We used the housekeeping

gene β-actin as a control for RNA loading.

Three dimensional tube forming assay - Type I collagen was prepared from the tail tendons of

adult Sprague Dawley rats. The collagen matrix gel was obtained by simultaneously raising the

pH and ionic strength of the collagen solution. Briefly, collagen was used to coat 24-well cluster

plates (0.3 ml/well). After polymerization of the collagen at 37°C for 0.5 h, the BAEC cells (2 X

10^4/0.5ml/well) were added to each well. Collagen solution (0.4ml) was carefully poured on top

of the cells. After the gel was formed, 0.4 ml of conditioned medium from *Par1* transfected

MCF-7 cells, mock transfected MCF-7 or control non-transfected MCF-7 cells was added and

replaced with fresh medium every other day. Tube formation and alignment of BAEC were

visualized by phase microscopy, and photographed at days 8-10 (43).

BAEC proliferation - Cells were seeded in DMEM containing 10% FCS at a density of 2×10^3 cells/16-mm well of a 24-well plate, in triplicate. The medium was replaced with conditioned medium 24 h after seeding, and the cells were cultured for 3 to 14 days in the different conditioned media. Every three days post-seeding, cells (three wells for each condition) were dissociated with trypsin/EDTA and counted with a Coulter counter (Coulter Electronics Ltd.)

Matrigel plug assay - The Matrigel plug assay was performed as previously described (44). Briefly, 300 μl Matrigel (kindly provided by Dr. H. Kleinman, NIDR, NIH, Bethesda, MD) containing 10^6 *Par1*-transfected SB-2 cells/ml at 4°C were injected, subcutaneously (s.c.) into an abdominal site between the hind limbs of seven-week-old male BALB/c mice (n=6). Injections were performed bilaterally, when always at the right side Matrigel mixed with naïve cells and transfection reagent. Control mice were injected with Matrigel mixed with empty vector transfected SB-2 cells lacking *Par1*. Matrigel plugs were removed after 10 days. The skin of the mouse was easily pulled back to expose the Matrigel plug, which remained intact. After qualitative differences were noted and photographed, the plugs were dissected out of the mouse and fixed with 4% formaldehyde/phosphate-buffered saline and embedded in paraffin for histological evaluation. For vessel density analysis, 5-μm thick sections from paraffin-embedded plugs were stained with H&E and either Mallory's or von Willebrand Factor (vWF) (DAKO, Glostrup, Denmark) staining. Vascular structures were recognized as luminal or slit-like structures that occasionally contained blood cells within them, as described previously (45). The microvessel density was determined in various plug areas. Individual vessels were counted on X200 microscopic fields (0.785mm^2). A total of six fields/plug (representative of at least 3 independent Matrigel plugs per condition) were analyzed.

"Tet-On" system - A 1.3 Kb DNA of *hPar1* was cut from PSL-301-PAR1 plasmid by BamHI and Xho I restriction enzymes. This fragment was cloned into the multiple cloning site of pAHygTet1 plasmid between BamH I and Xho I to generate pAHygTet1-*hPar1*.

Cells from a clone of AT2.1/Tet -On (generously provided by Dr. Hua-Quan Miao, Imclone systems, Inc., new York, NY 10014) were transfected with 2μg DNA of either pAHygTet1-*hPar1* or pAHygTet1 using FuGENE 6 transfection reagent (Roche, Mannheim Germany). After 48hr, the medium was changed and cells were selected by 800μg/ml hygromycine B (Calbiochem, La Jolla, CA). Stable pAHygTet1-*hPar1*-transfected clones were checked for *hPar1* expression by Northern blot analysis after a 48 hr induction with Doxycycline (Dox) (2μg/ml).

Tumor growth in vivo - 2 month old male Copenhagen rats were anesthetized. Cells (0.3 X 10^6 / 0.3 ml /rat) were injected subcutaneously at a dorsal site between the hind limbs. The rats (*n*=5, each group) were fed with drinking water containing 1% sucrose. To induce *h*PAR1 expression, 10 μg/ml Dox was added to the drinking water, which was changed every 2 days.

RESULTS

PAR1 promotes tumor angiogenesis *in vivo*. We have previously shown that introducing *Par1* cDNA into non-metastatic melanoma cells induced the invasive and adhesive properties of these cells (11). The molecular mechanisms underlying PAR1-induced tumor invasion include recruitment of αvβ5 integrin, focal adhesion complex formation, and cytoskeletal reorganization. We asked whether PAR1 is also capable of inducing tumor angiogenesis. To address this question, we applied a Matrigel plug assay to evaluate whether *Par1* can recruit blood vessels *in vivo*. We have characterized a stable *Par1* transfected, non-metastatic SB-2 melanoma cell line (Cl13) (11). Densitometric analysis of a representative Western blot (Fig. 1, ref. 11) revealed that Cl13 cells express 4.2 times more PAR1 than the parent SB-2 line which expresses very little PAR1. For comparison, the highly invasive melanoma cell line SM-A375 was determined to express 1.8 times the levels of PAR1 protein found in SB-2 parental cells. C113 cells were mixed at 4^0C with Matrigel (reconstituted basement membrane (BM) preparation extracted from EHS mouse sarcoma) and injected *s.c.* into BALB/c mice. Upon injection, the liquid Matrigel rapidly formed a solid gel plug that served not only as an inert vehicle for PAR1 producing cells, but also mimicked the natural interactions that exist between tumor cells and the surrounding extracellular matrix (ECM). Non-transfected SB-2 cells were similarly mixed with Matrigel and injected as a control. In some cases, C113 cells were treated with thrombin receptor activating peptide (TRAP) to activate *Par1* prior to embedding in Matrigel. 10 days after injection, the Matrigel plugs were exposed, examined and photographed. Plugs containing control SB-2 cells were pale, containing few blood vessels; however, those containing *Par1*-expressing C113 cells were reddish, indicative of recruited blood vessels. Plugs containing TRAP-activated C113 cells had the most pronounced red coloration (Fig.1 I). Matrigel plugs were subsequently removed, paraffin-embedded,

sectioned, and stained for either collagen (Mallory's staining; Fig.1 II A, C, D&E) or Factor VIII

(vWF staining Fig. 1 II, B&F) to allow histological evaluation of blood vessels in the plug. A

network of recruited capillary blood vessels is seen in plugs containing Cl13 cells while few

vessels appear in plugs containing non transfected cells (Fig. 1 II). The difference in angiogenesis

induced by activated PAR1-transfected cells (Fig. 1 IIF) as compared to non transfected, either

untreated or TRAP-treated (Fig. 1II, A&B), is particularly striking. Microscopic counts of the

microvessels in Matrigel sections indicated that these differences are statistically significant (Fig. 1

III). While low levels of blood vessels were obtained in SB-2 cells and somewhat induced levels

following activation, eight fold increase was seen in Cl13 following TRAP activation (Fig. 1 III).

To exclude the possibility that clonal variation is responsible for these effects, we analyzed several

other PAR1- transfected SB-2 clones (MixL and Cl15) and found similar angiogenic activity (data

not shown).

Inducible *Par1* expression in rat prostatic carcinoma increases tumor mass and angiogenesis.

Differential expression of *Par1* in the Dunning rat prostate carcinoma cell variants was observed

by RT-PCR. The AT2.1 variant expressed low levels of *Par1*, while AT3.1, which is more motile

and tumorigenic than AT2.1 (47), expressed high levels (Fig. 2 IA). In order to establish the

exclusive effect of *Par1* expression on prostate tumor progression, AT2.1 cells were transfected

with human *Par1* cDNA under the control of a tetracycline-inducible promoter (Fig. 2II). Two

clones (AT2.1/Tet-On/ *hPar1* clones Cl1 and Cl4) were isolated, in which *hPar1* expression was

strongly induced by the tetracycline analog Dox as determined by Northern blot analysis. *Par1*

expression was nearly undetectable in the absence of Dox. Following addition of Dox, the levels

of the 4.1 kb *Par1* mRNA were increased substantially (39 fold for Cl1 and 52 fold for Cl4; Fig.

2II, D & F). The optimal dose of Dox necessary to induce *Par1* expression was 1-2 μg/ml (not

shown). *Par1* mRNA could be detected as early as 4-6 h, and reached maximum levels at 20-24 h after Dox treatment (not shown). AT2.1 cells transfected with the pTet-On vector without the *Par1* gene did not express any detectable *Par1* mRNA levels either in the presence (Fig. 2II, lane B) or in the absence (Fig. 2II, lane A) of Dox.

To assess the effect of PAR1 on tumor growth *in vivo,* AT2.1/Tet-On/*hPar1* clone Cl4 cells or control transfected cells were injected *s.c.* into rats. Rats were then maintained for 2 weeks with either regular drinking water (supplemented with 1% sucrose) or drinking water containing Dox (and 1% sucrose) to induce *Par1*. In all injected rats, marked tumor growth occurred during this time period. In the absence of Dox the mean mass of AT2.1 clone Cl4 tumors was 0.35 ± 0.1 gr (Fig. 2 III, B). When PAR1 expression was induced by Dox in the drinking water, mean AT2.1 clone Cl4 tumor mass increased 3.7 fold to 1.30 ± 0.14 gr. This increase was statistically significant. In addition to being larger, tumors in these Dox –treated animals had a very reddish appearance (Fig. 2III, C) compared to the pale appearance of tumors from untreated animals (Fig. 2 III, B). In comparison, tumors from control-transfected and non-transfected AT2.1 tumors were significantly smaller and did not increase in mass or change in color when Dox was delivered in their drinking water (Fig. 2 IV). We conclude, therefore, that the regulated induction of the *Par1* gene markedly enhanced two critical determinants of tumor progression: tumor size and angiogenesis.

***Par1* expressing cells induce functional VEGF.** Next we analyzed the expression levels of VEGF165 in the stably *Par1*-transfected melanoma cells (Cl13 and Mix L) using Northern blot analysis (Fig. 3I). Parental SB-2 or control transfected cells (Fig. 3I, A&B respectively) showed no detectable levels of VEGF, but both Cl13 and MixL had significant levels of VEGF165 mRNA (Fig. 3I, C&D respectively). A probe for the house-keeping gene, β-actin, was used as a control for

loading. Activation of PAR1 by thrombin or TRAP further increased levels of VEGF165 mRNA (Fig. 3II). Maximal induction was obtained after 8 h of TRAP treatment (Fig. 3II, lane G), at concentrations of 100µM and 50 µM and was reduced markedly with lower concentrations (Fig. 3III, lanes B-F). When control SB-2 cells were treated with 100 µM of TRAP for 8 h there was no detectable change in VEGF mRNA levels compared to untreated SB-2 cells (data not shown). A similar pattern was obtained for VEGF145 but not for VEGF 189, which was slightly expressed only after 8h of TRAP treatment (Fig. 3IV). Since TRAP could be activating other endogenous PARs, it is important to point out that RT-PCR did not detect any expression of PAR2, PAR3 or PAR4 in our experimental system (data not shown). Using RT-PCR with primers targeting the start site (exon 1) and the end point (exon 8) of the VEGF gene, we could detect all the different splice forms induced by *Par1*. *Par1* markedly induced VEGF 121, VEGF 145, and VEGF 165; it induced only very low levels of VEGF 189 and VEGF 206 was not detected at all. No VEGF isoforms were detected in the absence of *Par1* in SB-2 parental cells, control-transfected SB-2 cells, or non metastatic cells (MCF-7) (Fig. 3 IV). Activation of PAR1 (TRAP; 8h) increased substantially the level of VEGF189, similar to the pattern obtained in the highly metastatic cells (MDA 435). To determine how much VEGF protein is actually produced and secreted, VEGF conditioned media was quantitated by ELISA. In conditioned medium (up to 24 hours) derived from control cells (not expressing *Par1*), there was no significant VEGF release (<15 pg/ml). In 8-hours conditioned medium derived from Cl13 cells activated with TRAP, VEGF levels were 1440 $\pm$39.8 pg/ml (p<0.01) as compared to 343.3 $\pm$ 39.8 pg/ml in non-activated Cl13 cells. Twenty four-hours conditioned medium from non-activated Cl13 cells contained 1467 $\pm$ 125.8 pg/ml VEGF; upon TRAP activation VEGF release was increased to 4863.1$\pm$ 267.1 pg/ml (p<0.005).

To determine whether the increased levels of VEGF mRNA and protein induced by *Par1* gene correspond to increases in functional VEGF protein, we collected conditioned medium from untreated or thrombin activated *Par1* transfected cells, as well as from control non transfected, non-metastatic cells. We used an endothelial tube forming assay to assess VEGF activity: BAEC cells were embedded in a 3 dimensional collagen (type I) mesh and the extent of tube-forming network was evaluated following application of the various conditioned media. While low vascular branching activity was obtained with untreated control conditioned medium, either treated with thrombin or not (Fig. 4I A-C), a more complex appearing network was obtained with activated PAR1 conditioned medium obtained from *Par1*-transfected cells (Fig. 4I, D-F). We also examined the effect of *Par1* transfected cell conditioned media on the rate of bovine aortic endothelial cell (BAEC) proliferation *in vitro*. BAEC proliferation was found to be maximal using conditioned medium from Cl13 cells activated with TRAP (8 hours) and was comparable to proliferation seen using conditioned medium from the highly invasive MDA 435 cell line (Fig. 4II). When neutralizing anti-VEGF antibodies were applied during the proliferation assay, a significant inhibition was obtained. Nearly complete inhibition is seen at a 1:100 dilution of the antibodies; the effect decreases in a dose-dependent manner at greater dilutions (Fig. 4 III). These data demonstrate that activated PAR1 expressing cells secrete high levels of functional VEGF.

VEGF induction by *Par1* is mediated via PKC, PI3K and Src. The phorbol ester PMA increased VEGF mRNA levels in Cl13 cells in a dose-dependent manner, with maximum induction achieved between 1 and 500 ng/ml (Fig. 5I). To determine whether PKC might play a role in PAR1-induced increases in VEGF, we used the potent PKC inhibitor, calphostin C. At concentrations of 500 ng/ml and higher, calphostin C potently blocked the TRAP-induced

increase in VEGF mRNA in Cl13 cells (Fig. 5II). No effect was observed at a lower

concentration (50 ng/ml). These data suggest that PKC plays a role in the induction of VEGF by

PAR1. Specific inhibitors of two other kinases also inhibited the PAR1-dependent increase in

VEGF expression in Cl13 cells. Wortmannin, a PI3K inhibitor, inhibited TRAP-induced

increases in VEGF mRNA levels (Fig. 5III). In addition, PP-2, a potent Src inhibitor, also

inhibited VEGF induction (Fig. 5IV). These data point to essential roles for PKC, Src and PI3K

in the molecular mechanisms underlying VEGF induction by PAR1.

Transformation of NIH 3T3 cells by the oncogenes v-Ha-Ras, V-Src, or VavK49 induces

VEGF mRNA. It has been shown previously that the PAR1 signaling pathway involves Src

family tyrosine kinases down stream (56), Ras (58,67) and increased phosphorylation of Vav

(55, 64). It was therefore of interest to see what effect their oncogenic (activated) forms had on

VEGF mRNA expression.

To determine the effect of oncogenic transformation on VEGF expression, mRNA from

transformed and control NIH3T3 cells was examined for VEGF transcripts (Fig. 6I). NIH3T3

cells were transfected with the active forms of *ras*, *src* or *vav* (K49) oncogenes, wild type (wt)

vav protooncogene, or two different SH2 domain mutants of *vav* (W622R and R647L). *Ras,*

src, and the oncogenic *vav* all have potent transforming capability. While the full-length *vav*

proto-oncogene and the W622R *vav* mutant exhibit greatly reduced transforming potential, the

R647L *vav* mutant retains the transforming potential of the oncogene. As shown in Fig. 6I, a

marked induction in VEGF mRNA expression was observed in the NIH3T3 cells transfected

with *src* or the *vav* oncogene. However, only low levels of VEGF mRNA are induced in cells

transfected with *ras* or the proto-oncogene *vav*, and no VEGF is detected when cells are

transfected with *vav* W622R, the SH2 mutant with reduced transforming ability (Fig. 6I). Low

levels of VEGF mRNA were present in cells transfected with vav R647L, which maintains its transforming capability (data not shown). These results suggest that cell transformation is sufficient to induce VEGF.

By performing RT-PCR with primers directed to exons 1 and 8 of the VEGF gene, we examined which VEGF splice forms are expressed in transformed cells. While control NIH 3T3 cells do not express any of the VEGF splice variants, *src*-transfected NIH 3T3 cells express VEGF121, 145, 165, and 189 but not VEGF 206 (Fig. 6III). The VEGF forms present in *src*-transformed NIH3T3 were similar to those found in activated (8 hours of TRAP) Cl13 cells.

DISCUSSION

We have previously shown that *Par1* is a critical gene involved in tumor invasion and metastasis (10, 11). Here we wished to determine the involvement of PAR1 in tumor angiogenesis. Although the association between the protease thrombin and angiogenesis has been previously documented (49-51), dissection of the role of PAR1 in tumor angiogenesis and its mechanism of activation are largely unknown.

Our results provide a comprehensive analysis of PAR1 involvement in tumor angiogenesis. We demonstrate here the ability of *Par1* to elicit tumor angiogenesis both *in vivo* in animal models and *in vitro* (as shown by the endothelial tube forming assay and cell proliferation). In addition, *Par1* expression induces VEGF mRNA. The data indicate that while the expression of *Par1* is sufficient to induce VEGF levels, activation of the PAR1 protein and initiation of the cell signaling machinery greatly enhance expression of 4 VEGF splice forms; VEGF121, VEGF145, VEGF165 and VEGF189 but not VEGF 206. This correlates with an increase in effects on angiogenesis in the Matrigel plug assay and on endothelial tube formation and cell proliferation following activation of PAR1. The fact that a greater angiogenic response is seen in Matrigel plugs containing pre-activated *Par1*- expressing cells indicates that active recruitment of blood vessels take place early on, immediately following the introduction of the Matrigel plugs. These findings, together with our previous results on the increased invasion potential of *Par1*-overexpressing cells, strongly support a significant role for *Par1* in the two critical events in tumor progression, tumor invasion and angiogenesis (10,11).

Activation of PAR1 leads to synthesis and secretion of functional VEGF protein as indicated by our observation that conditioned medium from *Par1*-overexpressing cells increases BAEC proliferation and 3 dimensional tube forming assay *in vitro*. The growth promoting

activity of activated PAR1 is mediated by VEGF as demonstrated by the dramatic inhibition of PAR1-induced endothelial cell proliferation in the presence of neutralizing anti-VEGF antibodies. *Par1* expression induces 4 VEGF splice forms (VEGF121, VEGF145, VEGF165, VEGF189), which are markedly further induced following activation of PAR1 by thrombin or TRAP. This increase in VEGF mRNA is most likely due to stabilization of VEGF mRNA rather than enhanced transcription as documented recently by Haung and S. Karpatkin (51) and our data (not shown). It appears therefore, that *Par1* plays a dual role in the control of blood vessel formation. The expression of *Par1* in tumor cells is sufficient to induce VEGF expression levels, leading to endothelial cell proliferation and sprouting. In addition, *Par1* is required in endothelial cells for maturation and stabilization of the blood vessels (22).

Previous studies have shown that thrombin activates PKC, Src, PI3K, and MAPK (52-54). Our studies show the involvement of these signaling enzymes in PAR1-induced angiogenesis, since PP-2, a Src inhibitor, Wortmannin-a PI3K inhibitor and Calphostin C, a PKC inhibitor, all potently inhibited VEGF165 mRNA induction. Furthermore, oncogenic transformation of NIH3T3 cells with genes which participate in PAR1 signaling (e.g. *ras, src* or *vav;* 55-59,67) is sufficient to induce the same 4 VEGF splice forms seen in *Par1*-transfected tumor cells. PAR1 couples to different G-proteins and activates the tyrosine kinases Src and Fyn (56, 57, 60). Thrombin has been shown to induce tyrosine phosphorylation of the adaptor protein Shc, which is then recruited to Grb2 (60). It has been reported that a dominant negative Shc that is deficient in Grb2 binding capability suppresses thrombin-mediated activation of p44 MAP kinase and cell growth, highlighting out the importance of Shc in this pathway. In CCL-39 fibroblasts, thrombin activates p21 *ras* in a manner that is inhibited by pertussis toxin and the tyrosine kinase inhibitor genistein suggesting that activation of Ras involves both G-proteins and activation of protein

tyrosine kinases (61). Although the mechanism by which PAR1 couples to Ras is still unclear, it is likely that Src and Fyn activate Ras through the adaptor protein Shc in complex with Grb2 and SOSRas exchange factor (56, 57). It has been documented previously that activated forms of Ras induce VEGF gene expression in NIH 3T3 cells and primary endothelial cells (62, 63) - our results confirm and support these data. Vav activates GTP-binding proteins and is part of the PAR1 signaling cascade (64, 65); we now show that it also induces low levels of VEGF. The oncogenic form of *vav* induces high levels of VEGF. The fact that two SH2 mutants of Vav (R647L and W622R), both shown to be defective in their tyrosine phosphorylation properties, had different abilities to induce VEGF suggests a correlation between VEGF production and transforming potential (48, 66). The W622R mutant, which is defective in transforming properties, does not induce VEGF expression while R647L, which maintains its transforming potential, does.

Together, these data strongly support the notion that PAR1 expression and the initiation of the PAR1 signaling cascade are highly significant in eliciting tumor angiogenesis.

REFERENCES

1. Ferrara, N., and Alitalo, K. (1999) Clinical application of angiogenic growth factor and their inhibitors. *Nature Med.* **5**, 1359-1364

2. Hynes, R.O., Bader, B.L., and Hodivala-Dilke, K. (1999) Integrins in vascular development. *Braz. J. Med. Biol.* Res. **32**, 501-510

3. Carmeliet, P., and Jain, R.K. (2000) Angiogenesis in cancer and other diseases. *Nature* **407**, 249-257

4. Folkman, J. (1971) Tumor angiogenic therapoeitic implications. *N. Engl. J. Med.* **285**, 1182-1186

5. Hanahan, D., and Folkman, J. (1996) Pattern and emerging mechanisms of angiogenic switch during tumorigenesis. *Cell* **86**, 353-364

6. Trousscau, A. (1872) *Lectures in Clinical Medicine, Delivered in Hotel-Dieu, paris. Pp 281-295. New Sydenham Society. London*

7. Rickles, F.R., and Edwards, R.L. (1983) Activation of blood coagulation in cancer: Trousseau's syndrome revisited. *Blood* **62**,14-31

8. Sloane, B.F., Rozhin, J., Johnson, K., Taylor, H., Crissman, J.D., and Honn, K.Y. (1986) Cathepsin B: association with plasma membrane in metastatic tumors. *Proc. Natl. Acad. Sci. USA.* **83**, 2483-2487

9. Zacharski, L.R., Memoli, V.A., Morian, W.D., Schlaeppi, J.M., and Roussceu, S.M. (1995) Cellular localization of enzymatically active thrombin in intact human tissues by hirudin binding. *Throm Haemostasis* **73**, 793-797

10. Even-Ram, S., Uziely, B., Cohen, P., Ginzburg, Y., Reich, R. Vlodavsky, I. and Bar-Shavit, R. (1998) Thrombin receptor overexpression in physiological and malignant invasion process. *Nature Med.* **4**, 909-914

11. Even-Ram, C. S., Maoz, M., Pokroy, E., Reich, R. Katz, B-Z., Gutwein, P., Altevogt, P., and Bar-Shavit, R. (2001) Tumor cell invasion is promoted by activation of protease activated Receptor-1 in cooperation with $\alpha v \beta 5$ integrin. *J. Biol. Chem.* **276**, 10952-10962

12. Vu, T-K., Hung, D.T., Wheaton V.I., and Coughlin, S.R. (1991) Molecular cloning of a functional thrombin receptor reveals a novel proteolytic mechanism of receptor activation. *Cell* **64**, 1057-1068

13. Rasmussen, U.B., Vouret-Craviari. V, Jallat, S., Schlesinger, Y., Pages, G., Pavirani, A., Lecocq, J.P., Pouyssegur, J., and Van Obberghen-Schilling, E. (1991)

cDNA cloning and expression of a hamster α-thrombin receptor coupled to Ca^{+2} mobilization. *FEBS Lett.* **288,** 123-128

14. Martin, C.B., Mahon, G.M., Klinger, M.B., Kay, R.J., Symons, M., Der, C.J., and Whitehead, I.P. (2001) The thrombin receptor, PAR-1, causes transformation by activation of Rho-mediated signaling pathways. *Oncogene* **20**, 1953-1963

15. Connolly, A.J., Ishihara, H., Kahn, M.L.,Fares,Jr. R.V., and Coughlin, S.R. (1996) Role of the thrombin receptor in development and evidence for a second receptor. *Nature* **381,** 516-519

16. Bugge, T.H., Xiao, Q., Kombrinck, K.W., Flick, M.J., Holmback, K., Danton, M.J., Colbert, M.C., Witte, D.P., Fujikawa, K., Davie, E.W., and Degen, J.L. (1996) Fatal embryonic bleeding events in mice lacking tissue factor, the cell-associated initiator of blood coagulation. *Proc. Natl. Acad. Sci. USA.* **93,** 6258-6263

17. Carmeliet, P., Ferreira, V., Breier, G., Pollefeyt, S., Kieckens, L., Gertsenstein, M., Fahrig, M., Vandenhoeck, A., Harpal, K., Eberhardt, C., Declercq, C., Pawling, J., Moons, L., Collen, D., Risau,, W., and Nagy, A. (1996) Abnormal blood vessel development and lethality in embryos lacking a single VEGF allele. *Nature* **380,** 435-439

18. Toomey, J.R., Kratzer, K.E., Lasky, N.M., Stanton, J.J., and Broze, Jr. G.J. (1996) Targeted disruption of the murine tissue factor gene results in embryonic lethality. *Blood* **88,** 1583-1587

19. Cui, J., O'Shea, K.S.M., Purkayastha, A., Saunders, T.L, and Ginsburg, D. (1996) Fatal haemorrhage and incomplete block to embryogenesis in mice lacking coagulation factor V. *Nature* **384,** 66-68

20. Sun, W.Y., Witte, D.P., Degen, J.L., Colbert, M.C., Burkart, M.C., Holmback K, Xiao Q, Bugge TH, and Degen SJ. (1998) Prothrombin deficiency results in embryonic and neonatal lethality in mice. *Proc. Natl. Acad. Sci. USA.* **95,** 7597-7602

21. Xue, J., Wu, Q., Westfield, L.A., Tuley, E.A., Lu, D., Zhang, Q., Shim, K., Zheng, X., and Sadler, J.E. (1998) Incomplete embryonic lethality and fatal neonatal hemorrhage caused by prothrombin deficiency in mice. *Proc. Natl Acad. Sci. USA.* **95,** 7603-7607

22. Griffin, C.T., Snirivasan, Y., Zheng, Y-W., Haung, W., and Coughlin, S.R. (2001) A role for thrombin receptor signaling in endothelial cells during embryonic development. *Science* **293,** 1666-1670

23. Preissner, K.T., Nawroth, P.P., and Kanse, S.M. (2000) Vascular protease receptors: integrating haemostasis and endothelial cell functions. *J. Pathol.* **190,** 360-372

24. Carmeliet, P. (2001) Clotting factors build blood vessels. *Science* **293,** 1602-1604

25. Shibuya, M., Yamaguchi, S., Yamane, A., Ikeda, T., Tojo, A., Matsushime, H., and Sato, M. (1990) Nucleotide sequence and expression of a novel human receptor-type tyrosine kinase gene (flt) closely related to the fms family. *Oncogene* **5,** 519-524

26. Terman, B.I., Carrion, M.E., Kovacs, E., rasmussen, B.A., Eddy, R.L., and Shows, T.B. (1991) Identification of a new endothelial cell growth factor receptor tyrosine kinase. *Oncogene* **6,** 1677-1683

27. Neufeld, G., Cohen, T., Gengrinovitch, S., and Poltorak, Z. (1999) Vascular endothelial growth factor (VEGF) and its receptors. *FASEB J.* **13,** 9-22.

28. Kim, K.J., Li, B., Winer, J., Armanini, M., Gillett, N., Phillips, H.S., and Ferrara, N. (1993) Inhibition of vascular endothelial growth factor-induced angiogenesis suppresses tumour growth in vivo. *Nature* **362,** 841-844

29. Millauer, B., Shawver, L.K., Plate, K.H., Risau, W., and Ullrich, A. (1994) Glioblastoma growth inhibited in vivo by a dominant-negative Flk-1 mutant. *Nature* **367,** 576-579

30. Carmeliet, P., Ferreira, V., Breier, G., Pollefeyt, S., Kieckens, L., Gertsenstein, M., Fahrig, M., Vandenhoeck, A., Harpal, K., Eberhardt, C., Declercq, C., Pawling, J., Moons, L., Collen, D., Risau, W., and Nagy, A. (1996) Abnormal blood vessel development and lethality in embryos lacking a single VEGF allele. *Nature* **380,** 435-439

31. Shalaby, F., Ho, J., Stanford, W.L., Fischer, K.D., Schuh, A.C,, Schwartz, L., Bernstein, A., and Rossant, J. (1997) A requirement for Flk1 in primitive and definitive hematopoiesis and vasculogenesis. *Cell* **89,** 981-90

32. Fong, G.H., Rossant, J., Gertsenstein, M., and Breitman, M.L. (1995) Role of Flt-1 receptor tyrosine kinase in regulating the assembly of vascular endothelium. *Nature* **376,** 66-70

33. Shweiki, D., Itin, A., Soffer, D., and Keshet, E. (1992) Vascular endothelial growth factor induced by hypoxia may mediate hypoxia-initiated angiogenesis. *Nature* **359,** 843-845

34. Plate, K.H., Breier, G., Weich, H.A., and Risau, W. (1992) Vascular endothelial growth factor is a potent tumor angiogenesis factor in human gliomas *in vivo*. *Nature* **359**, 845-848

35. Leung, D.W., Cachianes, G., Kuang, W.J., Goddel, D.V., and Ferrara, N. (1989) Vascular endothelial growth factor is a secreted angiogenic mitogen. *Science* **246**,1306-1309

36. Tischer, E., Gospadorowicz, D., Mitchell, R., Silva, M., Schilling, J., Lau, K., Crisp, T., Fiddes, J.C., and Abraham, J.A. (1989) Vascular endothelial growth factor: a new member of the platelet - derived growth gene family. *Bichem. Biophys. Res. Commun.* **165**, 1198-1206

37. Benjamin, L.E., Golijanin, D., Itin, A., Pode, D., and Keshet, E. (1999) Selective ablation of immature blood vessels in established human tumors follows vascular endothelial growth factor withdrawal. *J. Clin. Invest.* **103**, 159-165

38. Keck, P. J., Hauser, S,D., Krivi, G., Sanzo, K., warren, T., Feder, J., and Connolly, D.T. (1989) Vascular permeability factor, an endothelial cell mitogen related to PDGF. *Science* **246**, 1309-1312

39. Houck, K.A., Ferrara, N., Winer, J., Cachiaes, G., Li, B., and Leung, D.W. (1991) The vascular endothelial growth factor family-identification of a fourth molecular species and characterization of a alternative splicing RNA. *Mol. Endocrinol.* **5**, 1806-1814

40. Cohen, T., Gitay-Goren, H., Sharon, R., Shibuya, M., Halaban, R., Levi, B., and Neufeld, G. (1995) VEGF121, a vascular endothelial growth factor isoform lacking heparin binding ability, requires cell surface heparan sulfates for efficient binding to the VEGF receptors of human melanoma cells. *J. Biol. Chem.* **270**, 11322-11326

41. Park, J.E., Keller, G.A., and Ferrara, N. (1993) Vascular endothelial growth factor (VEGF) isoforms - differential deposition into the subepithelial eextracellular matrix and bioactivity of extracellular matrix–bound VEGF. *Mol. Biol. Cell* **4**,1317-1326

42. Poltorak, Z., Cohen, T., Sivan, R., Kandelis, Y., Spira, G., Vlodavsky, I., Keshet, E., and Neufeld, G. (1997) VEGF 145: a secreted VEGF form that binds to extracellular matrix. *J. Biol. Chem.* **272**, 7151-7158

43. Schnaper, H.W., Grant, D.S., Stetler-Stevenson, W.G., Fridman, R., D'Orazi, G., Murphy, A.N., Bird, R.E., Hoytha, M., Fuerst, T. R., French, D.L., et al. (1993) type IV collagenase(s) and TIMPs modulate endothelial cell morphogenesis in vitro. *J. Cell. Physiol.* **156**, 235-246

44. Passaniti, A., Taylor, R.M., Pili, R., Guo, Y., Long, P.V., Haney, J.A., Pauly, R. R., Grants, D.S., and Martin, G.R. (1992) A simple, quantitative method for assessing angiogenesis and antiangiogenic agents using reconstituted basement membrane, heparin, and fibroblast growth factor. *Lab. Invest.* **67**, 519-528

45. Itoh, T., Tanioka, M., Yoshida, H., Yoshioka, T., Nishimoto, H., and Itohara, S. (1998) Reduced angiogenesis and tumor progression in gelatinase A-deficient mice. *Cancer Res.* **58**,1048-1051

46. Fiedler, W., Graeven, U., Ergun, S., Verago, S., Kilic, N., Stockschlader, M.,Hossfeld, D. K. (1997) Vascular endothelial growth factor, a possible paracrine growth factor in human acute myeloid leukemia. *Blood* **89,** 1870-1875

47. Miao, H-Q., Lee, P., Lin, H., Soker, S., and Klagsbrun, M. (2000) Neuropilin-1 expression by tumor cells promotes tumor angiogenesis and progression. *FASEB J.* **14,** 2532-2539

48. Katzav, S. (1993) single point mutation in the SH2 domain impair the transforming potential of *vav* and fail to activate proto-*vav.* *Oncogene 8,* 1757-1763

49. Tsopanoglou, N.E., and Maragoudakis, M.E. (1999) On the mechanism of thrombin-induced angiogenesis. *J. Biol. Chem.* **274,** 23969-23976

50. Richard, D.E., Vouret-Craviari, V., and Pouyssegur, J. (2001) Angiogenesis and G-protein coupled receptors:signals and bridge the gap. *Oncogene* **20,**1556-1562

51. Huang, Y-Q., Li, J-J., Hu, L., Lee, M., and Karpatkin, S. (2001) Thrombin induces increased expression and secretion of VEGF from human FS4 fibroblasts, DU145 prostate cells and CHRF megakaryocytes. *Throm. Haemst.* **86,** 1094-1098

52. Carter, A.N., Haung, R., Sorisk, A., Downes, C.P., and Rittenhouse, S.E., (1994) Phosphatidylinositol 3,4,5-triphosphate is formed from phosphatidylinositol 4,5-bis-phosphate in thrombin –stimulated platelets. *Biochem. J.* **310,** 415-420

53. Gutkind, J.S., Lacal, P.M., and Robbins, K.C. (1990) Thrombin-dependent association of phosphatidylinositol –3-kinase with p60c-src and p59fyn in human platelets. *Mol. Cell. Biol.* **10,** 3806-3809

54. Leach, K., L., Ruff, V.A., Jarpe, M.B., Adams, L.D., Fabbro, D., and Raben, D.M., (1992) Alpha thrombin stimulates nuclear localization of protein kinse C isozyme in IIC9 cells. *J. Biol. Chem.* **267,** 21816-21822

55. Cichowski, K., Brugge, J.S., and Brass, L.F. (1996) Thrombin receptor activation and integrin engagement stimulate tyrosine phosphorylation of the proto-oncogene product, p95vav, in platelets. *J. Biol. Chem.* **271,** 7544-7550

56. Chen, Y.-H., Pouyssegur, J., Coutridge, S.A., and Van Obberghen-Schilling, E. (1994) Activation of Src family kinase activity by the G protein-coupled thrombin receptor in growth-responsive fibroblasts. *J. Biol. Chem.* **269,** 27372-27377

57. Chen, Y., Grall, D., Salcini, A.E., Pelicci, P.G., Pouyssegur, J., and Van Obberghen-Schilling, E. (1996) Shc adaptor proteins are key transducers of mitogenic signaling mediated by the G protein-coupled thrombin receptor. *EMBO J.* **15,** 1037-1044

58. Shock, D.D., He, K., Wencel-Drake, J.D., and Parise, L.V (1997) Ras activation in platelets after stimulation of the thrombin receptor, thromboxane A2 receptor or prote. *Biochem. J.* **321,** 525-530

59. Collins, L.R., Rickets, W. A., Olefsky, J. M., and Brown, J.H. (1997) The G12 coupled thrombin receptor stimulates mitogenesis through the Shc SH2 domain. *Oncogene* **15,** 595-600

60. Maulon, L., Mari, B., Bertolotto, C., Ricci, J.E., Luciano, F., Belhacene, N., Deckert, M, Baier, G., and Auberger, P. (2001) Differential requirements for ERK1/2 and P38 MAPK activation by thrombin in T cells. Role of P59Fyn and PKC epsilon. *Oncogene* **20,** 1964-1972

61. Ricketts,W. A., W., Brown, J.H., and Olefsky, J. M. (1999) Pertussis toxin-sensitive and -insensitive thrombin stimulation of Shc phosphorylation and mitogenesis are mediated through distinct pathways. *Mol. Endocrinol.* **13,** 1988-2001

62. Grugel, S., Finkenzeller, G., Weindel, K., Barleon, B. and Marme, D. (1995) Endothelial Growth factor in NIH 3T3 cells. *J. Biol. Chem.* **270,** 25915-25919

63. Meadows, K.N., Bryant, P., and Pumiglia, K. (2001) Vascular endothelial growth factor induction of the angiogenic phenotype requires Ras activation. *J. Biol. Chem.* **276,** 49289-49298

64. Bar-Shavit, R,, Maoz, M., Yongjun, Y., Groysman, M., Dekel, I. And Katzav, S. (2002) Signalling pathways induced by protease-activated receptors and integrins in T cells. *Immunology* **105,** 35-46

65. Landau E, Tirosh R, Pinson A, Banai S, Even-Ram S, Maoz M, Katzav S, Bar-Shavit R. (2000) Protection of thrombin receptor expression under hypoxia. *J. Biol. Chem.* 275(4), 2281-2287

66. Katzav, S., Packham, G., Sutherland, M., Aroca,P., Santos, E., and Cleavland, J.L. (1995) Vav and ras induce fibroblast transformation by overlapping signaling pathways which require c-Myc function. Oncogene 11, 1079-1088

67. Ellis C.A., Malik A.B., Gilchrist A, Hamm H, Sandoval R, Voyno-Yasenetskaya T, Tiruppathi C. (1999) Thrombin induces proteinase-activated receptor-1 gene expression in endothelialcells via activation of Gi-linked Ras/mitogen-activated protein kinase pathway. *J. Biol. Chem.* 274(19), 13718-27

LEGENDS

Figure 1. *Par1* induces angiogenesis *in vivo*. Matrigel plugs containing Cl13 (SB-2 cells stably transfected with *Par1)* or non-transfected SB-2 cells were injected *s.c.* into the peritoneal cavity of BALB/c mice in a bilateral fashion. Mice were divided into four groups dependent on the nature of the injected cells: Group A (n=9) untreated SB-2 cells; Group B (n=8) SB-2 cells treated with TRAP (100µM, 8 hours); Group C (n=11) untreated Cl13 cells; and Group D (n=12) Cl13 cells treated with TRAP (100µM, 8 hours). **I. Matrigel plugs under phase microscopy**. 10 days after *in vivo* implantation, Matrigel plugs were removed and examined. Matrigel containing SB-2 cells remained pale (A). The appearance of the Matrigel plugs containing SB-2 cells pretreated with TRAP was not significantly different (B). Matrigel plugs containing Cl13 cells exhibited a reddish color (C), which was more pronounced in Cl13 cells pretreated with TRAP (D). Magnification X 5. **II. Histolgical evaluation of Matrigel plugs.** Serial sections were prepared from Matrigel plugs, and processed either with Mallory's (A, C, D & E) or vWF (B&F) staining. A, B. Untreated SB-2 cells C. SB-2 cells pretreated with TRAP D. Untreated Cl13 cells E, F. Cl13 cells pretreated with TRAP. Magnification X 200. vWF staining shows clearly the lumind endothelial cells especially in the microvessels of activated Cl13 embedded plugs.

III. Quantification of capillary vessels in Matrigel plugs. Six separate fields of each Matrigel plug stained with H&E, Mallory's and vWF staining were examined under phase microscopy and capillary vessels were counted. Data shown are representative of at least 3 independent Matrigel plug sets of experiments.

Figure 2. Inducible *Par1* expression in rat prostatic carcinoma increases tumor mass and angiogenesis. I. Differential expression of *Par1* in the Dunning rat prostate carcinoma cell

variants was observed by RT-PCR using primers specific for PAR1. Primers for L19 were used as a loading control. **II.** Inducible *Par1* expression in a rat prostatic carcinoma cell line - AT2.1. AT2.1 cells were transfected with a plasmid containing the human *Par1* coding sequence under the control of a tet-inducible promoter. Two stably transfected clones, AT2.1/Tet-On/*hPar1* clones C14 and Cl1, were tested for the inducibility of human *Par1* expression by the tetracycline analog, Dox as evaluated by Northern blot analysis. **III.** AT2.1/Tet-On/*hPar1* clone 4 cells and control transfected (vector only) cells were injected into rats *s.c*. Animals were maintained for 2 weeks with regular drinking water or drinking water supplemented with Dox. After 2 weeks, the tumors were excised and examined. Tumors shown were from animals injected with: A. control transfected cells; B. AT2.1/Tet-On/*hPar1*, clone 4; C. AT2.1/Tet-On/*hPar1* clone 4, fed with Dox for 2 weeks. **VI.** Tumor weight. Data shown are the mean at least 3 independent sets of experiments.

Figure 3. Expression of VEGF isoforms by stable *Par1*-transfected clones. I. Northern blot analysis of VEGF expression. Total RNA was prepared from SB-2 cells (A), SB-2 cells transfected with an empty expression vector (B), and two clones stably expressing PAR1: Cl13 (C) and MixL(D). The Northern blot was hybridized with a probe specific for VEGF165. The bottom panel shows hybridization to the housekeeping gene L32, as a control for RNA loading. **II. Kinetics of VEGF165 mRNA induction following activation of PAR1.** Cl13 or SB-2 cells were treated with Thrombin (1u/ml) or TRAP (100μM) for the indicated times and RNA levels were analyzed by Northern blot. **III. Dose response of VEGF165 mRNA induction by TRAP.** Cl13 cells were treated with the indicated doses of TRAP for 8 hours. RNA was analyzed by Northern blot. **IV. RT-PCR for the detection of VEGF splice forms in *Par1* transfected cells.** RT-PCR was performed using primers directed to exons 1 and 8 to detect all splice forms. Four different

splice forms are detected in Cl13 cells: VEGF121, VEGF145, VEGF165, and VEGF189. None, or very little, is seen in non- transfected (SB-2) cells, cells transfected with empty vector (SB-2 Vector) and non-metastatic cells (MCF-7). The pattern of expression of *Par1* splice forms in TRAP- or thrombin-activated Cl13 cells is similar to that in highly metastatic cells (MDA435).

Figure 4. PAR1 activity induces functional VEGF. I. Conditioned medium from Cl13 cells increases the complexity of cell tube formation. Cultures of endothelial cells in a three-dimensional collagen type I matrix were grown with conditioned media from: A) Non metastatic MCF-7 cells transfected with an empty vector; B) Non metastatic MCF-7 cells /empty vector cells treated with thrombin; C) control, non metastatic MCF-7 cells; D) *Par1* transfected MCF-7 cells; E) *Par1* transfected MCF-7 cells treated with thrombin; or F) highly metastatic MDA435 cells.

II. Conditioned media from *Par1* transfected cells induce the proliferation of BAEC. BAEC cells were cultured in the presence of conditioned medium from the indicated cells. Cultures were refed with fresh conditioned medium every two days. At each indicated time point, cells were removed from plates with trypsin/EDTA and counted. The data exhibit a typical experiment representing triplicates. **III. Anti-VEGF antibodies inhibit the effects of activated *PAR1* cell conditioned medium on BAEC proliferation.** BAECs were cultured in the presence of conditioned medium from activated Cl13 cells (TRAP, 8 hours) Anti-VEGF antibodies were added to cultures at varying concentrations as indicated (0.05μg/ml - 2.5 μg/ml) and were present for the entire period of the assay. The effects of conditioned medium from control SB-2 cells and the highly metastatic MDA435 line are shown for comparison.

Figure 5. Induction of VEGF by PAR1 is mediated by PKC, PI3K and Src.

I. Dose response of VEGF mRNA induction by PMA. Various concentrations of PMA were added to cultures of Cl13 cells and VEGF mRNA levels were determined by Northern blot. RNA

from non-transfected, non-metastatic cells was included as a control (lane A). **II. Calphostin C inhibits PAR1-induced increases in VEGF mRNA.** Calphostin C was added to Cl13 cultures at the indicated concentrations 30 minutes prior to addition of TRAP. Cells were harvested after 8 hours of TRAP/ calphostin treatment and VEGF mRNA levels were determined by Northen blot. **III. Wortmannin, a PI3K inhibitor, b locks PAR1-induced increases in VEGF mRNA.** Inhbition by Wortmannin is observed at 1μM (F) and up to 10 μM (G) but not at 0.1 μM (E). **IV. PP-2, an inhibitor of Src, blocks PAR1-induced increases in VEGF mRNA.** Inhbition of VEGF is observed at 10 μM (B), 1 μM (C) as compared to *Par1* transfected cells (A) and parental non transfected cells (G).

Figure 6. Expression of VEGF mRNA splice forms in *ras-*, *src* -and *vav*-transformed NIH3T3 cells. I. Northern blot analysis of transformed NIH 3T3. NIH 3T3 cells were transfected with activated *ras* or *src* oncogenes, wild type (w.t.) *vav* proto-oncogene, oncogenic *vav* or an SH2 mutant of *vav*. Total RNA was isolated and 15μg were analyzed by Northern blotting using a probe for VEGF$_{165}$. **II. Quantitation of changes in VEGF mRNA levels in transformed cells.** Photoimage was used to quantitate VEGF165 mRNA levels from Northern blots. VEGF165 mRNA levels were normalized to β-actin mRNA levels to control for loading differences. Data shown are representative of 3 independent experiments. **III. RT-PCR analysis of VEGF splice forms.** A representative RT-PCR experiment shows elevated levels of VEGF121, VEGF145, VEGF165 and VEGF189 splice forms in *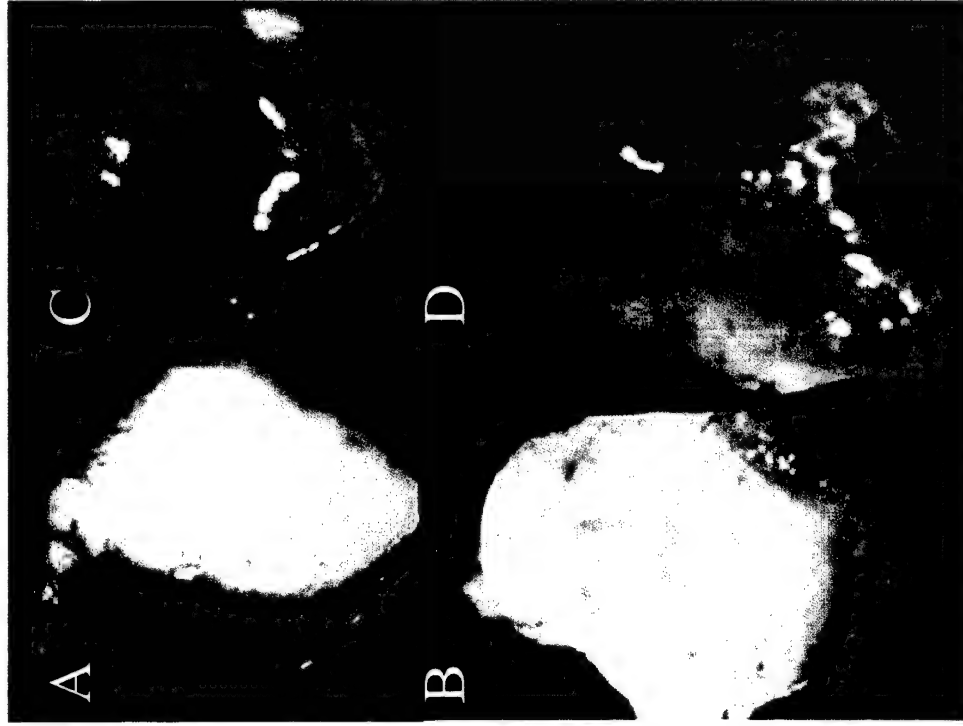src*-transformed NIH3T3 cells. *Par1* transfected/activated cells (Cl13/TRAP/8h) and non-transfected SB-2 cells are included as positive and negative controls.
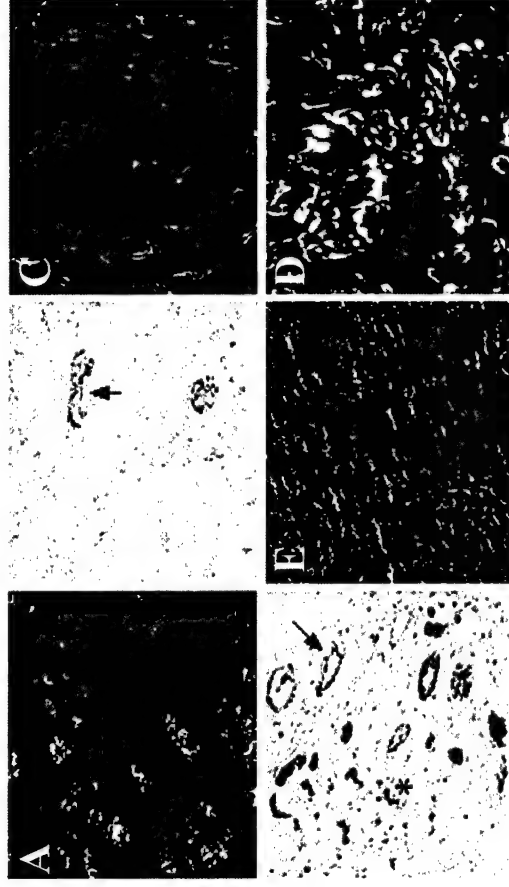
ACKNOWLEDGEMENTS

Figure 1   Appendix 3

hPar1 induces Angiogenesis *in vivo*

I.

II.

III.   Vessel density analysis in Matrigel micropocket experiment
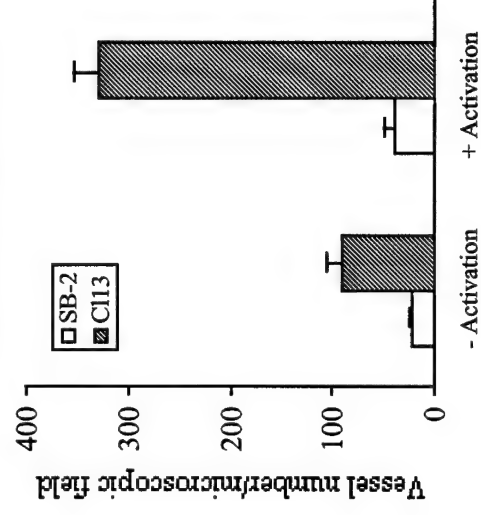
Figure 2   Appendix 3

I.
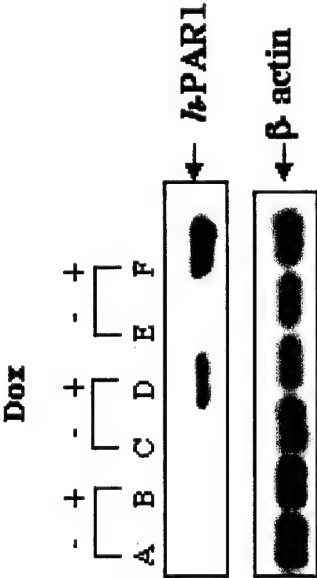
A   B   C

→ m-PAR1

→ L19

A- AT2.1
B- AT3.1
C- Baf 210

II.

Dox

A   B   C   D   E   F

→ h-PAR1

→ β actin
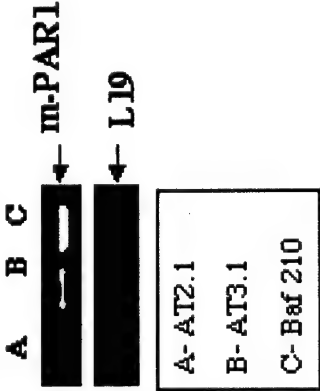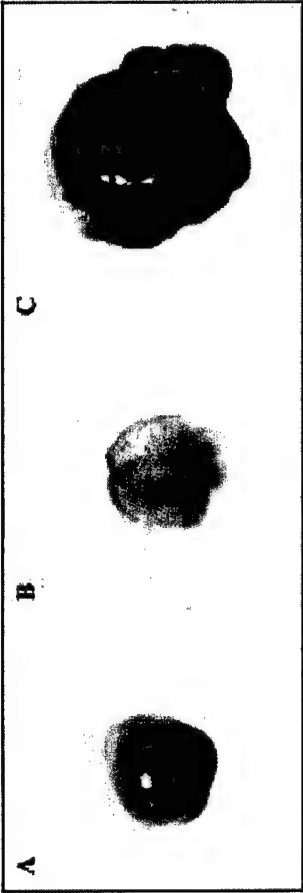
A- AT2.1/cont/ non induced
B- AT2.1/cont/ induced by Dox
C- Clone 1/PAR1/ non induced
D- Clone 1 /PAR1/ induced by Dox
E- Clone 4 /PAR1/ non induced
F- Clone 4 /PAR1/ induced by Dox

III.

A   B   C

IV.
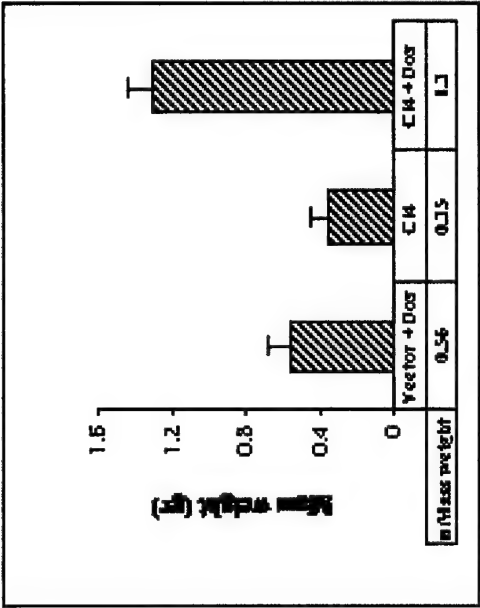
Figure 3 Appendix 3

I.

II.

III.

IV.
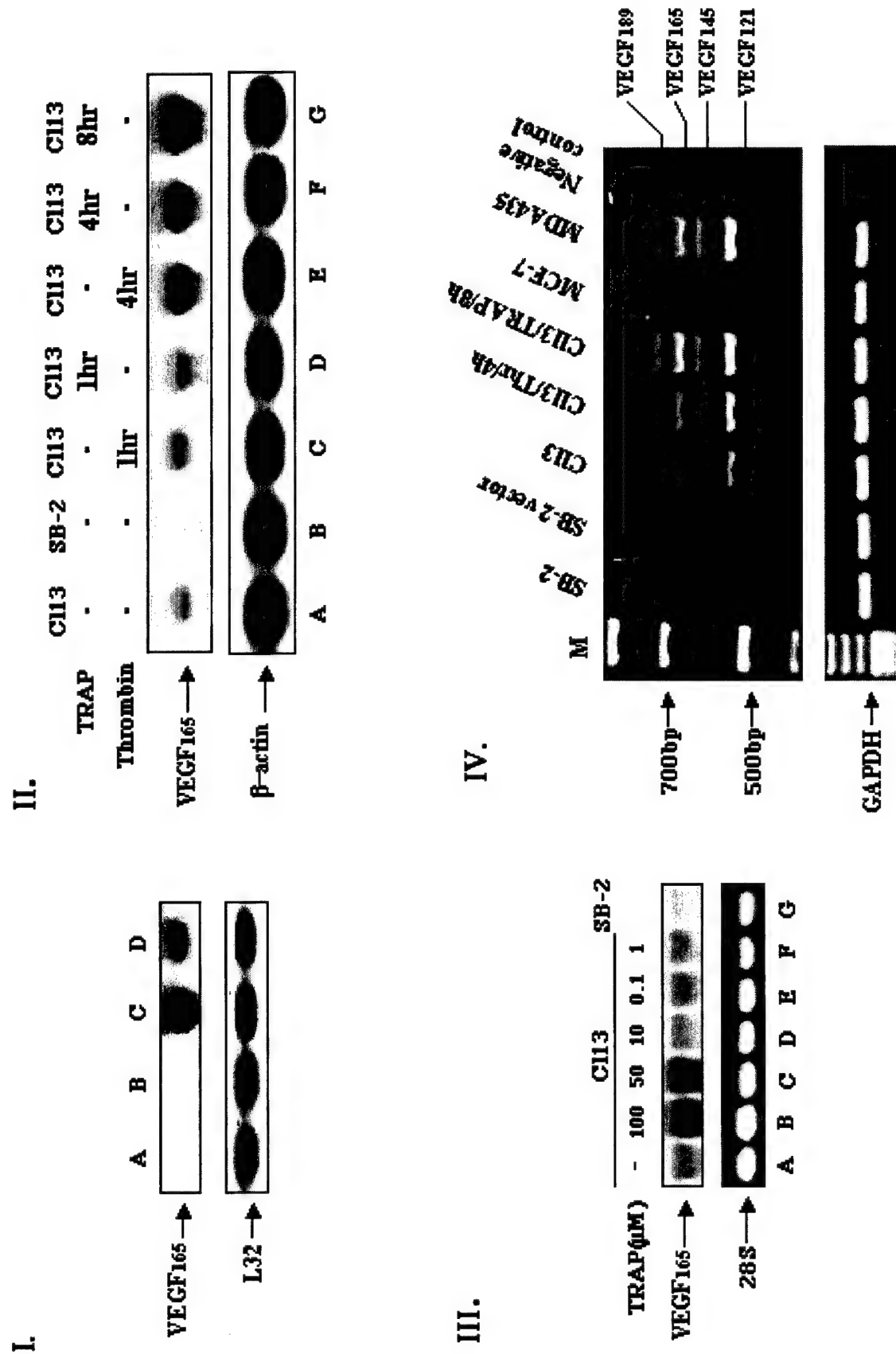
Figure 4 Appendix 3

A. CM-Vector
B. CM-Vector+Thr
C. CM-non metastic MCF-7
D. CM-MCF-7 F.L
E. CM-MCF-7 F.L +Thr
F. CM-highly metastic MDA435

I.
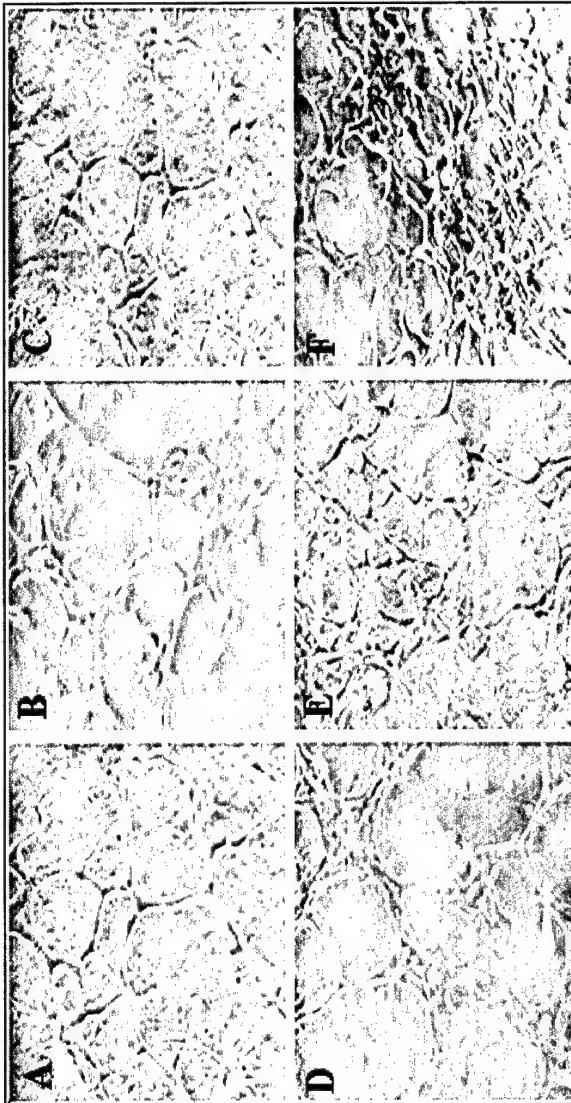
II.
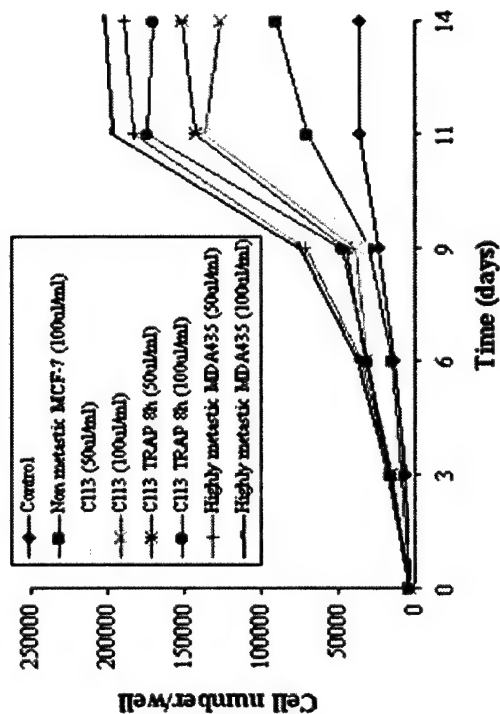
III.
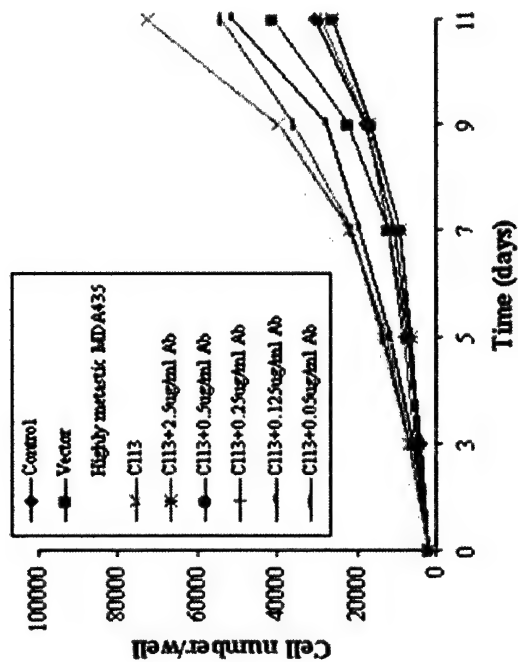
Figure 5   Appendix 3
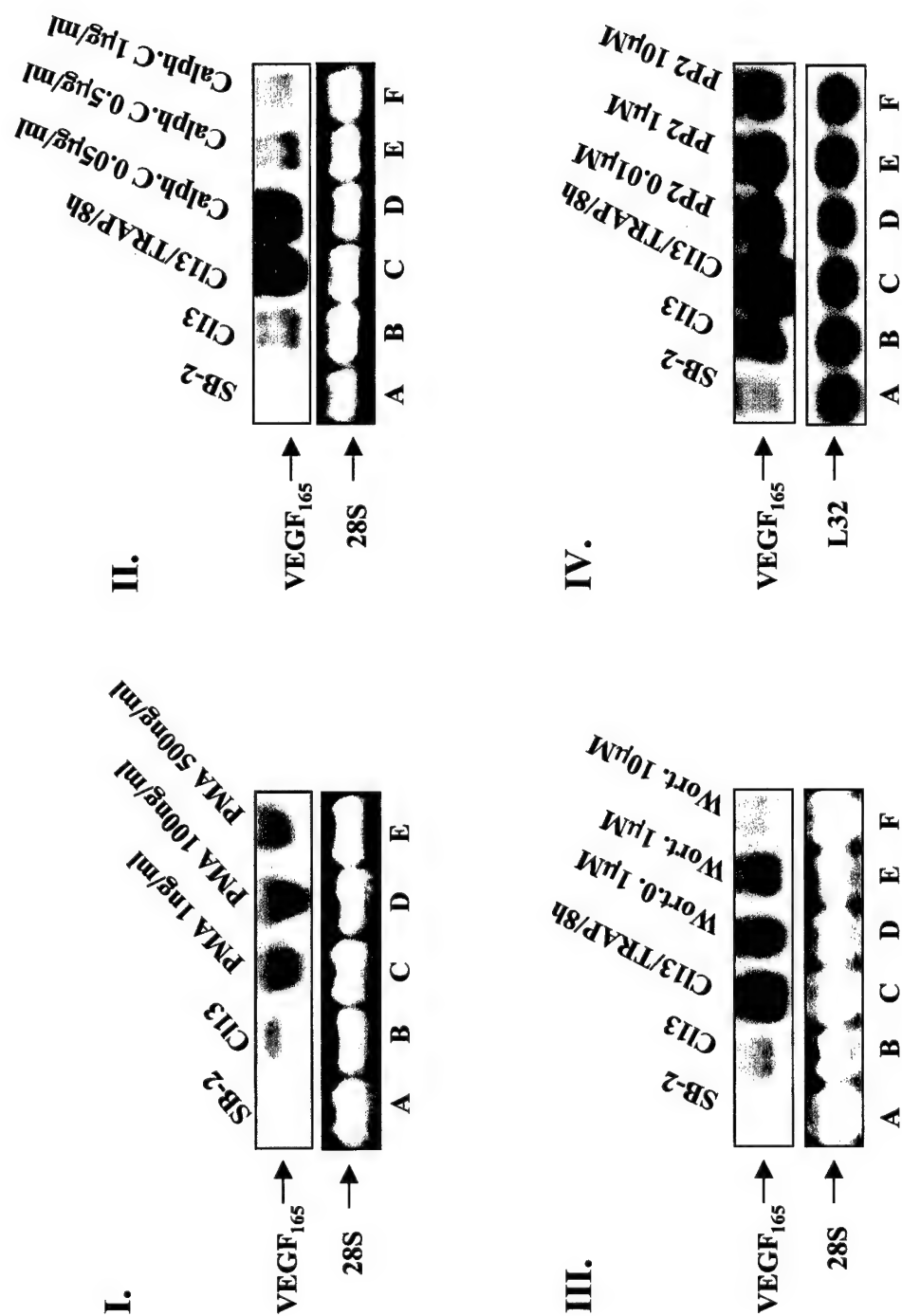
Figure 6   Appendix 3

I.
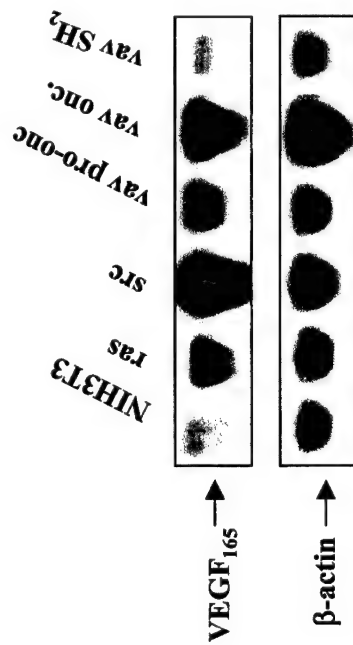
II.

Northern analysis of VEGF$_{165}$
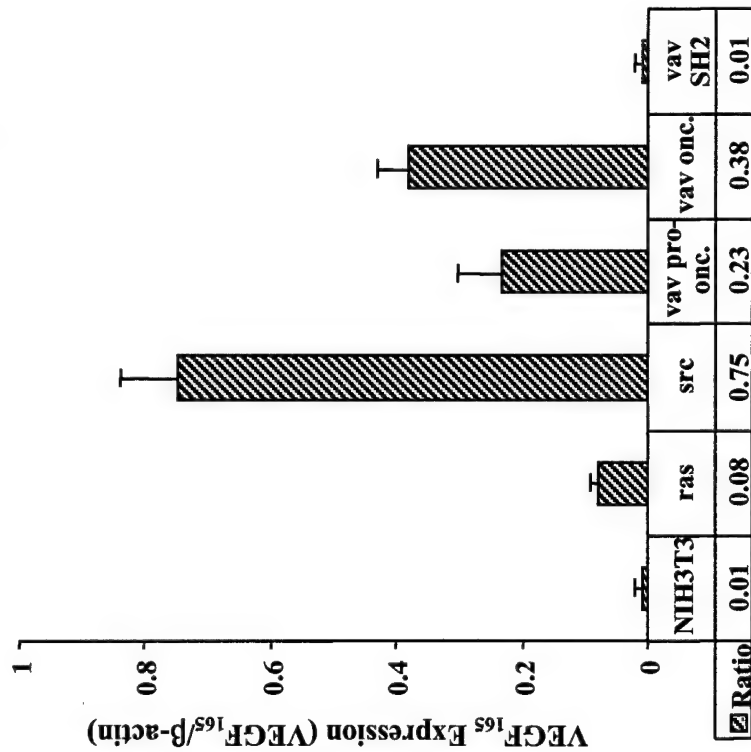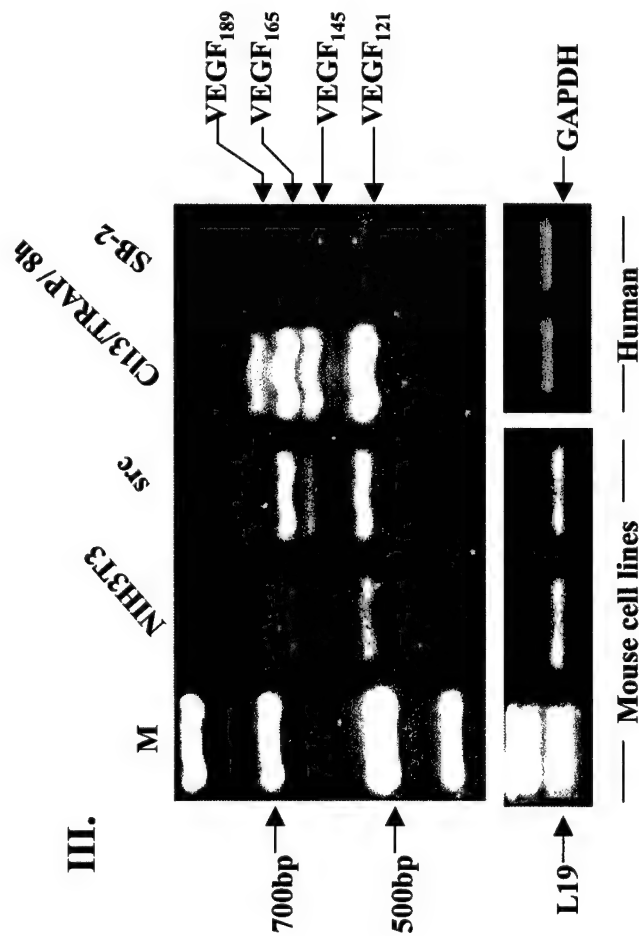
Ratio	NIH3T3	ras	src	vav pro-onc.	vav onc.	vav SH2
	0.01	0.08	0.75	0.23	0.38	0.01

VEGF$_{165}$ Expression (VEGF$_{165}$/β-actin)

III.

R1

Human Protease Activated Receptor1 (hPar1) expression in malignant epithelia: A role in invasiveness

Yong-Jun Yin, Zaidoun Salah, Sorina Grisaru-Granovsky, Irit Cohen, Sharona Cohen Even-Ram, Myriam Maoz, Beatrice Uziely and Rachel Bar-Shavit. *Department of Oncology Hadassah-University Hospital, Jerusalem 91120, Israel*

Runing title: *hPar1* involvement in tumor metastasis and angiogenesis

Word count:

Abstract: 78

Body (including references, legend): 3,713

Figures: 1

Correspondence address:

Bar-Shavit, Rachel Ph.D.

Department of Oncology

Hadassah-University Hospital

POB 12000, Jerusalem 91120, Israel

Phone: 972-2-6777563

Fax: 972-2-6422794

E-mail: barshav@md.huji.ac.il

Human Protease Activated Receptor1 (hPar1) expression in malignant epithelia: A role in invasiveness

Yong-Jun Yin, Zaidoun Salah, Sorina Grisaru-Granovsky, Irit Cohen, Sharona Cohen Even-Ram, Myriam Maoz, Beatrice Uziely and Rachel Bar-Shavit. *Department of Oncology Hadassah-University Hospital, Jerusalem 91120, Israel*

While *Protease Activated Receptors (PARs)* play a traditional role in vascular biology it emerges with a surprisingly new assignments in tumor biology. PAR1 expression correlates with the invasion properties of breast carcinoma while *hPar1* antisense reduces their ability to migrate through Matrigel. Part of the molecular mechanism of PAR1 invasion involves the formation of focal contact complexes upon PAR1 activation. PAR1 induces angiogenesis in animal models *in vivo* and exhibits an oncogenic phenotype of enhanced ductal complexity when overexpressed in the mice mammary glands.

PAR1 expression correlates with the invasion properties of breast carcinoma while *hPar1* antisense inhibits. PAR1 invasion involves the formation of focal contact complexes upon activation. PAR1 induces angiogenesis in animal models *in vivo* and exhibits an oncogenic phenotype of enhanced ductal complexity when overexpressed in the mice mammary glands.

Key words: PAR1, epithelia, invasion, metastasis, angiogenesis

Introduction

In addition to its central role in hemostasis and thrombosis, the serine protease thrombin is a potent mitogen of vascular endothelial and smooth muscle cells (1,2). Along with endothelial dysfunction, massive proliferation of vascular smooth muscle cells (VSMCs) is one of the prominent characteristics of atherosclerosis, suggesting a role for thrombin in the etiology of the disease. While vascular proliferation, inflammation, apoptosis, and extracellular matrix alterations all contribute to the pathobiology of atherosclerosis, the precise role of each of these processes is poorly understood. In this review, we will consider the role of the thrombin receptor in cell proliferation and invasiveness, which is likely to be relevant to atherolsclerotic VSMC proliferation.

Most thrombin - regulated cellular events are mediated via the *Protease Activated Receptors*; PAR-1, PAR-3 and PAR- 4 (3). The PARs are a family of seven transmembrane G-protein coupled receptors activated via proteolytic cleavage. This unique mode of activation appears to involve exposure of autoligated sites present on the receptor themselves (4-7). While the full repertoire of protease signaling through PARs remains to be determined, this family plays a distinct role in epithelial cell biology. Analysis of PAR1 in the context of normal epithelial function as well as under pathological conditions highlights a new function for this gene (and possibly other members of the PAR family) in normal development and in tumor progression.

Epithelial cells associate into intact polarized sheets and communicate through an intricate network of cell-cell junctions and cell-ECM interactions. This architectural restraint of cell-cell junctions underlined by a basement membrane serves as extra-strict boundaries to maintain normal cellular behavior. A critical event in malignant tumor development is the acquisition of the ability to invade through basement membranes, enter the circulatory system, and re-emerge from blood vessels to establish metastatic colonies at distant sites. This task is accomplished via a well-orchestrated set of events including the recruitment of enzymes to remodel targeted locations of the basement membrane microenvironment. We have shown that PAR1 has central roles in breast carcinoma invasion and

metastasis (8) as well as in other types of carcinomas (e.g., bladder, ovary, prostate and colon) (*in preparation*). In addition, recent studies by Martin *et al* (9) identified *Par1* as a potent oncogene in a cDNA expression library screen for genes that induce focus forming activity and transformation in NIH3T3 cells. Thus *Par1* joins the list of G-protein coupled receptors (GPCRs) that harbor oncogenic potential such as, *mas* and *g2a*. This property of *hPar1* was attributed to ectopic overexpression of the receptor, as also demonstrated for Wnt-1 and HER2/Neu (erbB2) (10, 11), rather than to a specifically inserted mutation as in the case of APC and β-catenin (10). A putative oncogenic role for *Par1* is further supported by our observations that *hPar1* is overexpressed in a series of carcinoma biopsy specimens and in a collection of differentially metastatic cell lines (8, 12).

PAR1 expression is associated with metastatic potential. A direct correlation has been established between the levels of PAR1 expression and the invasion properties of breast carcinomas (8*). In situ* hybridization performed on paraffin-embedded sections from a broad range of archival biopsy specimens showed a differential pattern of distribution. Invasive carcinoma specimens, selected from typical infiltrating ductal carcinoma (IDC) with vascular invasion and lymph node metastases, revealed high PAR1 expression, confined to the carcinoma of the primary tumors. Lower levels of expression were observed in *high grade* ductal carcinoma *in situ* (DCIS) of comedo type. In contrast, very little or no PAR1 was observed in *low grade* DCIS of solid type and in the pre-malignant atypical intraductal hyperplasia (AIDH). No PAR1 expression was observed in normal mammary sections obtained from reduction mammoplasty. Likewise, a panel of mammary carcinoma cell lines was surveyed for a correlation between PAR1 expression and established metastatic potential (8). The cell lines included a near-normal diploid immortalized breast epithelial cell line originating from fibrocystic disease (MCF10A), and six tumor cell lines with different doubling times, tumorigenicity, and metastatic potential in nude mice. In these cell lines, high levels of PAR1 expression were found in the highly metastatic cell lines, moderate PAR1 levels in moderately metastatic cell lines, and no expression was present in non-metastatic cells.

PAR1 expression does not merely correlate with tumor progression but appears likely to play an active role during metastatic breast carcinoma cell invasion. This is suggested by the fact that introduction of *Par1* antisense into the aggressively metastatic MDA- 435 cells markedly reduces their ability to migrate through Matrigel (a reconstituted basement membrane) *in vitro* (13). In the complementary experiment, cell lines overexpressing PAR1 exhibit increased invasion through Matrigel (12). These results identify PAR1 as a potential cellular target for cancer therapies.

Molecular mechanisms of PAR1 in tumor invasion: PAR1 cooperates with αvβ5 integrin to promote cytoskeletal reorganization. To begin to evaluate the molecular mechanisms by which PAR1 promotes tumor invasion and metastasis, stable clones of non-metastatic melanoma cells (SB-2) overexpressing *hPar1* were established. These clones exhibited increased adhesion to extracellular matrix components, accompanied by reorganization of cytoskeletal F-actin toward a morphology favoring migration (12). Activation of PAR1 by TRAP (100μM) increased the phosphorylation of focal adhesion kinase and paxillin, and induced the formation of focal contact complexes. In addition, PAR1 activation affected the distribution of cell-surface integrins without altering their level of expression: αvβ5, but not αvβ3 or α5β1, was specifically recruited to focal contact sites. PAR1-overexpressing cells showed selective reciprocal co-precipitation of paxillin with αvβ5 but not with αvβ3. This co-immunoprecipitation failed to occur in cells containing the truncated form of PAR1 lacking the entire cytoplasmic portion of the receptor (12). Thus, the PAR1 cytoplasmic tail is essential for recruitment of αvβ5 integrin. PAR1 overexpressing cells were invasive *in vitro*, as reflected by migration through a Matrigel barrier and invasion was further enhanced by ligand activation of PAR1. Moreover, the application of anti-αvβ5 antibodies specifically attenuated this PAR1-induced invasion (12). We conclude that activation of PAR1 may foster tumor cell invasion via a novel mechanism involving cooperation with αvβ5 integrin. While we observed induced invasion following PAR1 activation, Kamath *et al* have reported that activation of PAR1 inhibited the invasion and migration of MDA231 breast cancer cells (14). By the use of a truncated version of PAR1, devoid of the entire cytoplasmic tail one may resolve this controversy.

PAR1 expression correlates with normal physiological invasion during placental implantation.

Placental implantation into the uterus wall in early pregnancy is an example of a normal physiological invasion process. We hypothesized that genes such as PAR1 are part of an invasive program that should be turned off when the period of invasion is over. We therefore analyzed PAR1 expression during and after placenta implantation. Indeed, PAR1 is exclusively expressed during the time-limited invasion period and is completely shut off thereafter (15). In the first trimester of pregnancy, specialized placental epithelial cells, the cytotrophoblasts (CTBs), differentiate, proliferate and invade to initiate placental implantation. To address the involvement of PAR1 in a regulated invasion process, we examined PAR1 expression in CTBs in human placental tissue samples (obtained from elective terminations of pregnancies). In contrast to the PAR1 overexpression observed in the tumor biopsy specimens, the temporal and spatial pattern of PAR1 expression during placental implantation is tightly controlled. PAR1 is detected predominantly in the cytotrophoblast layer between 7 and 10 weeks of gestation and is undetectable by 12 weeks (15). During placental implantation CTBs differentiate, proliferate, and invade the uterine wall and the spiral arteries deep into the stroma to establish proper fetal-maternal interactions (16). Although poorly understood, the molecular basis of CTB invasion shares many features with tumor cell invasion (16-18). Furthermore, the pathobiology of several disorders of pregnancy involves dysregulated trophoblastic invasion. Shallow invasion of the uterine wall leads to preeclampsia and restriction of fetal growth (19) while excessive proliferation and invasion may result in gestational trophoblastic disease, ranging from partial hydatidiform moles to choriocarcinoma (20). Trophoblast cells from complete hydatidiform moles (CHM) proliferate rapidly, often show cytologic atypia, and bear an approximately 20% risk of becoming malignant (20). This condition provides an opportunity to study the expression of *Par1* in pathologically over-proliferative placental villi. *Par1* mRNA and protein expression in biopsies of CHM (12-14 weeks of gestation) were compared with age-matched normal placentas. In CHM, the trophoblast cells exhibit high levels of *hPar1* mRNA and protein, while very little or no expression is detected in the age matched controls (15). These results suggest that *hPar1* expression is part of an invasive program for both normal placental development and pathological trophoblastic disorders such as CHM.

PAR1 induces VEGF and tumor angiogenesis. The formation of new blood vessels is a critical determinant of tumor progression. Although the association between the protease thrombin and angiogenesis has been previously documented, the role of PAR1 in tumor angiogenesis and its mechanism of activation are largely unknown. Using *in vivo* injection of either Matrigel plugs containing *Par1*-expressing cells or of rat prostatic carcinoma cells transfected with a tetracycline-inducible *Par1* expression vector, we showed that *Par1* significantly enhances both angiogenesis and tumor growth (21). Several VEGF splice forms are induced in cells expressing *Par1* and activation of PAR1 markedly augments the expression of VEGF mRNAs and of functional VEGF proteins. Since neutralizing anti-VEGF antibodies potently inhibited *Par1*-induced endothelial cell proliferation (21), we conclude that *Par1*-induced angiogenesis requires VEGF. Specific inhibitors of PKC, Src and PI3K inhibit *Par1*-induced VEGF expression, suggesting the participation of these kinases in the process. In addition, oncogenic transformation by genes known to be part of PAR1 signaling machinery is sufficient to increase VEGF expression in NIH3T3 cells. These data identify players in the signaling process evoked by PAR1 activation and support the novel notion that initiation of the PAR1 signalling pathway, either by ligation of PAR1 or by the direct activation of downstream signaling components, is sufficient to induce VEGF and hence angiogenesis.

hPar1 **and mammary gland morphogenesis.** To further investigate the role of *h*PAR1 in breast cancer and normal development of the breast epithelia we have established a line of mice carrying *hPar-1* transgenes specifically overexpressed in the mammary glands (by using MMTV-LTR derived construct) (manuscript in preparation). Mammary glands from transgenic animals exhibited grossly hyperplastic features compared to non transgenic littermates. The growing branch ends from virgin transgenic animals showed enhanced complexity of alveolar side branching compared with normal virgin glands; a difference that is accentuated in pregnant *hPar 1*$^{+/-}$ mice. This phenotype is reminiscent of the effect of overexpression of several different oncogenes in the mouse breast (22). *In situ* hybridization analysis in sections of virgin mammary glands and during early pregnancy showed abundant *hPar1* expression at the

luminal phase of the mammary epithelium. Likewise, quantitative RT-PCR analysis showed high levels of *hPar1* expression in 5-, 8- and 13- week old virgin *hPar1*^{+/-} animals and further elevated *hPar1* levels in pregnant mice (P4d, P8d, P12d).

In normal wild-type mice, Wnt-4 expression is low in the virgin gland and increases during pregnancy (23, 24), suggesting Wnt-4 may play a role in the induction of ductal side branching. Wnt-4 expression is markedly induced in the *hPar1* [+/-] overexpressing glands compared to age matched wild type mice. This was demonstrated by both RT-PCR (at 5 &13 weeks in virgin mice and during pregnancy at 4, 8, and 12 days of gestation) and immunoblotting assays. Immunohistochemistry detected Wnt-4 confined to the epithelial compartment of mammary tissue from 13-week virgin and 4- and 8-day pregnant *hPar1*^{+/-} animals, compatible with the localization and expression of PAR1 in these mice. Wnts encode secreted glycoproteins that carry short-range signals between cells and bind to members of the Frizzled family of seven - transmembrane receptors. Wnt 7b levels were also increased compared to normal controls in both virgin and pregnant *hPar1*^{+/-} mammary tissue at the same time points as Wnt-4. The expression of other Wnt family members (Wnt 5a, 5b, 6, and 7a) in the mammary tissue of *hPar1* [+/-] animals was analyzed by RT-PCR and was not different from controls. The presence of elevated Wnt-4 and Wnt-7 in mammary glands from *hPar1* [+/-] mice suggests that PAR1 directly or indirectly controls their expression.

The possibility that PAR1 overexpression in the mammary gland induces alveologenesis (i.e., proliferation in the lobulo-alveolar structures) in addition to ductal side-branching was also investigated. Higher ductal network complexity results from enhanced alveoli proliferation, thus the epithelial cell proliferation rate was assessed *in situ* by immunostaining using antibodies to the "proliferating cell nuclear antigen" (PCNA). The proliferation index is defined as the number of PCNA - positive nuclei of alveolar epithelial cells divided by the total number of nuclei. These studies revealed that the proliferation of alveolar bud epithelium is significantly enhanced in *hPar1*^{+/-} mice as compared to wild type counterparts. In virgin *hPar1*^{+/-} mice, enhanced PCNA staining was observed at 5 weeks, declined at weeks 8 and 10, and was elevated again at 13 weeks. During pregnancy, active alveoli proliferation

takes place in wild type mice and PCNA staining is significantly increased in the alveolar bud epithelium. In the pregnant $hPar1^{+/-}$ mice (at 4, 8, and 12 days of gestation), PCNA staining is further elevated. In contrast to the alveolar epithelium, there were no obvious differences between wild type and $hPar1^{+/-}$ mice in the proliferation of the ductal epithelium in virgin or pregnant mice. Overall, the mammary glands of $hPar1^{+/-}$ transgenic mice show enhancement of alveoli proliferation and ductal side branching, both of which contribute to increased network complexity in the mammary ducts.

Future Perspective: Epithelial-mesenchymal transitions (EMTs) occur during critical phases of embryonic development and a similar transition occurs during the progression of carcinoma towards malignancy. Alterations of the normally strict epithelial architecture may reflect critical early events which ultimately lead to invasion and metastasis. The interrelation between PAR1 and E-cadherin and its signaling machinery (α-, β- and γ –catenins) is of primary interest. How does PAR1 affect epithelial cell morphology? Our preliminary data suggest that PAR1 suppresses E-cadherin expression. Does the mechanism involve regulators of E-cadherin expression, such as Snail and SiP1? Both of these proteins bind E-cadherin promoter regions and act as transcriptional repressors (25-28). Alternatively, promoting aberrant methylation of the normally unmethylated 5' - CpG-rich areas in E-cadherin is another way *hPar1* might regulate E-cadherin. This epigenic mechanism is associated with the transcriptional silencing of genes, including E-cadherin, in various forms of cancer (29).

Another important factor to consider when studying the role of PAR1 in tumor progression is the interactions between cancer cells and their microenvironment (30). The stroma microenvironment of the tumor can have profound influence on tumor progression. Whereas normal stroma can postpone or prevent tumorigenesis, abnormal stromal components can promote tumor development. This stromal effect is significant enough that in some cases, reintroduction of normal stroma can suppress transformed phenotype (31). Even after prolonged passaging, teratocarcinoma cells are still capable of differentiating and generating normal mice upon contact with a normal microenvironment (31). Therefore, tumor progression may be clinically reversible if the appropriate context and signaling are

supplied. It is feasible that serine- proteases capable of acivating PAR1 are present in the vicinity of the tumor. Prothrombin/thrombin , factor Xa as also the tissue factor (TF) TF-VIIa complex are possible candidates to serve as signaling cues for PAR1 (32). In the context of endothelial cells, for example, activated protein C (APC), a trypsin like enzyme was shown (along with other receptors) –to activate PAR1 (33). It remains to determine whether these proteins are expressed in the stroma of the tumor. Future studies will explore the involvement of PAR1 in epithelial morphology and the influence of the stromal microenvironment on PAR1 expression, activation, and function.

Acknowledgments

References
1. Madamanchi NR, Li S, Patterson C, Runge MS. Thrombin regulates vascular smooth muscle cell growth and heat shock proteins via JAK-STAT pathway. *J. Biol. Chem.* 2001; 276: 18915-18924

2. Rao GN, Katki KA, Madamachi NR, Wu Y, Birrer MJ. JunB forms the majority of the AP-1 complex and is a target for redox regulation by receptor tyrosine kinase and G-protein-coupled receptor agonists in smooth muscle cells. *J. Biol. Chem.* 1999; 274: 6003-6010.

3. Sambrano GR, Weiss EJ, Zheng YW, Huang W, Coughlin SR. Role of thrombin signalling in hemostasis and thrombosis. *Nature* 2001; 413: 74-78.

4. Vu T-K, Hung HDT, Wheaton VI, Coughlin SR. Molecular cloning of a functional thrombin receptor reveals a novel proteolytic mechanism of receptor activation. *Cell* 1991;.64:1057-1068.

5. Rasmussen UB, Vouret-Craviari V, Jallat S, Schlesinger Y, Pages G, Pavirani A, Lecocq JP, Pouyssegur J, Van Obberghen-Schilling E. cDNA cloning and expression of a hamster alpha-thrombin receptor coupled to Ca2+ mobilization. *FEBS Lett* 1991; 288: 123-128.

6. Kahn ML, Zheng YW, Huang W, Bigornia V, Zeng D, Moff S, Farese RV Jr, Tam C, Coughlin SR. A dual thrombin receptor system for platelet activation. *Nature* 1998; 394: 690-694.

7. Nakanishi-Matsui M, Zheng YW, Sulciner DJ, Weiss EJ, Ludeman MJ, Coughlin SR PAR3 is a cofactor for PAR4 activation by thrombin *Nature* 2000; 404: 609-613.

8. Even-Ram S, Uziely B, Cohen P, Ginzburg, Y, Reich R, Vlodavsky I, Bar-Shavit R. *Nature Medicine* 1998; 4: 909-914.

9.   Martin CB, Mahon GM, Klinger MB, Kay RJ, Symons M, Der CJ, Whitehead IP. The thrombin receptor, PAR-1, causes transformation by activation of Rho-mediated signaling pathways *Oncogene* 2001; 20: 1953-1963.

10. Nusse R, Varmus H. Wnt genes. *Cell* 1992; 69: 1073-1087.

11. Alroy I, Yarden Y. The ErbB signaling network in embryogenesis and oncogenesis: signal diversification through combinatorial ligand-receptor interactions. *FEBS Lett.* 1997; 410: 83-86.

12. Cohen Even-Ram S, Maoz M, Pokroy E, Reich R, Katz B-Z, Gutwein P, Altevogt P, Bar-Shavit R. Tumor cell invasion is promoted by activation of protease activated receptor-1 in cooperation with the alpha vbeta 5 integrin *J. Biol. Chem* 2001; 276: 10952-10962.

13. Albini A, Iwamoto Y, Kleinman HK, Martin GR, Aaronson SA, Kozlowsky JM, McEwan RN. A rapid in vitro assay for quantitating the invasive potential of tumor cells. *Cancer Research* 1987; 47: 3239-3245.

14. Kamath L, Meydani A, Foss F, Kuliopulos A. Signaling from protease-activated receptor-1 inhibits migration and invasion of breast cancer cells. *Cancer Res* 2001; 61: 5933-5940 .

15. Even-Ram Cohen, S, Grisaru-Granovsky S, Pruss D, Maoz M, Salah Z, Yin Y-J, Bar-Shavit R. The pattern of Protease Activated Receptors (PARs) expression during early trophoblast development *J Pathology In Press,* 2002.

16. Cross JC, Werb Z, Fisher SJ. Implantation and the placenta: key pieces of the development puzzle. *Science.* 1994; 266:1508-1518, Review.

17. Damsky CH, Fisher SJ. Trophoblast pseudo-vasculogenesis: faking it with endothelial adhesion receptors *Curr Opin Cell Biol* 1998; 10: 660-666, Review.

18. Flamigni C, Bulletti C, Polli V, Ciotti PM, Prefetto RA, Galassi A, Di Cosmo E. *Ann N Y Acad Sci* 1991; 622:176-190, Review.

19. Zhou Y, Damsky CH, Chiu K, Roberts JM, Fisher SJ. Preeclampsia is associated with abnormal expression of adhesion molecules by invasive cytotrophoblasts *J Clin Invest* 1993; 91: 950-960.

20. Coukos G, Makrigiannakis A, Chung J, Randall TC, Rubin SC, Benjamin I. Complete hydatidiform mole. A disease with a changing profile. *J Reprod Med* 1999; 44: 698-704.

21. Yin Y-J, Salah Z, Maoz M, Cohen Even Ram S, Ochayon S, Neufeld G, Katzav S, Bar-Shavit R. Oncogenic transformation induces tumor angiogenesis: A role for PAR1 activation. *FASEB J In Press,* 2002.

22. Siegel PM, Hardy WR, Muller WJ. Mammary gland neoplasia: insights from transgenic mouse models. *BioEssay* 2000; 22: 554-563,

23. Brisken C, Park S, Vass T, Lydon J, O'Malley B, Weinberg, RA. A paracrine role for the epithelial progesterone receptor in mammary gland development. *Proc. .Natl. Acad. Sci. USA* 1998; 95: 5076-5081.

24. Brisken C, Heineman A, Chavarria T, Elenbaas B, Tan J, Dey SK, McMahon JA, McMahon AP, Weinberg RA. Essential function of Wnt-4 in mammary gland development downstream of progesterone signaling. *Genes & Dev.* 2000; 14: 650-654.

25. Batlle E, Sancho E, Francí C, Domínguez D, Mercè Monfar M, Baulida J, de Herreros GA. The transcription factor Snail is a repressor of E-cadherin gene expression in epithelial tumor cells. *Nature Cell Biol.* 2000; 2: 84-89.

26. Cano A, Pérez-Moreno MA, Rodrigo I, Locascio A, Blanco MJ, del Barrio MG, Portillo F, Nieto MA. The transcription factor Snail controls epithelail-mesenchymaltransition by repressing E-cadherin expression. *Nature Cell Biol.* 2000; 2: 76-83.

27. Leptin M. Twist and Snail as positive and negative regulators during *Drosophila* mesoderm development. *Genes and Dev* 1991; 5: 1568-1576

28. Comijn J, Berx G, Vermassen P, Verschueren K, van Grunsven L, Bruyneel E, Mareel M, Huylebroeck D, van Roy F. The two handed E-box binding zinc finger protein SIP1 downregulates E-cadherin and induces invasion. *Mol. Cell* 2001; 7: 1267-1278.

29. Garinis AG, Menounos PG, Spanakis NE, Papadopoulos K, Karavitis G, Parassi I, Christeli E, Patrinos GP, Manolis EN, Peros G. Hypermethylation-associated transcriptional silencing of E-cadherin in primary sporadic colorectal carcinomas. *J Pathology* 2002; 198: 442-449.

30. Bissell MJ, Derek R. Putting tumors in context. *Nature Reviews* 2001; 1: 46-54.

31. Illmensee K, Minz B. Totipotency and normal differentiation of single teratocarcinoma cells cloned by injection into blastocysts. *Proc Natl Acad. Sci.* USA 1976; 73: 549-553.

32. Riewald M and Ruf, W., Orchestration of coagulation protease signaling by tissue factor. *Trends Cardiovasc Med* 2002;12(4):149-154.

33. Riewald M, Petrovan RJ, Donner A, Mueller BM, Ruf W. Activation of endothelial cell protease activated receptor 1 by the protein C pathway. *Science* 2002 ;296 (5574):1880-1882.

Legend to summarizing scheme

Steps in tumor carcinoma progression and metastasis. Normal epithelia consist of polarized sheets of cells with well organized junctions underlined by a basement membrane. In carcinoma *in situ*, epithelial cells proliferate locally, but are still confined by the basement membrane. The transition from epithelial to mesenchyme stage (EMT-epithelial mesenchyme transition) involves further alterations that can induce local dissemination, emergence through the basement membrane, intravasation and extravasation of lymph or blood vessels, and the establishment of metastatic colonies at distant sites. PAR1 is present at high levels in DCIS (ductal carcinoma *in situ*), but not in normal epithelia or dysplastic carcinoma. Active signaling initiated by PAR1 association with αvβ5 induces reorganization of the cytoskeleton and focal adhesion complex formation, which fosters invasion and metastasis. Part of the scheme is modified from Thiery, JP (*Nature Reviews* June 2002 volume 2 (6)p. 442-454).

Appendix 4 Scheme 1

Normal epithelium

Dysplasia/Adenoma

Loss of E-cadherin:
hypermethylation or
E-cadherin repressors
(Snail, Sip1, E12/E47)

Carcinoma *in situ*

E-cadherin

E-cadherin

E-cadherin

Basement membrane

EMT

Invasive carcinoma

PAR1

PAR1

α4β5

α4β5

PAR1 cross-talk with α4β5
integrin during invasion

ECM

RGD

Matrix degradation

Integrin
α4β5

Activation
Thrombin

α4β5

Src
Shc

Paxillin

P

FAK

Csk

P

Cytoskeleton
modulation

MMP

PAR1

G

G

Src

Src

Paxillin

Csk

RhoA

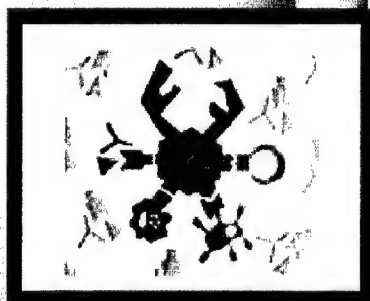Rac

Erk

Reprinted from:

Proceedings of
The 2nd International
Conference on

Tumor Microenvironment
Progression, Therapy & Prevention

Baden (Austria), June 25-29, 2002

Editor

Isaac P. Witz

The Role of *Protease Activated Receptor -1* (PAR-1) in Tumor Invasion and Metastasis, Angiogenesis, and Mammary Gland Morphogenesis

Z. Salah[1], Y.-J., Yin[2], M. Maoz, I. Cohen, B. Uziely, S. Grisaru-Granovsky and R. Bar-Shavit

Department of Oncology
The Hebrew University-Hadassah Medical School, Jerusalem, Israel
Authors[1&2] contributed equally

The *Protease Activated Receptors* (PARs) are a family of seven trans-membrane G-protein coupled receptors activated via proteolytic cleavage. This unique mode of activation appears to involve exposure of autoligand sites present on the receptors themselves (1-4). It is possible that the family members mediate responses to other proteases or peptide ligands *in vivo*. The prototype and first identified member is the thrombin receptor, PAR1. Three other family members (PARs 2,3, 4) have been identified to date. While the full repertoire of protease signaling through PARs remains to be determined, sufficient data exists to define a role for PAR1 in tumor invasion, metastasis and angiogenesis.

PAR1 Expression Is Associated with Metastatic Potential

The turning point in malignant tumor progression is the acquisition of the ability to invade basement membranes, infiltrate and reemerge from blood vessels to establish new metastatic colonies at distant sites. The well-orchestrated set of events that mediates this invasion includes the recruitment of enzymes to remodel targeted sites within the basement membrane microenvironment. We have identified PAR1 as a cellular marker of breast carcinoma invasion and metastasis (5) as well as of other types of carcinomas (i.e., bladder, ovary, prostate and colon) (*in preparation*). More importantly, our results suggest it is a good target for novel cancer therapies.

A direct correlation has been established between the levels of PAR1 expression and the invasion properties of breast carcinomas *(5)*. *In situ* hybridization performed on paraffin-embedded sections from a broad range of archival biopsy specimens showed a differential pattern of distribution. Invasive carcinoma specimens, selected from typical infiltrating ductal carcinoma (IDC) with vascular invasion and lymph node metastases, revealed high PAR1 expression, confined to the carcinoma of the primary tumors. Lower levels of expression were observed in *high grade* ductal carcinoma *in situ* (DCIS) of comedo type. In contrast, very little or no PAR1 was observed in *low grade* DCIS the solid type and in the pre-malignant atypical intraductal hyperplasia (AIDH). No PAR1 expression was observed in normal mammary sections obtained from reduction mammoplasty. Likewise, a panel of mammary carcinoma cells was surveyed for a correlation between the level of PAR1 expression and established degrees of metastasis (5). The cell lines included near-normal diploid immortalized breast epithelial cell line (MCF10A) originating from fibrocystic disease, and six tumor cell lines with different doubling times, tumorigenicity and metastases in nude mice. In these cell lines, high levels of PAR1 expression were found in the highly metastaic cell lines, moderate PAR1 levels in medium metastatic cell lines, and no expression in the non-metastatic cells.

Intriguingly, a recent screen of cDNA expression libraries for genes that induce focus forming activity and transformation in NIH3T3 cells identified *hPar1* as a potent oncogene (6). Thus *Par1* joins a growing list of G-protein coupled receptors that harbor oncogenic potential, including *mas* and *g2a*. This property of *hPar1* was attributed specifically to ectopic overexpression of the receptor as also demonstrated for *Wnt-1* and HER2/Neu (*erbB2*) (7, 8) and not to a specifically inserted mutation, for example. The correlation of *hPar1* expression with malignancy and the ability of ectopically expressed *Par1* to transform NIH3T3 cells strongly suggest that PAR1 is involved in tumor progression.

PAR1 expression does not merely correlate with tumor progression but appears likely to play an active role during metastatic breast carcinoma cell invasion. This is suggested by the fact that introduction of *Par1* antisense into the aggressively metastatic MDA- 435 cells markedly reduces their ability to migrate through Matrigel (a reconstituted basement membrane) *in vitro* (9). In the complementary experiment, cell lines overexpressing PAR1 exhibit increased invasion through Matrigel (10). These results assign PAR1 as a potential cellular target for cancer therapies.

PAR1 Involvement in Placental Implantation: A Physiological Invasion Process

We have analyzed the expression levels of PAR1 in a physiological invasion process of placental implantation in early pregnancy into the

uterus decidua. This was carried out based on the notion that genes that are part of an invasive program are expected to be turned off when the period is over. Indeed, PAR1 appears to be involved in this process also as it is exclusively expressed during the time-limited invasion period and is completely shut off thereafter (11). In the first trimester of pregnancy, specialized placental epithelial cells, the cytotrophoblasts (CTBs), differentiate, proliferate and invade to initiate placental implantation. To address the involvement of PAR1 in a regulated invasion process, we examined PAR1 expression in CTBs in human placental tissue samples (obtained from elective terminations of pregnancies).

In contrast to the PAR1 overexpression observed in the tumor biopsy specimens, the temporal and spatial pattern of PAR1 expression during placental implantation is tightly controlled. PAR1 is detected predominantly in the cytotrophoblast layer between 7 and 10 weeks of gestation and is undetectable by 12 weeks (11).

Mammalian embryonic development depends on successful implantation and proper placentation. During this process CTBs differentiate, proliferate, and invade the uterine wall and the spiral arteries deep into the stroma to establish proper fetal-maternal interactions (12). Although poorly understood, the molecular basis of CTB invasion shares many features with tumor cell invasion (12-14). Furthermore, the etiology of several disorders of pregnancy involves dysregulated trophoblastic invasion. Shallow invasion of the uterine wall leads to preeclampsia and restriction of fetal growth (15) while excessive proliferation and invasion may result in gestational trophoblastic disease, ranging from partial hydatidiform moles to choriocarcinoma (16). Trophoblast cells from complete hydatidiform moles (CHM) proliferate rapidly, often show cytologic atypia, and bear an approximately 20% risk of becoming malignant (16). This condition provides an opportunity to study the expression of *Par1* in pathologically over-proliferative placental villi. *Par1* mRNA and protein expression in biopsies of CHM (12-14 weeks of gestation) were compared with age-matched normal placentas. In CHM, the trophoblast cells exhibit high levels of *hPar1* mRNA and protein, while very little or no expression is detected in the age matched controls (11). These results suggest that *hPar1* expression is part of an invasive program for both normal placental development and pathological trophoblastic disorders such as CHM. The physiological control of PAR1 expression is therefore of great interest and characterization of the molecular mechanisms involved is underway.

hPar1 in Mammary Gland Morphogenesis and Hyperplasia

The MMTV promoter provides a powerful tool for targeting gene expression specifically to the mammary gland in transgenic animals.

Such studies have allowed the identification of genes involved in normal mammary gland development and in tumorigenesis. We have established a line of mice carrying an MMTV LTR – driven *Par-1* transgene which specifically overexpress *hPar1* in the mammary glands. The mammary glands of these animals exhibited grossly hyperplastic features while non transgenic littermates had normal mammary tissue (*in preparation*). Enhanced complexity of alveolar side branching was observed as compared with normal virgin glands, and this was accentuated in tissues from pregnant *hPar 1+/-* mice. This phenotype is reminiscent of the effect of overexpression of several oncogenes in the mouse breast. *In situ* hybridization analysis of mammary glands from *hPar 1+/-* mice (virgin or in early gestation) showed abundant *hPar1* expression at the luminal phase of the mammary epithelium. Likewise, RT-PCR showed high levels of *hPar1* expression in mammary glands of virgin *hPar1 +/- * mice at 5, 8 and 13 weeks postnatal. *hPar1* levels were further elevated in pregnant *hPar1 +/-* mice at 4, 8 and 12 days of gestation.

In normal wild-type mice, Wnt-4 is weakly expressed in the virgin gland with increased expression in pregnancy (17, 18) and thus may play a role in the induction of ductal side branching. Wnt-4 expression is markedly induced in the *hPar1 +/-* overexpressing glands as compared to age matched wild type mice. This was demonstrated by both RT-PCR (at 5 &13 weeks in virgin and during pregnancy at 4,8, and 12 days of gestation) and immunoblotting assays. Immunohistochemistry detected Wnt-4 confined to the epithelial compartment of mammary tissue from 13-week virgin and 4- and 8-day pregnant *hPar1+/-* animals, compatible with the localization and expression of PAR1 in these mice. Wnts encode secreted glycoproteins that carry short-range signals between cells and bind to members of the Frizzled family of seven - transmembrane receptors. Wnt 7b levels were also increased compared to normal controls in both virgin and pregnant *hPar1 +/-* mammary tissue at the same time points as Wnt-4. The expression of other Wnt family members (Wnt 5a, 5b, 6, and 7a) in the mammary tissue of *hPar1 +/-* animals was analyzed by RT-PCR and was not different from controls. The presence of elevated Wnt-4 and Wnt-7 in mammary glands from *hPar1 +/-* mice suggests that PAR1 directly or indirectly controls their expression.

The possibility that PAR1 overexpression in the mammary gland induces alveologenesis (i.e., proliferation in the lobulo-alveolar structures) in addition to ductal side-branching was explored. Higher ductal network complexity results from enhanced alveoli proliferation, thus the epithelial cell proliferation rate was assessed *in situ* by immunostaining using antibodies to the "proliferating cell nuclear antigen" (PCNA). The proliferation index is defined as the number of PCNA – positive nuclei of alveolar epithelial cells divided by the total number of nuclei. These studies revealed that the proliferation of alveolar bud epithelium is significantly enhanced in *hPar1+/-*

mice as compared to wild type counterparts. In virgin *hPar1*+/- mice, enhanced PCNA staining was observed at 5 weeks, declined at weeks 8 and 10, and was elevated again at 13 weeks. During pregnancy, active alveoli proliferation takes place in wild type mice and PCNA staining is increased in the alveolar bud epithelium. In pregnant *hPar1*+/- mice (at 4, 8, and 12 days of gestation), PCNA staining is further elevated. In contrast to the alveolar epithelium, there were no obvious differences between wild type and *hPar1*+/- mice in the proliferation of the ductal epithelium in virgin or pregnant mice. Overall, we conclude that the mammary glands of *hPar1*+/- transgenic mice show enhancement of both alveoli proliferation and ductal side branching, both of which contribute to increased network complexity in the mammary ducts.

Tumor Angiogenesis: A Role for PAR1 Activation

The formation of new blood vessels is a critical determinant of tumor progression. Although the association between the protease thrombin and angiogenesis has been previously documented, the role of PAR1 in tumor angiogenesis and its mechanism of activation are largely unknown. We find that *Par1* gene expression plays a central role in blood vessel recruitment in animal models (19). Using *in vivo* injection of either Matrigel plugs containing *Par1*-expressing cells or of rat prostatic carcinoma cells transfected with a tetracycline-inducible *Par1* expression vector, we show that *Par1* significantly enhances both angiogenesis and tumor growth. Several VEGF splice forms are induced in cells expressing *Par1*. Activation of PAR1 markedly augments the expression of VEGF mRNAs and of functional VEGFs as determined by *in vitro* assays for endothelial tube alignment and bovine aortic endothelial cell proliferation. Since neutralizing anti-VEGF antibodies potently inhibited *Par1*-induced endothelial cell proliferation, we conclude that *Par1*-induced angiogenesis requires VEGF. Specific inhibitors of PKC, Src and PI3K inhibit *Par1*-induced VEGF expression, suggesting the participation of these kinases in the process. In addition, oncogenic transformation by genes known to be part of PAR1 signaling machinery is sufficient to increase VEGF expression in NIH3T3 cells. These data support the novel notion that initiation of the PAR1 signalling pathway, either by ligation of PAR1 or by the direct activation of downstream signaling components, is sufficient to induce VEGF and hence angiogenesis.

Mechanisms of PAR1 Action: PAR1 Cooperates with αvβ5 Integrin To Promote Cytoskeletal Reorganization and Tumor Cell Invasion

To begin to evaluate the molecular mechanisms by which PAR1 promotes tumor invasion and metastasis, stable clones of non-metastatic

melanoma cells (SB-2) overexpressing *hPar1* were established. These clones exhibited increased adhesion to extracellular matrix components, accompanied by reorganization of cytoskeletal F-actin toward a morphology favoring migration (10). Activation of PAR1 by TRAP (100μM) increased the phosphorylation of focal adhesion kinase and paxillin, and induced the formation of focal contact complexes. In addition, PAR1 activation affected the distribution of cell-surface integrins without altering their level of expression: $\alpha v\beta5$, but not avb3 or $\alpha5\beta1$, was specifically recruited to focal contact sites. PAR1-overexpressing cells showed selective reciprocal co-precipitation of paxillin with $\alpha v\beta5$ but not with $\alpha v\beta3$. This co-immunoprecipitation failed to occur in cells containing the truncated form of PAR1 lacking the entire cytoplasmic portion of the receptor (10). Thus, the PAR1 cytoplasmic tail is essential for recruitment of $\alpha v\beta5$ integrin. PAR1 overexpressing cells were invasive *in vitro*, as reflected by migration through a Matrigel barrier and invasion was further enhanced by ligand activation of PAR1. Moreover, the application of anti-$\alpha v\beta5$ antibodies specifically attenuated this PAR1-induced invasion (10). We conclude therefore, that activation of PAR1 may lead to a novel cooperation with $\alpha v\beta5$ integrin to foster tumor cell invasion.

References

1. Vu, T-K., Hung, H.D.T., Wheaton V.I., & Coughlin, S.R. 1991. *Cell* 64:1057-1068.

2. Rasmussen UB, Vouret-Craviari V, Jallat S, Schlesinger Y, Pages G, Pavirani A, Lecocq JP, Pouyssegur J,, and Van Obberghen-Schilling E. 1991. *FEBS Lett* 288: 123-128.

3. Kahn ML, Zheng YW, Huang W, Bigornia V, Zeng D, Moff S, Farese RV Jr, Tam C., and Coughlin SR.1998. *Nature*. 394: 690-694.

4. Nakanishi-Matsui M, Zheng YW, Sulciner DJ, Weiss EJ, Ludeman MJ, and Coughlin SR 2000. *Nature*. 404: 609-613.

5. Even-Ram, S., Uziely, B., Cohen, P.,Ginzburg, Y., Reich, R. Vlodavsky, I., and Bar-Shavit, R. 1998. *Nature Medicine*. 4: 909-914.

6. Martin, CB., Mahon, GM., Klinger, MB., Kay, RJ, Symons, M., Der, CJ., and Whitehead IP., and 2001. *Oncogene*, 20: 1953-1963.

7. Nusse, R. and Varmus, H. 1992. *Cell* 69: 1073-1087.

8. Alroy, I. and Yarden Y. *FEBS Lett*. 410: 83-86.

9. Albini, A., Iwamoto, Y., Kleinman, H.K., Martin, G.R., Aaronson, S.A., Kozlowsky, J.M. and McEwan, R.N. 1987. *Cancer Research* 47: 3239-3245.

10. Cohen Even-Ram, S., Maoz, M., Pokroy, E., Reich, R. Katz, B-Z., Gutwein, P., Altevogt, P., and Bar-Shavit, R. 2001. *J. Biol. Chem* 276: 10952-10962.

11. Even-Ram, Cohen, S., Grisaru-Granovsky, S., Pruss, D., Maoz, M., Salah, Z., Yin, Y-J., and Bar-Shavit, R. *J Pathology In Press,* 2002.

12. Cross JC, Werb Z, and Fisher SJ. *Science* 1994; 266:1508-1518, Review.

13. Damsky CH and Fisher SJ. *Curr Opin Cell Biol* 1998; 10: 660-666, Review.

14. Flamigni C, Bulletti C, Polli V, Ciotti PM, Prefetto RA, Galassi A, and Di Cosmo E. *Ann N Y Acad Sci* 1991; 622:176-190, Review.

15. Zhou Y, Damsky CH, Chiu K, Roberts JM, and Fisher SJ. *J Clin Invest* 1993; 91:950-960.

16. Coukos G, Makrigiannakis A, Chung J, Randall TC, Rubin SC, and Benjamin I. *J Reprod Med* 1999; 44: 698-704.

17. Brisken, C., Heineman, A., Chavarria, T., Elenbaas, B., tan, J., Dey, S.K., McMahon, J.A., McMahon, A.P. and Weinberg R.A. 2000. Genes & Dev. 14: 650-654.

18. Gavin, B.J., and McMahon, A.P., 1992. *Mol. Cell Biol.* 12: 2418-2423.

19. Yin, Y-J, Salah, Z., Maoz, M., Cohen Even Ram, S., Ochayon, S., Neufeld, G., Katzav, S. and Bar-Shavit, R. *FASEB J In Press,* 2002.

Human Protease-Activated Receptor 1 Expression in Malignant Epithelia
A Role in Invasiveness

Yong-Jun Yin, Zaidoun Salah, Sorina Grisaru-Granovsky, Irit Cohen, Sharona Cohen Even-Ram,
Myriam Maoz, Beatrice Uziely, Tamar Peretz, Rachel Bar-Shavit

Abstract—While protease-activated receptors (PARs) play a traditional role in vascular biology, they emerge with surprisingly new assignments in tumor biology. PAR1 expression correlates with the invasion properties of breast carcinoma, whereas human PAR1 antisense reduces their ability to migrate through Matrigel. Part of the molecular mechanism of PAR1 invasion involves the formation of focal contact complexes on PAR1 activation. PAR1 induces angiogenesis in animal models in vivo and exhibits an oncogenic phenotype of enhanced ductal complexity when overexpressed in mouse mammary glands. (*Arterioscler Thromb Vasc Biol.* 2003;23:940-944.)

Key Words: PAR1 ■ epithelia ■ invasion ■ metastasis ■ angiogenesis

In addition to its central role in hemostasis and thrombosis, the serine protease thrombin is a potent mitogen of vascular endothelial and smooth muscle cells.[1,2] Along with endothelial dysfunction, massive proliferation of vascular smooth muscle cells (VSMCs) is one of the prominent characteristics of atherosclerosis, suggesting a role for thrombin in the etiology of the disease. While vascular proliferation, inflammation, apoptosis, and extracellular matrix alterations all contribute to the pathobiology of atherosclerosis, the precise role of each of these processes is poorly understood. In this review, we will consider the role of the thrombin receptor in cell proliferation and invasiveness, which is likely to be relevant to atherosclerotic VSMC proliferation.

Most thrombin-regulated cellular events are mediated via the protease activated receptors PAR1, PAR3, and PAR 4.[3]

The PARs are a family of seven transmembrane G-protein coupled receptors activated via proteolytic cleavage. This unique mode of activation appears to involve exposure of autoligated sites present on the receptor themselves.[4–7] While the full repertoire of protease signaling through PARs remains to be determined, this family plays a distinct role in epithelial cell biology. Analysis of PAR1 in the context of normal epithelial function as well as under pathological conditions highlights a new function for this gene (and possibly other members of the PAR family) in normal development and in tumor progression (Figure).

Epithelial cells associate into intact polarized sheets and communicate through an intricate network of cell-cell junctions and cell-extracellular matrix (ECM) interactions. This architectural restraint of cell-cell junctions underlined by a basement membrane serves as extra-strict boundaries to

Steps in tumor carcinoma progression and metastasis. Normal epithelia consist of polarized sheets of cells with well organized junctions underlined by a basement membrane. In carcinoma in situ, epithelial cells proliferate locally, but are still confined by the basement membrane. The transition from epithelial to mesenchyme stage (EMT) involves further alterations that can induce local dissemination, emergence through the basement membrane, intravasation and extravasation of lymph or blood vessels, and the establishment of metastatic colonies at distant sites. PAR1 is present at high levels in DCIS but not in normal epithelia or dysplastic carcinoma. Active signaling initiated by PAR1 association with $\alpha v \beta 5$ induces reorganization of the cytoskeleton and focal adhesion complex formation, which fosters invasion and metastasis. Part of the scheme is modified from Thiery, JP (*Nature Reviews* June 2002 volume 2 (6)p. 442 to 454).

PAR1 cross-talk with $\alpha_v\beta_5$ integrin during invasion

maintain normal cellular behavior. A critical event in malignant tumor development is the acquisition of the ability to invade through basement membranes, enter the circulatory system, and re-emerge from blood vessels to establish metastatic colonies at distant sites. This task is accomplished via a well orchestrated set of events including the recruitment of enzymes to remodel targeted locations of the basement membrane microenvironment. We have shown that PAR1 has central roles in breast carcinoma invasion and metastasis[8] as well as in other types of carcinomas (eg, bladder, ovary, prostate and colon) (S. Grisaru-Granovsky and Z. Salah, unpublished observations). In addition, recent studies by Martin et al[9] identified PAR1 as a potent oncogene in a cDNA expression library screen for genes that induce focus forming activity and transformation in NIH3T3 cells. Thus PAR1 joins the list of G-protein coupled receptors that harbor oncogenic potential such as, *mas* and *g2a*. This property of human PAR1 (hPAR1) was attributed to ectopic overexpression of the receptor, as also demonstrated for Wnt-1 and HER2/Neu (erbB2),[10,11] rather than to a specifically inserted mutation as in the case of adenomatous polyposis coli (APC).[10] A putative oncogenic role for PAR1 is further supported by our observations that hPAR1 is overexpressed in a series of carcinoma biopsy specimens and in a collection of differentially metastatic cell lines.[8,12]

PAR1 Expression Is Associated With Metastatic Potential

A direct correlation has been established between the levels of PAR1 expression and the invasion properties of breast carcinomas.[8] In situ hybridization performed on paraffin-embedded sections from a broad range of archival biopsy specimens showed a differential pattern of distribution. Invasive carcinoma specimens, selected from typical infiltrating ductal carcinoma (IDC) with vascular invasion and lymph node metastases, revealed high PAR1 expression, confined to

the carcinoma of the primary tumors. Lower levels of expression were observed in high-grade ductal carcinoma in situ (DCIS) of comedo type. In contrast, very little or no PAR1 was observed in low-grade DCIS of solid type and in the premalignant atypical intraductal hyperplasia (AIDH). No PAR1 expression was observed in normal mammary sections obtained from reduction mammoplasty. Likewise, a panel of mammary carcinoma cell lines was surveyed for a correlation between PAR1 expression and established metastatic potential.[8] The cell lines included a near-normal diploid immortalized breast epithelial cell line originating from fibrocystic disease (MCF10A), and six tumor cell lines with different doubling times, tumorigenicity, and metastatic potential in nude mice. In these cell lines, high levels of PAR1 expression were found in the highly metastatic cell lines, moderate PAR1 levels in moderately metastatic cell lines, and no expression was present in nonmetastatic cells.

PAR1 expression does not merely correlate with tumor progression but appears likely to play an active role during metastatic breast carcinoma cell invasion. This is suggested by the fact that introduction of PAR1 antisense into the aggressively metastatic MDA-435 cells markedly reduces their ability to migrate through Matrigel (a reconstituted basement membrane) in vitro.[13] In the complementary experiment, cell lines overexpressing PAR1 exhibit increased invasion through Matrigel.[12] These results identify PAR1 as a potential cellular target for cancer therapies.

Molecular Mechanisms of PAR1 in Tumor Invasion: PAR1 Cooperates With $\alpha v \beta 5$ Integrin to Promote Cytoskeletal Reorganization

To begin to evaluate the molecular mechanisms by which PAR1 promotes tumor invasion and metastasis, stable clones of nonmetastatic melanoma cells (SB-2) overexpressing

hPAR1 were established. These clones exhibited increased adhesion to extracellular matrix components, accompanied by reorganization of cytoskeletal F-actin toward a morphology favoring migration.[12] Activation of PAR1 by TRAP (100 μmol/L) increased the phosphorylation of focal adhesion kinase and paxillin and induced the formation of focal contact complexes. In addition, PAR1 activation affected the distribution of cell-surface integrins without altering their level of expression: $\alpha v\beta 5$, but not $\alpha v\beta 3$ or $\alpha 5\beta 1$, was specifically recruited to focal contact sites. PAR1-overexpressing cells showed selective reciprocal coprecipitation of paxillin with $\alpha v\beta 5$ but not with $\alpha v\beta 3$. This co-immunoprecipitation failed to occur in cells containing the truncated form of PAR1 lacking the entire cytoplasmic portion of the receptor.[12] Thus, the PAR1 cytoplasmic tail is essential for recruitment of $\alpha v\beta 5$ integrin. PAR1 overexpressing cells were invasive in vitro, as reflected by migration through a Matrigel barrier, and invasion was further enhanced by ligand activation of PAR1. Moreover, the application of anti-$\alpha v\beta 5$ antibodies specifically attenuated this PAR1-induced invasion.[12] We conclude that activation of PAR1 may foster tumor cell invasion via a novel mechanism involving cooperation with $\alpha v\beta 5$ integrin. While we observed induced invasion following PAR1 activation, Kamath et al[14] have reported that activation of PAR1 inhibited the invasion and migration of MDA231 breast cancer cells. By the use of a truncated version of PAR1, devoid of the entire cytoplasmic tail, one may resolve this controversy.

PAR1 Expression Correlates With Normal Physiological Invasion During Placental Implantation

Placental implantation into the uterus wall in early pregnancy is an example of a normal physiological invasion process. We hypothesized that genes such as PAR1 are part of an invasive program that should be turned off when the period of invasion is over. We therefore analyzed PAR1 expression during and after placenta implantation. Indeed, PAR1 is exclusively expressed during the time-limited invasion period and is completely shut off thereafter.[15] In the first trimester of pregnancy, specialized placental epithelial cells, the cytotrophoblasts (CTBs), differentiate, proliferate, and invade to initiate placental implantation. To address the involvement of PAR1 in a regulated invasion process, we examined PAR1 expression in CTBs in human placental tissue samples (obtained from elective terminations of pregnancies). In contrast to the PAR1 overexpression observed in the tumor biopsy specimens, the temporal and spatial pattern of PAR1 expression during placental implantation is tightly controlled. PAR1 is detected predominantly in the cytotrophoblast layer between 7 and 10 weeks of gestation and is undetectable by 12 weeks.[15] During placental implantation, CTBs differentiate, proliferate, and invade the uterine wall and the spiral arteries deep into the stroma to establish proper fetal-maternal interactions.[16] Although poorly understood, the molecular basis of CTB invasion shares many features with tumor cell invasion.[16–18] Furthermore, the pathobiology of several disorders of pregnancy involves dysregulated trophoblastic invasion. Shallow invasion of the uterine wall leads to preeclampsia

and restriction of fetal growth[19] while excessive proliferation and invasion may result in gestational trophoblastic disease, ranging from partial hydatidiform moles to choriocarcinoma.[20] Trophoblast cells from complete hydatidiform moles (CHMs) proliferate rapidly, often show cytologic atypia, and bear an $\approx$20% risk of becoming malignant.[20] This condition provides an opportunity to study the expression of PAR1 in pathologically over-proliferative placental villi. PAR1 mRNA and protein expression in biopsies of CHMs (12 to 14 weeks of gestation) were compared with age-matched normal placentas. In CHMs, the trophoblast cells exhibit high levels of hPAR1 mRNA and protein, while very little or no expression is detected in the age-matched controls.[15] These results suggest that hPAR1 expression is part of an invasive program for both normal placental development and pathological trophoblastic disorders such as CHM.

PAR1 Induces VEGF and Tumor Angiogenesis

The formation of new blood vessels is a critical determinant of tumor progression. Although the association between the protease thrombin and angiogenesis has been previously documented, the role of PAR1 in tumor angiogenesis and its mechanism of activation are largely unknown. Using in vivo injection of either Matrigel plugs containing PAR1-expressing cells or of rat prostatic carcinoma cells transfected with a tetracycline-inducible PAR1 expression vector, we showed that PAR1 significantly enhances both angiogenesis and tumor growth.[21] Several VEGF splice forms are induced in cells expressing PAR1 and activation of PAR1 markedly augments the expression of VEGF mRNAs and of functional VEGF proteins. Because neutralizing anti-VEGF antibodies potently inhibited PAR1-induced endothelial cell proliferation,[21] we conclude that PAR1-induced angiogenesis requires VEGF. Specific inhibitors of PKC, Src, and PI3K inhibit PAR1-induced VEGF expression, suggesting the participation of these kinases in the process. In addition, oncogenic transformation by genes known to be part of PAR1 signaling machinery is sufficient to increase VEGF expression in NIH3T3 cells. These data identify players in the signaling process evoked by PAR1 activation and support the novel notion that initiation of the PAR1 signaling pathway, either by ligation of PAR1 or by the direct activation of downstream signaling components, is sufficient to induce VEGF and hence angiogenesis.

hPar1 and Mammary Gland Morphogenesis

To further investigate the role of hPAR1 in breast cancer and normal development of the breast epithelia, we have established a line of mice carrying hPAR1 transgenes specifically overexpressed in the mammary glands (by using MMTV-LTR–derived construct) (Y.-J. Yin, unpublished observations). Mammary glands from transgenic animals exhibited grossly hyperplastic features compared with nontransgenic littermates. The growing branch ends from virgin transgenic animals showed enhanced complexity of alveolar side branching compared with normal virgin glands, a difference that is accentuated in pregnant hPar1$^{+/-}$ mice. This phenotype is reminiscent of the effect of overexpression of several

different oncogenes in the mouse breast.[22] In situ hybridization analysis in sections of virgin mammary glands and during early pregnancy showed abundant hPar1 expression at the luminal phase of the mammary epithelium. Likewise, quantitative reverse-transcriptase polymerase chain reaction (RT-PCR) analysis showed high levels of hPAR1 expression in 5-, 8- and 13-week-old virgin hPAR1^{+/-} animals and further elevated hPAR1 levels in pregnant mice (pregnant for 4, 8, and 12 days).

In normal wild-type mice, Wnt-4 expression is low in the virgin gland and increases during pregnancy,[23,24] suggesting Wnt-4 may play a role in the induction of ductal side branching. Wnt-4 expression is markedly induced in the hPar1^{+/-} overexpressing glands compared with age-matched wild-type mice. This was demonstrated by both RT-PCR (at 5 and 13 weeks in virgin mice and during pregnancy at 4, 8, and 12 days of gestation) and immunoblotting assays. Immunohistochemistry detected Wnt-4 confined to the epithelial compartment of mammary tissue from 13-week virgin and 4- and 8-day pregnant hPar1^{+/-} animals, compatible with the localization and expression of PAR1 in these mice. Wnts encode secreted glycoproteins that carry short-range signals between cells and bind to members of the Frizzled family of 7-transmembrane receptors. Wnt 7b levels were also increased compared with normal controls in both virgin and pregnant hPar1^{+/-} mammary tissue at the same time points as Wnt-4. The expression of other Wnt family members (Wnt 5a, 5b, 6, and 7a) in the mammary tissue of hPar1^{+/-} animals was analyzed by RT-PCR and was not different from controls. The presence of elevated Wnt-4 and Wnt-7 in mammary glands from hPar1^{+/-} mice suggests that PAR1 directly or indirectly controls their expression.

The possibility that PAR1 overexpression in the mammary gland induces alveologenesis (ie, proliferation in the lobulo-alveolar structures) in addition to ductal side-branching was also investigated. Higher ductal network complexity results from enhanced alveoli proliferation, thus the epithelial cell proliferation rate was assessed in situ by immunostaining using antibodies to the proliferating cell nuclear antigen (PCNA). The proliferation index is defined as the number of PCNA-positive nuclei of alveolar epithelial cells divided by the total number of nuclei. These studies revealed that the proliferation of alveolar bud epithelium is significantly enhanced in hPar1^{+/-} mice as compared with wild-type counterparts. In virgin hPAR1^{+/-} mice, enhanced PCNA staining was observed at 5 weeks, declined at weeks 8 and 10, and was elevated again at 13 weeks. During pregnancy, active alveoli proliferation takes place in wild-type mice, and PCNA staining is significantly increased in the alveolar bud epithelium. In the pregnant hPAR1 mice (at 4, 8, and 12 days of gestation), PCNA staining is further elevated. In contrast to the alveolar epithelium, there were no obvious differences between wild-type and hPAR1^{+/-} mice in the proliferation of the ductal epithelium in virgin or pregnant mice. Overall, the mammary glands of hPar1^{+/-} transgenic mice show enhancement of alveoli proliferation and ductal side branching, both of which contribute to increased network complexity in the mammary ducts.

Future Perspective

Epithelial-mesenchymal transitions (EMTs) occur during critical phases of embryonic development, and a similar transition occurs during the progression of carcinoma toward malignancy. Alterations of the normally strict epithelial architecture may reflect critical early events which ultimately lead to invasion and metastasis. The interrelation between PAR1 and E-cadherin and its signaling machinery (α-, β- and γ-catenins) is of primary interest. How does PAR1 affect epithelial cell morphology? Our preliminary data suggest that PAR1 suppresses E-cadherin expression. Does the mechanism involve regulators of E-cadherin expression, such as Snail and SiP1? Both of these proteins bind E-cadherin promoter regions and act as transcriptional repressors.[25-28] Alternatively, promoting aberrant methylation of the normally unmethylated 5'-CpG-rich areas in E-cadherin is another way hPAR1 might regulate E-cadherin. This epigenic mechanism is associated with the transcriptional silencing of genes, including E-cadherin, in various forms of cancer.[29]

Another important factor to consider when studying the role of PAR1 in tumor progression is the interactions between cancer cells and their microenvironment.[30] The stroma microenvironment of the tumor can have profound influence on tumor progression. Whereas normal stroma can postpone or prevent tumorigenesis, abnormal stromal components can promote tumor development. This stromal effect is significant enough that in some cases, reintroduction of normal stroma can suppress transformed phenotype.[31] Even after prolonged passaging, teratocarcinoma cells are still capable of differentiating and generating normal mice on contact with a normal microenvironment.[31] Therefore, tumor progression may be clinically reversible if the appropriate context and signaling are supplied. It is feasible that serine- proteases capable of activating PAR1 are present in the vicinity of the tumor. Prothrombin/thrombin, factor Xa as also the tissue factor (TF) TF-VIIa complex are possible candidates to serve as signaling cues for PAR1.[32] In the context of endothelial cells, for example, activated protein C (APC), a trypsin like enzyme, was shown (along with other receptors) to activate PAR1.[33] It remains to determine whether these proteins are expressed in the stroma of the tumor. Future studies will explore the involvement of PAR1 in epithelial morphology and the influence of the stromal microenvironment on PAR1 expression, activation, and function.

Acknowledgments

References

1. Madamanchi NR, Li S, Patterson C, Runge MS. Thrombin regulates vascular smooth muscle cell growth and heat shock proteins via JAK-STAT pathway. *J Biol Chem.* 2001;276:18915–18924.

2. Rao GN, Katki KA, Madamachi NR, Wu Y, Birrer MJ. JunB forms the majority of the AP-1 complex and is a target for redox regulation by receptor tyrosine kinase and G-protein-coupled receptor agonists in smooth muscle cells. *J Biol Chem.* 1999;274:6003–6010.

3. Sambrano GR, Weiss EJ, Zheng YW, Huang W, Coughlin SR. Role of thrombin signaling in hemostasis and thrombosis. *Nature.* 2001;413: 74–78.

4. Vu T-K, Hung HDT, Wheaton VI, Coughlin SR. Molecular cloning of a functional thrombin receptor reveals a novel proteolytic mechanism of receptor activation. *Cell.* 1991;64:1057–1068.

5. Rasmussen UB, Vouret-Craviari V, Jallat S, Schlesinger Y, Pages G, Pavirani A, Lecocq JP, Pouyssegur J, Van Obberghen-Schilling E. cDNA cloning and expression of a hamster alpha-thrombin receptor coupled to Ca2+ mobilization. *FEBS Lett.* 1991;288:123–128.

6. Kahn ML, Zheng YW, Huang W, Bigornia V, Zeng D, Moff S, Farese RV Jr, Tam C, Coughlin SR. A dual thrombin receptor system for platelet activation. *Nature.* 1998;394:690–694.

7. Nakanishi-Matsui M, Zheng YW, Sulciner DJ, Weiss EJ, Ludeman MJ, Coughlin SR. PAR3 is a cofactor for PAR4 activation by thrombin *Nature.* 2000;404:609–613.

8. Even-Ram S, Uziely B, Cohen P, Ginzburg Y, Reich R, Vlodavsky I, Bar-Shavit R. *Nat Med.* 1998; 4: 909–914.

9. Martin CB, Mahon GM, Klinger MB, Kay RJ, Symons M, Der CJ, Whitehead IP. The thrombin receptor, PAR-1, causes transformation by activation of Rho-mediated signaling pathways. *Oncogene.* 2001;20: 1953–1963.

10. Nusse R, Varmus H. Wnt genes. *Cell.* 1992;69:1073–1087.

11. Alroy I, Yarden Y. The ErbB signaling network in embryogenesis and oncogenesis: signal diversification through combinatorial ligand-receptor interactions. *FEBS Lett.* 1997;410:83–86.

12. Cohen Even-Ram S, Maoz M, Pokroy E, Reich R, Katz B-Z, Gutwein P, Altevogt P, Bar-Shavit R. Tumor cell invasion is promoted by activation of protease activated receptor-1 in cooperation with the alpha vbeta 5 integrin. *J Biol Chem.* 2001;276:10952–10962.

13. Albini A, Iwamoto Y, Kleinman HK, Martin GR, Aaronson SA, Kozlowsky JM, McEwan RN. A rapid in vitro assay for quantitating the invasive potential of tumor cells. *Cancer Res.* 1987;47:3239–3245.

14. Kamath L, Meydani A, Foss F, Kuliopulos A. Signaling from protease-activated receptor-1 inhibits migration and invasion of breast cancer cells. *Cancer Res.* 2001;61:5933–5940 .

15. Even-Ram Cohen S, Grisaru-Granovsky S, Pruss D, Maoz M, Salah Z, Yin Y-J, Bar-Shavit R. The pattern of protease activated receptors (PARs) expression during early trophoblast development. *J Pathology.* Published online March 3, 2003.

16. Cross JC, Werb Z, Fisher SJ. Implantation and the placenta: key pieces of the development puzzle. *Science.* 1994;266:1508–1518.

17. Damsky CH, Fisher SJ. Trophoblast pseudo-vasculogenesis: faking it with endothelial adhesion receptors. *Curr Opin Cell Biol.* 1998;10: 660–666.

18. Flamigni C, Bulletti C, Polli V, Ciotti PM, Prefetto RA, Galassi A, Di Cosmo E. *Ann N Y Acad Sci* 1991; 622:176–190.

19. Zhou Y, Damsky CH, Chiu K, Roberts JM, Fisher SJ. Preeclampsia is associated with abnormal expression of adhesion molecules by invasive cytotrophoblasts. *J Clin Invest.* 1993;91:950–960.

20. Coukos G, Makrigiannakis A, Chung J, Randall TC, Rubin SC, Benjamin I. Complete hydatidiform mole: a disease with a changing profile. *J Reprod Med.* 1999;44:698–704.

21. Yin Y-J, Salah Z, Maoz M, Cohen Even Ram S, Ochayon S, Neufeld G, Katzav S, Bar-Shavit R. Oncogenic transformation induces tumor angiogenesis: a role for PAR1 activation. *FASEB J.* 2003;17:163–174.

22. Siegel PM, Hardy WR, Muller WJ. Mammary gland neoplasia: insights from transgenic mouse models. *Bio Essay.* 2000;22:554–563.

23. Brisken C, Park S, Vass T, Lydon J, O'Malley B, Weinberg RA. A paracrine role for the epithelial progesterone receptor in mammary gland development. *Proc Natl Acad Sci U S A.* 1998;95:5076–5081.

24. Brisken C, Heineman A, Chavarria T, Elenbaas B, Tan J, Dey SK, McMahon JA, McMahon AP, Weinberg RA. Essential function of Wnt-4 in mammary gland development downstream of progesterone signaling. *Genes Dev.* 2000;14:650–654.

25. Batlle E, Sancho E, Francí C, Domínguez D, Mercè Monfar M, Baulida J, de Herreros GA. The transcription factor Snail is a repressor of E-cadherin gene expression in epithelial tumor cells. *Nat Cell Biol.* 2000;2:84–89.

26. Cano A, Pérez-Moreno MA, Rodrigo I, Locascio A, Blanco MJ, del Barrio MG, Portillo F, Nieto MA. The transcription factor Snail controls epithelial-mesenchymaltransition by repressing E-cadherin expression. *Nat Cell Biol.* 2000;2:76–83.

27. Leptin M. Twist and Snail as positive and negative regulators during *Drosophila* mesoderm development. *GenesDev.* 1991;5:1568–1576.

28. Comijn J, Berx G, Vermassen P, Verschueren K, van Grunsven L, Bruyneel E, Mareel M, Huylebroeck D, van Roy F. The two handed E-box binding zinc finger protein SIP1 downregulates E-cadherin and induces invasion. *Mol Cell.* 2001;7:1267–1278.

29. Garinis AG, Menounos PG, Spanakis NE, Papadopoulos K, Karavitis G, Parassi I, Christeli E, Patrinos GP, Manolis EN, Peros G. Hypermethylation-associated transcriptional silencing of E-cadherin in primary sporadic colorectal carcinomas. *J Pathology.* 2002;198:442–449.

30. Bissell MJ, Derek R. Putting tumors in context. *Nature Reviews.* 2001; 1:46–54.

31. Illmensee K, Minz B. Totipotency and normal differentiation of single teratocarcinoma cells cloned by injection into blastocysts. *Proc Natl Acad Sci U S A.* 1976;73:549–553.

32. Riewald M, Ruf W, Orchestration of coagulation protease signaling by tissue factor. *Trends Cardiovasc Med.* 2002;12:149–154.

33. Riewald M, Petrovan RJ, Donner A, Mueller BM, Ruf W. Activation of endothelial cell protease activated receptor 1 by the protein C pathway. *Science.* 2002;296(5574):1880–1882.

Original Paper

The pattern of expression of protease-activated receptors (PARs) during early trophoblast development

Sharona Cohen Even-Ram,[1][†] Sorina Grisaru-Granovsky,[1][†] Diana Pruss,[2] Miriam Maoz,[1] Zaidoun Salah,[1] Yin Yong-Jun[1] and Rachel Bar-Shavit[1]*

[1]Department of Oncology, Pathology, Hadassah University Hospital, Jerusalem, Israel
[2]Department of Pathology, Hadassah University Hospital, Jerusalem, Israel

*Correspondence to:
Rachel Bar-Shavit, Ph.D.
Department of Oncology,
Hadassah - University Hospital,
POB 12000 Jerusalem 91120,
Israel.
E-mail: barshav@md2.huji.ac.il

† These authors have contributed
equally to this paper.

Abstract

Human fetal development depends on the ability of the embryo to gain access to the maternal circulation. Thus, specialized stem cells of the newly formed placenta, trophoblast, invade the uterus and its arterial network to establish an efficient feto-maternal molecular exchange. To accomplish this task, trophoblast differentiation during the first trimester of pregnancy involves cell proliferation, invasion, and extracellular matrix (ECM) remodelling. Trophoblast invasion shares many features with tumour cell invasion, with the distinction that it is strictly spatially and temporally controlled. We have previously demonstrated that PAR1, the first member of the protease-activated receptor (PAR) family, plays a central role in tumour cell invasion. In the present study we have examined the pattern of expression of PAR1 and other PAR family candidates during early human placental development. We show that PAR1 and PAR3 are highly and spatially expressed between the 7th and 10th weeks of gestation but not at the 12th week and thereafter. Likewise, high expression levels of PAR1 and PAR3 were observed in the cytotrophoblast cells of complete hydatidiform mole as compared to minimal levels in normal age-matched placenta. Together, our data suggest the involvement of PAR1 and PAR3 in restricted and unrestricted pathological trophoblast invasion. Copyright © 2003 John Wiley & Sons, Ltd.

Introduction

During early human placentation, specialized placenta epithelial cells, termed cytotrophoblast (CTB) differentiate, proliferate, and invade the uterine wall and the spiral arteries [1]. Although poorly understood, the molecular basis of CTB invasion shares many features with the process of tumour cell invasion [1–3]. A subpopulation of CTB cells must detach from the fetal basement membrane where it initially resides and invade the uterine wall where it can survive. Cytotrophoblast cells in anchoring villi either fuse to form the syncytiotrophoblast layer or break through the syncytium to form columns of extravillous trophoblast (EVT) cells that connect the embryo to the uterine wall. Since the tumour-like properties of this subset population are critical for appropriate fetal maternal interactions the molecular mechanisms involved are carefully programmed and tightly regulated [4]. Furthermore, the aetiological basis of diseases during pregnancy involves unregulated trophoblastic invasion. Shallow invasion of the uterus leads to pre-eclampsia and restriction of fetal growth [5], while excessive proliferation and invasion may result in gestational trophoblastic disease and choriocarcinoma [6].

The interaction of differentiating CTB cells with the surrounding ECM is a critical feature of the invasion programme identified by a specific integrin switching profile [5,7,8]. CTB cells within the uterine spiral arteries, however, express a typical vascular integrin profile such as VE-cadherin, VCAM-1 and PECAM-1 of the IgG family and the integrins $\alpha v \beta 3$ and $\alpha 1 \beta 1$ [5,7,9]. The activated form of focal adhesion kinase (FAK), the major signalling molecule of integrin clustering, has recently been identified as a potent marker for cytotrophoblast invasion. While the expression of FAK is found at all stages of placental differentiation, the auto-phosphorylated FAK (pY397FAK) is specifically expressed under conditions facilitating CTB invasion and inhibited under conditions that abrogate CTB invasion [10,11].

In the process of trophoblast invasion, both serine- and matrix metalloproteases (MMPs) play a central role in the remodelling of the placental microenvironment as well as in trophoblast outgrowth [12,13]. One outcome of the enhanced proteolytic function is the activation of a family of cell surface receptors, collectively termed protease-activated receptors (PARs) [14]. Presently, there are four members of the PAR family, namely PAR 1–4. While PAR 1, 3, and 4 are activated by thrombin [15], PAR2 is activated by trypsin

and tryptase, as well as the coagulation factors VIIa and Xa, but not by thrombin [16]. This family shares a similar mode of activation, the exposure of an internal ligand following cleavage at a unique cleavage site within the N-terminal exo-domain of the seven transmembrane receptor. Thus PARs are G-coupled receptors that carry their own ligand and are activated either by cleavage of thrombin or by tethered binding of a peptide that mimics the internal ligand sequence.

We have previously shown that PAR1 is overexpressed in biopsy specimens of breast carcinomas as well as in a collection of differentially metastatic cell lines [17]. Activation of PAR1 led to focal adhesion complex formation, cytoskeletal reorganization and the recruitment of $\alpha_V\beta_5$ integrin into focal adhesion sites [18]. This study was undertaken to assess the expression pattern of three members of the PAR family (PAR1–3), during the first trimester of pregnancy. The expression levels of PARs in proliferating and potentially invasive trophoblast cells of complete hydatidiform mole (CHM) [6] were also analysed to assist in evaluating the significance of PARs involvement in early normal placenta development.

Methods

Placental specimens

Placental specimens were obtained from elective terminations of pregnancies as described [19]. Paraffin-embedded complete hydatidiform mole (CHM) biopsies were obtained from the Hadassah Hospital, Department of Pathology archives. All specimens were obtained according to the Hadassah Hospital local Ethics Committee Guidelines.

PCR detection of PAR levels

RNA was isolated (according to the manufacturer's instructions) using TRI-REAGENT (Molecular Research Center Inc, Ohio, USA) from pure villi preparation that had been dissected from the placental structures under a dissecting microscope (Zeiss, Schott KL1500, Germany). One microgram of RNA was used for complementary DNA (cDNA) synthesis employing MuMLV reverse-transcriptase and Oligo d(T) (both from Promega, Wisconsin, USA) and amplified by PCR using the following sets of primers:

PAR1: (1) 5′ ATG GGA TTC TGC CAC CTT AGA TCC 3′ (sense)
(2) 5′ ATG GGA TCC GGA GGC TGA CTA CAA 3′ (antisense)
PAR2: (1) 5′ TGC TCC GAT ATC TTT GTA CAG GAC 3′ (sense)
(2) 5′ TAG GTG GTA GGA AAG CTT CAG GGG 3′ (antisense)
PAR3: (1) 5′ GCT GAC ACA TGG AAC TGA GGT 3′ (sense)

(2) 5′ GAG GTA GAT GGC AGG TAT CAG 3′ (antisense)

These primers were selected to include the coding region for the specific internal ligand of each of the genes which is a unique, conserved region.

PARs transcripts were amplified using Taq polymerase (Bioline, London, UK) per 20 μl of PCR reaction. 95 °C for 3 min for initial melting was followed by 30 cycles of 95 °C for 1 min, 56 °C (PAR1 and PAR2), or 60 °C (PAR3) for 30 s, and 72 °C for 1 min; 7 min at 72 °C was used for final extension following cycling.

In situ hybridization

Specimens of placenta (8 samples for each week of gestation) were fixed in 4% paraformaldehyde and embedded in paraffin. Fifteen CHM biopsies were selected from the Pathology Department archives. Hybridization was carried out as previously described [17]. Briefly, RNA probes were transcribed and labelled by T7 RNA polymerase (for antisense orientation) or T3 RNA polymerase (for sense, control orientation) using DIG-UTP labelling mixture (Boerhinger, Germany). Probes were labelled by utilizing a plasmid of a 462-base pair fragment of the human *Par1* (pBh*Par1*-462S) inserted into the EcoR1-HindIII site. Final concentration for hybridization was 1 μg/ml, according to the manufacturer's instructions for a non-radioactive *in situ* hybridization application. Hybridization was performed overnight at 45 °C on paraffin-embedded placental tissue sections. Slides were washed three times in 0.2 × SSPE at 50 °C, 1 h for each washing, and blocked by blocking reagent (Boehringer). Detection was done by incubation with alkaline phosphatase-conjugated anti-DIG antibodies (Fab fragment, diluted 1 : 300; Boehringer) overnight at room temperature. Alkaline phosphatase was detected by NBT/BCIP reagents (Boehringer) according to the manufacturer's instructions.

Immunohistochemistry

Placental tissue samples of 6–15 weeks were fixed in 4% paraformaldehyde, and processed as described [17]. The tissue was further denatured for 4 min in a microwave oven in a citrate buffer (0.01mol/l, pH 6.0), then blocked in 0.2% glycine, 3% H_2O_2 in methanol and 5% goat serum. The sections were incubated overnight at 4 °C with either an antibody to PAR1 [(C-18): sc-8202, Santa Cruz Biotechnology, Inc, CA, USA] at 1 μg/ml, or a control IgG at the same concentration as anti-PAR1. Detection was performed using a horseradish peroxidase-conjugated goat anti-mouse IgG + IgM antibody (Jackson, Bar Harbor, ME, USA), followed by Zymed aminoethyl carbazole (AEC) substrate kit (Zymed, South San Francisco, CA, USA) and counterstained with Mayer's haematoxylin.

Western blot analysis

Placental villi were solubilized in lysis buffer as described [19]. Membranes (Immobilon-P; Millipore) were blocked and probed with 1 µg/ml of anti PAR3 receptor (anti-human rabbit polyclonal IgG) and detected as described [17].

Results

PAR family expression in human placental villi

To study the pattern of expression and specific localization of *Par1* we performed *in situ* hybridization analysis. *Par1* mRNA was detected predominantly in the cytotrophoblast layer and not in the syncytiotrophoblast layer (Figure 1 IC, insert). This expression was found in the 7th, 8th, and 10th week specimens, compatible with the northern blot and RT-PCR data (Figure 1 IIa, b). Minimal expression was observed at weeks 12 and 14 of gestation and thereafter. Quantification of the PAR family (*Par1–3*) mRNA was carried

out via RT-PCR and northern blot analysis (Figure 1 II and Figure 2). *Par1* expression was first observed in the 7th week of gestation and peaked in the 8th and 10th weeks (Figure 1 II). By the 12th week, *Par1* expression was no longer detectable (Figure 1 IIa), and remained undetectable until at least the end of the first trimester (data not shown). The same pattern of *Par1* mRNA levels was detected using northern blot analysis (Figure 1 IIb). The levels of *Par2* mRNA on the other hand, as detected by PCR, were relatively low and remained constant throughout the first trimester of pregnancy (Fig 1 IIa).

Immunohistochemical staining of PAR1 within the cytotrophoblast layer at 7, 8, and 10 weeks gestation showed high expression, recapitulating essentially the RNA pattern of expression. No staining was detected within the villous stroma at 12-week placenta sample (Figure 1 IIID, E) or when a control IgG was applied.

While no expression of *Par3* was observed in the 6th week of gestation (Figure 2 IA), high and abundant expression levels were found in the cytotrophoblast
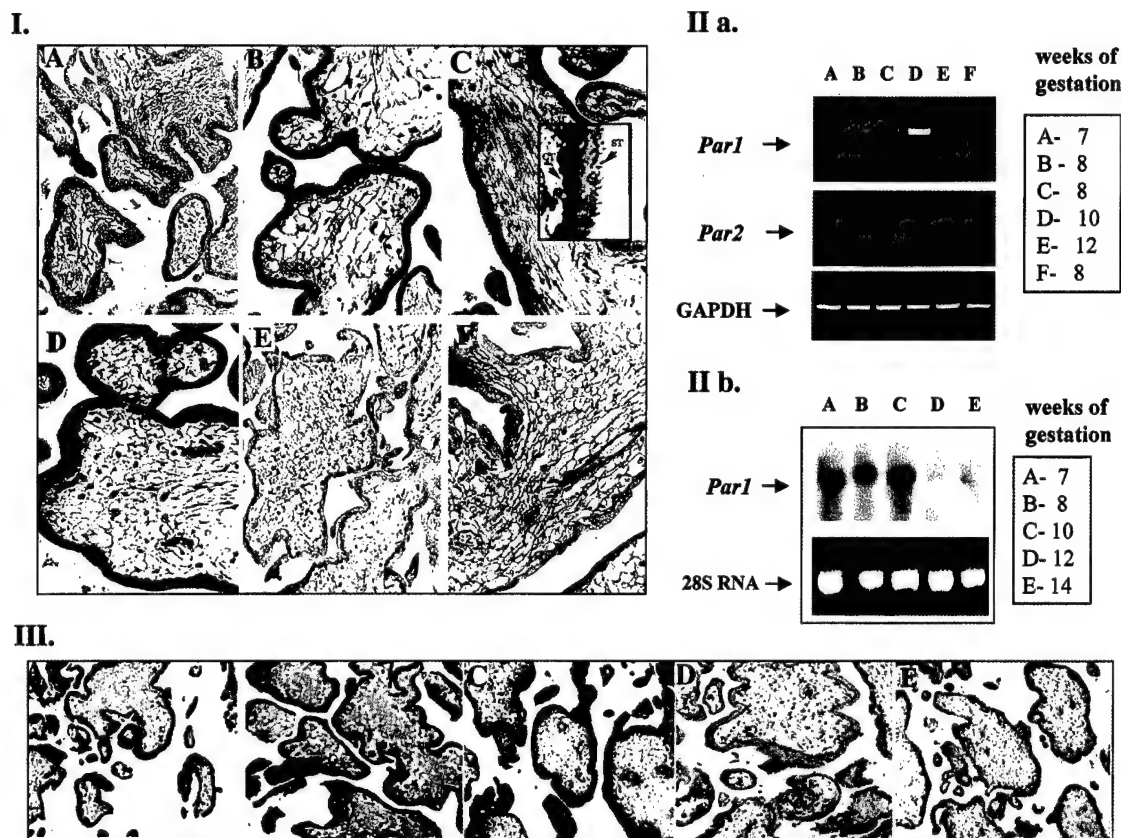
Figure 1. Tissue expression and distribution of PAR1 in the first-trimester placenta. I. *In situ* hybridization of *Par1*. Normal placental specimens were analysed for *Par1* mRNA by *in situ* hybridization, using a DIG-labelled RNA probe for *Par1*. *Par1* antisense riboprobe was applied on tissues from week (A) 6; (B) 7; (C) 8; (D) 10; (E) 10; sense control riboprobe 10; (F) 14. An enlarged view of the placental villi border is shown in section C (note the abundant staining of *Par1* in the cytotrophoblast layer but not in the syncytiotrophoblast). II. Levels of *Par1* and *Par2* mRNA. (a) For PCR detection, 0.25 µg of RNA was reverse-transcribed and amplified, using the appropriate set of primers and compared with the control housekeeping gene GAPDH. (b) *Par1* mRNA levels were evaluated by northern blot analysis and compared to the levels of 28S RNA. III. PAR1 Immunostaining. Immunohistochemical staining of PAR1 shows high immunoreactivity in placental samples obtained at 7 (A), 8 (B), and 10 (C) weeks of gestation. Minimal levels of staining were observed at week 12 (E) of gestation and in a control sample using bovine IgG at week 10 (D). Data shown are representative of at least five independent experiment series of early placenta samples
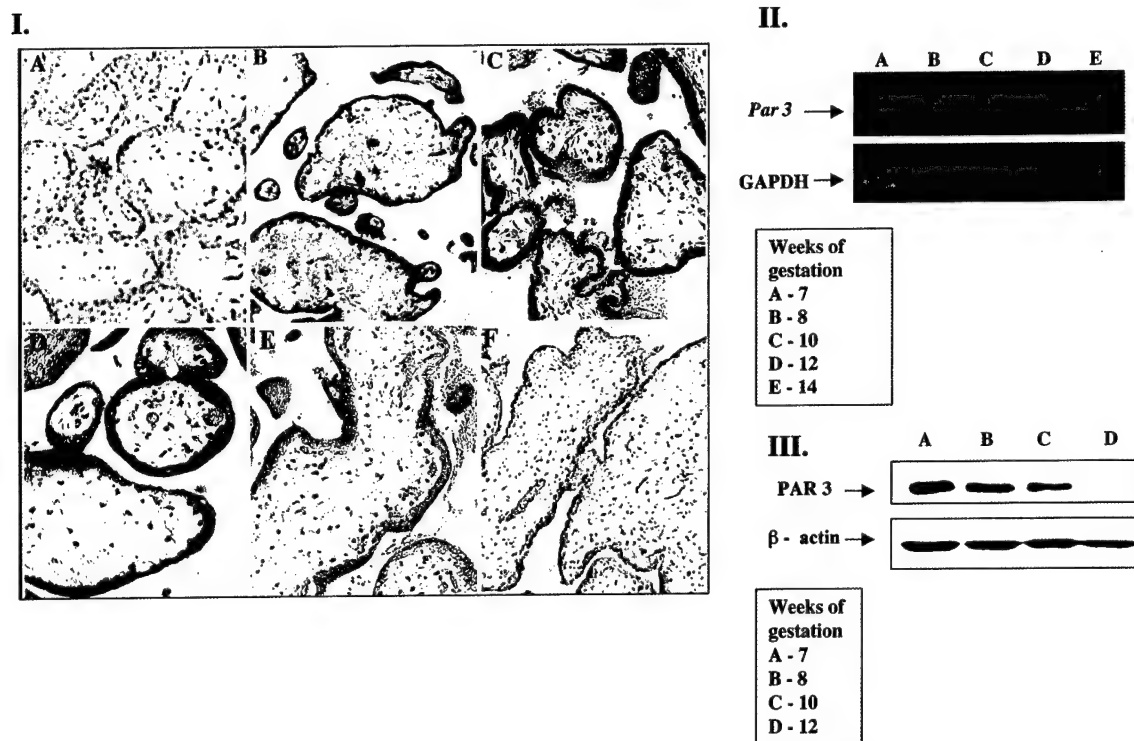
Figure 2. Tissue expression and distribution of PAR3 in the first-trimester placenta. I. *In situ* hybridization. Normal placental specimens were analysed for *Par3* mRNA by *in situ* hybridization using a DIG-labelled RNA probe. An antisense *Par3* riboprobe was applied on tissues from placenta villi following week (A) 6; (B) 7; (C) 8; (D) 10; (E) 10; sense control riboprobe, at week (F) 12. II. RT-PCR analysis of *Par3*. For PCR detection as in Figure I, using specific primers of *Par3*. III. Western blot analysis of PAR3. PAR3 protein levels were detected at weeks 7, 8 and 10 of gestation and were absent at week 12 (D). Equal levels of protein were applied as detected by β-actin housekeeping levels. Data shown are representative of at least three independent set of experiments of early placenta samples

layer of weeks 7–10 of gestation (Figure 2 IB–D). These levels declined thereafter (Figure 2 I F). This pattern of cell distribution corresponded to the expression data observed by RT-PCR analysis (Figure 2 II). The expression profile of the RNA levels was confirmed by western blot analysis for the PAR3 protein quantification similar to the mRNA pattern (Figure 2 III).
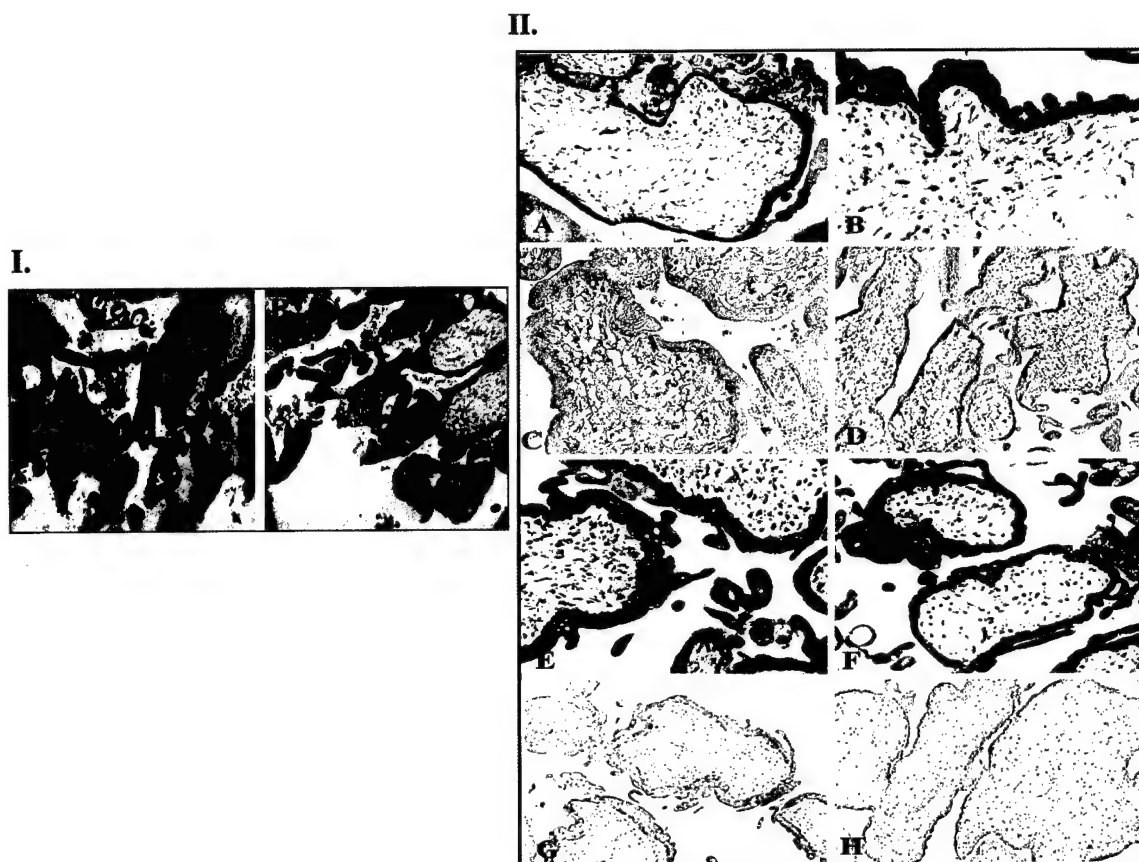
CHMs are linked with a failure to down-regulate the trophoblast expression of PAR1 and PAR3

Trophoblast cells of CHM proliferate rapidly, often show cytological atypia, and bear an approximately 20% risk of becoming a trophoblastic malignancy [6]. This pathological condition of uncontrolled trophoblast hyperplasia provides an opportunity to study the expression levels of *Par1* and *Par3* genes in pathological proliferative placental villi. We have compared tissue localization of *Par1* and *Par3* mRNAs in biopsies of CHM (12–14 weeks of gestation) with that of age-matched normal placentas. *In situ* hybridization analysis of *Par1* RNA probes revealed a high level of expression in the CHM trophoblast cells (Figure 3 II A, B), with very little or no expression detected in trophoblast cells from the normal age-matched pregnancies (Figure 3 II C, D). Immunohistological staining

showed that specific PAR1 protein is localized within the molar cytotrophoblast cells in a tissue distribution similar to that of RNA (Figure 3 I). *Par3* was highly expressed in CHM (Figure 3 II E, F) and absent from normal placenta of the same gestational age (Figure 3 II H). The protein levels of PAR3 essentially recapitulated the mRNA profile (data not shown). Overall, our results show that in complete molar trophoblast cells high levels of PAR1 and PAR3 are found. In contrast, these levels are very low in normal age-matched placenta. Our data indicate that PAR1 and 3 are involved in the invasive phase of trophoblast cells. This was shown in the expression pattern of normal developing placenta during the first trimester of pregnancy as well as in the overexpression demonstrated in pathological trophoblast of CHM.

Discussion

Human placental development involves the differentiation of CTB stem cells (organized in a polarized fashion on top of a basement membrane) toward a non-polarized cytotrophoblast subpopulation (that subsequently lose cell–cell contact and invade). During early pregnancy cytotrophoblast cells proliferate, differentiate, and become motile. While the net invasiveness of trophoblast during early placental development

Figure 3. *Par1* and *Par3* expression levels remain high in CHM. I. Immunohistochemistry of PAR1. A representative experiment of immunohistochemical staining of CHM trophoblast cells, showed strong staining of PAR1 (A) using PAR 1 antibodies. No staining was observed when a control (B) bovine IgG was applied. II. *In situ* hybridization of *Par1* and *Par3*. *Par1* and *Par3* mRNA levels were evaluated in biopsy specimens of CHM that were evacuated at the 12th and 14th weeks of gestation. These samples were compared with normal age-matched placental tissues. (A) *Par1* from CHM placentas at the 12th gestational week; (B) *Par1* from CHM placentas at the 14th gestational week; as compared to normal age-matched placenta; (C) normal villi from placentas at the 12th week; (D) normal villi at the 14th week; (E) and (F) *Par3* from CHM placentas at the 12th and 14th gestational week, respectively; (G) *Par3* sense control from CHM placentas at the12th gestational week; (H) *Par3* antisense on normal villi placenta at 14th gestation week

is regulated in part by integrin-mediated ECM interactions, a specific pattern of integrins was identified to either facilitate or restrain invasion [5,7,8]. Indeed, FAK, a major focal adhesion complex (FAC) protein, was reported to be highly expressed between 5 and 8 weeks of gestation, localized especially to both villous stem cell cytotrophoblasts and extravillous trophoblast cells [10,11]. We have previously demonstrated a central role for PAR1 in tumour invasion via the activation of integrins, cytoskeletal reorganization, and the phosphorylation of FAK and paxillin during the assembly of FACs [17,18]. We show here that PAR1 and PAR3 are highly and abundantly expressed during early placental differentiation, specifically at weeks 7–10 of gestation. This time-frame coincides with the period when the developing trophoblast cells in early pregnancy proliferate, differentiate, and become motile.

During early pregnancy several critical proteins are upregulated: HIF1α, $\alpha6\beta4$ and $\alpha5\beta1$ integrins, fibronectin, and metalloproteinases MMP2 [5,19–21].

Our preliminary observations indicated that overexpression of *Par1* cDNA in EVT cultures facilitated villus outgrowth and induced MMP2 and MMP9 activities (unpublished results). This strengthens the notion that PAR1 contributes to the invasion-like properties of trophoblast cells. The high expression levels of PAR1 and PAR3 occur when the oxygen levels in trophoblast cells are low [22,23]. It appears that the low oxygen tension provides a critical regulator of trophoblast differentiation through the HIF1α transcription factor [24]. We are currently examining whether the expression of PARs in villous explants, cultured in a low (3%) O_2 environment, is elevated as compared with a normal (20%) O_2 environment.

Collectively, our data are the first to demonstrate that PAR1 and PAR3 are overexpressed in pathological trophoblast cells in CHM and during a limited time period of normal early pregnancy (7–10 weeks gestation). The relation between PARs and trophoblast invasiveness is reaffirmed by the over–expression of PAR1 and PAR3 in pathological trophoblast cells

from CHM tissues. In these tissues, uncontrolled trophoblast proliferation is associated with an increased invasive/malignant potential as described in 56% of patients 50 years of age and older [6]. We suggest that the extended expression levels of PAR1 and PAR3 in molar trophoblast cells is directly correlated with their invasive phenotype, although their role remains yet to be fully elucidated.

The trophoblast differentiation system, during early pregnancy, provides an opportunity to study the physiological pattern of PARs in invading cytotrophoblast cells. These data complement our earlier observation that PAR1 is overexpressed in a collection of tumour biopsy specimens and plays a central role in tumour invasion and metastasis [17,18]. Yet, the fact that PAR1 and PAR3 are temporally and spatially expressed and their expression is turned off at week 12 and thereafter is intriguing. The nature of the molecular mechanisms involved in the shut-off of expression of PAR1 and PAR3 is currently being explored.

Acknowledgements

References

1. Cross JC, Werb Z, Fisher SJ. Implantation and the placenta: key pieces of the development puzzle. *Science* 1994; **266**: 1508–1518.
2. Damsky CH, Fisher SJ. Trophoblast pseudo-vasculogenesis: faking with endothelial adhesion receptors. *Curr Opin Cell Biol* 1998; **10**: 660–666.
3. Pijnenborg R, Bland JM, Robertson WB, Dixon G, Brosens I. The pattern of interstitial trophoblastic invasion of the myometrium in early human pregnancy. *Placenta* 1981; **2**: 303–316.
4. Flamigni C, Bulletti C, Polli V, *et al.* Factors regulating interaction between trophoblast and human endometrium. *Ann NY Acad Sci* 1991; **622**: 176–190.
5. Zhou Y, Damsky CH, Chiu K, Roberts JM, Fisher SJ. Preeclampsia is associated with abnormal expression of adhesion molecules by invasive cytotrophoblasts. *J Clin Invest* 1993; **91**: 950–960.
6. Coukos G, Makrigiannakis A, Chung J, Randall TC, Rubin SC, Benjamin I. Complete hydatidiform mole: a disease with a changing profile. *J Reprod Med* 1999; **44**: 698–704.
7. Damsky CH, Fitzgerald ML, Fisher SJ. Distribution patterns of extracellular matrix components and adhesion receptors are intricately modulated during first trimester cytotrophoblast differentiation along the invasive pathway, in vivo. *J Clin Invest* 1992; **89**: 210–222.
8. Damsky CH, Librach C, Lim KH, Fitzgerald M. Integrin switching regulates normal trophoblast invasion. *Development* 1994; **120**: 3657–3666.
9. Vicovac L, Jones CJ, Aplin JD. Trophoblast differentiation during formation of anchoring villi in a model of the early human placenta in vitro. *Placenta* 1995; **16**: 41–56.
10. Ilic D, Genbacev O, Jin F, *et al.* Plasma membrane-associated pY397FAK is a marker of cytotrophoblast invasion in vivo and in vitro. *Am J Pathol* 2001; **159**: 93–108.
11. MacPhee DJ, Mostachfi H, Han R, Lye SJ, Post M, Caniggia I. Focal adhesion kinase is a key mediator of human trophoblast development. *Lab Invest* 2001; **81**: 1469–1483.
12. Hurskainen T, Seiki M, Apte SS, *et al.* Production of membrane-type matrix metalloproteinase-1 (MT-MMP-1) in early human placenta: a possible role in placental implantation? *J Histochem Cytochem* 1998; **46**: 221–229.
13. Librach CL, Werb Z, Fitzgerald ML, *et al.* 92-kD type IV collagenase mediates invasion of human cytotrophoblasts. *J Cell Biol* 1991; **113**: 437–449.
14. Coughlin SR. How the protease thrombin talks to cells. *Proc Natl Acad Sci USA* 1999; **96**: 11 023–11 027.
15. O'Brien PJ, Molino M, Kahn M, Brass LF. Protease activated receptors: theme and variations. *Oncogenes* 2001; **20**(13): 1570–1581.
16. Camerer E, Huang W, Coughlin SR. Tissue factor- and factor X-dependent activation of protease activated receptor 2 by factor VIIa. *Proc Natl Acad Sci USA* 2000; **97**(10): 5255–5260.
17. Even-Ram S, Uziely B, Cohen P, *et al.* Thrombin receptor overexpression in malignant and physiological invasion processes. *Nat Med* 1998; **4**: 909–914.
18. Even-Ram CohenS, Maoz M, Pokroy E, *et al.* Tumour cell invasion is promoted by activation of protease activated receptor-1 in cooperation with $\alpha v \beta 5$ integrin. *J Biol Chem* 2001; **276**: 10 952–10 962.
19. Caniggia I, Grisaru-Gravnosky S, Kuliszewsky M, Post M, Lye SJ. Inhibition of TGF-beta 3 restores the invasive capability of extravillous trophoblasts in preeclamptic pregnancies. *J Clin Invest* 1999; **103**(12): 1641–1650.
20. Caniggia I, Taylor CV, Ritchie JW, Lye SJ, Letarte M. Endoglin regulates trophoblast differentiation along the invasive pathway in human placental villous explants. *Endocrinology* 1997; **138**: 4977–4988.
21. Caniggia I, Mostachfi H, Winter J, *et al.* Hypoxia-inducible factor-1 mediates the biological effects of oxygen on human trophoblast differentiation through TGFbeta(3). *J Clin Invest* 2000; **105**: 577–587.
22. Genbacev O, Joslin R, Damsky CH, Polliotti BM, Fisher SJ. Hypoxia alters early gestation human cytotrophoblast differentiation/invasion in vitro and models the placental defects that occur in preeclampsia. *J Clin Invest* 1996; **97**: 540–550.
23. Genbacev O, Zhou Y, Ludlow JW, Fisher SJ. Regulation of human placental development by oxygen tension. *Science* 1997; **277**: 1669–1672.
24. Cannigia I, Winter J, Lye SJ, Post M. Oxygen and placental development during the first trimester: implications for the pathophysiology of pre-eclampsia. *Placenta* 2000; **21**(Suppl A): S25–S30.

Oncogenic transformation induces tumor angiogenesis: a role for PAR1 activation

YONG-JUN YIN,* ZAIDOUN SALAH,* MYRIAM MAOZ,* SHARONA COHEN EVEN RAM,* SHALOM OCHAYON,* GERA NEUFELD,[‡] SHULAMIT KATZAV,[†] AND RACHEL BAR-SHAVIT*,[1]

*Departments of Oncology, [†]Hubert H. Humphrey Center for Experimental Medicine and Cancer Research, Hebrew University-Hadassah Medical School, Jerusalem; and [‡]Department of Biology, Technion, Israel Institute of Technology, Haifa, Israel

ABSTRACT The formation of new blood vessels is a critical determinant of tumor progression. We find that *Par1* gene expression plays a central role in blood vessel recruitment in animal models. By in vivo injection of either Matrigel plugs containing *Par1*-expressing cells or of rat prostatic carcinoma cells transfected with tetracycline-inducible *Par1* expression vectors, we show that *Par1* significantly enhances both angiogenesis and tumor growth. Several vascular endothelial growth factor (VEGF) splice forms are induced in cells expressing *Par1*. Activation of PAR1 markedly augments the expression of VEGF mRNAs and of functional VEGFs as determined by in vitro assays for endothelial tube alignment and bovine aortic endothelial cell proliferation. Because neutralizing anti-VEGF antibodies potently inhibited *Par1*-induced endothelial cell proliferation, we conclude that *Par1*-induced angiogenesis requires VEGF. Specific inhibitors of protein kinase C (PKC), Src, and phosphatidylinositol 3-kinase (PI3K) inhibit *Par1*-induced VEGF expression, suggesting the participation of these kinases in the process. We also show that oncogenic transformation by genes known to be part of PAR1 signaling machinery is sufficient to increase VEGF expression in NIH 3T3 cells. These data support the novel notion that initiation of cell signaling either by activating PAR1 or by the activated forms of oncogenes is sufficient to induce VEGF and hence angiogenesis. Yin, Y.-J., Salah, Z., Maoz, M., Cohen Even Ram, S., Ochayon, S., Neufeld, G., Katzav, S., Bar-Shavit, R. Oncogenic transformation induces tumor angiogenesis: a role for PAR1 activation. *FASEB J.* 17, 163–174 (2003)

Key Words: thrombin receptor · vascular endothelial growth factor · invasion · metastasis

THE FORMATION of new blood vessels (vasculogenesis and angiogenesis) involves the coordinated functions of endothelial cell proliferation, migration, and tube alignment. The emergence of new blood vessels from preexisting vasculature is a process that is highly affected by growth factor receptors such as KDR/*flk-1* and *flt-1* and by a spectrum of adhesion molecules, primarily integrins (1, 2). Angiogenesis has been designated a

hallmark of cancer and determined to be a prerequisite for tumor growth (3, 4) as well as for various ischemic diseases such as retinopathy of prematurity (3). This process takes place as a consequence of an angiogenic genetic switch, which allows the recruitment of blood vessels from neighboring tissues (5). The critical determinants of this angiogenic switch remain to be elucidated.

The relationship between thrombosis and cancer/metastasis was first recognized by the classical observations of Trousseau in 1872 (6). Many studies since have described a systemic activation of the blood coagulation cascade in patients with cancer (7–9). During initiation of the thrombosis/hemostasis cascade, a complex of factors Va and Xa (Va/Xa) acts to convert prothrombin to the serine protease thrombin. Thrombin ligates the protease activated receptor (PAR) family to initiate cellular functions. We have shown previously that PAR1, the first identified member of the PAR family, plays a direct role in both normal (physiological placental implantation) and pathological (malignancy) cell invasion processes (10). Molecular mechanisms underlying PAR1 involvement in tumor invasion and metastasis include increased phosphorylation of focal adhesion complex proteins, cytoskeletal reorganization, and the recruitment of $\alpha v \beta 5$ integrin after PAR1 ligation (11).

PARs are G-coupled cell surface proteins mediating intracellular responses to the serine protease thrombin (12, 13). PAR1 was recently recognized as an oncogene, promoting transformation in NIH 3T3 cells. In addition to its potent focus forming activity, constitutive overexpression of PAR1 in NIH 3T3 cells promoted the loss of anchorage- and serum-dependent growth. PAR1 activity was found to be directly linked to Rho A and inhibited by pertussis toxin and thus mediated via the $G_{\alpha 13}$ subunit (14). The oncogenic function of PAR1 is especially significant in light of our observation that PAR1 is overexpressed in a series of biopsy specimens of

---

[1] Correspondence: Department of Oncology, Hadassah-University Hospital, POB 12000, Jerusalem 91120, Israel. E-mail: barshav@md.huji.ac.il

breast tumors (10) as well as in a collection of cell lines exhibiting differential metastatic potentials (11).

Mouse embryos lacking *Par1* or several coagulation factors die with varying frequencies at midgestation, often with signs of bleeding (15–21). Recently (22), it has been shown that *Par1* plays a critical role in endothelial cell embryonic development, rescuing *Par 1*$^{-/-}$ mice from bleeding to death; however, its function in tumor angiogenesis is unknown. It was unclear whether bleeding in embryos lacking *Par1* results from impairment of hemostasis or of blood vessel formation. Griffin et al. (22) provided elegant evidence demonstrating that loss of *Par1* does not prevent vessel formation but rather impairs the stabilization and maturation of the newly forming vessels, thereby causing abnormal fragility and ruptures in the vessel wall (22, 23). By initiating the PAR1 signaling cascade in endothelial cells, Griffin et al. (22) were able to rescue *Par1* deficient mouse embryos from bleeding to death. These results demonstrate that activation of PAR1 and its signaling pathway in endothelial cells is essential for vascular integrity. It is interesting to note the phenotypic similarities between *Par1*$^{-/-}$ embryos and various coagulation factor knockout embryos (e.g., factor V$^{-/-}$, tissue factor $^{-/-}$, and prothrombin $^{-/-}$). Most die at midgestation with yolk sac defects and bleeding (16–24).

The major angiogenic factor vascular endothelial growth factor (VEGF) acts mainly through two tyrosine kinase receptors present almost exclusively on endothelial cells, VEGF receptor-1 (VEGFR-1; also termed *flt*-1) and VEGF receptor-2 (*KDR/flk-1*) (25, 26), and via neuropilins expressed on tumor cells (27). The importance of the VEGF/VEGFR system in angiogenesis is strongly supported by data showing early embryonic lethality in mice either heterozygous or completely deficient in VEGFR (25, 27–31). The crucial biological role of VEGF in angiogenic-related functions was shown in studies using targeted gene disruption in mice. Because VEGFR-2 is required for the differentiation of endothelial cells and the recruitment of endothelial cell precursors (31), embryos lacking the VEGFR-2 gene die before birth because the blood vessels do not form (32). Likewise, inhibition of VEGF activity using neutralizing antibodies or by the introduction of dominant negative VEGF receptors into endothelial cells derived from tumor-associated blood vessels resulted in the inhibition of tumor growth and even in tumor regression. This indicates that VEGF is a major initiator of tumor angiogenesis (32, 33). Furthermore, VEGF expression is potentiated by hypoxia and the induced VEGF production in hypoxic areas of solid tumors contributes significantly to tumor angiogenesis (34–36). VEGF also functions as a survival factor for immature blood vessels. These vessels become VEGF independent once they recruit periendothelial cells and undergo maturation. However, the newly formed vascular network will regress if VEGF is prematurely withdrawn. Thus, VEGF deprivation may lead not only to inhibition of further angiogenesis but also to regression of already formed, immature tumor vessels (37).

Several VEGF isoforms are produced from the VEGF gene by alternative splicing. Five human VEGF mRNA splice forms have been identified, encoding VEGFs of various lengths (121, 145, 165, 189, and 206 amino acids; VEGF 121–206) (29–36, 38, 39). They are mainly distinguished by their heparin and heparan sulfate binding ability. Whereas VEGF121 lacks the amino acids encoded by exons 6 and 7 of the VEGF gene (40) and does not bind heparin or extracellular matrix (41), VEGF165 includes exon 7 and does bind heparin (40, 41) and VEGF145 includes exon 6 and binds tightly to the extracellular matrix (ECM) (42). VEGF189 and VEGF206 contain the amino acids encoded by both exons 6 and 7 and display a higher affinity for heparin and heparan sulfate than VEGF145 or VEGF165. It is not clear which of these splice forms are involved in the known effects of VEGF on angiogenesis and tumor growth. In addition, it is not known whether the effects of VEGF and PAR1 on tumor progression are interrelated in any way. We investigated this question and explored the role of PAR1 in tumor angiogenesis.

MATERIALS AND METHODS

Cells

SB-2 noninvasive human melanoma cells (kindly provided by J. Fidler and M. Bar-Eli, Dept. of Cell Biology, University of Texas, M. D. Anderson Cancer Center, Houston, TX) were grown in 10% FCS-DMEM supplemented with 50 U/mL penicillin and streptomycin (GIBCO-BRL, Gaithersburg, MD) and maintained in a humidified incubator with 8% CO_2 at 37°C. The *Par1* stable transfectants, clone Cl13, and clone MixL were grown under the same conditions; for long-term maintenance these were supplemented with 200 µg/mL G418 antibiotics (11). MCF-7 (adenocarcinoma) and MDA435 cells (ductal carcinoma) were maintained as described previously (10). NIH 3T3 cells transfected with Vav, Src, and Ras were grown in DMEM supplemented with 10% calf serum.

Cell transfection

Cells were grown to 30–40% confluency and then transfected with 0.5–2 µg/mL of plasmid DNA in Fugene 6 transfection reagent (Boehringer Mannheim, Germany) according to the manufacturer's instructions (11). After 10 days of selection, stable, transfected clones were established in medium containing 400 µg/mL G418. Antibiotic resistant cell colonies were transferred to separate culture dishes and were grown in 200 µg/mL G418 medium. Forty-eight hours after transfection, transiently transfected cells were collected and tested (RNA was extracted either for RT-PCR and/or Northern blot or for preparation of conditioned medium).

Densitometric evaluations

The relative intensities of PAR1 protein bands (obtained by Western blot analysis) were determined by Fluor-S™ Multi Imager and Multi-Analyst/PC software (Bio-Rad laboratories, Herecules, CA) normalized to the total amount of protein

loaded and expressed relative to PAR1 levels in parental SB-2 cells.

Preparation of conditioned medium

Cells at 90% confluence were fed with fresh medium and incubated for 24 h. For thrombin receptor-activating peptide (TRAP) activation, 100 μM TRAP was added to the medium 8 or 24 h before medium collection. Conditioned medium was then collected and centrifuged at 1000 rpm for 5 min. The supernatant was either used immediately or stored at 4°C before use.

TRAP

TRAP was comprised of H-Ser-Phe-Leu-Leu-Arg-Asn-Pro-Asn-Asp-Lys-NH$_2$ (SFLLRNPNDK).

ELISA

Quantification of the levels of VEGF secreted by *hPar1*-expressing clones was carried out using an ELISA (Quantikine/human VEGF; R&D Systems, MN) performed according to the manufacturer's instructions.

RNA extraction and RT-PCR

Total RNA was prepared, using the *TRI REAGENT* (Molecular Research Center, Inc., Cincinnati, OH) as described by the manufacturer. One microgram of RNA was used for complementary DNA (cDNA) synthesis, employing M-MLV reverse transcriptase and oligo dT (both from Promega, Heidelberg, Germany). VEGF transcripts were amplified, using *Taq* polymerase (Bioline, London, UK) for 20 μL total PCR reaction; 95°C for 3 min for initial melting was followed by 24–30 cycles of 95°C for 1 min, 59°C for 30 s, and 72°C for 1 min; 7 min at 72°C was used for final extension after cycling. PCR primers were as follows: upstream mouse L19, 5'-CTGAAG-GTGAAGGGGAATGTG-3'; downstream mouse L19, 5'-GGATAAAGTCTTGATGATCTC-3' (24cycles); upstream human GADPH, 5'-CCACCCATGGCAAATTCCATGGCA-3'; downstream human GADPH, 5'-TCTAGACGGCAGGTCAG-GTCCACC (26cycles); upstream VEGF, 5'-TCGGGCCTC-CGAAACCATGA-3'; downstream VEGF, 5'-CCTCCT-GAGAGATCTGGTTC-3' (30 cycles). For VEGF, sequences in the 3' and 5' translated regions were used, allowing the amplification of the known splice variants (516 bp, 648 bp, 720 bp, and 771 bp) (43). PCR products were separated on a 2% Nusieve (FMC; Rockland, ME) 3:1 agarose gel, stained with ethidium bromide, and visualized under ultraviolet light.

Northern blot analysis

Total RNA (20 μg) was electrophoresed on 1% formaldehyde-agarose gels and transferred to Hybond-N$^+$ membranes (Amersham Pharmacia Biotech UN Limited). The membranes were hybridized (42°C, 18 h) with α-^{32}P-dCTP labeled (Rediprimer II, Amersham Biosciences UK Limited) probe for human VEGF165 (690 bp obtained by RT-PCR). After hybridization, membranes were washed and exposed to X-ray films. We used the housekeeping genes β-actin and L32 as a control for RNA loading.

Three-dimensional tube forming assay

Type I collagen was prepared from the tail tendons of adult Sprague-Dawley rats. The collagen matrix gel was obtained by simultaneously raising the pH and ionic strength of the collagen solution. Briefly, collagen was used to coat 24-well cluster plates (0.3 mL/well). After polymerization of the collagen at 37°C for 0.5 h, the bovine aortic endothelial cells (BAEC) (2×10^4cells/0.5 mL^{-1}/well^{-1}) were added to each well. Collagen solution (0.4 mL) was carefully poured on top of the cells. After the gel was formed, 0.4 mL of conditioned medium from *Par1* transfected MCF-7 cells, mock transfected MCF-7, or control nontransfected MCF-7 cells were added and replaced with fresh medium every other day. Tube formation and alignment of BAEC were visualized by phase microscopy and photographed at days 8–10 (44).

BAEC proliferation

Cells were seeded in DMEM containing 10% FCS at a density of 2×10^3 cells/16 mm well of a 24-well plate in triplicate. The medium was replaced with conditioned medium 24 h after seeding, and the cells were cultured for 3–14 days in the different conditioned media. Every 3 days postseeding, cells (3 wells for each condition) were dissociated with trypsin/EDTA and counted with a Coulter counter (Coulter Electronics, Ltd.).

Matrigel plug assay

The Matrigel plug assay was performed as described previously (45). Briefly, 300 μL Matrigel [kindly provided by Dr. H. Kleinman, National Institute of Dental Research (NIDR), National Insititutes of Health (NIH), Bethesda, MD] containing 10^6 *Par1*-transfected SB-2 cells/mL at 4°C were injected subcutaneously into an abdominal site between the hind limbs of 7-wk-old male BALB/c mice ($n=6$). Injections were performed bilaterally, when always at the right side Matrigel mixed with naïve cells and transfection reagent. Control mice were injected with Matrigel mixed with empty vector transfected SB-2 cells lacking *Par1*. Matrigel plugs were removed after 10 days. The skin of the mouse was easily pulled back to expose the Matrigel plug, which remained intact. After qualitative differences were noted and photographed, the plugs were dissected out of the mouse and fixed with 4% formaldehyde/phosphate-buffered saline and embedded in paraffin for histological evaluation. For vessel density analysis, 5 μm thick sections from paraffin-embedded plugs were stained with hematoxylin and eosin (H&E) and either Mallory's or von Willebrand Factor (vWF) (DAKO, Glostrup, Denmark) staining. Vascular structures were recognized as luminal or slit-like structures that occasionally contained blood cells within them, as described previously (46). The microvessel density was determined in various plug areas. Individual vessels were counted on ×200 microscopic fields (0.785 mm (2). A total of six fields/plug (representative of at least 3 independent Matrigel plugs per condition) was analyzed.

"Tet-On" system

A 1.3 Kb DNA of *hPar1* was cut from PSL-301-PAR1 plasmid by *Bam*HI and *Xho*I restriction enzymes. This fragment was cloned into the multiple cloning site of pAHygTet1 plasmid between *Bam*HI and *Xho*I to generate pAHygTet1-*hPar1*.

Cells from a clone of AT2.1/Tet-On (generously provided by Dr. Hua-Quan Miao, Imclone Systems, Inc., New York, NY) were transfected with 2 μg DNA of either pAHygTet1-*hPar1* or pAHygTet1 using FuGENE 6 transfection reagent (Roche, Mannheim Germany). After 48 h, the medium was changed and cells were selected by 800 μg/mL hygromycin B (Calbiochem, La Jolla, CA). Stable pAHygTet1-*hPar1*-transfected clones were checked for *hPar1* expression by Northern blot

analysis after a 48 h induction with doxycycline (Dox) (2 μg/mL).

Tumor growth in vivo

Two-month-old male Copenhagen rats were anesthetized. Cells ($0.3 \times 10^6/0.3$ mL/rat) were injected subcutaneously at a dorsal site between the hind limbs. The rats (n=5, each group) were fed with drinking water containing 1% sucrose. To induce *hPar1* expression, 10 μg/mL Dox was added to the drinking water, which was changed every 2 days.

RESULTS

PAR1 promotes tumor angiogenesis in vivo

We have previously shown that introducing *Par1* cDNA into nonmetastatic melanoma cells induced the invasive and adhesive properties of these cells (11). The molecular mechanisms underlying PAR1-induced tumor invasion include recruitment of αvβ5 integrin, focal adhesion complex formation, and cytoskeletal reorganization. We asked whether PAR1 is also capable of inducing tumor angiogenesis. To address this question, we applied a Matrigel plug assay to evaluate whether *Par1* can recruit blood vessels in vivo. We have characterized a stable *Par1* transfected, nonmetastatic SB-2 melanoma cell line (Cl13) (11). Densitometric analysis of a representative Western blot (Fig. 1, ref 11) revealed that Cl13 cells express 4.2-fold more PAR1 than the parent SB-2 line, which expresses very little PAR1. For comparison, the highly invasive melanoma cell line SM-A375 was determined to express 1.8-fold the levels of PAR1 protein found in SB-2 parental cells. Cl13 cells were mixed at 4°C with Matrigel [reconstituted basement membrane (BM) preparation extracted from EHS mouse sarcoma] and injected subcutaneously into BALB/c mice. On injection, the liquid Matrigel rapidly formed a solid gel plug that served not only as an inert vehicle for PAR1 producing cells but also mimicked the natural interactions that exist between tumor cells and the surrounding extracellular matrix (ECM). Nontransfected SB-2 cells were similarly mixed with Matrigel and injected as a control. In some cases, Cl13 cells were treated with TRAP to activate *Par1* before embedding in Matrigel. At 10 days after injection, the Matrigel plugs were exposed, examined, and photographed. Plugs containing control SB-2 cells were pale, containing few blood vessels; however, those containing *Par1*-expressing Cl13 cells were reddish, indicative of recruited blood vessels. Plugs containing TRAP-activated Cl13 cells had the most pronounced red coloration (**Fig. 1I**). Matrigel plugs were subsequently removed, paraffin-embedded, sectioned, and stained for either collagen (Mallory's staining; Fig. 1II*A*, *C*, *D*, *E*) or Factor VIII (vWF staining Fig. 1II*B* and *F*) to allow histological evaluation of blood vessels in the plug. A network of recruited capillary blood vessels is seen in plugs containing Cl13 cells, whereas few vessels appear in plugs containing nontransfected cells (Fig.

1II). The difference in angiogenesis induced by activated PAR1-transfected cells (Fig. 1II*E*, *F*) as compared to nontransfected, either untreated or TRAP-treated cells (Fig. 1II*A–C*), is particularly striking. Microscopic counts of the microvessels in Matrigel sections indicated that these differences are statistically significant (Fig. 1III). Whereas low levels of blood vessels were obtained in SB-2 cells and somewhat induced levels after activation, an eightfold increase was seen in Cl13 after TRAP activation (Fig. 1III). To exclude the possibility that clonal variation is responsible for these effects, we analyzed several other PAR1-transfected SB-2 clones (MixL and Cl15) and found similar angiogenic activity (data not shown).

Inducible *Par1* expression in rat prostatic carcinoma increases tumor mass and angiogenesis

Differential expression of *Par1* in the Dunning rat prostate carcinoma cell variants was observed by RT-PCR. The AT2.1 variant expressed low levels of *Par1*, while AT3.1, which is more motile and tumorigenic than AT2.1 (47), expressed high levels (**Fig. 2I***B*). To establish the exclusive effect of *Par1* expression on prostate tumor progression, AT2.1 cells were transfected with human *Par1* cDNA under the control of a tetracycline-inducible promoter (Fig. 2I). Two clones (AT2.1/Tet-On/*hPar1* clones Cl1 and Cl4) were isolated, in which *hPar1* expression was strongly induced by the tetracycline analog Dox as determined by Northern blot analysis. *Par1* expression was nearly undetectable in the absence of Dox. After addition of Dox, the levels of the 4.1 kb *Par1* mRNA were increased substantially (39-fold for Cl1 and 52-fold for Cl4; Fig. 2II*D*, *F*). The optimal dose of Dox necessary to induce *Par1* expression was 1–2 μg/mL (not shown). *Par1* mRNA could be detected as early as 4–6 h and reached maximum levels at 20–24 h after Dox treatment (not shown). AT2.1 cells transfected with the pTet-On vector without the *Par1* gene did not express any detectable *Par1* mRNA levels either in the presence (Fig. 2II, lane B) or in the absence (Fig. 2II, lane A) of Dox.

To assess the effect of PAR1 on tumor growth in vivo, AT2.1/Tet-On/*hPar1* clone Cl4 cells or control transfected cells were injected subcuanteously into rats. Rats were then maintained for 2 wk with either regular drinking water (supplemented with 1% sucrose) or drinking water containing Dox (and 1% sucrose) to induce *Par1*. In all injected rats, marked tumor growth occurred during this time period. In the absence of Dox, the mean mass of AT2.1 clone Cl4 tumors was 0.35 ± 0.1 g (Fig. 2III*B*). When *hPar1* expression was induced by Dox in the drinking water, mean AT2.1 clone Cl4 tumor mass increased 3.7-fold to 1.30 ± 0.14 g. This increase was statistically significant. In addition to being larger, tumors in these Dox-treated animals had a very reddish appearance (Fig. 2III*C*) compared to the pale appearance of tumors from untreated animals (Fig. 2III*B*). In comparison, tumors from control-transfected and nontransfected AT2.1 tu-
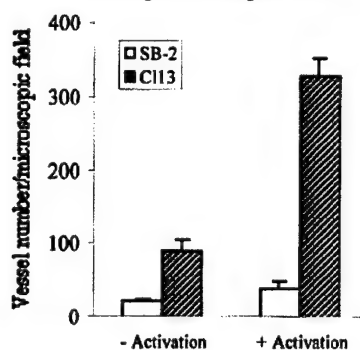
I.

II.
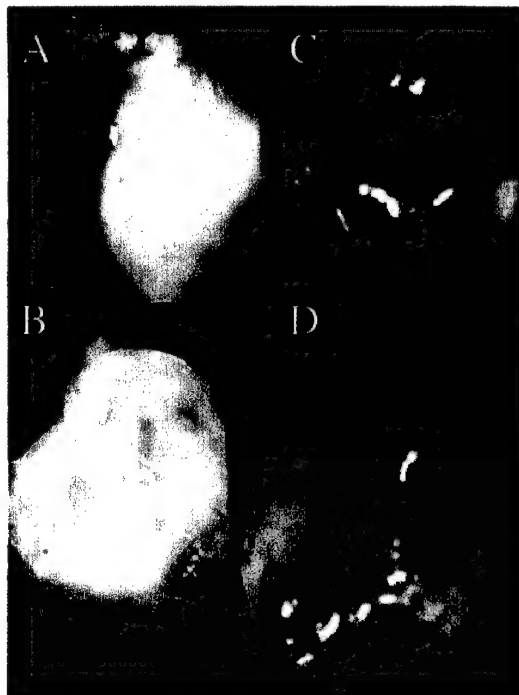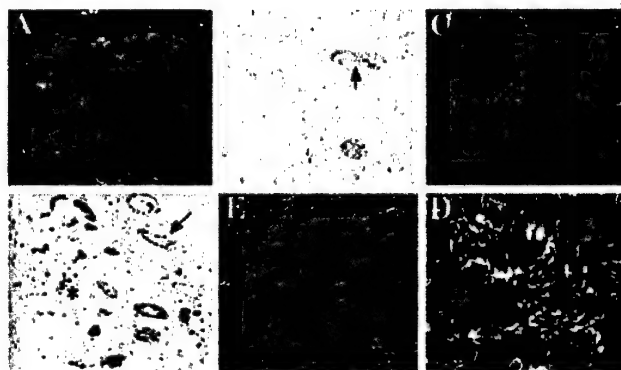
III. **Vessel density analysis in Matrigel micropocket experiment**

Figure 1. *Par1* induces angiogenesis in vivo. Matrigel plugs containing Cl13 (SB-2 cells stably transfected with *Par1*) or nontransfected SB-2 cells were injected subcutaneously into the peritoneal cavity of BALB/c mice in a bilateral fashion. Mice were divided into four groups dependent on the nature of the injected cells: group A ($n=9$) untreated SB-2 cells; group B ($n=8$) SB-2 cells treated with TRAP (100 μM, 8 h); group C ($n=11$) untreated Cl13 cells; and group D ($n=12$) Cl13 cells treated with TRAP (100 μM, 8 h). I: Matrigel plugs under phase microscopy; 10 days after in vivo implantation, Matrigel plugs were removed and examined. Matrigel containing SB-2 cells remained pale (*A*). The appearance of the Matrigel plugs containing SB-2 cells pretreated with TRAP was not significantly different (*B*). Matrigel plugs containing Cl13 cells exhibited a reddish color (*C*), which was more pronounced in Cl13 cells pretreated with TRAP (*D*). ×5. II: Histological evaluation of Matrigel plugs. Serial sections were prepared from Matrigel plugs, and processed either with Mallory's (*A, C, D, E*) or vWF (*B, F*) staining. *A, B*) Untreated SB-2 cells; *C*) SB-2 cells pretreated with TRAP; *D*) Untreated Cl13 cells. *E, F*) Cl13 cells pretreated with TRAP. ×200. vWF staining shows clearly the lumind endothelial cells especially in the microvessels of activated Cl13 embedded plugs. III: Quantification of capillary vessels in Matrigel plugs. Six separate fields of each Matrigel plug stained with H&E, Mallory's, and vWF staining were examined under phase microscopy and capillary vessels were counted. Data are representative of at least 3 independent Matrigel plug sets of experiments.
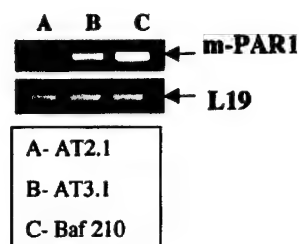
mors were significantly smaller and did not increase in mass or change in color when Dox was delivered in their drinking water (Fig. 2IV). We conclude therefore that the regulated induction of the *Par1* gene markedly enhanced two critical determinants of tumor progression: tumor size and angiogenesis.

Par1-expressing cells induce functional VEGF

Next, we analyzed the expression levels of VEGF165 in the stably *Par1*-transfected melanoma cells (Cl13 and Mix L) using Northern blot analysis (**Fig. 3I**). Parental SB-2 or control transfected cells (Fig. 3I*A* and *B*, respectively) showed no detectable levels of VEGF, but

both Cl13 and MixL had significant levels of VEGF165 mRNA (Fig. 3I*C* and *D*, respectively). A probe for the house-keeping gene β-actin was used as a control for loading. Activation of PAR1 by thrombin or TRAP further increased levels of VEGF165 mRNA (Fig. 3II). Maximal induction was obtained after 8 h of TRAP treatment (Fig. 3II, lane G) at concentrations of 100 μM and 50 μM and was reduced markedly with lower concentrations (Fig. 3III, lanes B–F). When control SB-2 cells were treated with 100 μM of TRAP for 8 h there was no detectable change in VEGF mRNA levels compared to untreated SB-2 cells (data not shown). A similar pattern was obtained for VEGF145 but not for VEGF189, which was slightly expressed only after 8 h of
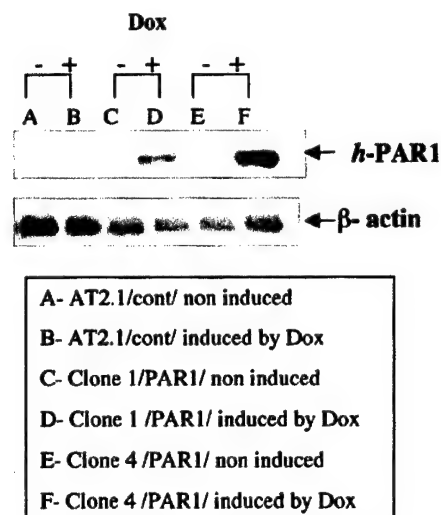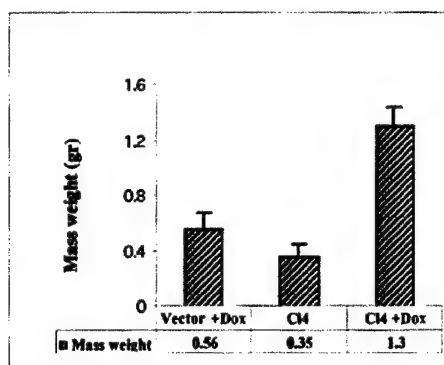
I.

A B C
← m-PAR1
← L19

A- AT2.1
B- AT3.1
C- Baf 210

III.

A   B   C

II.

Dox

- + - + - +

A B C D E F

← h-PAR1

← β- actin

A- AT2.1/cont/ non induced

B- AT2.1/cont/ induced by Dox

C- Clone 1/PAR1/ non induced

D- Clone 1 /PAR1/ induced by Dox

E- Clone 4 /PAR1/ non induced

F- Clone 4 /PAR1/ induced by Dox

IV.

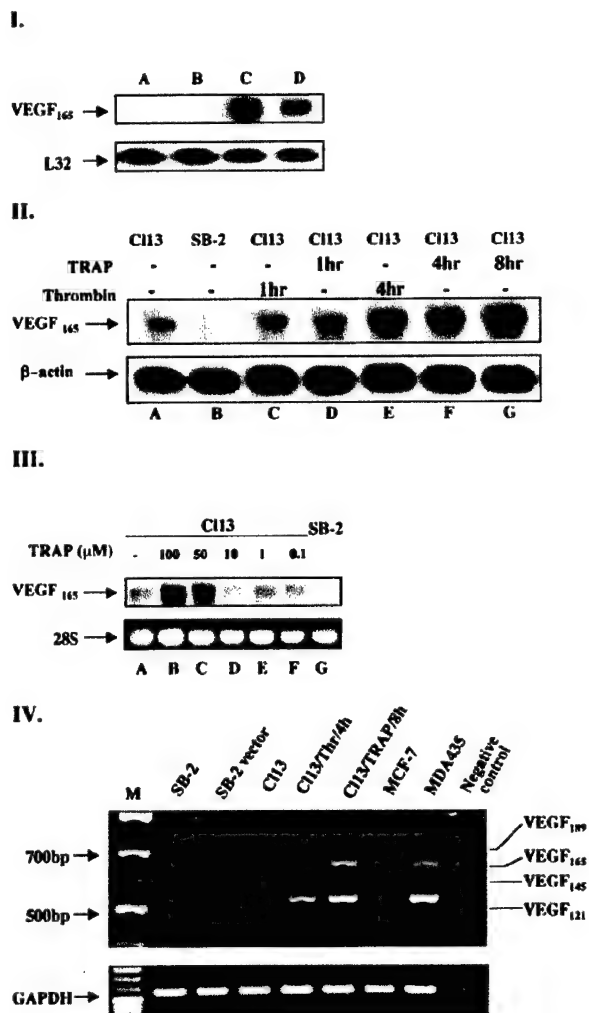|	Vector +Dox	Cl4	Cl4 +Dox
Mass weight	0.56	0.35	1.3

Figure 2. Inducible *Parl* expression in rat prostatic carcinoma increases tumor mass and angiogenesis. I: Differential expression of *Parl* in the Dunning rat prostate carcinoma cell variants was observed by RT-PCR using primers specific for PAR1. Primers for L19 were used as a loading control. II: Inducible *Parl* expression in the rat prostatic carcinoma cell line AT2.1. AT2.1 cells were transfected with a plasmid containing the human *Parl* coding sequence under the control of a tet-inducible promoter. Two stably transfected clones, AT2.1/Tet-On/*hParl* clones Cl4 and Cl1, were tested for the inducibility of human *Parl* expression by the tetracycline analog, Dox as evaluated by Northern blot analysis. III: AT2.1/Tet-On/*hParl* clone Cl4 cells and control transfected (vector only) cells were injected into rats subcutaneously. Animals were maintained for 2 wk with regular drinking water or drinking water supplemented with Dox. After 2 wk, the tumors were excised and examined. Tumors shown were from animals injected with the following: *A*) control transfected cells; *B*) AT2.1/Tet-On/*hParl*, clone Cl4; *C*) AT2.1/Tet-On/*hParl* clone Cl4, fed with Dox for 2 wk. IV: Tumor weight. Data shown are the mean at least 3 independent sets of experiments.

TRAP treatment (Fig. 3IV). Because TRAP could be activating other endogenous PARs, it is important to point out that RT-PCR did not detect any expression of PAR2, PAR3, or PAR4 in our experimental system (data not shown). Using RT-PCR with primers targeting the start site (exon 1) and the end point (exon 8) of the VEGF gene, we could detect all the different splice forms induced by *Parl*. *Parl* markedly induced VEGF 121, VEGF145, and VEGF165; it induced only very low levels of VEGF 189, and VEGF 206 was not detected at all. No VEGF isoforms were detected in the absence of *Parl* in SB-2 parental cells, control-transfected SB-2 cells, or nonmetastatic cells (MCF-7) (Fig. 3IV). Activation of PAR1 (TRAP; 8 h) increased substantially the level of VEGF189, similar to the pattern obtained in the highly metastatic cells (MDA435). To determine how much VEGF protein is actually produced and secreted,

VEGF conditioned media were quantitated by ELISA. In conditioned medium (up to 24 h) derived from control cells (not expressing *Parl*), there was no significant VEGF release (<15 pg/mL). In 8 h conditioned medium derived from Cl13 cells activated with TRAP, VEGF levels were 1440 ± 39.8 pg/mL (*P*<0.01) as compared with 343.3 ± 39.8 pg/mL in nonactivated Cl13 cells. Twenty four hour conditioned medium from nonactivated Cl13 cells contained 1467 ± 125.8 pg/mL VEGF; on TRAP activation VEGF release was increased to 4863.1 ± 267.1 pg/mL (*P*<0.005).

To determine whether the increased levels of VEGF mRNA and protein induced by *Parl* gene correspond to increases in functional VEGF protein, we collected conditioned medium from untreated or thrombin-activated *Parl* transfected cells, as well as from control nontransfected, nonmetastatic cells. We used an endo-

I.

II.

III.

IV.

Figure 3. Expression of VEGF isoforms by stable *Par1*-transfected clones. I: Northern blot analysis of VEGF expression. Total RNA was prepared from SB-2 cells (lane A), SB-2 cells transfected with an empty expression vector (lane B), and two clones stably expressing PAR1: Cl13 (lane C) and MixL (lanet D). The Northern blot was hybridized with a probe specific for VEGF165. Bottom panel shows hybridization to the housekeeping gene L32, as a control for RNA loading. II: Kinetics of VEGF165 mRNA induction after activation of PAR1. Cl13 or SB-2 cells were treated with thrombin (1 U/mL) or TRAP (100 μM) for the indicated times and RNA levels were analyzed by Northern blot. III: Dose response of VEGF165 mRNA induction by TRAP. Cl13 cells were treated with the indicated doses of TRAP for 8 h RNA was analyzed by Northern blot. IV: RT-PCR for the detection of VEGF splice forms in *Par1*-transfected cells. RT-PCR was performed using primers directed to exons 1 and 8 to detect all splice forms. Four different splice forms are detected in Cl13 cells: VEGF121, VEGF145, VEGF165, and VEGF189. None, or very little, is seen in nontransfected (SB-2) cells, cells transfected with empty vector (SB-2 Vector) and nonmetastatic cells (MCF-7). The pattern of expression of *Par1* splice forms in TRAP- or thrombin-activated Cl13 cells is similar to that in highly metastatic cells (MDA435).
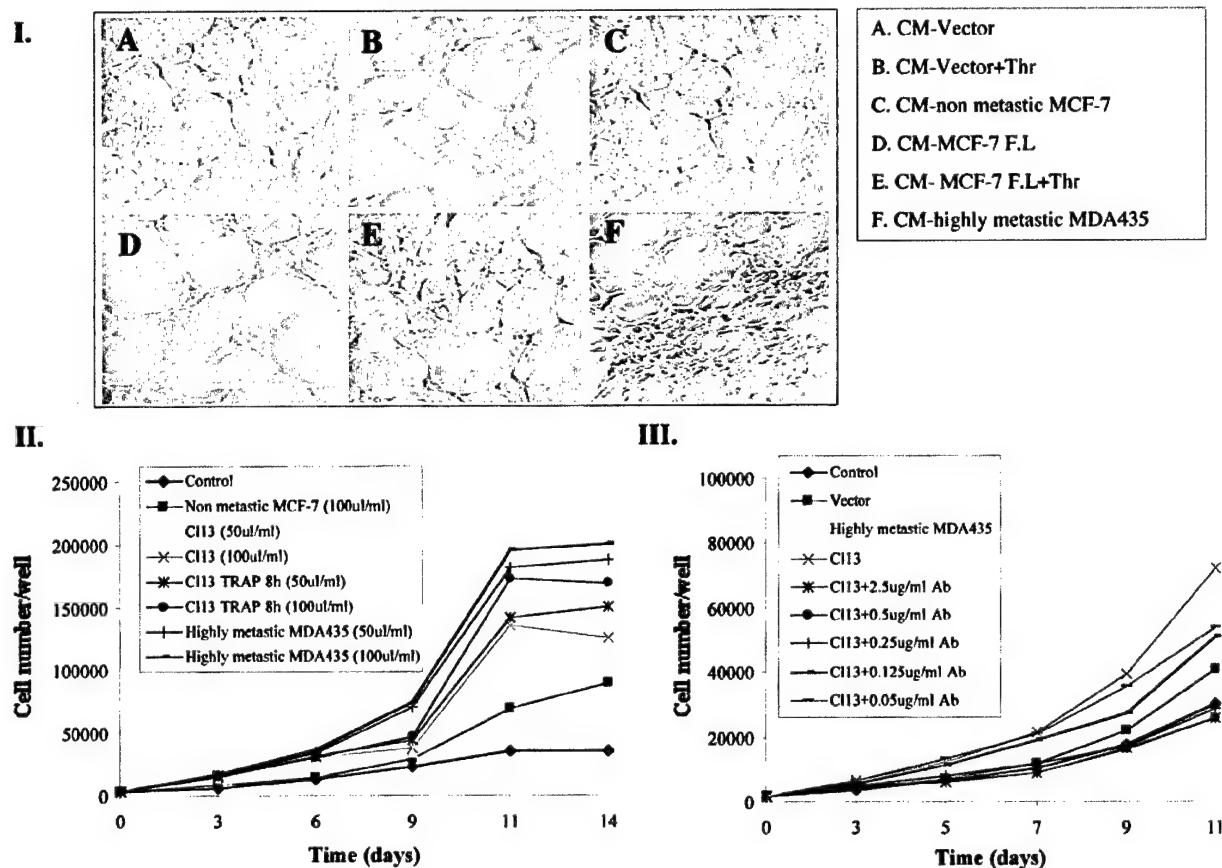
thelial tube forming assay to assess VEGF activity: BAEC cells were embedded in a three-dimensional collagen (type I) mesh and the extent of tube-forming network was evaluated after application of the various conditioned media. Although low vascular branching activity was obtained with untreated control conditioned medium, either treated with thrombin or not (**Fig. 4IA–C**), a more complex appearing network was obtained with activated PAR1 conditioned medium obtained from *Par1*-transfected cells (Fig. 4I*D, E*). We also examined the effect of *Par1* transfected cell conditioned media on the rate of BAEC proliferation in vitro. BAEC proliferation was found to be maximal using conditioned medium from Cl13 cells activated with TRAP (8 h) and was comparable to proliferation seen using conditioned medium from the highly invasive MDA 435 cell line (Fig. 4II). When neutralizing anti-VEGF antibodies were applied during the proliferation assay, a significant inhibition was obtained. Nearly complete inhibition is seen at a 1:100 dilution of the antibodies; the effect decreases in a dose-dependent manner at greater dilutions (Fig. 4III). These data demonstrate that activated PAR1-expressing cells secrete high levels of functional VEGF.

VEGF induction by *Par1* is mediated via protein kinase C, Src, and phosphatidylinositol 3-kinase and Src

The phorbol ester PMA increased VEGF mRNA levels in Cl13 cells in a dose-dependent manner, with maximum induction achieved between 1 and 500 ng/mL (**Fig. 5I**). To determine whether protein kinase C (PKC) might play a role in PAR1-induced increases in VEGF, we used the potent PKC inhibitor calphostin C. At concentrations of 500 ng/mL and higher, calphostin C potently blocked the TRAP-induced increase in VEGF mRNA in Cl13 cells (Fig. 5II). No effect was observed at a lower concentration (50 ng/mL). These data suggest that PKC plays a role in the induction of VEGF by PAR1. Specific inhibitors of two other kinases also inhibited the PAR1-dependent increase in VEGF expression in Cl13 cells. Wortmannin, phosphatidylinositol 3-kinase (PI3K) inhibitor, inhibited TRAP-induced increases in VEGF mRNA levels (Fig. 5III). PP-2, a potent Src inhibitor, also inhibited VEGF induction (Fig. 5IV). These data point to essential roles for PKC, Src, and PI3K in the molecular mechanisms underlying VEGF induction by PAR1.

Transformation of NIH 3T3 cells by the oncogenes v-Ha-Ras, V-Src, or VavK49 induces VEGF mRNA

It has been shown previously that the PAR1 signaling pathway involves Src family tyrosine kinases downstream (48), Ras (49, 50), and increased phosphorylation of Vav (51, 52). It was therefore of interest to see what effect their oncogenic (activated) forms had on VEGF mRNA expression.
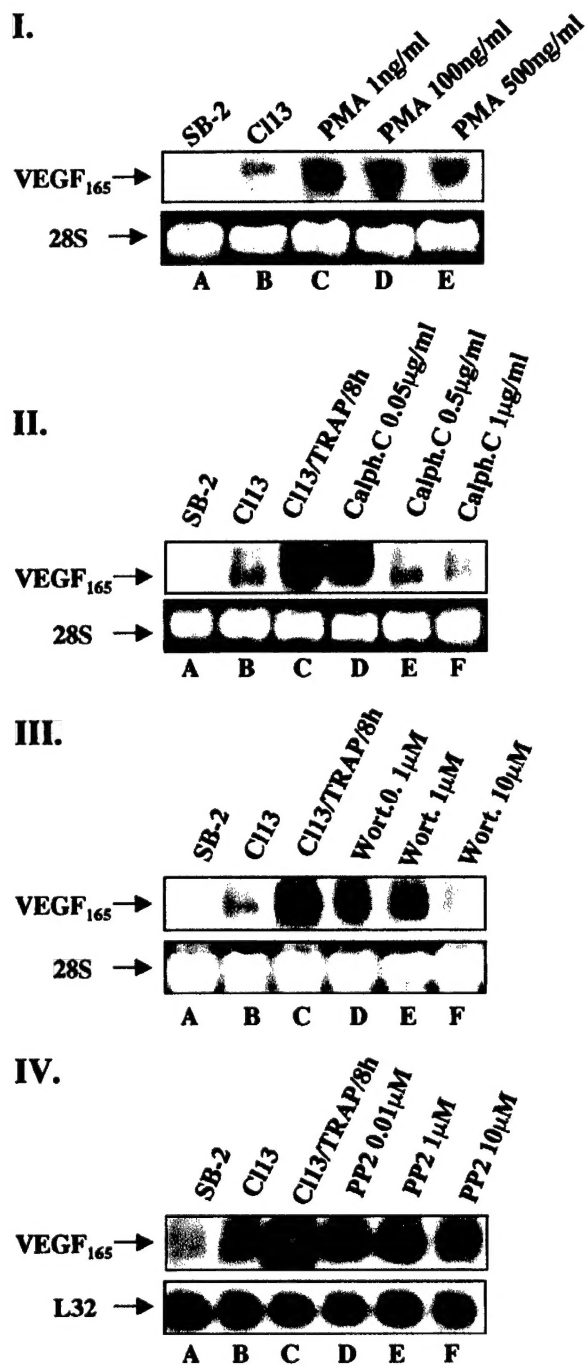
I.

A. CM-Vector

B. CM-Vector+Thr

C. CM-non metastic MCF-7

D. CM-MCF-7 F.L

E. CM- MCF-7 F.L+Thr

F. CM-highly metastic MDA435

II.

Control
Non metastic MCF-7 (100ul/ml)
Cl13 (50ul/ml)
Cl13 (100ul/ml)
Cl13 TRAP 8h (50ul/ml)
Cl13 TRAP 8h (100ul/ml)
Highly metastic MDA435 (50ul/ml)
Highly metastic MDA435 (100ul/ml)

Cell number/well

Time (days)

III.

Control
Vector
Highly metastic MDA435
Cl13
Cl13+2.5ug/ml Ab
Cl13+0.5ug/ml Ab
Cl13+0.25ug/ml Ab
Cl13+0.125ug/ml Ab
Cl13+0.05ug/ml Ab

Cell number/well

Time (days)

Figure 4. PAR1 activity induces functional VEGF. I: Conditioned medium from Cl13 cells increases the complexity of cell tube formation. Cultures of endothelial cells in a three-dimensional collagen type I matrix were grown with conditioned media from nonmetastatic MCF-7 cells transfected with an empty vector (A); nonmetastatic MCF-7 cells/empty vector cells treated with thrombin (B); control, nonmetastatic MCF-7 cells (C); *Par1* transfected MCF-7 cells (D); *Par1* transfected MCF-7 cells treated with thrombin (E); or highly metastatic MDA435 cells (F). II: Conditioned media from *Par1* transfected cells induce the proliferation of BAEC. BAEC cells were cultured in the presence of conditioned medium from the indicated cells. Cultures were refed with fresh conditioned medium every 2 days. At each indicated time point, cells were removed from plates with trypsin/EDTA and counted. Data exhibit a typical experiment representing triplicates. III: Anti-VEGF antibodies inhibit the effects of activated *PAR1* cell conditioned medium on BAEC proliferation. BAECs were cultured in the presence of conditioned medium from activated Cl13 cells (TRAP, 8 h) Anti-VEGF antibodies were added to cultures at varying concentrations as indicated (0.05 μg/mL-2.5 μg/mL) and were present for the entire period of the assay. The effects of conditioned medium from control SB-2 cells and the highly metastatic MDA435 line are shown for comparison.

To determine the effect of oncogenic transformation on VEGF expression, mRNA from transformed and control NIH 3T3 cells was examined for VEGF transcripts (**Fig. 6I**). NIH3T3 cells were transfected with the active forms of *ras, src,* or *vav* (K49) oncogenes, wild-type (wt) *vav* proto-oncogene, or two different SH2 domain mutants of *vav* (W622R and R647L). *Ras, src,* and the oncogenic *vav* all have potent transforming capability. Whereas the full-length *vav* proto-oncogene and the W622R *vav* mutant exhibit greatly reduced transforming potential, the R647L *vav* mutant retains the transforming potential of the oncogene. As shown in Fig. 6I, a marked induction in VEGF mRNA expression was observed in the NIH 3T3 cells transfected with *src* or the *vav* oncogene. However, only low levels of VEGF mRNA are induced in cells transfected with *ras* or

the proto-oncogene *vav,* and no VEGF is detected when cells are transfected with *vav* W622R, the SH2 mutant with reduced transforming ability (Fig. 6I). Low levels of VEGF mRNA were present in cells transfected with vav R647L, which maintains its transforming capability (data not shown). These results suggest that cell transformation is sufficient to induce VEGF.

By performing RT-PCR with primers directed to exons 1 and 8 of the VEGF gene, we examined which VEGF splice forms are expressed in transformed cells. Although control NIH 3T3 cells do not express any of the VEGF splice variants, *src*-transfected NIH 3T3 cells express VEGF121, 145, 165, and 189 but not VEGF 206 (Fig. 6III). The VEGF forms present in *src*-transformed NIH 3T3 were similar to those found in activated (8 h of TRAP) Cl13 cells.
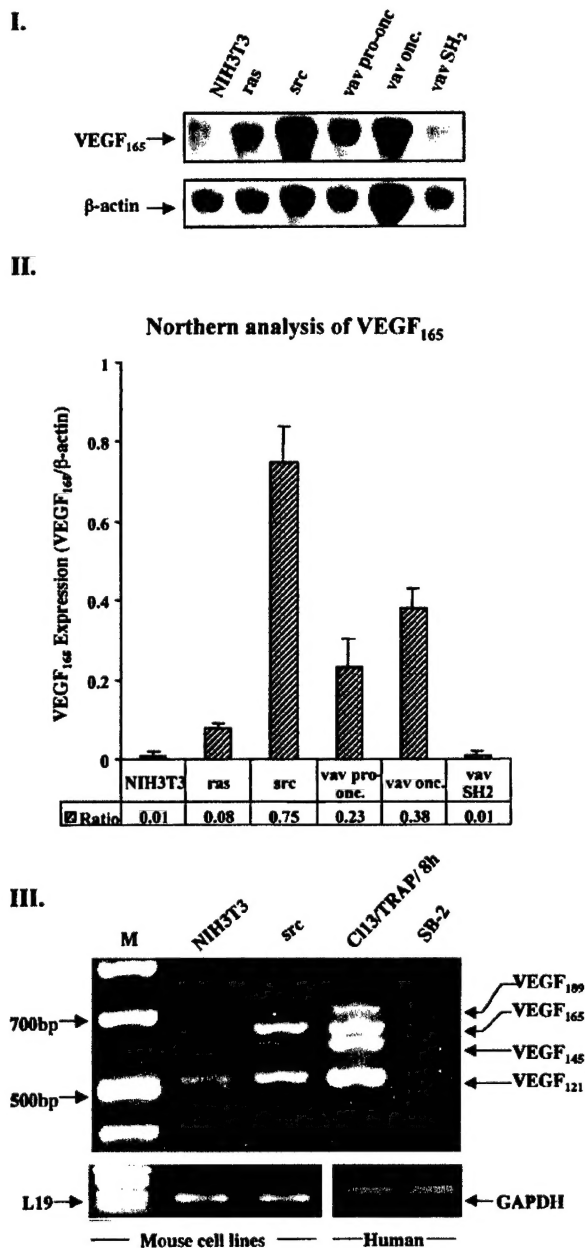
DISCUSSION

We have previously shown that *Par1* is a critical gene involved in tumor invasion and metastasis (10, 11). Here we wished to determine the involvement of PAR1 in tumor angiogenesis. Although the association between the protease thrombin and angiogenesis has been previously documented (53–55), dissection of the role of PAR1 in tumor angiogenesis and its mechanism of activation are largely unknown.

Our results provide a comprehensive analysis of PAR1 involvement in tumor angiogenesis. We demonstrate here the ability of *Par1* to elicit tumor angiogenesis both in vivo in animal models and in vitro (as shown by the endothelial tube forming assay and cell proliferation). In addition, *Par1* expression induces VEGF mRNA. The data indicate that whereas the expression of *Par1* is sufficient to induce VEGF levels, activation of the PAR1 protein and initiation of the cell signaling machinery greatly enhance expression of four VEGF splice forms: VEGF121, VEGF145, VEGF165, and VEGF189 but not VEGF206. This correlates with an increase in effects on angiogenesis in the Matrigel plug assay and on endothelial tube formation and cell proliferation after activation of PAR1. The fact that a greater angiogenic response is seen in Matrigel plugs containing preactivated *Par1*-expressing cells indicates that active recruitment of blood vessels take place early on, immediately after the introduction of the Matrigel plugs. These findings, together with our previous results on the increased invasion potential of *Par1*-overexpressing cells, strongly support a significant role for *Par1* in the two critical events in tumor progression, tumor invasion and angiogenesis (10, 11).

Activation of PAR1 leads to synthesis and secretion of functional VEGF protein as indicated by our observation that conditioned medium from *Par1*-overexpressing cells increases BAEC proliferation and three-dimensional tube forming assay in vitro. The growth-promoting activity of activated PAR1 is mediated by VEGF as demonstrated by the dramatic inhibition of PAR1-induced endothelial cell proliferation in the presence of neutralizing anti-VEGF antibodies. *Par1* expression induces four VEGF splice forms (VEGF121, VEGF145, VEGF165, VEGF189), which are markedly further induced after activation of PAR1 by thrombin or TRAP. This increase in VEGF mRNA is most likely due to stabilization of VEGF mRNA rather than enhanced transcription as documented recently by Haung et al. (55) and our data (not shown). It appears, therefore, that *Par1* plays a dual role in the control of blood vessel formation. The expression of *Par1* in tumor cells is sufficient to induce VEGF expression levels, lead-

Figure 5. Induction of VEGF by PAR1 is mediated by PKC, PI3K, and Src. I: Dose response of VEGF mRNA induction by PMA. Various concentrations of PMA were added to cultures of Cl13 cells and VEGF mRNA levels were determined by Northern blot. RNA from nontransfected, nonmetastatic cells was included as a control (lane A). II: Calphostin C inhibits PAR1-induced increases in VEGF mRNA. Calphostin C was added to Cl13 cultures at the indicated concentrations 30 min before addition of TRAP. Cells were harvested after 8 h of TRAP/calphostin treatment and VEGF mRNA levels were determined by Northern blot. III: Wortmannin, a PI3K inhibitor, blocks PAR1-induced increases in VEGF mRNA. Inhi-

bition by Wortmannin is observed at 1 µM (lane E) and up to 10 µM (lane F) but not at 0.1 µM (lane D). IV: PP2, an inhibitor of Src, blocks PAR1-induced increases inVEGF mRNA. Inhibition of VEGF is observed at 10 µM (lane F), 1 µM (lane E) as compared to *Par1* transfected cells (lane B) and parental nontransfected cells (lane A).

I.

VEGF₁₆₅ →

β-actin →

II.

Northern analysis of VEGF₁₆₅

| ⬚ Ratio | 0.01 | 0.08 | 0.75 | 0.23 | 0.38 | 0.01 |

III.

Figure 6. Expression of VEGF mRNA splice forms in *ras*-, *src*-and *vav*-transformed NIH 3T3 cells. I: Northern blot analysis of transformed NIH 3T3. NIH 3T3 cells were transfected with activated *ras* or *src* oncogenes, wild type (w.t.) *vav* proto-onco-gene, oncogenic *vav* or an SH2 mutant of *vav*. Total RNA was isolated, and 15 μg were analyzed by Northern blotting using a probe for VEGF165. II: Quantitation of changes in VEGF mRNA levels in transformed cells. Photoimage was used to quantitate VEGF165 mRNA levels from Northern blots. VEGF165 mRNA levels were normalized to β-actin mRNA levels to control for loading differences. Data shown are representative of 3 independent experiments. III: RT-PCR analysis of VEGF splice forms. A representative RT-PCR experiment shows elevated levels of VEGF121, VEGF145, VEGF165, and VEGF189 splice forms in *src*-transformed NIH 3T3 cells. *Par1* transfected/activated cells (Cl13/TRAP/8h) and nontransfected SB-2 cells are included as positive and negative controls.

ing to endothelial cell proliferation and sprouting. In addition, *Par1* is required in endothelial cells for matura-tion and stabilization of the blood vessels (22).

Previous studies have shown that thrombin activates PKC, Src, PI3K, and mitogen-activated protein kinase (56–58). Our studies show the involvement of these signaling enzymes in PAR1-induced angiogenesis, be-cause PP2, a Src inhibitor, wortmannin, a PI3K inhibi-tor, and walphostin C, a PKC inhibitor, all potently inhibited VEGF165 mRNA induction. Furthermore, oncogenic transformation of NIH 3T3 cells with genes that participate in PAR1 signaling (e.g., *ras, src*, or *vav*; refs 48, 51, 59, 60) is sufficient to induce the same four VEGF splice forms seen in *Par1*-transfected tumor cells. PAR1 couples to different G-proteins and activates the tyrosine kinases Src and Fyn (48, 59, 61). Thrombin has been shown to induce tyrosine phosphorylation of the adaptor protein Shc, which is then recruited to Grb2 (61). It has been reported that a dominant negative Shc that is deficient in Grb2-binding capability suppresses thrombin-mediated activation of p44 MAP kinase and cell growth, highlighting out the importance of Shc in this pathway. In CCL-39 fibroblasts, thrombin activates p21 *ras* in a manner that is inhibited by pertussis toxin and the tyrosine kinase inhibitor genistein suggesting that activation of Ras involves both G-proteins and activation of protein tyrosine kinases (62). Although the mechanism by which PAR1 couples to Ras is still unclear, it is likely that Src and Fyn activate Ras through the adaptor protein Shc in complex with Grb2 and SOSR as an exchange factor (48, 59). It has been documented previously that activated forms of Ras induce VEGF gene expression in NIH 3T3 cells and primary endothelial cells (63, 64); our results confirm and support these data. Vav activates GTP-binding proteins and is part of the PAR1 signaling cascade (52, 65); we now show that it also induces low levels of VEGF. The oncogenic form of *vav* induces high levels of VEGF. The fact that two SH2 mutants of Vav (R647L and W622R), both shown to be defective in their tyrosine phosphorylation properties (66, 67), had dif-ferent abilities to induce VEGF suggests a correlation between VEGF production and transforming potential. The W622R mutant, which is defective in transforming properties, does not induce VEGF expression while R647L, which maintains its transforming potential, does.

Together, these data strongly support the notion that PAR1 expression and the initiation of the PAR1 signal-ing cascade are highly significant in eliciting tumor angiogenesis. ⬛

REFERENCES

1. Ferrara, N., and Alitalo, K. (1999) Clinical application of angiogenic growth factor and their inhibitors. *Nature Med.* **5**, 1359–1364
2. Hynes, R. O., Bader, B. L., and Hodivala-Dilke, K. (1999) Integrins in vascular development. *Braz. J. Med. Biol. Res.* **32**, 501–510
3. Carmeliet, P., and Jain, R. K. (2000) Angiogenesis in cancer and other diseases. *Nature (London)* **407**, 249–257
4. Folkman, J. (1971) Tumor angiogenic therapoeitic implications. *N. Engl. J. Med.* **285**, 1182–1186
5. Hanahan, D., and Folkman, J. (1996) Pattern and emerging mechanisms of angiogenic switch during tumorigenesis. *Cell* **86**, 353–364
6. Trousscau, A. (1872) *Lectures in Clinical Medicine Delivered in Hotel-Dieu, Paris* pp. 281–295, New Sydenham Society, London
7. Rickles, F. R., and Edwards, R. L. (1983) Activation of blood coagulation in cancer: Trousseau's syndrome revisited. *Blood* **62**, 14–31
8. Sloane, B. F., Rozhin, J., Johnson, K., Taylor, H., Crissman, J. D., and Honn, K. Y. (1986) Cathepsin B: association with plasma membrane in metastatic tumors. *Proc. Natl. Acad. Sci. USA* **83**, 2483–2487
9. Zacharski, L. R., Memoli, V. A., Morian, W. D., Schlaeppi, J. M., and Rousseu, S. M. (1995) Cellular localization of enzymatically active thrombin in intact human tissues by hirudin binding. *Throm. Haemostasis* **73**, 793–797
10. Even-Ram, S., Uziely, B., Cohen, P., Ginzburg, Y., Reich, R. Vlodavsky, I., and Bar-Shavit, R. (1998) Thrombin receptor overexpression in physiological and malignant invasion process. *Nature Med.* **4**, 909–914
11. Even-Ram, C. S., Maoz, M., Pokroy, E., Reich, R., Katz, B.-Z., Gutwein, P., Altevogt, P., and Bar-Shavit, R. (2001) Tumor cell invasion is promoted by activation of protease activated receptor-1 in cooperation with αvβ5 integrin. *J. Biol. Chem.* **276**, 10952–10962
12. Vu, T.-K., Hung, D. T., Wheaton, V. I., and Coughlin, S. R. (1991) Molecular cloning of a functional thrombin receptor reveals a novel proteolytic mechanism of receptor activation. *Cell* **64**, 1057–1068
13. Rasmussen, U. B., Vouret-Craviari. V., Jallat, S., Schlesinger, Y., Pages, G., Pavirani, A., Lecocq, J. P., Pouyssegur, J., and Van Obberghen-Schilling, E. (1991) cDNA cloning and expression of a hamster α-thrombin receptor coupled to Ca^{+2} mobilization. *FEBS Lett.* **288**, 123–128
14. Martin, C. B., Mahon, G. M., Klinger, M. B., Kay, R. J., Symons, M., Der, C. J., and Whitehead, I. P. (2001) The thrombin receptor. *PAR*-1 causes transformation by activation of Rho-mediated signaling pathways. *Oncogene* **20**, 1953–1963
15. Connolly, A. J., Ishihara, H., Kahn, M. L., Fares, Jr., R. V., and Coughlin, S. R. (1996) Role of the thrombin receptor in development and evidence for a second receptor. *Nature (London)* **381**, 516–519
16. Bugge, T. H., Xiao, Q., Kombrinck, K. W., Flick, M. J., Holmback, K., Danton, M. J., Colbert, M. C., Witte, D. P., Fujikawa, K., Davie, E. W., and Degen, J. L. (1996) Fatal embryonic bleeding events in mice lacking tissue factor, the cell-associated initiator of blood coagulation. *Proc. Natl. Acad. Sci. USA* **93**, 6258–6263
17. Carmeliet, P., Ferreira, V., Breier, G., Pollefeyt, S., Kieckens, L., Gertsenstein, M., Fahrig, M., Vandenhoeck, A., Harpal, K., Eberhardt, C., Declercq, C., Pawling, J., Moons, L., Collen, D., Risau, W., and Nagy, A. (1996) Abnormal blood vessel development and lethality in embryos lacking a single VEGF allele. *Nature (London)* **380**, 435–439
18. Toomey, J. R., Kratzer, K. E., Lasky, N. M., Stanton, J. J., and Broze, Jr., G. J. (1996) Targeted disruption of the murine tissue factor gene results in embryonic lethality. *Blood* **88**, 1583–1587
19. Cui, J., O'Shea, K. S. M., Purkayastha, A., Saunders, T. L., and Ginsburg, D. (1996) Fatal haemorrhage and incomplete block to embryogenesis in mice lacking coagulation factor V. *Nature (London)* **384**, 66–68
20. Sun, W. Y., Witte, D. P., Degen, J. L., Colbert, M. C., Burkart, M. C., Holmback, K., Xiao, Q., Bugge, T. H., and Degen, S. J. (1998) Prothrombin deficiency results in embryonic and neonatal lethality in mice. *Proc. Natl. Acad. Sci. USA.* **95**, 7597–7602
21. Xue, J., Wu, Q., Westfield, L. A., Tuley, E. A., Lu, D., Zhang, Q., Shim, K., Zheng, X., and Sadler, J. E. (1998) Incomplete embryonic lethality and fatal neonatal hemorrhage caused by prothrombin deficiency in mice. *Proc. Natl. Acad. Sci. USA* **95**, 7603–7607
22. Griffin, C. T., Snirivasan, Y., Zheng, Y.-W., Haung, W., and Coughlin, S. R. (2001) A role for thrombin receptor signaling in endothelial cells during embryonic development. *Science* **293**, 1666–1670
23. Preissner, K. T., Nawroth, P. P., and Kanse, S. M. (2000) Vascular protease receptors: integrating haemostasis and endothelial cell functions. *J. Pathol.* **190**, 360–372
24. Carmeliet, P. (2001) Clotting factors build blood vessels. *Science* **293**, 1602–1604
25. Shibuya, M., Yamaguchi, S., Yamane, A., Ikeda, T., Tojo, A., Matsushime, H., and Sato, M. (1990) Nucleotide sequence and expression of a novel human receptor-type tyrosine kinase gene (flt) closely related to the fms family. *Oncogene* **5**, 519–524
26. Terman, B. I., Carrion, M. E., Kovacs, E., Rasmussen, B. A., Eddy, R. L., and Shows, T. B. (1991) Identification of a new endothelial cell growth factor receptor tyrosine kinase. *Oncogene* **6**, 1677–1683
27. Neufeld, G., Cohen, T., Gengrinovitch, S., and Poltorak, Z. (1999) Vascular endothelial growth factor (VEGF) and its receptors. *FASEB J.* **13**, 9–22
28. Kim, K. J., Li, B., Winer, J., Armanini, M., Gillett, N., Phillips, H. S., and Ferrara, N. (1993) Inhibition of vascular endothelial growth factor-induced angiogenesis suppresses tumour growth in vivo. *Nature (London)* **362**, 841–844
29. Millauer, B., Shawver, L. K., Plate, K. H., Risau, W., and Ullrich, A. (1994) Glioblastoma growth inhibited in vivo by a dominant-negative Flk-1 mutant. *Nature (London)* **367**, 576–579
30. Carmeliet, P., Ferreira, V., Breier, G., Pollefeyt, S., Kieckens, L., Gertsenstein, M., Fahrig, M., Vandenhoeck, A., Harpal, K., Eberhardt, C., Declercq, C., Pawling, J., Moons, L., Collen, D., Risau, W., and Nagy, A. (1996) Abnormal blood vessel development and lethality in embryos lacking a single VEGF allele. *Nature (London)* **380**, 435–439
31. Shalaby, F., Ho, J., Stanford, W. L., Fischer, K. D., Schuh, A. C, Schwartz, L., Bernstein, A., and Rossant, J. (1997) A requirement for Flk1 in primitive and definitive hematopoiesis and vasculogenesis. *Cell* **89**, 981–990
32. Fong, G. H., Rossant, J., Gertsenstein, M., and Breitman, M. L. (1995) Role of Flt-1 receptor tyrosine kinase in regulating the assembly of vascular endothelium. *Nature (London)* **376**, 66–70
33. Shweiki, D., Itin, A., Soffer, D., and Keshet, E. (1992) Vascular endothelial growth factor induced by hypoxia may mediate hypoxia-initiated angiogenesis. *Nature (London)* **359**, 843–845
34. Plate, K. H., Breier, G., Weich, H. A., and Risau, W. (1992) Vascular endothelial growth factor is a potent tumor angiogenesis factor in human gliomas in vivo. *Nature (London)* **359**, 845–848
35. Leung, D. W., Cachianes, G., Kuang, W. J., Goddel, D. V., and Ferrara, N. (1989) Vascular endothelial growth factor is a secreted angiogenic mitogen. *Science* **246**, 1306–1309
36. Tischer, E., Gospadorowicz, D., Mitchell, R., Silva, M., Schilling, J., Lau, K., Crisp, T., Fiddes, J. C., and Abraham, J. A. (1989) Vascular endothelial growth factor: a new member of the platelet-derived growth gene family. *Bichem. Biophys. Res. Commun.* **165**, 1198–1206
37. Benjamin, L. E., Golijanin, D., Itin, A., Pode, D., and Keshet, E. (1999) Selective ablation of immature blood vessels in established human tumors follows vascular endothelial growth factor withdrawal. *J. Clin. Invest.* **103**, 159–165
38. Keck, P. J., Hauser, S, D., Krivi, G., Sanzo, K., Warren, T., Feder, J., and Connolly, D. T. (1989) Vascular permeability factor, an endothelial cell mitogen related to PDGF. *Science* **246**, 1309–1312
39. Houck, K. A., Ferrara, N., Winer, J., Cachiaes, G., Li, B., and Leung, D. W. (1991) The vascular endothelial growth factor family-identification of a fourth molecular species and characterization of a alternative splicing RNA. *Mol. Endocrinol.* **5**, 1806–1814
40. Cohen, T., Gitay-Goren, H., Sharon, R., Shibuya, M., Halaban, R., Levi, B., and Neufeld, G. (1995) VEGF121, a vascular endothelial growth factor isoform lacking heparin binding ability, requires cell surface heparan sulfates for efficient bind-

ing to the VEGF receptors of human melanoma cells. *J. Biol. Chem.* **270**, 11322–11326

41. Park, J. E., Keller, G. A., and Ferrara, N. (1993) Vascular endothelial growth factor (VEGF) isoforms-differential deposition into the subepithelial eextracellular matrix and bioactivity of extracellular matrix-bound VEGF. *Mol. Biol. Cell* **4**, 1317–1326

42. Poltorak, Z., Cohen, T., Sivan, R., Kandelis, Y., Spira, G., Vlodavsky, I., Keshet, E., and Neufeld, G. (1997) VEGF 145: a secreted VEGF form that binds to extracellular matrix. *J. Biol. Chem.* **272**, 7151–7158

43. Fiedler, W., Graeven, U., Ergun, S., Verago, S., Kilic, N., Stockschlader, M., and Hossfeld, D. K. (1997) Vascular endothelial growth factor, a possible paracrine growth factor in human acute myeloid leukemia. *Blood* **89**, 1870–1875

44. Schnaper, H. W., Grant, D. S., Stetler-Stevenson, W. G., Fridman, R., D'Orazi, G., Murphy, A. N., Bird, R. E., Hoytha, M., Fuerst, T. R., French, D. L., Quigley, J. P., and Klienman, H. K. (1993) type IV collagenase(s) and TIMPs modulate endothelial cell morphogenesis in vitro. *J. Cell. Physiol.* **156**, 235–246

45. Passaniti, A., Taylor, R. M., Pili, R., Guo, Y., Long, P. V., Haney, J. A., Pauly, R. R., Grants, D. S., and Martin, G. R. (1992) A simple, quantitative method for assessing angiogenesis and antiangiogenic agents using reconstituted basement membrane, heparin, and fibroblast growth factor. *Lab. Invest.* **67**, 519–528

46. Itoh, T., Tanioka, M., Yoshida, H., Yoshioka, T., Nishimoto, H., and Itohara, S. (1998) Reduced angiogenesis and tumor progression in gelatinase A-deficient mice. *Cancer Res.* **58**, 1048–1051

47. Miao, H.-Q., Lee, P., Lin, H., Soker, S., and Klagsbrun, M. (2000) Neuropilin-1 expression by tumor cells promotes tumor angiogenesis and progression. *FASEB J.* **14**, 2532–2539

48. Chen, Y.-H., Pouyssegur, J., Coutridge, S. A., and Van Obberghen-Schilling, E. (1994) Activation of Src family kinase activity by the G protein-coupled thrombin receptor in growth-responsive fibroblasts. *J. Biol. Chem.* **269**, 27372–27377

49. Shock, D. D., He, K., Wencel-Drake, J. D., and Parise, L. V. (1997) Ras activation in platelets after stimulation of the thrombin receptor, thromboxane A2 receptor or prote. *Biochem. J.* **321**, 525–530

50. Ellis, C. A., Malik, A. B., Gilchrist, A., Hamm, H., Sandoval, R., Voyno-Yasenetskaya, T., and Tiruppathi, C. (1999) Thrombin induces proteinase-activated receptor-1 gene expression in endothelialcells via activation of Gi-linked Ras/mitogen-activated protein kinase pathway. *J. Biol. Chem.* **274**, 13718–13727

51. Cichowski, K., Brugge, J. S., and Brass, L. F. (1996) Thrombin receptor activation and integrin engagement stimulate tyrosine phosphorylation of the proto-oncogene product, p95vav, in platelets. *J. Biol. Chem.* **271**, 7544–7550

52. Bar-Shavit, R., Maoz, M., Yongjun, Y., Groysman, M., Dekel, I., and Katzav, S. (2002) Signalling pathways induced by protease-activated receptors and integrins in T cells. *Immunology* **105**, 35–46

53. Tsopanoglou, N. E., and Maragoudakis, M. E. (1999) On the mechanism of thrombin-induced angiogenesis. *J. Biol. Chem.* **274**, 23969–23976

54. Richard, D. E., Vouret-Craviari, V., and Pouyssegur, J. (2001) Angiogenesis and G-protein coupled receptors:signals and bridge the gap. *Oncogene* **20**, 1556–1562

55. Huang, Y.-Q., Li, J.-J., Hu, L., Lee, M., and Karpatkin, S. (2001) Thrombin induces increased expression and secretion of VEGF from human FS4 fibroblasts. DU 145 prostate cells and CHRF megakaryocytes. *Throm. Haemst.* **86**, 1094–1098

56. Carter, A. N., Haung, R., Sorisk, A., Downes, C. P., and Rittenhouse, S. E. (1994) Phosphatidylinositol 3,4,5-triphosphate is formed from phosphatidylinositol 4,5-bis-phosphate in thrombin-stimulated platelets. *Biochem. J.* **310**, 415–420

57. Gutkind, J. S., Lacal, P. M., and Robbins, K. C. (1990) Thrombin-dependent association of phosphatidylinositol-3-kinase with p60c-src and p59fyn in human platelets. *Mol. Cell. Biol.* **10**, 3806–3809

58. Leach, K., L., Ruff, V. A., Jarpe, M. B., Adams, L. D., Fabbro, D., and Raben, D. M. (1992) Alpha thrombin stimulates nuclear localization of protein kinse C isozyme in IIC9 cells. *J. Biol. Chem.* **267**, 21816–21822

59. Chen, Y., Grall, D., Salcini, A. E., Pelicci, P. G., Pouyssegur, J., and Van Obberghen-Schilling, E. (1996) Shc adaptor proteins are key transducers of mitogenic signaling mediated by the G protein-coupled thrombin receptor. *EMBO J.* **15**, 1037–1044

60. Collins, L. R., Rickets, W. A., Olefsky, J. M., and Brown, J. H. (1997) The G12 coupled thrombin receptor stimulates mitogenesis through the Shc SH2 domain. *Oncogene* **15**, 595–600

61. Maulon, L., Mari, B., Bertolotto, C., Ricci, J. E., Luciano, F., Belhacene, N., Deckert, M., Baier, G., and Auberger, P. (2001) Differential requirements for ERK1/2 and P38 MAPK activation by thrombin in T cells. Role of P59Fyn and PKC epsilon. *Oncogene* **20**, 1964–1972

62. Ricketts, W.A., Brown, J. H., and Olefsky, J. M. (1999) Pertussis toxin-sensitive and -insensitive thrombin stimulation of Shc phosphorylation and mitogenesis are mediated through distinct pathways. *Mol. Endocrinol.* **13**, 1988–2001

63. Grugel, S., Finkenzeller, G., Weindel, K., Barleon, B., and Marme, D. (1995) Endothelial growth factor in NIH 3T3 cells. *J. Biol. Chem.* **270**, 25915–25919

64. Meadows, K. N., Bryant, P., and Pumiglia, K. (2001) Vascular endothelial growth factor induction of the angiogenic phenotype requires Ras activation. *J. Biol. Chem.* **276**, 49289–49298

65. Landau, E., Tirosh, R., Pinson, A., Banai, S., Even-Ram, S., Maoz, M., Katzav, S., and Bar-Shavit, R. (2000) Protection of thrombin receptor expression under hypoxia. *J. Biol. Chem.* **275**, 2281–2287

66. Katzav, S. (1993) Single point mutation in the SH2 domain impair the transforming potential of *vav* and fail to activate proto-*vav*. *Oncogene* **8**, 1757–1763

67. Katzav, S., Packham, G., Sutherland, M., Aroca, P., Santos, E., and Cleavland, J. L. (1995) Vav and ras induce fibroblast transformation by overlapping signaling pathways which require c-Myc function. *Oncogene* **11**, 1079–1088